

MASTER THESIS IN PHYSICS/ACOUSTICS

Finite element modeling and experimental characterization of piezoelectric ceramic disk in air

Espen Fosse
June 2022



UNIVERSITY OF BERGEN

Department of Physics and Technology

NORWAY

Abstract

Understanding the piezoelectric disk characteristics and behaviors is essential to achieve a good system model and can increase accuracy and reduce measurement uncertainties. This work uses finite element modeling to compare simulations to experimentally obtained measurements of electrical and acoustic characteristics of the piezoelectric disk Pz27.

The electrical measurements are performed with an impedance analyzer, which measures the electrical properties of the piezoelectric disk conductance and susceptance. For the acoustic measurements of the directivity, on-axis pressure, and 2-D horizontal pressure field of the piezoelectric disk, a MatLab app has been developed to automate the measurements and control the acoustic measuring setup. The sensitivity of the directivity related to small dislocations of the transducer has been studied.

The finite element simulations compared to experimentally obtained results agree well, but somewhat low signal-to-noise ratio for some of the frequencies are observed. These results imply that the finite element simulation software used in this work proves to be a good tool for predicting measurements.

Acknowledgment

I want to express my gratitude to my supervisor, Prof. Per Lunde, and co-supervisors Mathias Myrtveit Sæther and Assoc. Prof. Emer. Magne Vestrheim for their guidance, informative meetings, and remarks that have been helpful to me in completing this master's thesis.

I want to thank Sverre Kongsro Finstad for his introduction to the acoustic measurement setup. I want to give a big thanks to Eivind Nag Mosland for helping me answer questions on FEMP, sharing knowledge of previously used scripts in the acoustic measurement setup, and providing general information about instruments in the acoustic measurement setup. I also want to thank Assoc. Prof. Audun Oppedal Pedersen for always keeping his door open for questions and discussions that have been very useful. I thank Philip Trætteberg for sharing knowledge, fruitful discussions, and motivation.

Lastly, I want to thank my family and friends, and my biggest thanks to my partner for her patience and support and for taking extra good care of our son in times I have worked a lot.

E.F.

Bergen 2022

Contents

Abstract	i
Acknowledgment	ii
1 Introduction	1
1.1 Background and motivation	1
1.2 Previous work	2
1.2.1 Previous work at UiB	4
1.3 Objectives	5
1.4 Thesis outline	6
2 Theory	8
2.1 Modes in the piezoelectric element	8
2.2 System Model	10
2.3 Fourier transform	11
2.4 Speed of sound in air	12
2.5 Coordinate system	12
2.6 Absorption in air	13
2.7 Electronics	15
2.7.1 Cables	15
2.7.2 Transmitting electronics	16
2.7.3 Receiving electronics	18
2.8 Microphone sensitivity	21
2.9 Finite element modeling	22
3 Experimental setup and measurement method	28
3.1 Equipment list	28
3.2 Electrical measurement setup	29
3.3 Acoustical measurement setup	32
3.3.1 Signal generator (I)	34
3.3.2 Transmitter electronics (II)	35

3.3.3	Transmitter (III)	35
3.3.4	Medium (IV)	36
3.3.5	Receiver (V)	36
3.3.6	Amplifier (VI)	36
3.3.7	Filter (VII)	37
3.3.8	Oscilloscope (VIII)	37
3.3.9	Environmental parameters	38
3.3.10	Cables	38
3.4	Brüel & Kjær 4138 microphone	39
3.4.1	Microphone sensitivity calibration using a pistonphone	41
3.5	Motor's setup	45
3.5.1	Travel distance adjustments of Y-stage	46
3.6	Reflections	48
3.7	Signal setup and processing	52
3.7.1	Transmitted signal	53
3.7.2	Received signal	53
3.7.3	Signal filtering	54
3.7.4	Method for calculating peak-to-peak voltage by using the fast Fourier transform	55
3.7.5	Method of calculating pressure	56
3.7.6	Signal to noise ratio	57
4	Positioning setup and measurements with the MatLab app	59
4.1	MatLab app screen	60
4.2	Startup of the MatLab app	62
4.3	Positioning of the piezoelectric disk	64
4.3.1	Setup 1	66
4.3.2	Setup 2	69
4.3.3	Setup 3	73
4.3.4	Setup 4	74
4.4	Single or series of measurements of electrical and acoustical signals	75
4.5	Transmitter and receiver mounting and positioning sensitivity analysis	76
5	Finite element setup	88
5.1	FEMP 6.1	88
5.2	Material parameters	90
5.2.1	Piezoelectric element, Pz27	91
5.2.2	Air	91

5.3	Simulation parameters	92
5.4	Simulated pressure	93
5.5	Structure setup	94
6	Results and discussion	96
6.1	Electrical properties of the piezoelectric disk	96
6.1.1	Comparison of electrical properties between FE simulations in a vacuum and air	96
6.1.2	Comparison of electrical properties between measurements and FE simulations	98
6.2	Acoustic characteristics of the piezoelectric disk	101
6.2.1	Frequency selection for measurements and FE simulations	101
6.2.2	Acoustic signals examples over three different angles and for all used frequencies	102
6.2.3	Comparison of directivity between FE simulations and measurements	104
6.2.4	SNR of directivity measurements	112
6.2.5	Comparison of directivity at different z distances of FE simulations and measurements	114
6.2.6	Comparison of on-axis pressure between FE simulations and measurements	117
6.2.7	SNR of on-axis pressure measurements	124
6.2.8	Comparison of 2-D sound pressure field between FE simulations and measurements	124
7	Conclusions and further work	130
7.1	Conclusions	130
7.2	Further work	132
	References	134
A	MatLab-scripts	142
A.1	impanal.m	142
A.2	positioninganalyze_directivity.m	143
A.3	MeasParameters.m	145
A.4	HVV_0m1.m	148
A.5	HVV_55m.m	149
A.6	Vpp.m	150
A.7	Receiver_Sensitivity.m	151
A.8	plorthorizontalpressurefield_basic.m	160

A.9	polarPcolor.m	162
A.10	absorption_in_air.m	171
A.11	Admittance_plotting.m	172
B	MatLab-app	174
B.1	App's startup values	174
B.2	Initialize machine function	176
B.3	Homing function	183
B.4	Step function	185
B.5	Position function	187
B.6	Moving function	189
B.7	Instrument connect	191
B.8	Initialize instruments	195
B.9	Measure function	197
B.10	DPO read function	203
B.11	Environmental measurements	204
B.12	Setup functions	205
B.13	Overall functions	211
B.14	Button functions	222
C	FEMP-scripts	253
C.1	read_inn_project.m (vacuum)	253
C.2	read_inn_project.m (fluid)	254
C.3	init_const_project.m	256
C.4	Pz27.inn	257
C.5	material5.dat	259
D	Additional information	261
D.1	Derivation of R	261
D.2	Derivation of j	262
D.3	Derivation of θ_r	263

Chapter 1

Introduction

1.1 Background and motivation

The use of ultrasound in industries, commercial products, and science is numerous. In these areas, ultrasound applications can be topography mapping the sea floor [58][34], detecting cracks in pipes both on and offshore [77][10][74], fiscal flow measuring [33][3], pregnancy check [75], or motion detections [59]. A piezoelectric material is often used in such applications due to the material's ability to transmit or receive ultrasound due to the piezoelectric effect and with given structural dimensions [73]. Therefore, there is a need to understand the behaviors and characteristics of these piezoelectric materials. A good understanding can increase accuracy and reduce uncertainties in measurements. Fiscal flow measurements for exporting and selling gas [3][33][69][43] are one field where accuracy and low uncertainties are crucial. Suppose ultrasonic flow meters are chosen over non-ultrasonic. In that case, it is often due to one or more reasons, such as reasonable purchase price, operation, maintenance, and installation costs, or the equipment is easy to use [45]. Ultrasonic gas meters use several measurement methods such as transit time, doppler, and correlation [30]. The more commonly used method is the transit time. This method measures the time difference of sound propagation between the transmitter and receiver caused by fluid velocity and produces high accuracy measurements [14].

To better understand an ultrasound measurement system, it is necessary to describe a complete system model beyond the transmitter and receiver [72]. A complete system model often consists of a computer, signal generator, transmitter electronics, transmitter transducer, propagation medium, receiver microphone/transducer, receiver electronics, and termination at oscilloscope [72]. Describing this system model as a whole or as individual parts can theoretically improve the understanding of the measurement system considerably. It also opens up to analyze each individual part of the system model and optimize parameters within each individual block, which further leads to improvements in the measurement

system as a whole.

Understanding the piezoelectric element characteristics and behaviors is essential to achieving a good system model. In a transducer construction, piezoelectric elements are the main component to transmit and receive ultrasound. Since piezoelectric elements are often only a part of several components in a larger transducer structure, other components can be used, for example, to improve the impedance matching of the transducer structure to the medium [72]. A transducer construction could be matching layers, backing, piezoelectric material, and housing designed to increase the efficiency of transmitting and receiving ultrasound in a given medium [73]. Before designing a transducer structure, it is essential to have appropriate piezoelectric and material parameters to perform sufficiently good finite element simulation approximations, such as admittance, axis pressure, and directionality, that will largely match measurements.

Simulating piezoelectric elements requires knowledge and control over the parameters of the surrounding mediums, materials, and elements. Several years of research on the parameters of the element used in the present work have provided good approximations of the parameters. These good approximations come from comparing finite element modeling with actual measurements and fine-tuning the parameters. This method is well established within the research community when studying transducer elements.

1.2 Previous work

Knowledge and a good understanding of a transmit-receive ultrasonic measurement system are necessary to predict the measurement system's behaviors and electrical and acoustical characteristics. After years of research on transmitter receiving ultrasonic measurement systems, the developed modeling software FLOSIM was investigated for use in simulations of 1-D ultrasonic transit time systems. These investigations concluded that it would be an effective tool in developing future ultrasonic transit time flowmeters [44]. In later years, software such as FLOSIM (1-D), FEMP (2-D), and COMSOL (3-D) is used extensively to simulate and predict various parts of a transmit-receive ultrasonic measuring system. Examples of works that have used these different software are [71][44][49][22].

Work done by Benny et al. [11] investigates a method to predict and measure the acoustic radiation induced by ultrasonic transducers radiating in the air for frequencies less than 1 MHz. This work used a laser vibrometer to map the surface displacement. This surface displacement is used to predict the 2-D sound field, and the predicted sound field is compared with finite element modeling (FEM) simulations and measured pressure using an ultrasonic detector. These predictions and measurements were compared in the near-field range of ± 20 mm in the radial direction and from 5 to 300 mm in the axial direction relative to the

transducer surface. The results gave good agreement between the theory and experimental obtained results. With this method of predicting the sound field of the transducer, problems arising from standing waves and non-planar waves in near fields are avoided.

Sanabria et al. [62] use a closed reradiation method that combines the Rayleigh-Sommerfeld integral and time-reversal acoustics, which allows for calculating the entire near and far-field based on a single 2-D sound pressure field measurement. This sound pressure field is produced by an air-coupled ultrasound (ACU) probe, where measurements are done in a plane parallel to the probe's surface in the near field, and measurements are performed with a calibrated microphone. This method works for both 3-D (circular, square) and 2-D (rectangular) planar transducers in the frequency range from 50 to 230 kHz, and it is stated that this method outperforms baffled piston models.

The article by Øyerhamn et al. [49] developed a model describing a transit-receiver measurement system based on the transducer's radial mode operating in a homogeneous fluid medium. It uses axisymmetric FEM of two piezoelectric ceramic disks as transmit receiver pair and sound propagation in the medium air. The simulated model is compared with experimental measurements of the transmit-receive voltage-to-voltage transfer function in the frequency range over the two first radial modes of the two disks and at 1 atm. It is also compared simulation with the time domain electrical terminals voltages signals of the transmitting and receiving transducers. Compared to the measurements, this model simulation of the measurement system provides good agreement, but improvements are potentially identified and discussed.

An article by Chillara et al. [22] studies the generation of ultrasonic Bessel beams from radial modes to a piezoelectric disk transducer. Laser Doppler Vibrometry is used to measure the Bessel vibration pattern of the radial mode, which is found to agree well with the numerical simulations. The beam profiles from the four first radial modes of the disc are measured with a hydrophone in a water tank and compared to predicted results obtained from the analytical model, and they are in good agreement. These experimental measurements use similar methods of measuring directivity, on-axis pressure, and 2-D sound pressure field as the measurements conducted in this work.

There are few articles published regarding radial modes and characterization of the piezoelectric disk's radial modes. This leads to the majority of the articles covered in this section being written about complete transducer constructions and other transducers then used in this work. However, several of the measurement methods and models are similar to what has been done in this work.

1.2.1 Previous work at UiB

Over the years, much work has been conducted at the University of Bergen with the acoustical measurement setup, focusing on investigating the behaviors of piezoelectric disks and transducers in transmitting and receiving ultrasound in the air. The primary investigation by the work performed by Storheim [65] is diffraction correction of non-uniformly vibrating sources. These sources are baffled uniform piston, baffled piezoceramic disk, unbaffled piezoceramic disk, and side baffled piezoceramic disc. It is used finite element (FE) to simulate and investigate these sources and then compares them to numerical and analytical expressions and electrical and acoustic measurements. The diffraction correction behavior is defined by the sound pressure generated by the source simulations and compared to the widely used baffled piston diffraction correction. The FE simulation program used to perform the simulations was developed by Kocbach [38] in cooperation between the University of Bergen (UiB) and Christian Michelsen Research AS (CMR) and called Finite Element Modeling of Piezoelectric structures (FEMP).

The work of Mosland and Hauge [48][29] is partially co-written. Mosland's primary focus is developing and implementing a modified three-transducer reciprocity calibration method for use in the surrounding fluid air in a frequency range of 50-300 kHz. This calibration method includes correction due to absorption in air, diffraction effects, and transmitting and receiving electronics. The experiment's final results are compared to simulations and acoustical measurements with a calibrated condenser microphone. The produced transmitting voltage response result by Mosland is given in Fig. 1.1 [48] and is used in this work's discussion of signal-to-noise results. Hauge's primary focus is developing and implementing an FE-based linear system model that describes an air measurement system with arbitrary distances between transmitter and receiver and compares the system model with experiments performed in air.

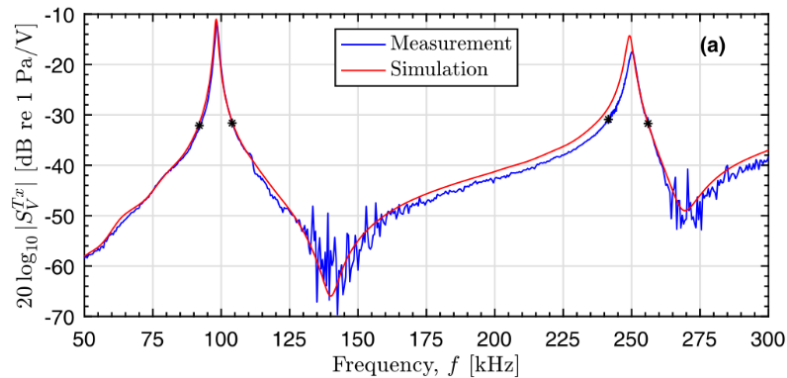


Figure 1.1: Comparison of the measurement and simulation of the transmitting voltage response $|S_V|$ for the transmitting piezoelectric disk Pz27 with $d/t = 10$ and plotted from 50 kHz to 300 kHz. The boundaries between "x" in the resonance peaks is $V_{0pp} = 2$ V and $V_{0pp} = 20$ V elsewhere. The result is taken from [48].

Andersen [7] used the three-transducer reciprocity calibration method to calibrate two piezoelectric disks for air in a frequency range of 50-300 kHz and compared the experiment's final results with FE simulations. Andersen [7] also implemented lasers to conduct high-accuracy separation measurements between the two disks.

The work of Søvik [64] is based upon the work of [48][29], where it is further developed the FE-based linear system model describing a measurement system for gas. This further development includes the slowly varying phase in the air at 1 atm, with room temperature and assumption of no airflow, and then compared to experimental measurements.

Hagen [27] is studying improvements to the work of [7] measurement system to simplify the measurements of the system model's transmission functions at short distances between transmitter and receiver. It is presented a method to reduce crosstalk, and the experimental result performed is compared to FE simulation by using both FEMP and COMSOL.

Work conducted by Grindheim [26] investigates and measures the transfer function of a transmit-receiver system and compares results with FE simulations. It is provided good similarities between calculated and simulated results, but misalignment causes uncertainty in the transfer function $H_{15_{open}}^{VV}$ amplitude, especially around the second radial mode.

The work executed by Finstad [24] measures the electrical characteristics with an impedance analyzer and acoustical characteristics with a condenser microphone in the air with a piezoelectrical disk Pz27 and compares results to FE simulations. The frequency of interest covers the two first radial modes of the disk, where the electrical measurement results show good comparison with FE simulations. For the acoustical measurements of directivity, it shows good similarities compared to FE simulations. However, for the acoustical measurement results of on-axis pressure and transmitter sensitivity, a deviation of around 8 dB is seen.

1.3 Objectives

The main objectives of this work are to experimentally measure the electrical and acoustical characteristics of a circular piezoelectric disk of type Pz27 with a diameter/thickness (d/t) ratio of 10, and measure in the frequency range covering the two first radial modes, then compare the measured results with the FE simulations performed in FEMP. Other primary objectives of this work are to improve and facilitate the positioning of the piezoelectric disk in the measurement setup and to automate and reduce the measuring time of the measurements.

The electrical characteristics measurements are the conductance and susceptance, used to calculate the admittance, and measurements are conducted in the frequency range of 1-300 kHz. The acoustical characteristics measurements are the on-axis pressure, directivity, and 2-D horizontal pressure field in the near and far field of the piezoelectric disk.

These acoustical measurements are performed with several different frequencies covering the disk's first radial mode, and directivity measurements also cover the second radial mode. All measurements are then compared with FE simulations of a modeled piezoelectric disk radiating in air. The FE simulation program used to perform the simulations is called FEMP and was developed by Kocbach [38] in cooperation between UiB and CMR. The current version of FEMP is 6.1.

The method for improving and facilitating the positioning of the piezoelectric disk is firstly done by building a MatLab app that controls all stages in the measurement setup. Secondly, creating a setup guide to find the origo on the piezoelectric disk's front center with the app significantly reduces the setup time. It allows for visual control over the position of the disk via the app by having control of the absolute position of the stages and by knowing the disk's position. The necessity of automating the measurements is due to work done by Finstad [24], which states that acoustical measurements are highly time-consuming, especially for the 2-D pressure field. Integrating communication with all instruments in the experimental setup through the app and controlling the disk's position makes it possible to automate the measurements.

Method for analyzing the measurements includes Fourier transforming the measured signal from time to frequency domain with Matlab's fast Fourier transform (FFT) function. This transformation opens up to extracting the peak-to-peak voltage amplitude of the transmitting frequency. This method of finding the voltage is used when calibrating the microphone sensitivity, where microphone sensitivity allows for converting the measured voltage into pressure. This method for calculating pressure is used when comparing simulated pressure with measurements.

1.4 Thesis outline

Chapter 2 presents the theoretical background and equations used in this work. Chapter 3 presents the instruments used, the experimental setup of electrical and acoustic measurements, and the method for analyzing measurement results. Chapter 4 presents the method of finding the correct position of the piezoelectric disk relative to the microphone and the developed MatLap app. Chapter 5 presents the finite element method to simulate the piezoelectric disk Pz27 vibrating in a vacuum and fully immersed in air. Chapter 6 presents the results obtained with the FE simulations method, the results obtained from the measurements of the electrical characteristics, the results obtained from the measurements of the acoustical characteristics, and a discussion of all results. Chapter 7 gives a conclusion and suggestions for further work.

Chapter 2

Theory

This chapter presents the theoretical background and equations used in this work. Sect. 2.1 goes through modes and resonances in the piezoelectric disk and the resonances central to this work. Sect. 2.2 describes the system model used in the present work. Sect. 2.3 presents the Fourier transformation theory and its use in this work. Sect. 2.4 presents how the speed of sound is calculated and used to estimate signal arrival time and length. Sect. 2.5 goes through the coordinate system used. Sect. 2.6 describes the theory of absorption in air. Sect. 2.7 presents the transfer functions of transmitter and receiver electronics to calculate electrical corrections. Sect. 2.8 represents the theory behind the calculations of microphone sensitivity. Sect. 2.9, the last section in this theory chapter, summarizes the theory behind finite element modeling.

2.1 Modes in the piezoelectric element

The vibration of a piezoelectric element shaped like a disk with electrodes on each end surface can be described as a weighted superposition of eigenmodes, either with an applied voltage or displacement [73]. For large d/t ratios, where d is the diameter of the disk and t is the thickness of the disk, studies show that the piezoelectric disks can oscillate in two kinds of radial modes (R-modes and A-modes) and four types of thickness modes (T-mode, TE-mode, TS-mode, and E-mode) [41][38]. The type of modes of interest in this work is the two first radial extension modes (R-modes), which correspond to standing waves in the radial direction, as illustrated in Fig. 2.1. These modes are the lowest kinds in piezoelectric disks [28], where R1 is the fundamental radial mode, and R2 is the second radial mode. These first two modes occur at 98.1 kHz and 249 kHz for the simulated Pz27, as shown as an example in Fig. 2.2, with a d/t ratio matching the element used in this work, see Table 5.3. The displacement will be at its maximum at these resonance frequencies and is known as the serial resonance f_s [25].

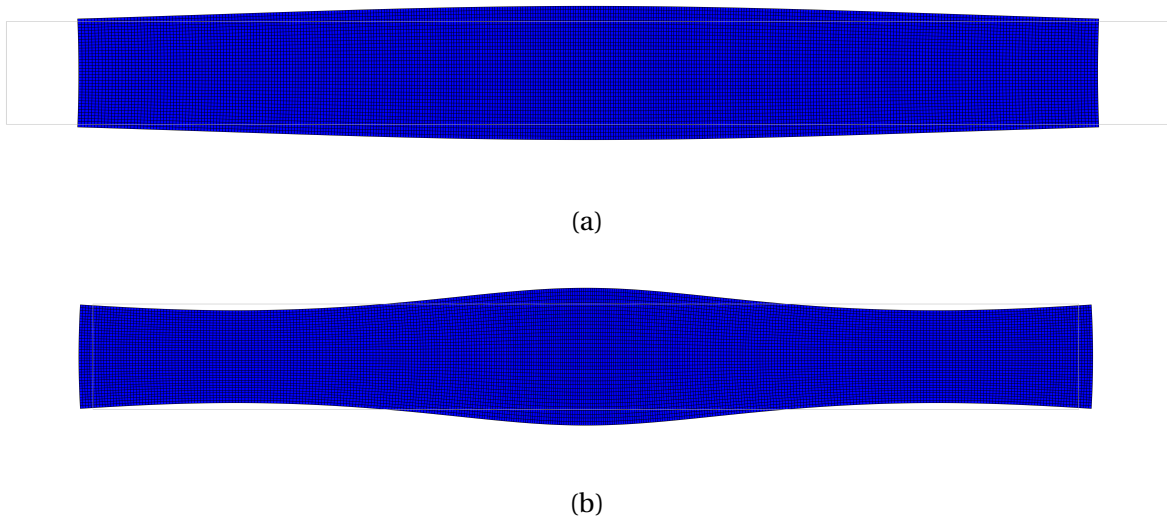


Figure 2.1: Simulated displacement of the piezoelectric disk's Pz27 two first radial extension modes with a d/t ratio ≈ 10 mm **(a)** The fundamental radial mode R1, occurring at 98.1 kHz **(b)** the second radial mode R2, occurring at 249 kHz.

Because of the maximum displacement, the piezoelectric disk transmits a maximal amount of mechanical energy leading to an optimal transmission performance [25]. By performing measurements of the admittance Y and over the frequency span from 1-300 kHz, which covers the two first radial modes of the disk used in this work, the series resonances of the piezoelectric disk occur when conductance G is at its maximum [32]. The expression for the admittance is

$$Y(f) = G(f) + iB(f) = \frac{1}{Z(f)} = \frac{1}{R(f) + iX(f)} \quad (2.1)$$

where B is the susceptance and the unit for admittance is Siemens [S], Z is the impedance, R is the resistance, X is the reactance, and the unit for impedance is ohm [Ω], and f is the frequency.

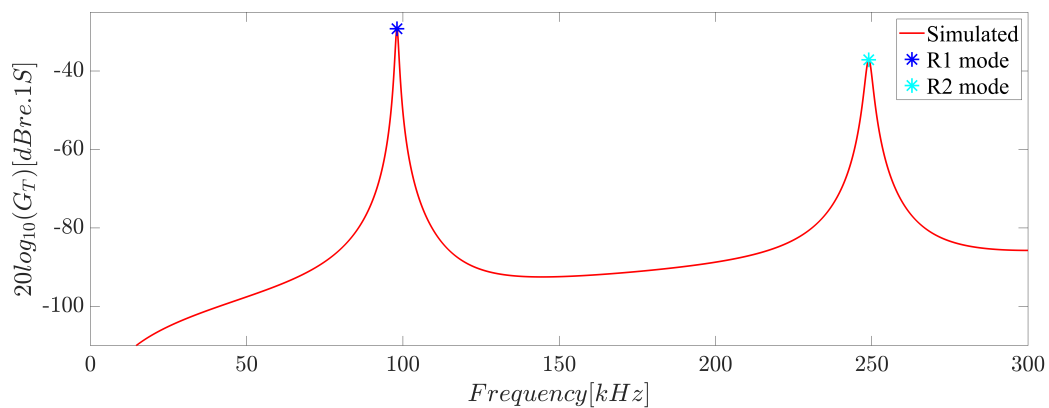


Figure 2.2: Simulated $G_T(f)$ of a piezoelectric disk with matching d/t ratio of disk used in present work and markings of the corresponding R1 and R2 modes of the $\max(G(f)_T)$.

2.2 System Model

The system model is used to describe the electro-acoustic signal propagation chain via an ultrasonic measurement system, all the way from the signal generator to the measuring instrument consisting of an oscilloscope [49]. The system model in this work, shown in Fig. 2.3, consists of modules connected by nodes. These connections between the modules generate inputs and outputs. With the assumption that the system can be described as linear relations, the different nodes can be characterized by transfer functions [72]. An example of such a transfer function is

$$H_{12}^{vV} = \frac{v_2}{V_1}, \quad (2.2)$$

where V_1 is the voltage over the transmitter and v_2 is the particle velocity normal to the transmitter surface. Each node in Fig. 2.3 represents either the input or the output variables for the associated modules [72].

node

- 0** V_0 is the generated output voltage by the signal generator.
- 0m** V_{0m} is the measured voltage at the oscilloscopes channel one or seen as the voltage into the transmitting electronics.
- 1** V_1 is the voltage over the electrodes of the transmitter or seen as the voltage out from transmitting electronics.
- 2** v_2 is the particle velocity normal to the transmitter surface.
- 3** p_3 is the free field, on axis pressure in the medium.
- 4** p_4 is the free field on axis pressure at the front surface of the receiver.
- 5** V_5 is the voltage out from the receiver or seen as the voltage into the receiver electronics.
- 5m** V_{5m} is the measured voltage at the oscilloscopes channel two or seen as the voltage out of the receiver electronics.

A piezoelectric ceramic disk Pz27 is used as the transmitter, and transmitter electronics couples the transmitter to the oscilloscope, which receives a generated signal from the signal generator. The receiver in this work is a pressure-field microphone, which measures the received signal, and induces a voltage. The receiver electronics, consisting of an amplifier and a filter, before being terminated in the oscilloscope.

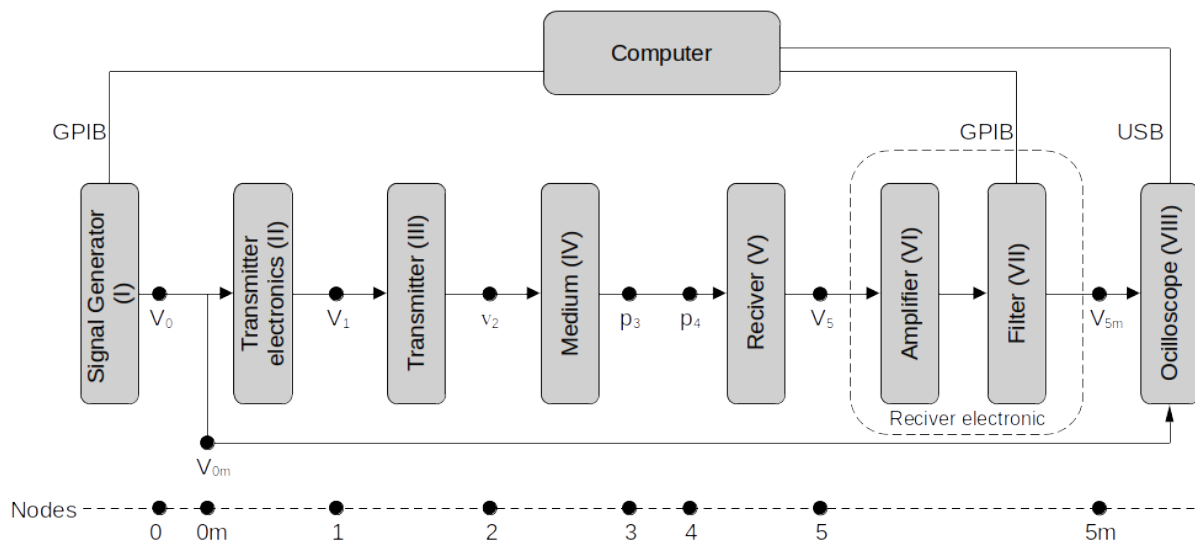


Figure 2.3: Representation of the system model used in this work in the form of a block diagram which is based on [72]

When analyzing the voltages $V_{0m}(t)$ and $V_{5m}(t)$ measured at the oscilloscope, the voltages are Fourier transformed from the time domain to the frequency domain. This transform enables voltage extraction $V(f)$ for its corresponding frequency spectrum and acts as an additional frequency filter.

2.3 Fourier transform

When measuring a signal on an oscilloscope, the amplitude is dependent on the time in the time domain. If the amplitude of interest lies in a specific frequency, such as the transmitting frequency, Fourier transform (FT) is used to extract the information on the amplitude for that given frequency in the frequency domain. This method converts the measured voltage signal from time domain $V(t)$ to frequency domain $V(f)$. There is also a method to reverse this process by taking the inverse Fourier transform (IFT), which takes the signal from the frequency domain $V(f)$ to the time domain $V(t)$. Both these transformations, FT and IFT, can mathematically be expressed [15] as

$$V(f) = FTV(t) = \int_{-\infty}^{\infty} V(t)e^{-i2\pi ft} dt \quad (2.3)$$

$$V(t) = IFTV(f) = \int_{-\infty}^{\infty} V(f)e^{i2\pi ft} df \quad (2.4)$$

In the present work, the FFT algorithm in MatLab is used [68], which is just an efficient and fast computation method of discrete Fourier transform (DFT), and returns both negative and positive frequencies. The negative frequency values correspond to the conjugates

of the positive frequency values. The FFT algorithm also uses zero-padding, which increases the length of the signal time in the form of an array of zero amplitude. This array of zeroes increases the bins in the signal, increasing the frequency resolution of the solved FFT and finding the amplitude more accurately for the transmitted signal or other frequencies present in the signal.

2.4 Speed of sound in air

For a signal with a known frequency and number of cycles, it is of interest in this work to roughly estimate the signal length and the arrival time of the signal at the receiver. This is of interest because it is used to set the correct time window of the oscilloscope for a given distance between the transmitter and receiver, which efficiently discards unnecessary signal information. Since only a rough estimation is needed, the sound speed in the air c_{air} used to calculate the signal length and arrival time does not need to be as accurate. Assuming the fluid is an adiabatic process, and the gas preserves the ideal gas laws, this will give a speed of sound that only depends on temperature as [36]

$$c_{air} = \sqrt{\frac{\gamma RT}{M}}. \quad (2.5)$$

Here the γ is the adiabatic constant, R is the gas constant, T is the absolute temperature, and M is the molar mass of air. Calculating the speed of sound for the temperature T_K in kelvin equal to 273.15 K will give a constant equal to approximately 331 meters per second. Then, by measuring the temperature in kelvin, the sound speed becomes

$$c_{air} \approx 331 \sqrt{\frac{T}{T_K}}, \quad (2.6)$$

which is the method used to roughly calculate the sound speed in the air in this work.

2.5 Coordinate system

Two coordinate systems are used in this work. The coordinate system X, Y, and the Z-axes correspond to the surface of the piezoelectric disk, see Fig. 2.4, and the coordinates of the X, Y, and Z-stages which is defined by the travel direction of the different positioning motor's in the experimental setup. X, Y, and Z-stages coordinates are found with induction sensors where the stages reference points are defined, see Table 4.1. There are two categories of coordinate systems based on the reference points: the machine coordinate system, defined by the reference points and travel limits of the positioning motor's; the user coordinate system,

defined by an offset from the reference point. Ideally, the user coordinate system should overlap the coordinate system of the piezoelectric disk, such that when the X, Y, and Z-stages move, they are ideally moved in the coordinate system of the X, Y, and Z axis in Fig. 2.4. A rotating stage, R-stage, is also used in this work, where the axis out of the R-stage should ideally be parallel and overlap the Y-axis. It is studied in Sect. 4.5 what happens if the user coordinates do not overlap the coordinate system of the piezoelectric disk and what uncertainty this entails.

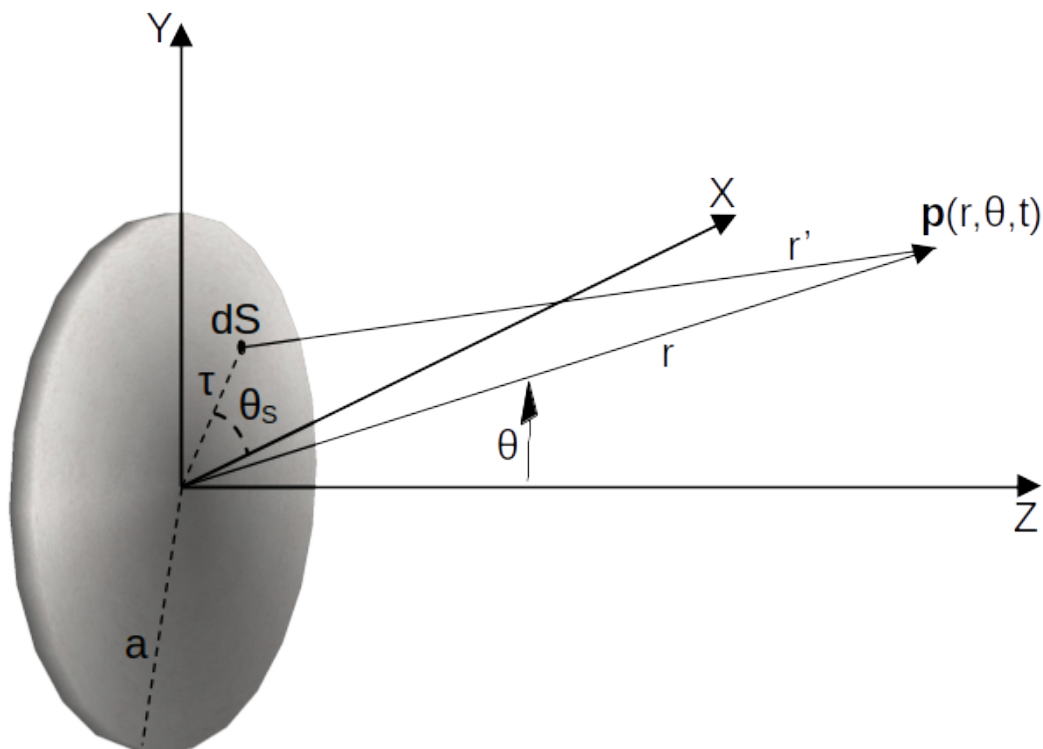


Figure 2.4: Illustration of the front surface of the piezoelectric disk with a radius a and the corresponding X, Y, and Z-axis with the origo in the disk's center, an angle θ to, and arbitrary pressure point $p(r, \theta, t)$ and with a θ_s representing the symmetrical angle around Z-axis.

2.6 Absorption in air

When using FEMP to simulate the pressure, it considers a lossless fluid. But in reality, when measuring sound pressure that has propagated through a fluid, there are different mechanisms in the fluid that absorb the sound pressure depending on the propagation distance z . To compare the experimentally measured pressure with FE simulated pressure in this work, then absorption must be known. This leads to the equation for the measured free field pressure [72]

$$p_A = p_i e^{-\alpha_{Np/m} z}, \quad (2.7)$$

where p_i is the initial free field pressure without losses and α is the absorption coefficient given in Neper per meter. Generally, the absorption coefficient is favorable to describe in dB per meter, which leads to the absorption coefficient [72]

$$\alpha_{Np/m} = \frac{\alpha_{dB/m}}{20 \log_{10}(e)} \approx 0.1151 \alpha_{dB/m}. \quad (2.8)$$

This atmospheric absorption coefficient combines several different attenuations, such as shear viscosity, thermal conductivity, molecular relaxation, and thermal diffusion [5]. This combination of attenuation sums up as [72]

$$\alpha_{Np/m} = \alpha_{cl} + \alpha_{rot} + \alpha_{vib,O} + \alpha_{vib,N}, \quad (2.9)$$

where α_{cl} stands for the classical absorption coefficient, α_{rot} stands for rotational relaxation, and $\alpha_{vib,O}$ and $\alpha_{vib,N}$ are the molecular vibrational relaxation absorption coefficient of oxygen and nitrogen in the air. The cause of α_{cl} is shear viscosity, heat conduction, and thermal diffusion [5]. In terms of dB per meter, the combined absorption coefficient becomes [5]

$$\alpha_{dB/m} = 8.686 f^2 \left(\left[1.84 \cdot 10^{-11} \left(\frac{p_r}{p_a} \right) \left(\frac{T}{T_r} \right)^{1/2} \right] + \left(\frac{T_r}{T} \right)^{5/2} \right. \\ \left. \left[0.01275 e^{-\frac{2239.1}{T}} \frac{f_{rO}}{f_{rO}^2 + f^2} + 0.1068 e^{-\frac{3352.0}{T}} \frac{f_{rN}}{f_{rN}^2 + f^2} \right] \right), \quad (2.10)$$

where the relaxation frequency of oxygen is [5]

$$f_{rO} = \frac{p_a}{p_r} \left(24 + \frac{(4.04 \cdot 10^4 h)(0.02 + h)}{0.391 + h} \right), \quad (2.11)$$

and the relaxation frequency of nitrogen is [5]

$$f_{rN} = \frac{p_a}{p_r} \left(\frac{T_r}{T} \right)^{1/2} \left(9 + 280 h \cdot e^{-4.170 \left(\left(\frac{T_r}{T} \right)^{1/3} - 1 \right)} \right). \quad (2.12)$$

Here is p_a , the measured pressure in kPa, and p_r the reference pressure, 101.325 kPa—further, T is the measured air temperature, and T_r the reference temperature, 293.15 K. Furthermore, h is the percent molar concentration of water vapor, and f is the frequency used [5]. In the given molar concentration of water vapor [5]

$$h = h_{rel} \left(\frac{p_{sat}}{p_r} \right) \left(\frac{p_r}{p_a} \right), \quad (2.13)$$

there is a need to know the relative humidity h_{rel} and saturated pressure p_{sat} . Measurements could provide the relative humidity and give the necessary temperature T value to calculate

[5]

$$\begin{aligned}
V = & 10.79586 \left(1 - \frac{T_{01}}{T} \right) - 5.02808 \log_{10} \left(\frac{T}{T_{01}} \right) + 1.50474 \cdot 10^{-4} \left(1 - 10^{-8.29692 \left(\frac{T}{T_{01}} - 1 \right)} \right) \\
& + 0.42873 \cdot 10^{-3} \left(10^{4.76955 \left(1 - \frac{T_{01}}{T} \right)} - 1 \right) - 2.2195983,
\end{aligned} \tag{2.14}$$

used to calculate the saturated pressure [5]

$$p_{sat} = p_r 10^V. \tag{2.15}$$

T_{01} is the isothermal triple point temperature for water, 273.16 K.

The calculated absorption coefficient α in dB per meter and the measured pressure open up to calculating the initial pressure using Eq. 2.7 and 2.8, giving

$$p_i = \frac{p_4}{e^{-0.1151 \alpha_{dB/m} \cdot z}}. \tag{2.16}$$

Using this Eq. 2.16, one can compare p_i calculated from the measured pressure p_4 with the simulated pressure after the simulated pressure has been adjusted for the differences in the voltage across the piezoelectric disk and simulated voltage, see Sect. 5.4. It is worth noting that this absorption coefficient used in this work does not consider factors such as refraction, scattering by turbulence, and non-linear propagation effects [5], which are assumed to be negligible.

2.7 Electronics

Cables connect instruments to the piezoelectric disk and the microphone together within the transmitting or receiving electronics. In these systems, the ideal voltages across the piezoelectric disk V_1 and the microphone output V_5 can not be measured directly. This is due to the finite impedance of the measurement system as a whole, which affects the voltage signal flowing through the system. Therefore it is deduced transfer functions that transfer the input voltages of the transmitted voltage V_{0m} and received voltage V_{5m} to ideal voltage V_1 and V_5 .

2.7.1 Cables

A well-known phenomenon is that signals flowing through cables are affected by the characteristics of the cable. This phenomenon is experimentally proven and, therefore, essential to consider when calculating the voltage V_1 and V_5 , which lead to seeing the cable as an ideal uniform transmission line using distributed constants [61]. The coaxial cables terminated

in a load impedance Z_L can then be described as an equivalent circuit [73], as shown in Fig. 2.5.

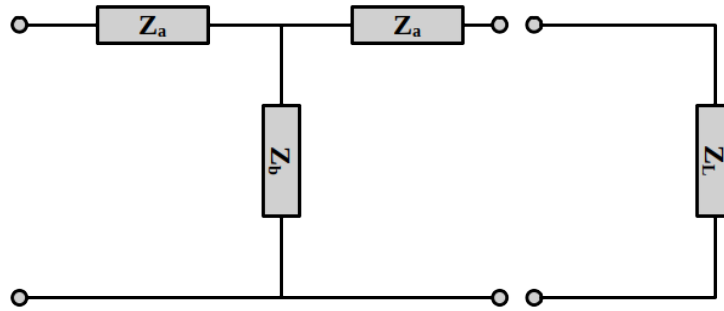


Figure 2.5: Equivalent circuit of a ideal lossless transmission line with coaxial cable terminated in a load impedance Z_L , where distributed constants are Z_a and Z_b .

The distributed constants used in describing the coaxial cable could be defined as two different impedances Z_a and Z_b , as seen in Fig. 2.5. These impedances are determined by the characteristic impedance of the cable Z_0 , the electromagnetic wave number k_{em} , and the cable length x in meters and given as [73]

$$Z_a = i Z_0 \tan\left(\frac{k_{em}x}{2}\right) \quad (2.17)$$

and

$$Z_b = \frac{Z_0}{i \sin(k_{em}x)}. \quad (2.18)$$

The characteristic impedance and the electromagnetic wave number is [73]

$$Z_0 = \sqrt{\frac{L_x}{C_x}} \quad (2.19)$$

and

$$k_{em} = \omega \sqrt{L_x C_x}, \quad (2.20)$$

respectively, where L_x and C_x are the inductance and capacitance per meter, respectively, and ω is the angular frequency.

2.7.2 Transmitting electronics

In this work, transmitting electronics links the signal generator to the oscilloscope and the piezoelectric disk with coaxial cables. This part of the system model, seen in Fig. 2.3, can be described with a circuit diagram, as shown in Fig. 2.6. In this diagram, the voltage over the piezoelectric disk is V_1 , and the voltage measured with the oscilloscope is V_{0m} . A transfer

function can describe this relationship between these two voltages as

$$H_{0m1}^{VV} = \frac{V_1}{V_{0m}}. \quad (2.21)$$

From the circuit diagram, the voltage V describes the Thevenin equivalent voltage of the signal generator, and Z_{GEN} is the Thevenin equivalent impedance. The Z_{OSC} is the oscilloscope's termination impedance, Z_T is the piezoelectric disk's impedance, and Z_a and Z_b are the coaxial cable impedances. The impedance of the piezoelectric disk is measured with an impedance analyzer.

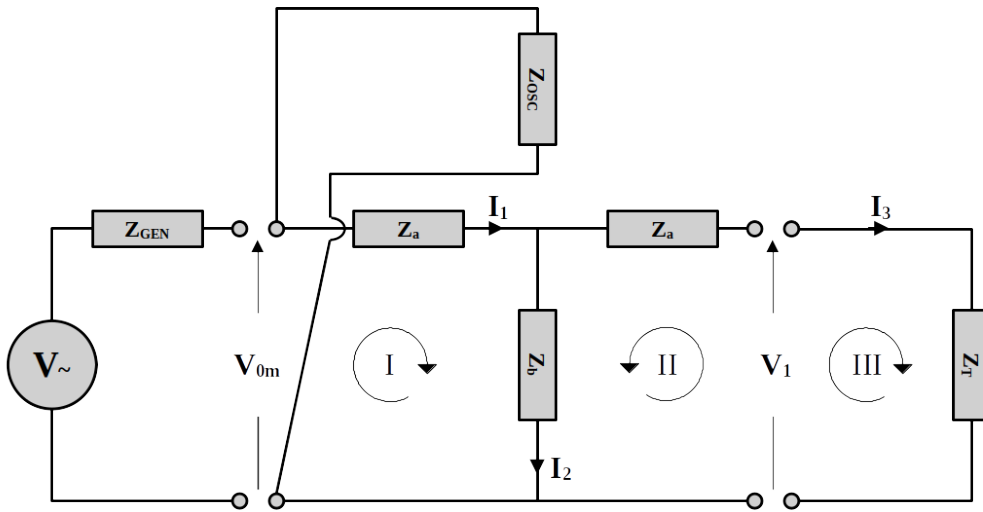


Figure 2.6: Circuit diagram of the transmitting electronics, connecting to a signal generator as a Thevenin equivalent circuit, the piezoelectric disk, and the oscilloscope.

Applying Kirchhoff's voltage law in the three directions indicated by arrows in Fig. 2.6, three voltage equations can be deduced,

$$V_{0m} = Z_a I_1 + Z_b I_2 \quad (2.22)$$

$$V_1 = Z_b I_2 - Z_a I_3 \quad (2.23)$$

$$V_1 = Z_T I_3 \quad (2.24)$$

and with Kirchhoff's current law, the relation between the three currents I_1 , I_2 , and I_3 shown in Fig. 2.6 is

$$I_1 = I_2 + I_3. \quad (2.25)$$

By setting Eqs. 2.23 and 2.24 equal to another and solving for the current I_3 ,

$$I_3 = \frac{Z_b I_2}{Z_T + Z_a}, \quad (2.26)$$

and using substitution and algebraic manipulation of Eqs. (2.22,2.24-2.26), then the transfer function in Eq. 2.21 is easily derived and gives

$$H_{0m1}^{VV} = \frac{Z_T Z_b}{Z_T(Z_a + Z_b) + (Z_a + Z_b)^2 - Z_b^2}, \quad (2.27)$$

which is a transfer function given in only known impedances and, therefore, used to solve the voltage V_5 with measured voltage V_{0m} .

2.7.3 Receiving electronics

In this work, receiver electronics link the amplifier and filter to the oscilloscope and the microphone with coaxial and microphone cables, respectively, as seen in Fig. 2.3. Describing the voltage signal that flows in via input on the filter or amplifier and out via output can quickly become unnecessarily complicated. This becomes complicated due to the electronics inside the filter or amplifier, which are unknown. Therefore, the electronics are described as a complex frequency-dependent factor $F(f)$ to simplify this part, which is given as the black dotted lines, illustrating unknown electronics in Fig. 2.7, separating the input and the output. In this circuit description of the filter (or amplifier), the input is seen as an open input with a voltage $V_{5'open}$ and an impedance Z_{filt_open} . The output is seen as a Thevenin equivalent voltage generator $V_{5'}$ with a Thevenin equivalent impedance Z_{filt_out} which is the output impedance given by the manufacturer. The relation between the input and output of the filter becomes

$$V_{5'} = V_{5'open} F(f) \quad (2.28)$$

and applies to the amplifier and all filters in this work.

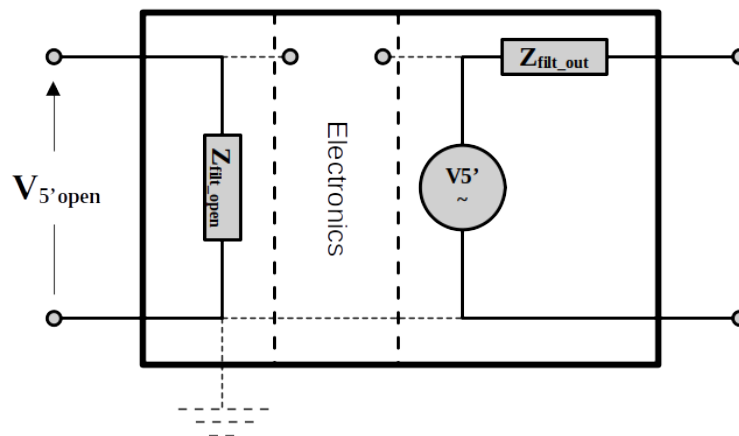


Figure 2.7: Illustration of input and output of the filter separated by unknown electronics. This illustration applies to the amplifier and all filters in this work.

With the theory of voltage flow from input to the output of the amplifier and the filters covered, it is necessary to describe what happens between the instruments. In this work, the microphone cable is neglected, and only the coaxial cables are considered. This leads to three circuit diagrams, shown in Fig. 2.8. These three circuit diagram transfer functions are almost identical to derive as for the transmitter electronics. The only difference between the transmitter and receiver electronics is that with the receiver electronics, one of Kirchoff's voltage law directions indicated changes, and the values of the receiver electronics are changed.

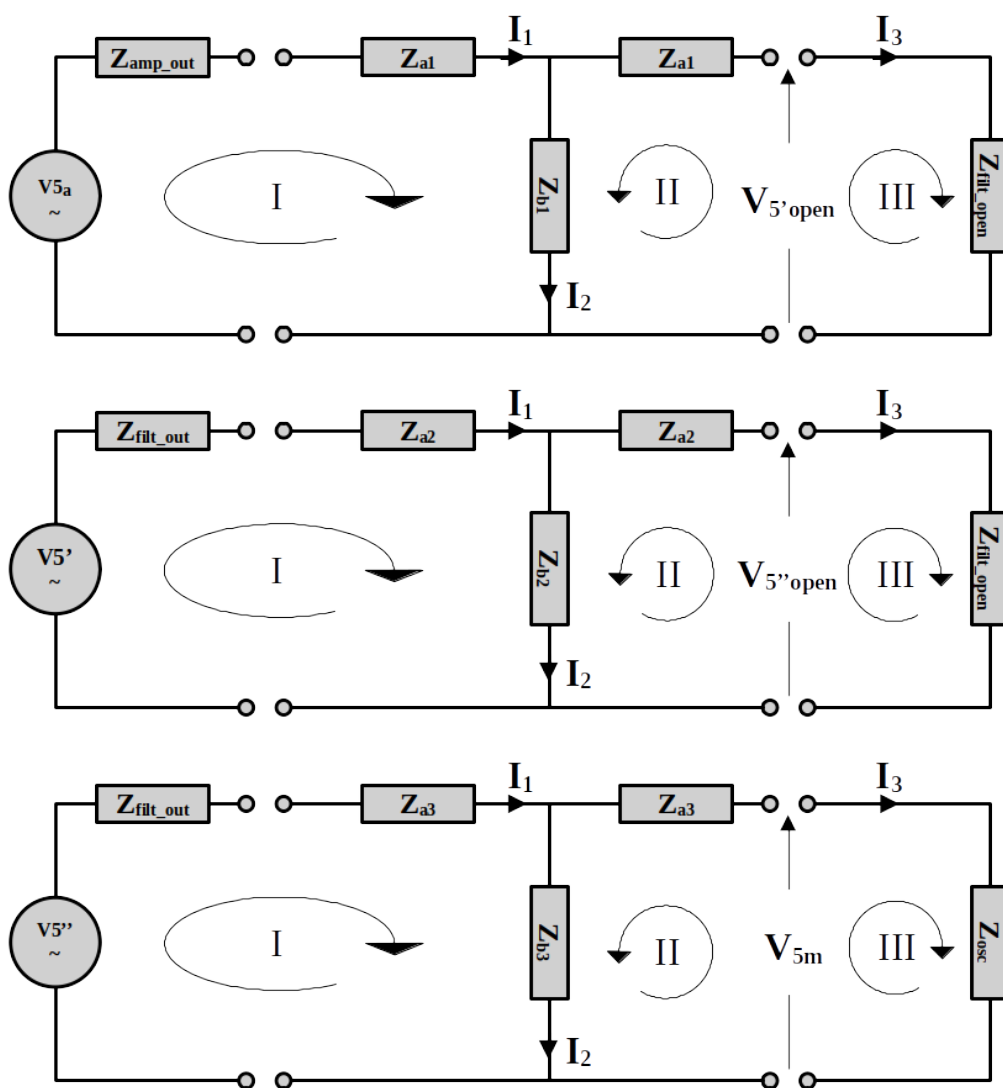


Figure 2.8: Three circuit diagrams: Top circuit diagram is the Thevenin equivalent generated output voltage from the amplifier connected to the filter's open input channel one via coaxial cable; the middle circuit diagram is the Thevenin equivalent generated output voltage from the filter's output channel one connected to the filter's open input channel two via coaxial cable; the bottom circuit diagram is the Thevenin equivalent generated output voltage from the filter's output channel two connected to the oscilloscope's channel two via coaxial cable.

The transfer function describing the relation of the output voltage of the microphone V_5 and the input voltage in channel two of the oscilloscope V_{5m} is given as

$$H_{55m}^{VV} = H_{55a}^{VV} \cdot H_{5a5'_{open}}^{VV} \cdot H_{5'_{open}5'}^{VV} \cdot H_{5'5''_{open}}^{VV} \cdot H_{5''_{open}5''}^{VV} \cdot H_{5''5m}^{VV} = \frac{V_{5m}}{V_5}. \quad (2.29)$$

This transfer function is a combination of multiple transfer functions: the relation of the voltage V_5 and the output voltage of the amplifier V_{5a} as H_{55a}^{VV} ; the relation of the voltage V_{5a} and the input voltage of the filters channel one $V_{5'_{open}}$ as $H_{5a5'_{open}}^{VV}$; the relation of the voltage $V_{5'_{open}}$ and the output voltage of the filters channel one $V_{5'}$ as $H_{5'_{open}5'}^{VV}$; the relation of the voltage $V_{5'}$ and the input voltage of the filters channel two $V_{5''_{open}}$ as $H_{5'5''_{open}}^{VV}$; the relation of the $V_{5''_{open}}$ and the output voltage of the filters channel two $V_{5''}$ as $H_{5''_{open}5''}^{VV}$; the relation of the voltage $V_{5''}$ and the V_{5m} as $H_{5''5m}^{VV}$.

The complex frequency-dependent factor given in Eq. 2.28 equals the transfer functions over the amplifier and the filters. The factor is given as a dB gain over the amplifier. The factor is assumed lossless and equal to one over the filters. These three transfer functions become

$$H_{55a}^{VV} = 10^{\frac{Gain}{20}}, \quad (2.30)$$

$$H_{5'_{open}5'}^{VV} = 1, \quad (2.31)$$

and

$$H_{5''_{open}5''}^{VV} = 1. \quad (2.32)$$

Using substitution and algebraic manipulation of the equation that is possible to derive from each circuit in Fig. 2.8, the transfer function from the output voltage of the amplifier to the input voltage of the filter's channel one becomes

$$H_{5a5'_{open}}^{VV} = \frac{Z_{filt,open}}{\left[(Z_{amp,out+Za_1}) \left(1 + \frac{Z_{filt,open+Za_1}}{Z_{b_1}} \right) \right] + Z_{filt,open+Za_1}}, \quad (2.33)$$

the transfer function from the output voltage of the filter's channel one to the input voltage of the filter's channel two becomes

$$H_{5'5''_{open}}^{VV} = \frac{Z_{filt,open}}{\left[(Z_{filt,out+Za_2}) \left(1 + \frac{Z_{filt,open+Za_2}}{Z_{b_2}} \right) \right] + Z_{filt,open+Za_2}}, \quad (2.34)$$

and the transfer function from the output voltage of the filter's channel two to the input voltage of the oscilloscope channel two becomes

$$H_{5''5m}^{VV} = \frac{Z_{osc}}{\left[(Z_{filt,out+Za_3}) \left(1 + \frac{Z_{osc+Za_3}}{Z_{b_3}} \right) \right] + Z_{osc+Za_3}}. \quad (2.35)$$

2.8 Microphone sensitivity

Calibration of the Brüel & Kjær 4138 microphone [17] is performed with a Brüel & Kjær 4228 pistonphone [16], which operates at a known frequency of 250 Hz and produces a known sound pressure level, SPL [20]. The frequency response of the Brüel & Kjær 4138 microphones is given relative to the microphone reference sensitivity $|M_{ref}(250Hz)|$ when it is electrically unloaded [19]. It is possible to use the specified microphone sensitivity shown in the calibration papers, but it is recommended to calibrate the microphone by measuring and calculating microphone sensitivity using the pistonphone. This is due to changes in conditions such as air pressure, temperature, and any other conditions that may affect the sensitivity. Other conditions are not known, but aging effects or the receiver electronics may have additional effects that give a reason to calibrate. To calculate, in general, the free-field open circuit microphone sensitivity it is used the definition [73]

$$M_V(f) = \frac{V_5(f)}{p_4(f)} = |M_V(f)|e^{i\phi_{M_V}}, \quad (2.36)$$

where V_5 is the measured voltage at the electrically unloaded receiver, p_4 is the free field pressure at the microphone position when the microphone is not present, $|M_V(f)|$ is the magnitude of the free-field open circuit microphone sensitivity, and ϕ_{M_V} is the phase difference [73]. Since the open circuit pressure response relative to $|M_{ref}(250Hz)|$ for Brüel & Kjær 4138 microphone [19] does not specify the phase difference, it is disregarded, and only the microphone sensitivity is taken into account. The microphone sensitivity is then defined as [73]

$$|M_V(f)| = \frac{V_{eff}(f)}{p_{eff}(f)}, \quad (2.37)$$

where V_{eff} is the effective voltage amplitude calculated from the measured voltage V_{5m} as

$$V_{eff}(f) = \frac{V_{5pp}(f)}{2\sqrt{2}} = \frac{1}{2\sqrt{2}} \frac{V_{5mpp}(f)}{H_{55m}^{VV}(f)}, \quad (2.38)$$

and the pressure p_{eff} is the effective pressure amplitude and can be calculated from the sound pressure level defined as

$$SPL = 20 \log_{10} \left(\frac{p_{eff}(f)}{p_{ref}} \right). \quad (2.39)$$

where p_{ref} is the reference pressure for air which is 20 μPa , and SPL in this work is the known sound pressure level produced by the pistonphone at 250 Hz.

2.9 Finite element modeling

This work uses Finite Element Modeling of Piezoelectric structures (FEMP) software to simulate the electrical characteristic of $Y_T(f)$ (admittance in a vacuum and air) and acoustic characteristics of, $D(r, \theta, f)$ (directivity), $p_{ax}(z, f)$ (on-axis pressure), and $p(x, z, f)$ (2-D sound pressure field) of a piezoelectric disk. This section presents only a brief overview of the theory behind FEMP, where [38] provides a full description. In FEMP, the FE simulation is simplified by reducing the structure from being a 3-D structure to 2-D by assuming symmetry in the axisymmetric disk [38]. This assumption implies [38]

$$\frac{\partial}{\partial \theta_S} = 0 ,$$

where θ_S is the angle around the Z-axis in Fig. 2.4, and it further assumes no torsion modes [38]

$$u_{\theta_S} = 0 ,$$

where u_{θ_S} is displacement in the angle θ_S direction. Other benefits these assumptions provide are the reduction of the number of piezoelectric constants for the dielectric stiffness $[\epsilon^S]$, piezoelectric stiffness $[e]$, and elastic stiffness $[c^E]$ matrices used in FE calculations, which decreases computation time [38].

In the FE simulations, a structure is approximated using a finite number of volume elements [38]. Within each volume element, it is defined a number of nodes, see Fig 5.1. With an increasing number of volume elements, the accuracy of the simulation increases. Other factors that define the precision of the simulation are the number of nodes, and the interpolations function used to solve for quantitative values in an arbitrary position inside the structure's elements [38]. The starting equations to find the FE formulation for an unloaded piezoelectric disc with no surrounding fluids are as follows [32]

$$-\omega^2 \rho_p u_i = T_{ij,i} , \quad (2.40)$$

$$D_{i,i} = 0 , \quad (2.41)$$

$$T_{ij} = c_{ijkl}^E S_{kl} - e_{kij} E_k , \quad (2.42)$$

and

$$D_i = e_{ikl} S_{kl} + \epsilon_{ik}^S E_k , \quad (2.43)$$

where $T_{ij,i}$ is the motion for a piezoelectric medium, $D_{i,i}$ is the Maxwell equation, T_{ij} and D_i is the constitutive relations for the piezoelectric medium [38], and the rest of the variable's descriptions are given in Table 2.2.

Table 2.2: Description of variables used in Eqs.(2.42) and (2.43) [38].

Variable	Description [38]	Unit
T_{ij}	Mechanical stress tensor	$[N/m^2]$
S_{kl}	Mechanical strain tensor	$[-]$
D_i	Electric flux density	$[C/m^2]$
E_k	Electric field vector	$[V/m]$
c_{ijkl}^E	Elastic stiffness constant tensor with constant electric field	$[N/m^2]$
e_{ikl}	Piezoelectric constant tensor	$[C/m^2]$
ϵ_{ik}^S	Dielectric constant tensor with constant strain	$[F/m]$
ω	Angular frequency	$[rad/s]$
ρ_p	Piezoelectric medium density	$[kg/m^3]$
u	Displacement	$[m]$

The piezoelectric structure's surface, facing a vacuum, is imposed with boundary conditions [38]. With boundary conditions introduced, the Eqs. 2.40-2.43 is used when setting up weak formulations using test functions and solving each part of the weak formulation equations using Gauss Legendre quadrature [38]. With each part solved using Gauss, the final FE formulation for the unloaded case is given as [38]

$$-\omega^2 \begin{bmatrix} M_{uu} & 0 \\ 0 & 0 \end{bmatrix} \begin{Bmatrix} \hat{u} \\ \hat{\phi} \end{Bmatrix} + \begin{bmatrix} K_{uu} & K_{u\phi} \\ K_{\phi u} & K_{\phi\phi} \end{bmatrix} \begin{Bmatrix} \hat{u} \\ \hat{\phi} \end{Bmatrix} = \begin{Bmatrix} F \\ -Q \end{Bmatrix}, \quad (2.44)$$

and the variables of this Eq. 2.44 are given in Table 2.3. The FE formulation, Eq. 2.44 are transformed to H-form to simplify the calculation of the piezoelectric structure's resonance frequencies and response function [38]. With the potentials in the nodes of the elements condensed out from FE equations and V and I are introduced as voltage and current [39], Eq. 2.44 becomes [38]

$$-\omega^2 \begin{bmatrix} M_{uu} & 0 \\ 0 & 0 \end{bmatrix} \begin{Bmatrix} \hat{u} \\ V \end{Bmatrix} + \begin{bmatrix} H_{uu} & H_{u\phi} \\ H_{\phi u} & H_{\phi\phi} \end{bmatrix} \begin{Bmatrix} \hat{u} \\ V \end{Bmatrix} = \begin{Bmatrix} F \\ -I/i\omega \end{Bmatrix}. \quad (2.45)$$

Solving the piezoelectric disk with the direct harmonic analysis method in a vacuum where there is no outer traction ($F = 0$) [38], the first expression in Eq. (2.45), is used to calculate the particle displacement of a piezoelectric structure as [38]

$$\{\hat{u}\} = -[D]^{-1} \{H_{u\phi}\} V, \quad (2.46)$$

where Figs. 2.1a and 2.1b are examples of solved piezoelectric structure displacement $\{\hat{u}\}$,

and the matrix $[D]$ is just a simplified notation and is given as [38]

$$[D] = [H_{uu}] - \omega^2 [M_{uu}]. \quad (2.47)$$

By inserting the global displacement vector into the second expression in Eq. 2.45, and if the admittance Y is defined by the current I divided by the voltage V , the admittance of the piezoelectric structure is given as [38]

$$Y(\omega) = \frac{I}{V} = i\omega \left(\{H_{u\phi}\}^T [D]^{-1} \{H_{u\phi}\} - H_{\phi\phi} \right). \quad (2.48)$$

In the case of the piezoelectric structure is in a vacuum, the only volume studied is Ω_p , which is the volume of the piezoelectric structure, see Figs. 5.2/5.3. Reviewing the disc submerged into an inviscid and irrotational fluid, a new region, Ω_f , occurs which is the fluid volume [38], see Figs. 5.2/5.4. In the time-harmonic case, the relationship between the acoustic pressure p and the velocity potential ψ in the fluid is [38]

$$p = i\omega\rho_f\psi. \quad (2.49)$$

where ρ_f is the density of the fluid. The Helmholtz equation governing the fluid velocity potential ψ [36] is given as

$$\psi_{,ii} = -k^2\psi, \quad (2.50)$$

where k is the wave number, which is $k = \omega/c_f$, where c_f is the sound speed in the fluid. The piezoelectric structure's surface, facing a fluid, is imposed with new boundary conditions [38]. With boundary conditions introduced, the FE-formulations Eqs 2.40-2.43 and 2.50 is used when setting up weak formulations using test functions and solving each part of the weak formulation equations using Gauss Legendre quadrature [38]. With each part solved using Gauss, the final FE formulation for the fluid loading is written as [38]

$$-\omega^2 \begin{bmatrix} M_{uu} & 0 & 0 \\ 0 & 0 & 0 \\ 0 & 0 & -M_{\psi\psi} \end{bmatrix} \begin{Bmatrix} \hat{u} \\ \hat{\phi} \\ \hat{\psi} \end{Bmatrix} + i\omega \begin{bmatrix} 0 & 0 & C_{u\phi} \\ 0 & 0 & 0 \\ C_{\psi u} & 0 & 0 \end{bmatrix} \begin{Bmatrix} \hat{u} \\ \hat{\phi} \\ \hat{\psi} \end{Bmatrix} + \begin{bmatrix} K_{uu} & K_{u\phi} & 0 \\ K_{\phi u} & K_{\phi\phi} & 0 \\ 0 & 0 & -K_{\psi\psi} \end{bmatrix} \begin{Bmatrix} \hat{u} \\ \hat{\phi} \\ \hat{\psi} \end{Bmatrix} = \begin{Bmatrix} 0 \\ -Q \\ 0 \end{Bmatrix}, \quad (2.51)$$

and the variables of this Eq. 2.51 are given in Table 2.3.

Table 2.3: Description of variables and matrices used in Eq.2.44 and 2.51 [38].

Variable	Description [38]
$[M_{uu}]$	Global mass matrix
$[M_{\psi\psi}]$	Global fluid mass matrix
$[C_{u\psi}]$	Global fluid/structure coupling matrix
$[C_{\psi u}]$	Global fluid/structure coupling matrix
$[K_{uu}]$	Global stiffness matrix
$[K_{u\phi}]$	Global piezoelectric stiffness matrix
$[K_{\phi u}]$	Global piezoelectric stiffness matrix
$[K_{\phi\phi}]$	Global dielectric stiffness matrix
$[K_{\psi\psi}]$	Global fluid stiffness matrix
$\{F\}$	Global force vector
$\{Q\}$	Global charge vector
$\{\hat{u}\}$	Global displacement vector
$\hat{\phi}$	Global electric potential
$\hat{\psi}$	Global fluid velocity potential
V	Voltage
I	Current

The FE formulation, Eq. 2.51 are transformed to H-form and given as [38]

$$-\omega^2 \begin{bmatrix} M_{uu} & 0 & 0 \\ 0 & 0 & 0 \\ 0 & 0 & -M_{\psi\psi} \end{bmatrix} \begin{Bmatrix} \hat{u} \\ V \\ \hat{\psi} \end{Bmatrix} + i\omega \begin{bmatrix} 0 & 0 & C_{u\phi} \\ 0 & 0 & 0 \\ C_{\psi u} & 0 & 0 \end{bmatrix} \begin{Bmatrix} \hat{u} \\ V \\ \hat{\psi} \end{Bmatrix} + \begin{bmatrix} H_{uu} & H_{u\phi} & 0 \\ H_{\phi u} & H_{\phi\phi} & 0 \\ 0 & 0 & -K_{\psi\psi} \end{bmatrix} \begin{Bmatrix} \hat{u} \\ V \\ \hat{\psi} \end{Bmatrix} = \begin{Bmatrix} 0 \\ -I/i\omega \\ 0 \end{Bmatrix}. \quad (2.52)$$

From Equation (2.52), the global fluid velocity potential and global displacement vector can be written as [38]

$$\{\hat{\psi}\} = -i\omega (\omega^2 [M_{\psi\psi}] - [K_{\psi\psi}])^{-1} [C_{\psi u}] \{\hat{u}\}, \quad (2.53)$$

and

$$\{\hat{u}\} = -[E]^{-1} \{H_{u\phi}\} V, \quad (2.54)$$

respectively, where the matrix $[E]$ is just a simplified notation and is given as [38]

$$[E] = \left\{ [H_{uu}] - \omega^2 [M_{uu}] + \omega^2 [C_{u\psi}] (-[K_{\psi\psi}] + \omega^2 [H_{\psi\psi}])^{-1} [C_{\psi u}] \right\}, \quad (2.55)$$

The admittance is obtained by inserting the global displacement into the second expression

in Eq. 2.52 and written as [38]

$$Y(\omega) = \frac{I}{V} = i\omega \{ [H_{u\phi}]^T [G]^{-1} [H_{u\phi}] - [H_{\phi\phi}] \}. \quad (2.56)$$

The global fluid velocity potential is inserted into Eq. (2.49) for the acoustic pressure and then expressed as [38]

$$\{\hat{p}\} = -i\omega\rho_f \{\hat{\psi}\}. \quad (2.57)$$

Chapter 3

Experimental setup and measurement method

This chapter presents the instruments used, the experimental setup of electrical and acoustic measurements, and the method for analyzing measurement results. Sect. 3.1 shows a table of all the equipment that has been used. Sect. 3.2 goes through the method for electrical measurements. Sect. 3.3 goes through the method for acoustic measurements. Sect. 3.4 describes how the microphone sensitivity is calibrated. Sect. 3.5, motor setup and adjustment of the Y-stage travel length is described. Sect. 3.6 describes reflections that can affect the measured signal. Finally Sect. 3.7 describes the signal setup and processing of the signals.

3.1 Equipment list

Table 3.1 is the overview of the equipment connected to the movements of the experimental setup, and Table 3.2 shows the remaining equipment used in the experimental setup

Table 3.1: Equipment used in present work.

Brand/Model	Equipment	Serial number	Documentation/Manual
SMC Hydra TT	Motion Controller	1404-0153	[56]
PI C-843.41	Motion Controller	0095103296	[55]
PI C-852.12	Signal processor/Encoder	1460497	[51]
PI M-531.DG	Linear stage (X-stage)	-	[53]
PI M-535.22	Linear stage (Y-stage)	1460497	[52]
PI LS270	Linear stage (Z-stage)	414000926	[57]
PI M-037.PD	Rotation stage (R-stage)	109040312	[54]

Table 3.2: Equipment used in present work.

Brand/Model	Equipment	Serial number	Documentation/Manual
Mitutoyo M310-25	Micrometer	102-301	[47]
Cocraft HL10-S	Cross-line laser level	18081157898	[23]
HP 4192A	Impedance analyzer	2150J01344	[31]
Vaisala HMT313	Humidity and temperature	F4850018	[70]
ASL F250 MkII	Thermometer	1365026993	[8]
Paroscientific 740	Barometer	67325	[50]
Agilent 33220A	Signal generator	MY44023589	[4]
Tektronix DPO3012	Oscilloscope	C010246	[66]
Krohn-Hite 3940	Filter	AM2626	[40]
Brüel & Kjær 2636	Measurement amplifier	1815638	[18]
Brüel & Kjær 4138	1/8-inch pressure-field microphone	1832479	[17]
Brüel & Kjær UA-160	Adaptor - microphone to preamplifier	-	[17]
Brüel & Kjær 2633	Preamplifier	-	[17]
Brüel & Kjær 4228	Pistonphone	1918465	[16]
KEYENCE LK-G3001PV	Controller with display	1741187	[35]
KEYENCE LK-G32	Laser sensor	2041141/2041143	[35]
Meggitt A/S Pz27 Ceramic disc	Piezoelectric element	-	[46]

3.2 Electrical measurement setup

The impedance analyzer HP4192A [31] in Fig. 3.1 measures the electrical conductance and susceptance of the piezoelectric disk used in this work. The conductance, G_T , and susceptance, B_T , determine the piezoelectric element's electrical characteristics and are used to calculate Y_T . The admittance is given as

$$Y_T(f) = G_T(f) + iB_T(f) . \quad (3.1)$$

Before measurements are conducted of the piezoelectric disk, the impedance analyzer is turned on for at least 30 minutes to warm up the electronics and stabilize the instrument [31]. After the warm-up, it is necessary to do a zero calibration of the impedance analyzer to account for the electrical properties of external wires connected to the instrument. The calibration is performed in two steps: The first calibration is when the external wires connected to the analyzer are separated from each other, leading to an open circuit where the impedance is $Z = \infty \Omega$; The second calibration is when the external wires are kept together, making a shorted circuit where the impedance $Z \approx 0 \Omega$. These calibrations are generally performed with the highest measuring frequency of the measurement series, which is 300 kHz in this work. The complete calibration description is in section 3-50 in the manual [31]. Then by connecting the wires to each of the electrodes or wires soldered to the electrodes, see Fig. 3.2, the element of interest is ready for measurement. The MatLab script **impanel.m** in Appendix

[A.1] sets all measurement parameters before performing measurements and connects to the analyzer through GPIB. The adjustable parameters are the frequency range, frequency resolution, time delay before measurement after a frequency change, and the root mean square voltage V_{rms} . The frequency range of interest in the present work is 1-300 kHz. This range covers the piezoelectric element's first and second radial modes relevant for air/gas measurements. After performing a rough measurement of the G_T and B_T , the radial modes are identified. A new measurement is conducted from 1-300 kHz with a higher frequency resolution around the radial modes. The voltage range of the impedance analyzer is from 0.1-1.1 V_{rms} , where higher voltage can trigger non-linear effects but reduce the signal-to-noise ratio [13] or lower voltage increase uncertainties [31]. Previous work done by [48][29] has used 0.3 V_{rms} to maximize the accuracy of the measurement of the G_T and B_T , and therefore is this voltage used in the present work.

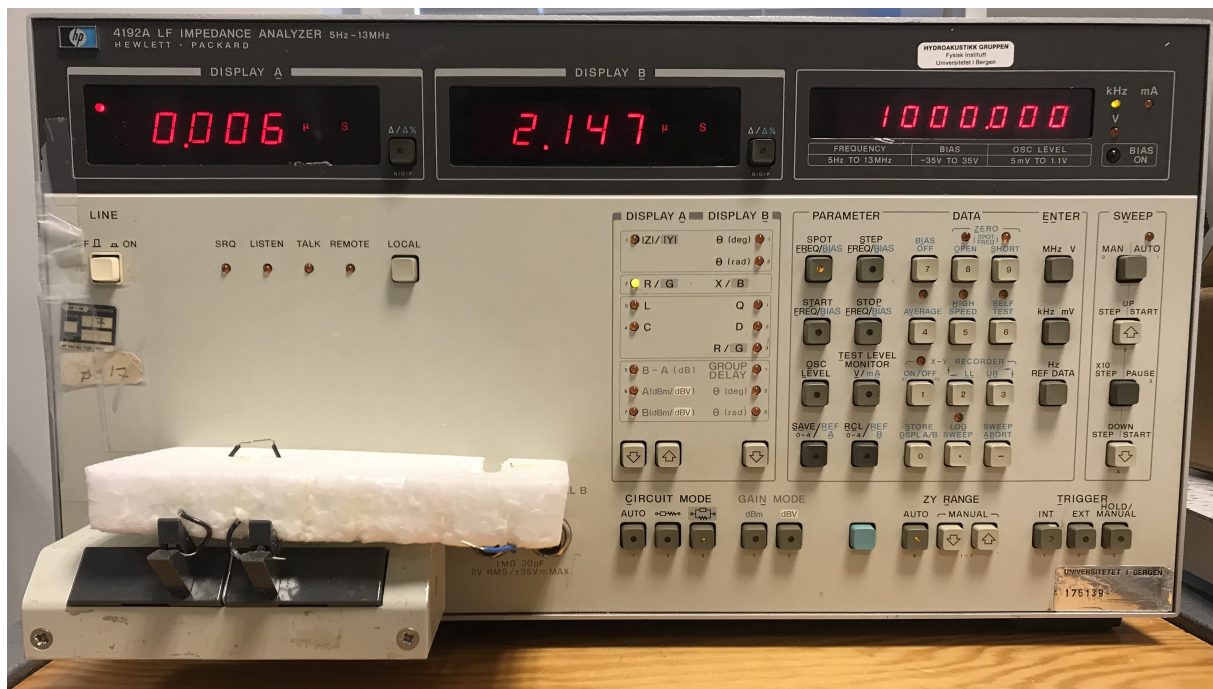


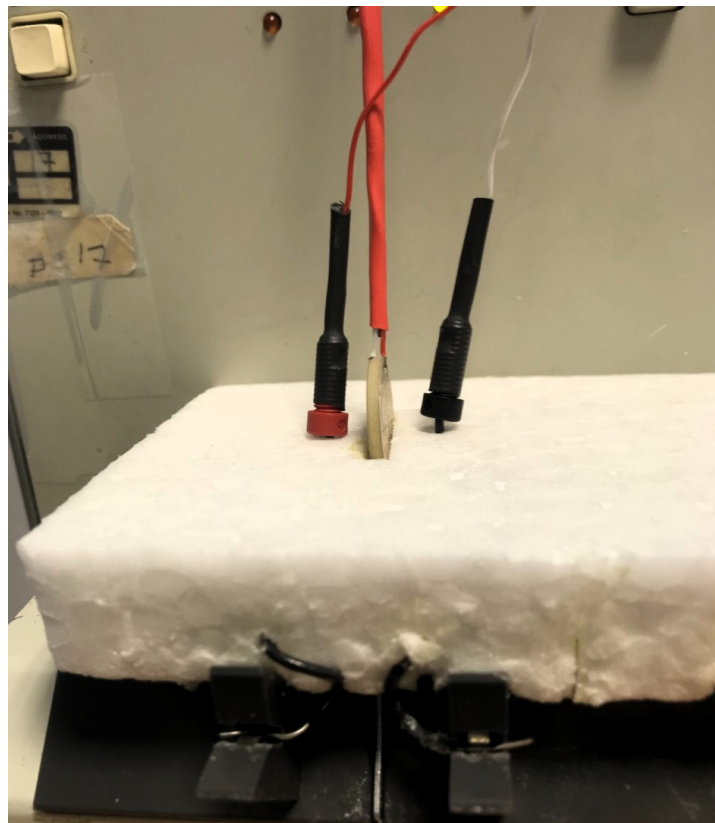
Figure 3.1: Impedance Analyzer HP 4192A [31], with a styrofoam block on the left side and the external wires used to connect the analyzer to the electrodes on the piezoelectric disk, pass through the styrofoam block.

When conducting measurements of the piezoelectric element, it is desirable to minimize the mechanical load on the disk. With a styrofoam block, the disk placed in a groove in the styrofoam, see Fig. 3.2, and wires connected to the electrodes with a slight inward force, this setup intends to minimize this load. This minimization helps the element to vibrate more freely and is essential when compared to FE simulations of the admittance of the piezoelectric disk in vacuum and fluid. It also helps to give more accurate measurements. However, in previous work, repeatability problems have been observed around the

resonances of measurements performed by [48][29]. It has been suggested that repeatability problems arise due to variations in the disk location in the styrofoam groove, the location of the wires on the electrodes, or different spring-like forces exerted by the wires placed on the electrodes [48][29]. It is also performed measurements directly on the wires plugs, where the wires are soldered to the electrodes, see Fig. 3.2b. These measurements are used to compare to the measurements conducted directly on the electrodes.



(a)



(b)

Figure 3.2: A styrofoam block with a groove holds the piezoelectric element when measuring the admittance. (a) Measurement is performed with wires from the analyzer placed directly on the electrodes and (b) to the wires soldered to the electrodes.

3.3 Acoustical measurement setup

Previous works [65][48][29] started developing the current acoustical measurement setup and have been continued to be developed by [6][7][64][26][24]. The block diagram in Fig. 3.3 is a detailed description of the current acoustical measurement setup. Figs. 3.4 and 3.5 gives the setup's visual overview, and the remaining instruments are shown in Fig. 3.6. There are two ways to go forward with acoustical measurements, set the settings directly in MatLab app for single measurements or predefining settings in the **MeasurementParameters.m** in Appendix A.3 script for a measurement series, see Sect. 4.4 for changeable settings.

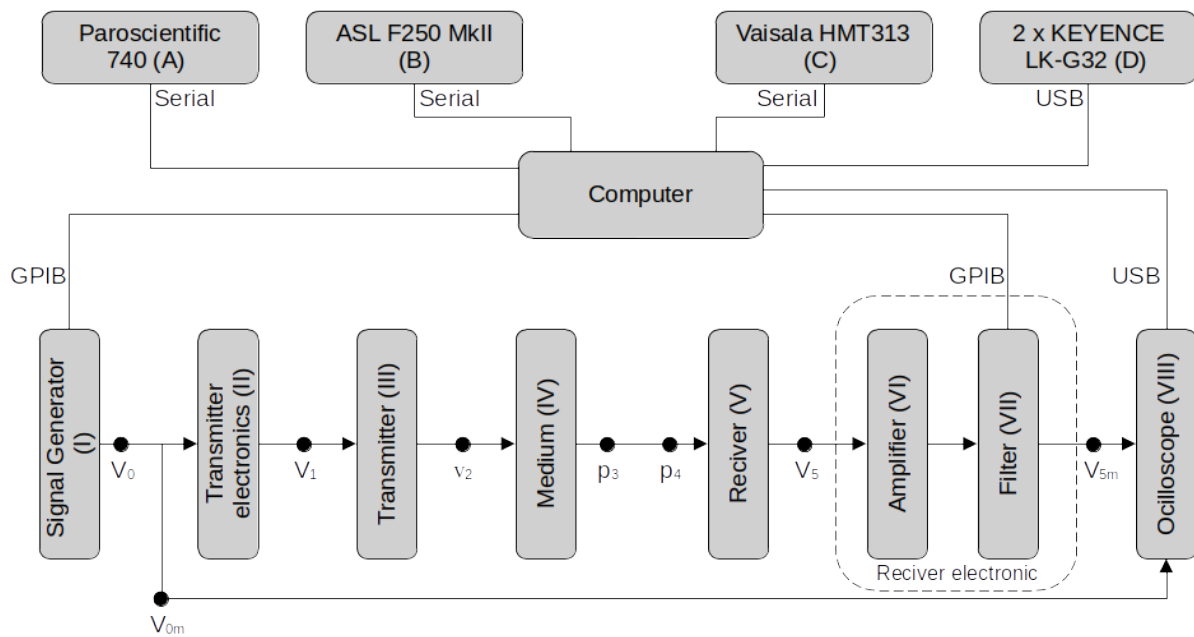


Figure 3.3: Block diagram of the acoustical setup and signal path. The blocks represent different equipment and are given in Table 3.2.

From the measurement system shown in Fig. 3.3, the measurements start with settings being sent from the computer to the signal generator (I), oscilloscope (VIII), and filter (VII). The signal generator creates the desired signal and sends it out through the output port. The oscilloscope reads the signal in channel one, which is connected to the signal generator and transmitter electronics (II) via BNC T-connector. The signal continues through the transmitter electronics, connected to the transmitter (III) via coaxial cable. Further, the transmitter sends the signal through the air (IV) before reaching the receiver (V). The received signal continues further to receiver electronics which amplifies (VI) the signal and filters the signal with a band-pass filter. The termination of the signal happens at the oscilloscope channel two after being amplified and filtered.



Figure 3.4: A overview of some of the equipment in the acoustical setup, where (A) is the barometer, (I) is the signal generator, (VI) is the amplifier, (VII) is the filter, and (VIII) is the oscilloscope (Table 3.2).

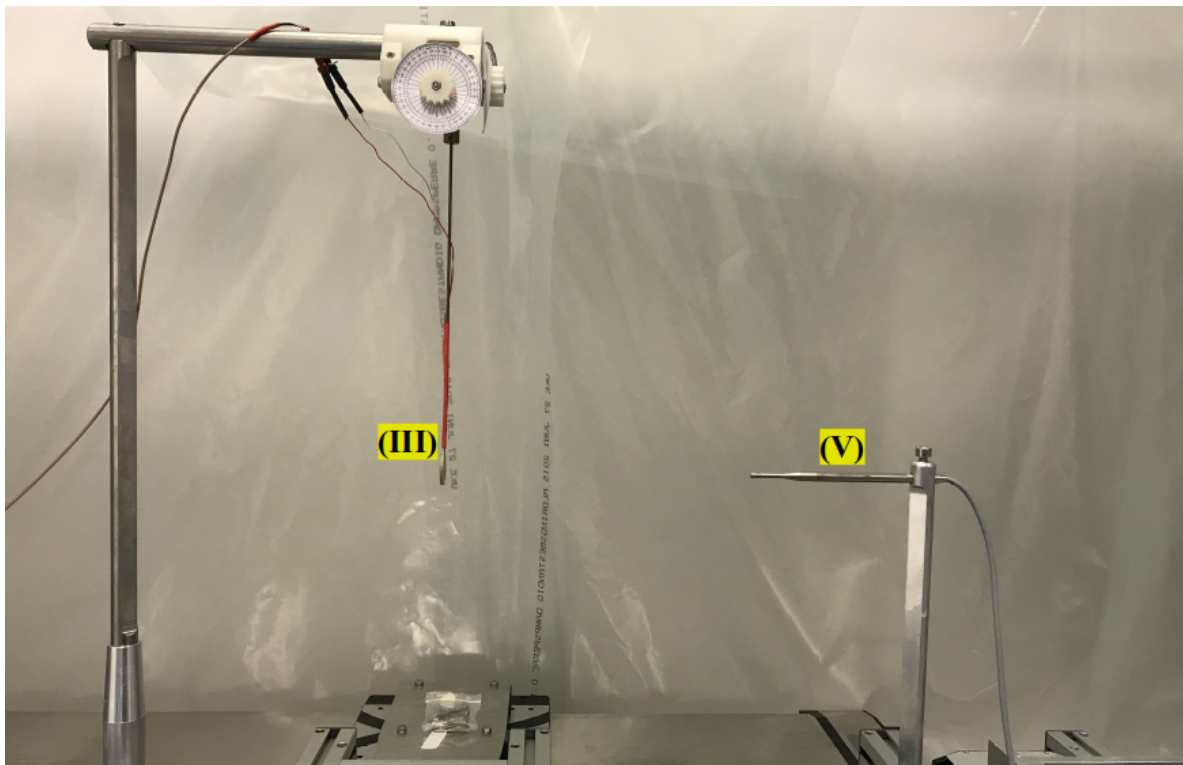


Figure 3.5: A overview of the chamber in the acoustical setup, where (III) is the piezoelectric disk/transmitter and (V) is the microphone/receiver (Table 3.2).

The setup frame is built up of aluminum profiles and placed inside a plastic sheet chamber. The chamber intends to lower the airflow to increase the accuracy of measurements. The measurements of the environmental parameters that take place inside the chamber are temperature (B)(C) and humidity (C), see Fig. 3.6. Inside the chamber is the placement of the transmitter, receiver, lasers stage (D), and all the moving stages as well. The only environmental parameter measured outside the chamber is the pressure (A).



Figure 3.6: A overview of some of the equipment in the acoustical setup, where (B) is the ASLF250 measuring the temperature, (C) the Vaisala measuring temperature and humidity, and (D) is the laser stage.

3.3.1 Signal generator (I)

The signal generator used in the present work is the Agilent 33220A [4], which communicates with the computer through GPIB. By predefining the settings, the instrument generates a sinusoidal burst and sends it out through the output port as V_0 . Changeable settings are the number of cycles, frequency, burst rate, and signal voltage amplitude. This work uses a 60-cycle sine burst and several different frequencies, a burst rate of 25Hz, and a peak-to-peak voltage signal $V_{0,pp}$ of 1 volt to avoid non-linearities of the piezoelectric disk at resonance frequencies. The low burst rate frequency used is because of letting reverberations of the piezoelectric disk die out and not letting any reflection interfere with the next burst. The output impedance of the signal generator is $50\ \Omega$, and at low output impedance, the output voltage V_0 usually is twice the programmed voltage. This doubling of the voltage is because, with high frequency and broadband signals, coaxial cables have a characteristic impedance of $50\ \Omega$ for practical reasons and will halve the voltage V_0 to 1 volt peak-to-peak. This halving of the voltage could easily be calculated by putting a load impedance in series to a Thevenin circuit, and the output voltage over the load impedance becomes

$$V_{0m} = V_0 \left(\frac{50\ \Omega}{50\ \Omega + 50\ \Omega_{sig}} \right) = V_0 \frac{1}{2}. \quad (3.2)$$

However, since the termination impedance of the oscilloscope is $1\text{ M}\Omega$, the read voltage will be approximately 2 volts peak-to-peak due to

$$V_{0m} = V_0 \left(\frac{1E6\Omega}{1E6\Omega + 50\Omega_{sig}} \right) \approx V_0 . \quad (3.3)$$

With the piezoelectric disk considered in this Thevenin circuit and parallel to the load impedance of the oscilloscope, this voltage V_{0m} measured changes dependent on the frequencies. Outside resonance of the disk, the perceived impedance is much higher than at the resonances. This change in impedance leads to the voltage V_{0m} measured being closer to 2 volts outside resonances and closer to 1 volt at resonance.

3.3.2 Transmitter electronics (II)

Transmitting electronics in this work is only a cable linking the piezoelectric disk to the BNC-T connector at the oscilloscope. It is assumed that this cable has the same characteristics as an RG58 coaxial cable, see Sect. 3.3.10. This transmitting electronics transfer the voltage V_{0m} measured at channel one at the oscilloscope to the piezoelectric disk electrodes. The voltage V_1 over the disk is calculated using the transfer function Eq. 2.21.

3.3.3 Transmitter (III)

The transmitter used in the present work is the piezoelectric ceramic disk Pz27. This ceramic disk, made by Meggit, states low aging rates and stable performance [46]. This ceramic disk type is a soft lead zirconate titanate (PZT) [46]. It has characteristics such as; high Curie temperature, low-temperature coefficients, and low mechanical quality factors [46], which allows the disk to be used in a variety of applications, such as flow meters, and therefore of interest in this work. The stated dimension of the disk is 2 mm in the thickness direction and 20 mm in diameter. However, the more accurate dimensions are measured and given in Table 5.3 in Sect. 5.3. The disk used in this work has previously been used by [26][7][64], and named #7. This disk has two wires soldered to the electrodes and hung up in a steel rod attached to the axis of rotation. A voltage V_1 applied to the electrodes is generated at the signal generator and sent through the transmitting electronics. The voltage sets the disk into motion and starts oscillating with a given frequency. This oscillation excites the piezoelectric disk with a velocity v_2 normal to the electrode front and is transmitted into longitudinal free-field pressure waves p_3 out in the medium.

3.3.4 Medium (IV)

The medium in this work that surrounds the transmitter and receiver is air. By monitoring the environmental parameters by measuring the temperature T in $^{\circ}\text{C}$, relative humidity RH in percentage %, and pressure P in hPa, the air absorption is calculated by Eq. 2.10. The absorption is essential when correcting for losses in pressure amplitude p_4 , which makes the measurement pressure comparable to the FE simulation pressure.

3.3.5 Receiver (V)

The receiver in this work is a 1/8-inch pressure-field microphone of the brand Brüel & Kjær and is the type 4138 [17]. It measures the free-field pressure p_4 and converts it into a voltage V_5 . More about the microphone in Sect. 3.4, later in this chapter. This section also covers the calibration of the microphone sensitivity.

3.3.6 Amplifier (VI)

The amplifier used in the present work is the Brüel & Kjær 2636 Measuring Amplifier and is adjusted manually [18]. This amplifier is one of two receiver instruments in this acoustical setup. In this work, the amplifier gain setting is 60 dB and split between the input and output ports by 40 dB and 20 dB, respectively. Brüel & Kjær state the amplifier's frequency response to be flat, 0 dB in the range from 1 Hz to 200 kHz, see Fig 3.7 and can provide up to 100 dB gain with a step of 10 ± 0.05 dB [18]. However, previous work done by Mosland and Hauge [48][29] did investigate the amplifier's frequency response and found a more accurate frequency response, see Fig 3.8. This new frequency response shows that in the frequency range from approx. 170 kHz to 220 kHz, an additional gain of 0.1 dB must be taken into account.

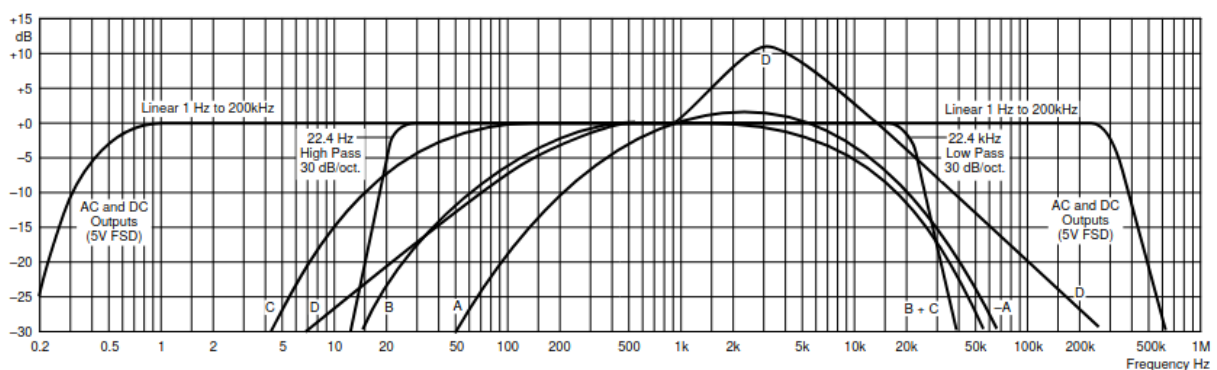


Figure 3.7: Typical overall frequency response of the Brüel & Kjær 2636 Measuring Amplifier [18].

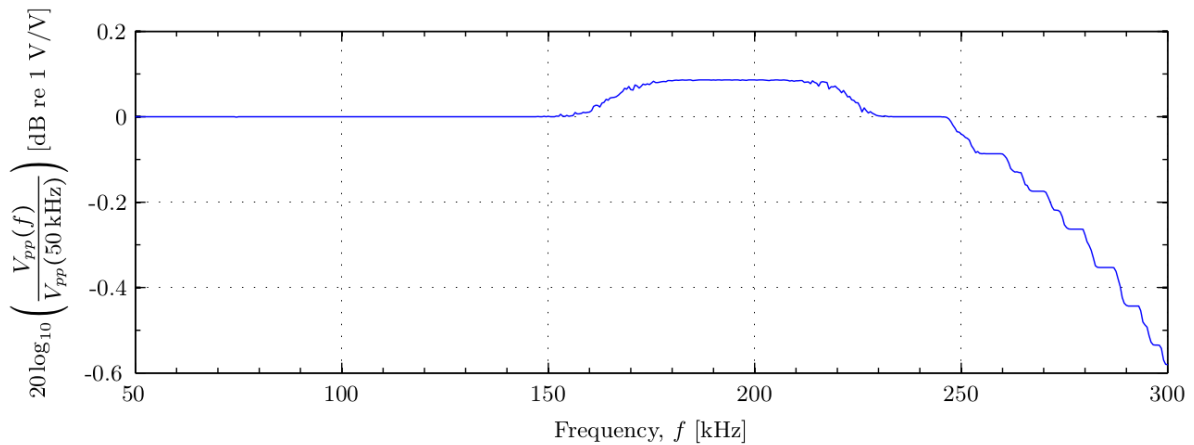


Figure 3.8: The frequency response of the Brüel & Kjær 2636 Measuring Amplifier created by [48] by conducting peak-to-peak voltage measurement in the frequency range from 50-300 kHz and normalizing measurements to the peak-to-peak voltage at 50 kHz. This frequency response is taken from [48].

3.3.7 Filter (VII)

The filter used in the present work is the Krohn-Hite 3940 filter [40], which communicates with the computer through GPIB. It has two channels, the first for a high-pass filter and the second for a low-pass filter. The cutoff frequency for the high-pass filter is set to half the measurement frequency and twice the measurement frequency for the low-pass filter. The attenuation outside the band-pass for this filter is 24 dB per octave [40]. It is possible to adjust the filter setting with the `MeasurementParameters.m` script in Appendix A.3.

3.3.8 Oscilloscope (VIII)

The oscilloscope used in the present work is the Tektronix DPO3012 [66], which communicates with the computer through USB. The oscilloscope has two input channels with termination impedance of 1 M Ω and 11 pF. Channel one read voltage V_0 from the signal generator connected to the oscilloscope by coaxial cable and measured as V_{0m} . Channel two read the output voltage V_5 from the microphone treated by the amplifier and band-pass filter connected by coaxial cables, terminated at the oscilloscope, and measured as V_{5m} . The oscilloscope's changeable settings are averaging, sample count, time per division (t/div), voltage per division (V/div), and bits. The voltage signal measured is averaged by 128 bursts. The t/div and V/div are automatically updated with scripts in the MatLab app, where t/div and V/div depend on the currently displayed signal length and voltage amplitude. The sample count is set to 10 000 samples, the t/div is usually 40 μ s or 100 μ s, and it is ten divisions on the oscilloscope, leading to a 0.4 ms to 1 ms time window. This time window leads to a sampling frequency of 25 MS/s or 10 MS/s and is more than sufficient for frequencies between 50 kHz

to 250 kHz. The bits resolution of the oscilloscope is set to 16-bit.

3.3.9 Environmental parameters

The monitored environmental parameters are pressure, temperature, and relative humidity. The barometer Paroscientific 740 (A) measures the pressure in hPa with a DIGIQUARTZ® pressure transducer. This pressure transducer gives high accuracy, resolution, and long-term stability resulting in an uncertainty of ± 0.01 % [50]. Both the ASL F250 MkII (B) and the Vaisala HMT313 (C) measure the temperature inside the plastic sheet chamber. They use a PT100 sensor with an uncertainty of ± 0.01 °C and ± 0.1 °C, respectively [8][70]. Vaisala HMT313 also measures relative humidity with a HUMICAP® with an uncertainty of ± 0.6 % when relative humidity is below 40 % and ± 1.0 % for above 40 % [70].

3.3.10 Cables

In the acoustical air setup, are two types of cables used. The first cable connects the piezoelectric disk to the BNC-T connector at the oscilloscope and is assumed to have the same characteristics as an RG58 coaxial cable. The second type is RG58 coaxial cables connecting the instruments. The coaxial cables are of different lengths, see Table 3.3, and the characteristic impedance of type RG58 coaxial cable is 50 Ω . There are also typical specifications for the RG58 coaxial cable listed in Table 3.4 [73].

Table 3.3: Measured or given length of the cables in the measurement setup.

Cable connection		Cable length
Input1	Input2	
Signal generator	BNC-T connector	0.25 m
BNC-T connector	Piezoelectric disk	3.00 m
Amplifier	Filter (Ch.1)	0.50 m
Filter (Ch.1)	Filter (Ch.2)	0.80 m
Filter (Ch.2)	Oscilloscope	1.50 m

Table 3.4: Typical specifications for RG58 coaxial cables [73]

Description	Value	Unit
Inductance (L) per meter	250	[nH/m]
Capacitance (C) per meter	100	[pF/m]

3.4 Brüel & Kjær 4138 microphone

The receiver in the acoustical setup is a microphone of the brand Brüel & Kjær type 4138 [17], which is a 1/8-inch microphone. This microphone is used together with a 1/4-inch Brüel & Kjær preamplifier type 2633 [17]. The preamplifier is necessary since the microphone needs a polarization voltage of 200 V. Brüel & Kjær states that the preamplifier has a flat frequency response [17]; therefore, only the microphone's frequency response $|M(f)|$ is considered in calibration. The given frequency response from the calibration chart of the microphone [19] goes from 20 Hz to 200 kHz, and is calibrated with an electrostatic actuator and plotted relative to reference microphone sensitivity $|M_{ref}(250Hz)|$ at 250 Hz. The calibration chart is digitized by importing a scanned image of the frequency response into an online software [60] and recreating the chart by manually inserting data points. The final result of the data points is plotted, see Fig. 3.9. This method of recreating a plot will give some errors. Factors that give errors are the thickness of the line, manually placing the data points on the line, and limitation on pixel movement of the points. Previous work by [24] estimated this error to be ± 0.1 dB.

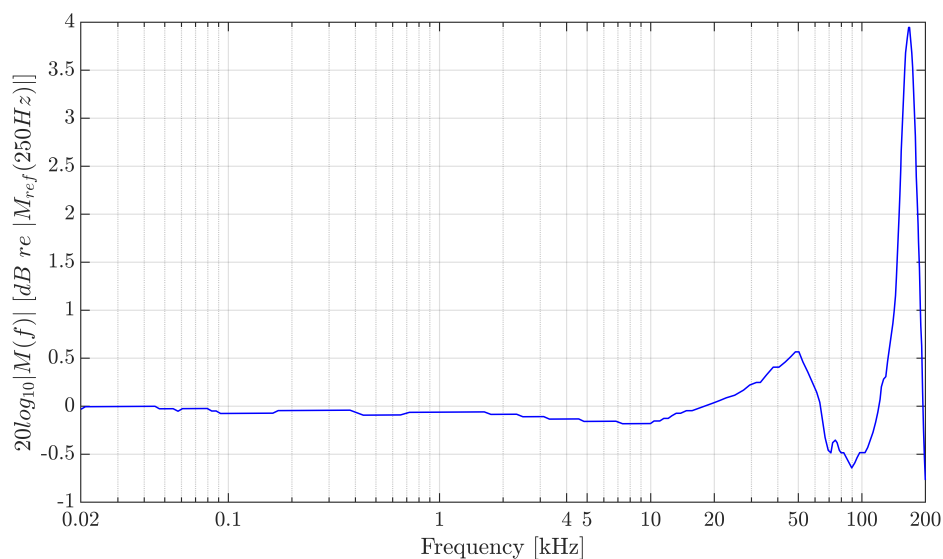


Figure 3.9: Open-circuit pressure response relative to 250 Hz for Brüel & Kjær microphone type 4138 with the serial number: 1832479.

In addition to the open-circuit pressure response, it is necessary to include the free field correction for a given incident angle of sound pressure θ_i . The free-field correction describes the increase of sound pressure caused by diffractions [17]. This increase happens at high frequencies when the wavelength becomes comparable to the diameter of the microphone. By assuming the incident angle of sound pressure between transmitter and receiver is θ_i equals 0 degrees, which is the case in this work, the Brüel & Kjær free-field correction chart is digitized for this angle and added to the open-circuit pressure response. The chart

used is for the 4138 microphone with a protection grid over the diaphragm [17] and digitized with the same method earlier, and the result is given in Fig. 3.10. This chart goes from 4-200 kHz. The open-circuit pressure response added to the free-field correction gives the microphone system's free-field open-circuit pressure response from 4-200 kHz, see Fig. 3.11.

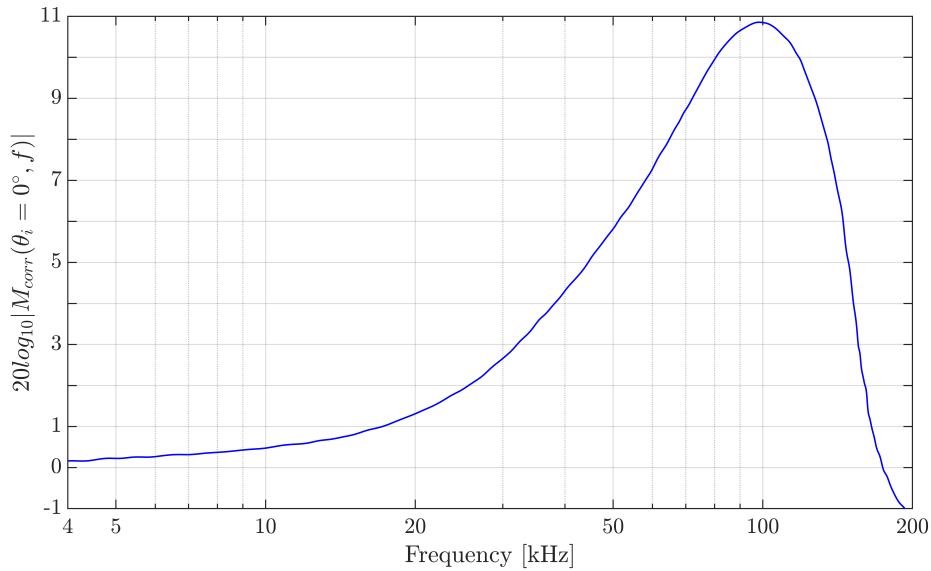


Figure 3.10: Free-field correction relative to 250 Hz for Brüel & Kjær microphone type 4138 with protection grid [17].

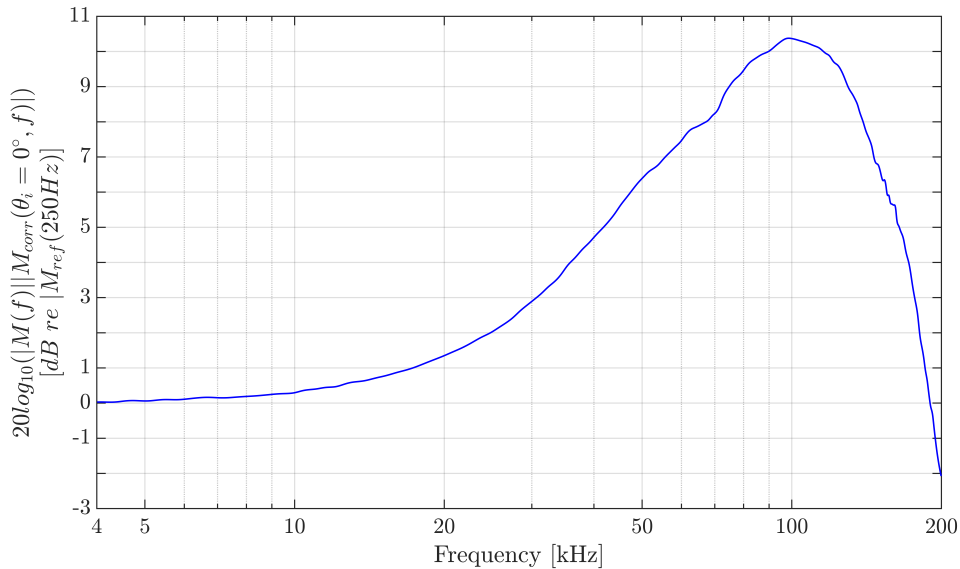


Figure 3.11: Open-circuit pressure response, including free-field correction, relative to 250 Hz for Brüel & Kjær microphone type 4138 with the serial number: 1832479.

3.4.1 Microphone sensitivity calibration using a pistonphone

This work uses a Brüel & Kjær 4228 pistonphone to find the microphone's system sensitivity [16]. This pistonphone produces a nominal sound pressure level *Stated SPL* of 124.11 ± 0.09 dB relative to $20 \mu\text{Pa}$ [20]. It also has a nominal frequency of 250 Hz, or the exact frequency is $10^{2.4}$ Hz (ISO266) ± 0.1 % [20]. If the calibration is under conditions other than the reference condition, the sound pressure level is given as [20]

$$\text{Actual SPL} = \text{Stated SPL} + \Delta L_V + \Delta L_p, \quad (3.4)$$

where ΔL_V is the load volume correction, ΔL_p is a correction if ambient pressure deviates from 1013 mbar, and *Actual SPL* is the corrected sound pressure level. The load volume correction ΔL_V for the given microphone 4138 is 0 dB when using the pistonphone adaptor DP 0774, see Table 3.5. The ambient pressure correction ΔL_p can be read directly off barometer UZ0004 supplied with the pistonphone calibration set [16], see Fig. 3.12. Alternatively, calculated using an interpolation function between different points read of the barometer UZ0004, see Table 3.6, and then using the ambient pressure measured with the Paroscien-tific 740, during the calibration.

Table 3.5: The load volume correction ΔL_V given by [20].

Size	Piston- phone Adaptor	Micro- phone Type	Load Volume Correction ΔL_V (dB)			
			With Protection Grid	Without Protection Grid	With Adaptor Ring DB0111	With Adaptor Ring UA0825
1"	None	4131/32	-0.05	—	+0.25	—
		4144/45	+0.05	—	+0.25	—
		4160	+0.43	+0.28	—	—
		4179	-0.05	—	—	—
1/2"	DP 0776	4129/30	-0.02	—	—	—
		4133/34	0.00	—	—	+0.08
		4147	0.00	—	—	+0.08
		4148	-0.04	—	—	—
		4149	0.00	—	—	—
		4155	-0.03	—	—	—
		4165/66	-0.03	—	—	—
		4176	-0.02	—	—	—
		4180	—	+0.08	—	—
		4181	0.00	—	—	—
4183	-0.02	—	—	—		
1/4"	DP 0775	4135/36	0.00	—	—	—
1/8"	DP 0774	4138	0.00	—	—	—

Table 3.6: Different points read of the supplied barometer UZ0004 in the pistonphone calibration set [16], see Fig. 3.12, used to calculate the ambient pressure correction ΔL_p .

Pressure	685 mbar	800 mbar	940 mbar	990 mbar	1013 mbar	1060 mbar
Correction	-3.4 dB	-2.05 dB	-0.65 dB	-0.20 dB	0.00 dB	0.39 dB



Figure 3.12: Supplied barometer UZ0004 in the pistonphone calibration set [16].

Using the definition of the microphone sensitivity given in Eq. 2.37 and using the pistonphone, the microphone sensitivity $|M_V|$ is calculated as

$$M_V(250 \text{ Hz}) = \frac{V_{eff}(250 \text{ Hz})}{p_{eff}(250 \text{ Hz})}, \quad (3.5)$$

where V_{eff} is the calculated open-circuit effective voltage with Eq. 2.38, and the pressure p_{eff} is the free-field effective pressure at the front of the microphone with the assumptions of normal incidence and plane waves. The oscilloscope records the microphone's voltage signal $V_{5m}(t)$ produced by the pistonphone, see Fig. 3.13, and fast Fourier transformed to the voltage $V_{5m}(f)$, see Sect. 3.7.2, where $V_{5m_{pp}}(250 \text{ Hz})$ is then calculated as

$$V_{5m_{pp}}(250 \text{ Hz}) = 4 * V_{5m}(250 \text{ Hz}) = 402.55 \text{ mV}, \quad (3.6)$$

where $V_{5m_{pp}}(250 \text{ Hz})$ is the calculated peak-to-peak voltage from the fast Fourier transformed voltage $V_{5m}(250 \text{ Hz})$. Then, with the calculated $V_{5m_{pp}}(250 \text{ Hz})$, the effective voltage V_{eff} is then deduced by using the Eq. 2.38, which gives

$$V_{eff}(250 \text{ Hz}) = \frac{V_{5pp}(250 \text{ Hz})}{2\sqrt{2}} = \frac{1}{2\sqrt{2}} \frac{V_{5m_{pp}}(250 \text{ Hz})}{H_{55m}^{VV}(250 \text{ Hz})} = \frac{1}{2\sqrt{2}} \frac{402.55}{9.998} \text{ mV} = 14.235 \text{ mV}, \quad (3.7)$$

where H_{55m}^{VV} is the transfer function in Eq. 2.29 and V_{5pp} is the peak-to-peak voltage out of the microphone. In this calibration, the amplifier gain is set to 20 dB.

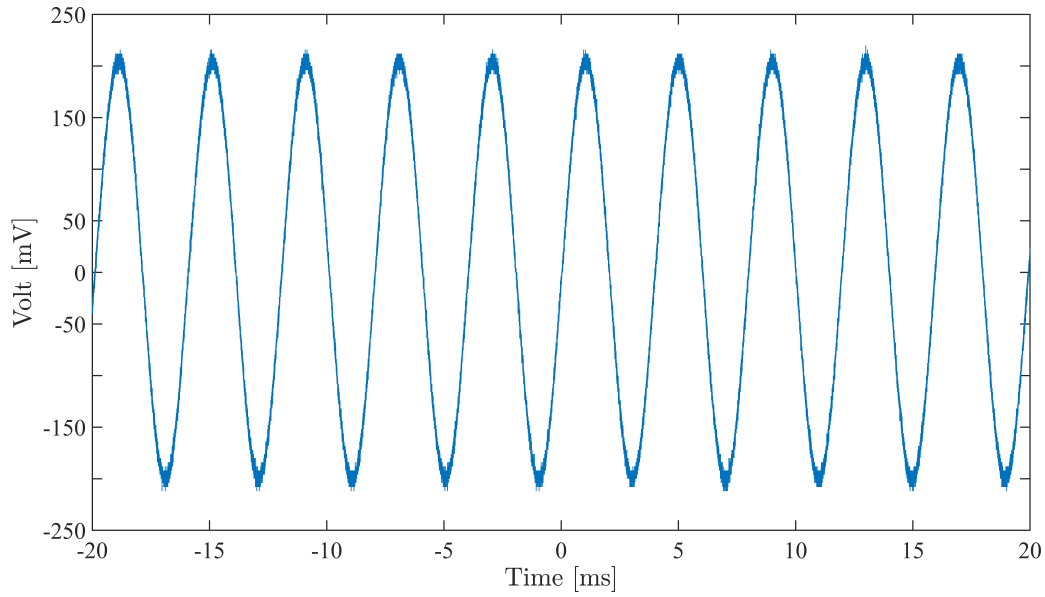


Figure 3.13: $V_{5m}(t)$ measurement generated by the pistonphone with an amplifier gain of 20 dB.

By calculating the *Actual SPL* with Eq 3.4, which gives

$$\text{Actual SPL} = 124.11 \text{ dB} - 0.251 \text{ dB} + 0 \text{ dB} = 123.859, \quad (3.8)$$

where ΔL_V equals 0 dB and ΔL_p equals -0.251 dB, the free-field effective pressure can be calculated using the Eq. 2.39, which gives

$$p_{eff}(250 \text{ Hz}) = p_{ref} \cdot 10^{\frac{\text{Actual SPL}}{20}} = 20 \mu\text{Pa} \cdot 10^{\frac{123.859}{20}} = 31.1875 \text{ Pa} \quad (3.9)$$

where p_{ref} is the reference pressure 20 μPa . Then with Equation 3.5, the microphone sensitivity is calculated as

$$M_V(250 \text{ Hz}) = \frac{14.235 \text{ mV}}{31.1875 \text{ Pa}} = 0.456433 \text{ mV/Pa}. \quad (3.10)$$

This calibrated microphone sensitivity $|M_V(250 \text{ Hz})|$ at 250 Hz has changed largely in previous works and calculated to 0.3157 mV/Pa [1], 0.535 mV/Pa [6], 0.493 mV/Pa [48][29], and now 0.456433 mV/Pa. None of the previous studies answers the significant changes in calibration results. An observation made in this work was that the higher the gain, the higher the signal distortion of the measured signal of the pistonphone. This distortion is the reason why 20 dB gain is used in this work, while it has previously been used as 30 dB by [1] and [6] and 20 dB by [48][29]. The calibration and calculated microphone sensitivity at 250 Hz are then added to the open-circuit pressure response, including a free-field correction in Fig.

3.11, to deduce the free-field open-circuit receiver sensitivity, which is given as

$$20\log_{10}|M_{cal}(f)| = 20\log_{10}\left(\frac{|M(f)| |M_{corr}(\theta_i = 0, f)| |M_V(250Hz)|}{|M_{ref}(250Hz)|}\right) [dB \text{ re. } 1V/Pa] \quad (3.11)$$

where $|M_{cal}(f)|$ is the calibrated microphone sensitivity and plotted in Fig. 3.14. The Fig. 3.15 is the equivalent free-field open-circuit receiver sensitivity in mV/Pa.

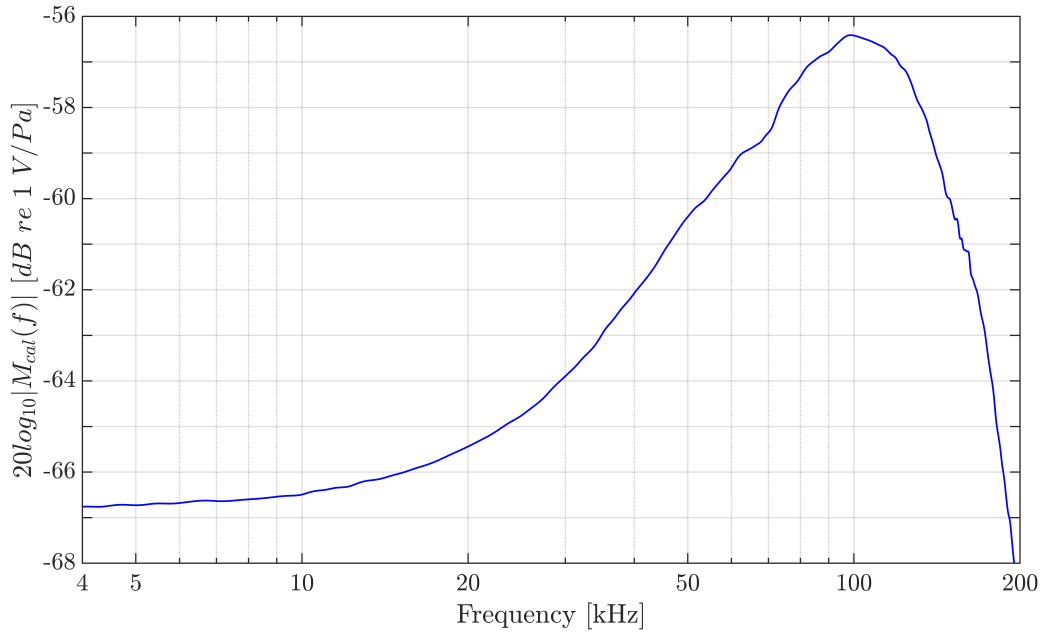


Figure 3.14: The free-field open-circuit microphones sensitivity from 4-200 kHz in dB.

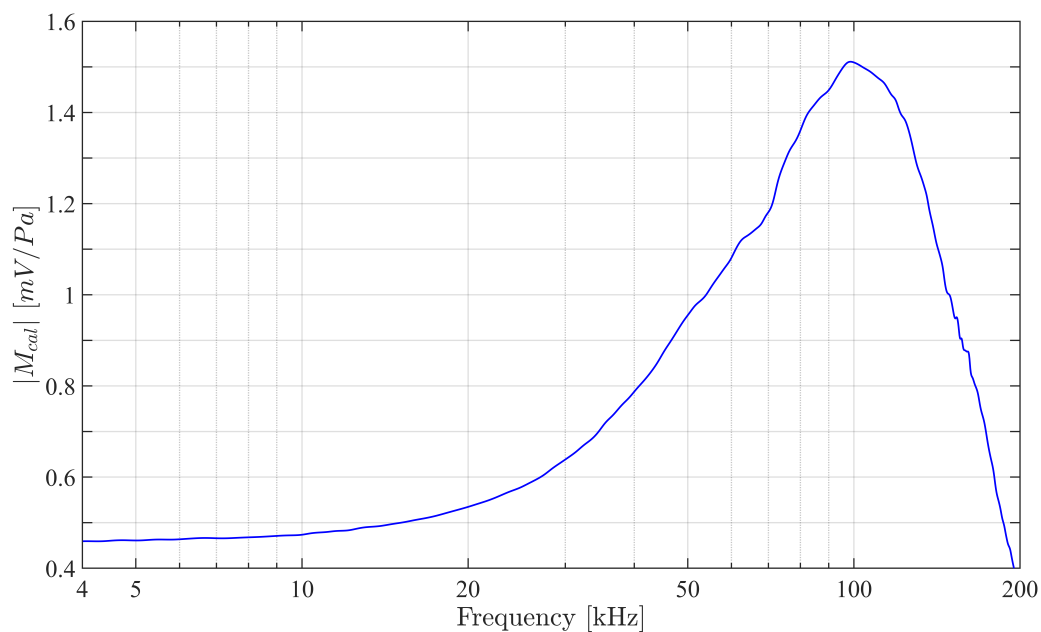


Figure 3.15: The free-field open-circuit microphones sensitivity from 4-200 kHz in mV/Pa.

3.5 Motor's setup

The present work's motor setup contains two motion controllers, one encoder for Y-stage, three linear stages (X, Y, and Z-stage), and one rotation stage (R-stage). For an illustration of the motor setup, see the block diagram of the motor setup, Fig. 3.16. All linear stages use reference coordinates found by an induction sensor at the end of each linear stage. These reference coordinates are repetitive and therefore used to find the origin position of the transducer. More details about using reference coordinates to find the origin position of the transducer are in the Chapter 4, and the importance of finding the origin position of the transducer is in the Sect. 4.5.

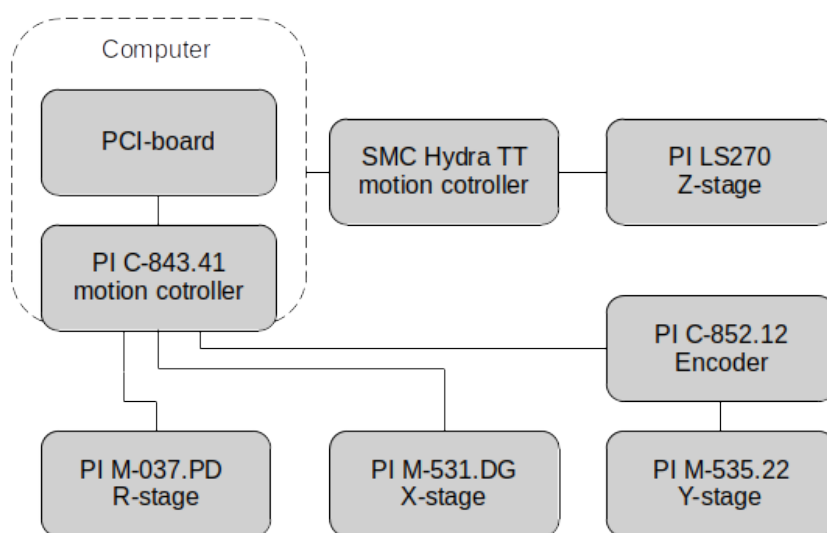


Figure 3.16: Block diagram of the acoustical motor setup and signal path. The blocks represent different motors and motor controllers and are given in Table 3.1.

The X and Y-stage set the microphone's position, and the Z-stage set the distance between the microphone and transducer. The R-stage rotate the transducer and is used to set the angle θ_R of the transducer relative to the microphone. The travel length of the X and Y-stage is 300 mm, and the Z-stage is 1016 mm, but it is limited to about 900 mm because the X and Y-stage are a part of the Z-stage linear rail system. The R-stage has no limits and can rotate an infinite number of degrees, but it is limited to roughly ± 90 degrees in this work. All linear stages move in steps, where one step is equivalent to one mm, or ten step is equivalent to ten mm, for the rotation stage, one step is equivalent to one degree. In this work, it is needed to adjust the Y-stage after observing wrong travel distance in mm relative to the given input step.

3.5.1 Travel distance adjustments of Y-stage

The internal settings of the Y-stage are given by [52] and are:

- the ball screw pitch, b , equal to 2 mm per revolution
- the encoder resolution, e_{res} , equal to 2000 counts per revolution
- the backlash-free gear head, g , which is 29.64197531:1
- the stage resolution, y_{res} , (calculated from $b/e_{res}/g$) equal to $0.34 \mu\text{m}$ per count

Suppose any of the internal settings deviate from [52]. In that case, it will lead to the encoder interpreting an inaccurate y_{res} and reading the incorrect number of counts leading to a wrong travel distance. It is observed that the Y-stage does not move the desired travel length but moves a shorter distance. The error is proportional to the input value by a common factor, e.g., an input value of one step results in a travel distance of half an mm, or two step results in a travel distance of one mm. The repetitive error in the travel distance indicates that the error comes from the internal settings of the Y-stage and not because of damaged parts. Since changing the internal settings has not been possible, a common alternative way of adjusting the travel length has been used. This alternative way is to look at the ratio of the output travel distance and the input value and define this ratio as travel resolution, d_{res} as

$$d_{res} = \frac{d}{s} = 1, \quad (3.12)$$

where s is the step and d is the travel distance in mm. If the input value is not equal to the travel distance, which is the case for the Y-stage, then d_{res} deviates from one and must be adjusted with a factor f as

$$f \cdot d_{res} = f \cdot \frac{d}{s} = 1. \quad (3.13)$$

The purpose of this is to alter the number of counts to be counted by the encoder without physically changing the internal settings but still achieving the correct travel distance. The travel distance d is measured with a dial gauge with an uncertainty of ± 0.01 mm. This dial gauge is made by the brand TESA Technology [67]. The positioning of the dial gauge, shown in Fig. 3.17, is as parallel as possible to the Y-stage such that the dial gauge plunger moves parallel with the stage. The travel distance is measured ten times using s set to 25, and the average of d is calculated as

$$\hat{d} = \frac{\sum_{i=1}^N |d_i|}{N}, \quad (3.14)$$

and the uncertainty of the travel distance is

$$\sigma_d = \sqrt{\sigma_{std}^2 + \sigma_{dial}^2}, \quad (3.15)$$

where σ_{dial} is the uncertainty of the dial gauge and σ_{std} is the estimated standard deviation calculated as

$$\sigma_{std} = \sqrt{\frac{\sum_{i=1}^N (d_i - \hat{d})^2}{N-1}}. \quad (3.16)$$



Figure 3.17: Dial gauge lined up parallel to the Y-stage, ready to measure the travel distance of the stage.

After calculating the factor with Eq. 3.13, f is tested to find the accuracy of d_{res} by taking the input value, s , multiplying it with f , and repeating ten distance measurements. If the distance resolution still deviates from one, a new factor is calculated as

$$f_{new} \cdot d_{res} = f_{new} \cdot \frac{d}{s \cdot f_{old}} = 1, \quad (3.17)$$

where f_{new} is the new factor and f_{old} is the old factor. Then to test f_{new} to find the accuracy of d_{res} , f_{new} is replaced with f_{old} , and the ten distance measurements are repeated.

This process is repeated until d_{res} reaches appropriate values, see Fig 3.18. To calculate the uncertainty of the d_{res} from Eq. 3.17 the uncertainty $\sigma_{d_{res}}$ becomes

$$\sigma_{d_{res}} = \sqrt{\left(\frac{\partial d_{res}}{\partial d} \cdot \sigma_d\right)^2 + \left(\frac{\partial d_{res}}{\partial s} \cdot \sigma_s\right)^2 + \left(\frac{\partial d_{res}}{\partial f_{old}} \cdot \sigma_{f_{old}}\right)^2} = \sqrt{\left(\frac{1}{s \cdot f_{old}} \cdot \sigma_d\right)^2}, \quad (3.18)$$

where $\sigma_{f_{old}}$ and σ_s equals zero because the factor and step are exact quantities with zero uncertainty. The final adjustment factor, f used, equals 1.69028, and the calculated distance resolution, d_{res} , equals 1.0000 ± 0.00024 .

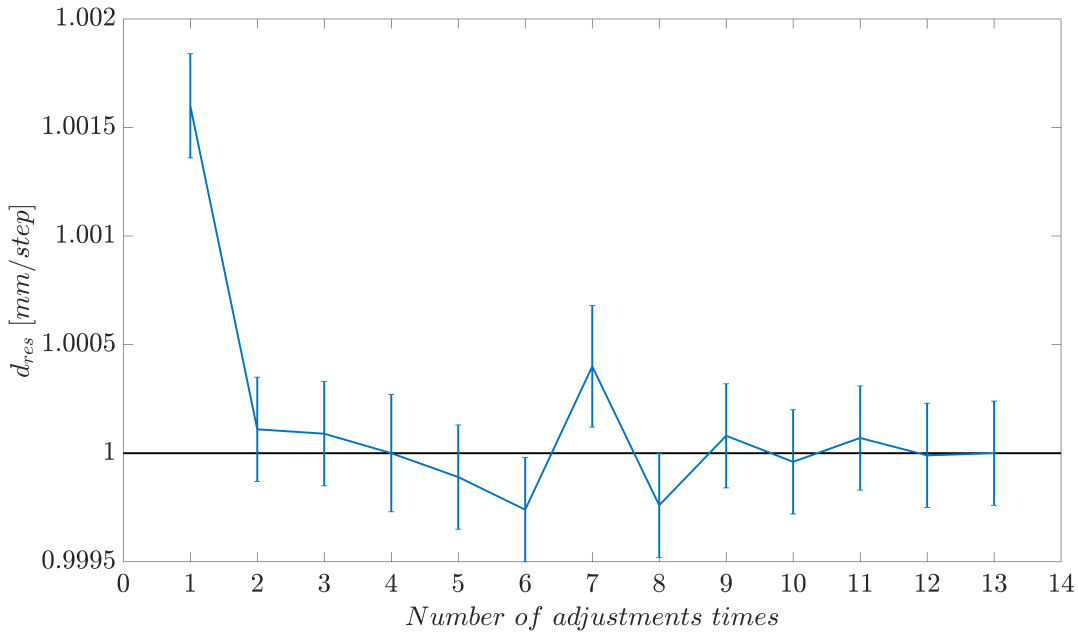


Figure 3.18: The change in distance resolution, d_{res} , is adjusted by the factor f found using the input step, s , equal to 25 steps and the calculated distance \hat{d} of ten distance measurements.

3.6 Reflections

This acoustic measurement setup contains many surfaces that can reflect a transmitted sound wave. Such as flat aluminum profiles, steel rods and plates, walls, floor and roof, plastic sheets, and wood frames. Most of these reflections are non-destructive on the received signal because of the late arrival time compared to the transmitted signal. The one destructive reflection that needs to be considered when measuring is the reflection from the vertical rod behind the transducer. The vertical steel rod has a wedge shape to reduce the reflections, see Figs. 3.5 and 3.19. This reflection from the vertical rod becomes apparent after the rotation angle θ_R deviates from 0 degrees, and the reflection starts to become a problem for the acoustic measurement signal, as illustrated in Fig. 3.19. Calculating the arrival time t_{refl} of

this reflection for every angle of θ_R is possible with the given equation

$$t_{refl}(\theta_R) = \frac{\sqrt{(d_{rod}\cos(\theta_R) + z_0)^2 + (d_{rod}\sin(\theta_R))^2} + d_{rod}}{c_{air}} = \frac{d_h(\theta_R) + d_{rod}}{c_{air}}, \quad (3.19)$$

where d_{rod} is the distance between the rod and piezoelectric disk, z_0 is the direct length between disk and microphone, and d_h is the distance from the vertical rod to the microphone, which is dependent on the R-stage rotation angle θ_R .

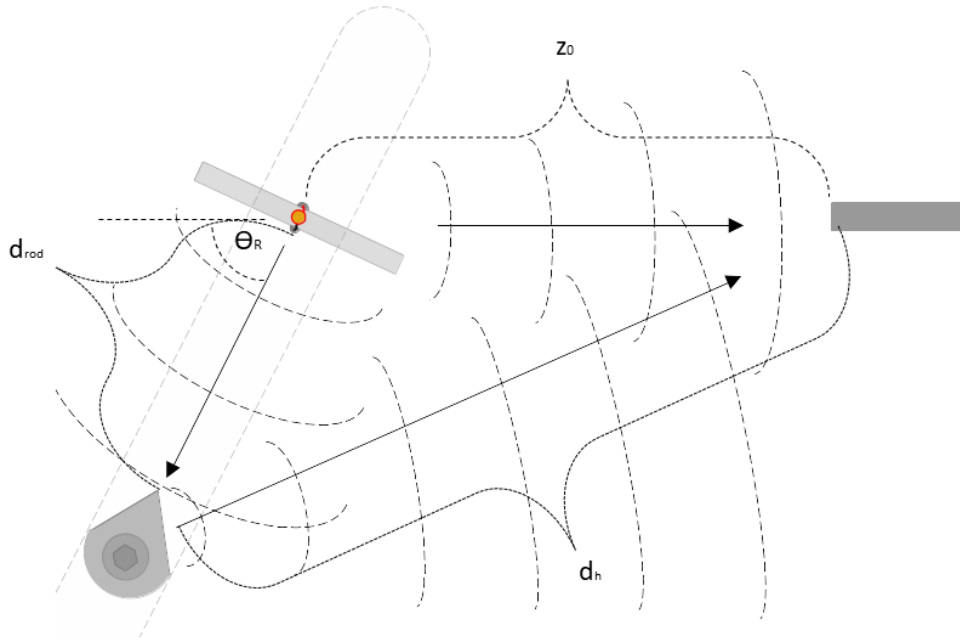


Figure 3.19: Illustration of direct travel path z_0 , and reflection path through d_{rod} and d_h from piezoelectric disk to microphone.

By knowing the arrival time of the reflection t_{refl} at every angle θ_R , the interval used to calculate the voltage $V_{5m}(f)$ can be set from the start of the steady state of the acoustic measurement signal to the reflection's arrival time. This interval prevents the acoustic measurement signal from being interfered with by reflections and intends to get the best results possible by the acoustic measurement signal. However, this work uses a sinus burst with a calculated standard number of cycles, which is used throughout this work. In order to calculate the number of cycles to be used in the measurements in this work, it is first calculated the time difference between the acoustic measurement signal coming directly from the piezoelectric disk and the arrival time of the reflection from the vertical rod Δt as

$$\Delta t(\theta_R, z_0) = t_{refl}(\theta_R) - \frac{z_0}{c_{air}} = t_{refl}(\theta_R) - t_{dir}, \quad (3.20)$$

where t_{dir} is the direct signal between the disk and microphone. In this work, final measurements are not performed further out than distance z_0 equal to 0.3 m. To calculate the

shortest Δt for this distance (z_0 equal to 0.3), which is when θ_R is equal to 90 degrees, then Δt can be used to calculate the number of cycles without reflection interfering with the direct signal of interest. The number of cycles is then calculated for the frequency 98860 Hz as

$$cycles = f \cdot \Delta t(\theta_R = 90^\circ, z_0 = 0.3 \text{ m}) = 98860 \text{ Hz} \cdot 0.737 \text{ ms} \approx 73. \quad (3.21)$$

With a calculated number of cycles to be 73, the standard number of cycles is set to 60-cycles. With a measurement signal combined as a short duration signal t_{dur} , which can be calculated as

$$t_{dur} = \frac{cycles}{f}, \quad (3.22)$$

and with a short burst period i.e. 25 Hz, it is accounted for that all reflections, and any reverberations in the piezoelectric disk die out before the next sine burst is transmitted.

By studying the received acoustic measurement signal, it is possible to confirm that the one destructive reflections come from the vertical steel rod. It can be confirmed by blocking the interference and seeing the reflection die out from the live signal at the oscilloscope. Alternatively, measuring and calculate the arrival time of the reflecting signal from different angles and compare it to the actual measurements, see Figs. 3.20-3.23. The present work uses both these methods. By analyzing the signals in Figs. 3.20-3.23, the estimated arrival time of the direct signal and reflection signal fits well with the several different angles' predictions.

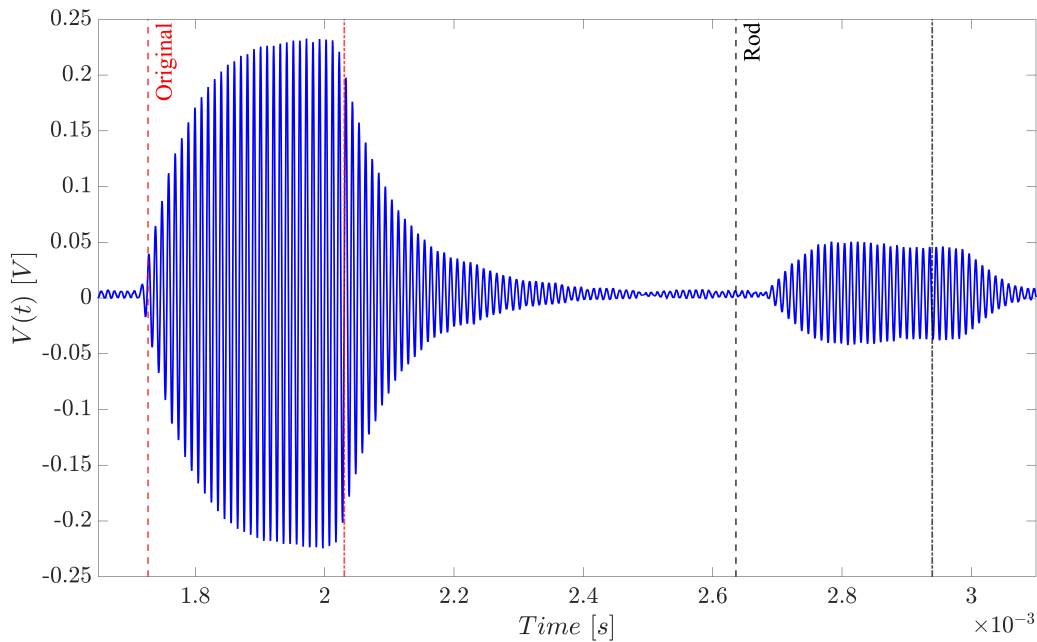


Figure 3.20: Reflection at θ_R equal to 55 degrees, a distance from the microphone to piezoelectric disk z_0 equals 600 mm, and a 30-cycle sine burst with frequency 98860 Hz.

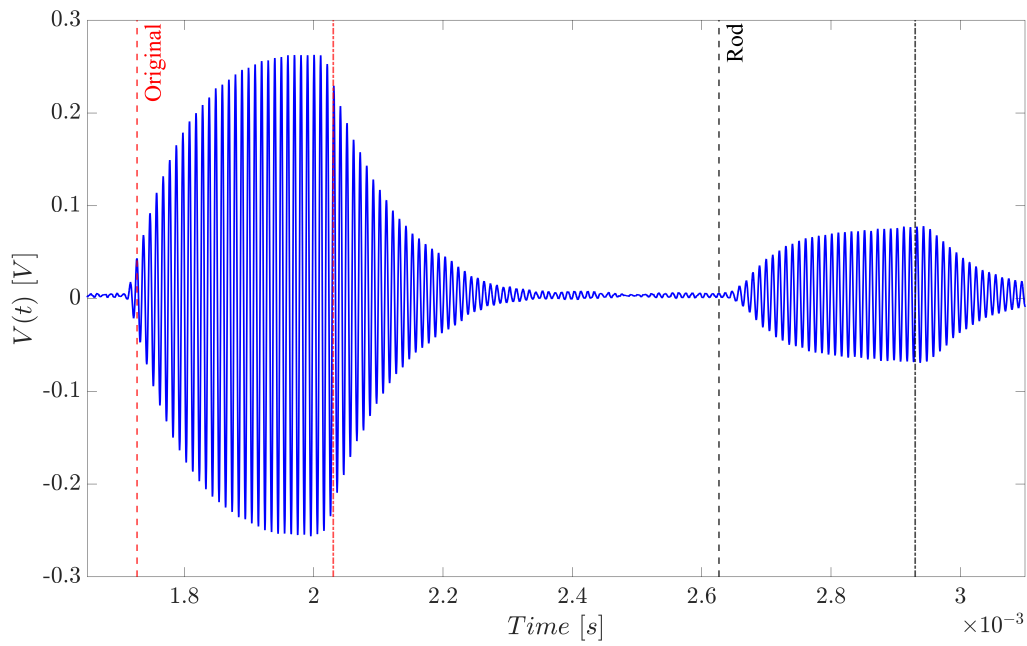


Figure 3.21: Reflection at θ_R equal to 60 degrees, a distance from the microphone to piezo-electric disk z_0 equals 600 mm, and a 30-cycle sine burst with frequency 98860 Hz.

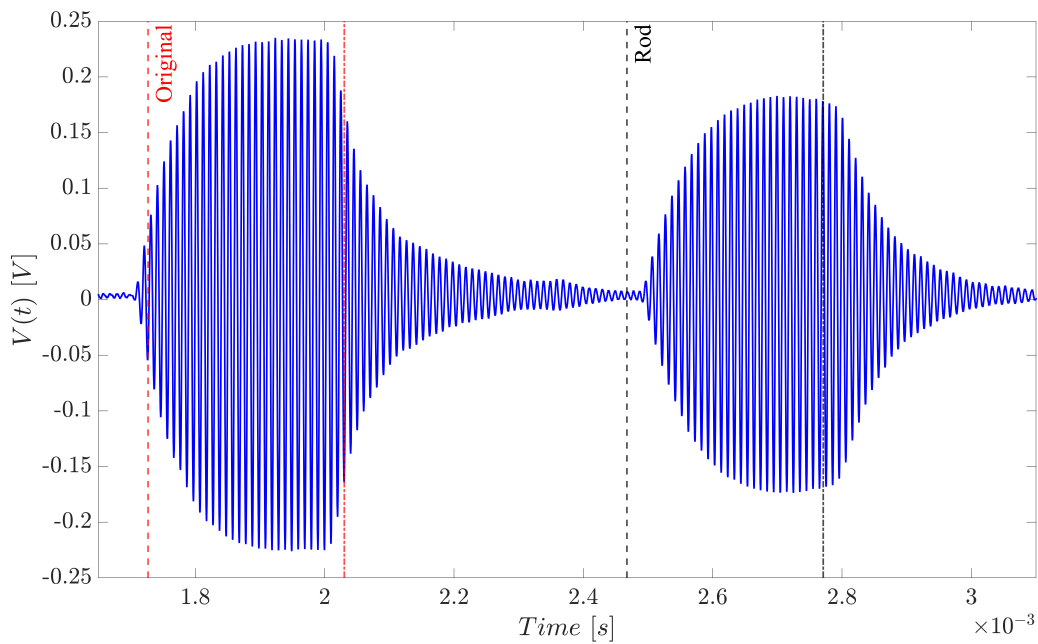


Figure 3.22: Reflection at θ_R equal to 80 degrees, a distance from the microphone to piezo-electric disk z_0 equals 600 mm, and a 30-cycle sine burst with frequency 98860 Hz.

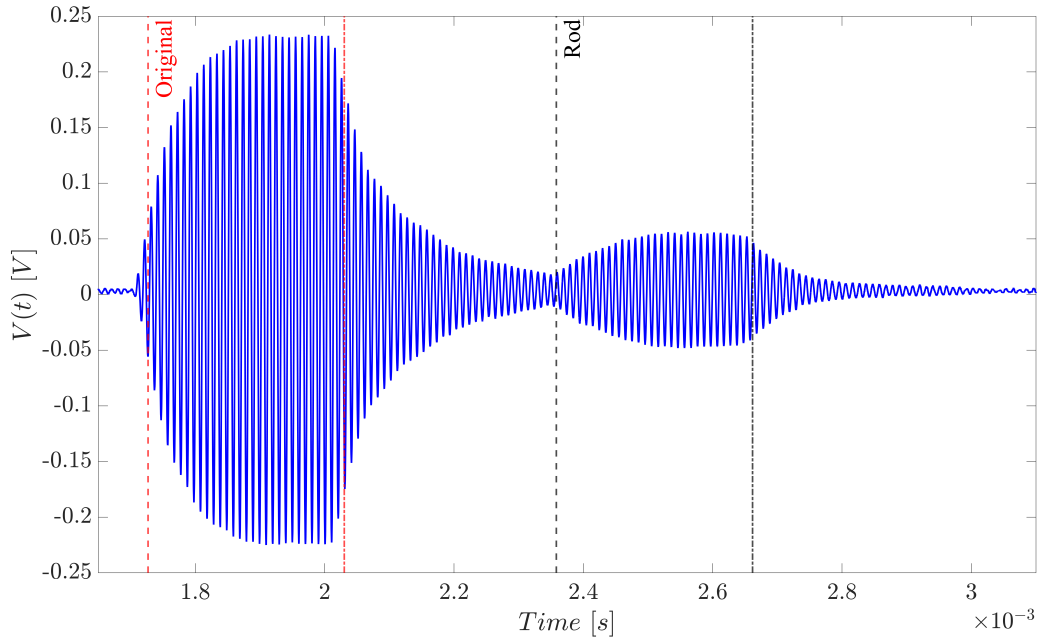


Figure 3.23: Reflection at θ_R equal to 90 degrees, a distance from the microphone to piezoelectric disk z_0 equals 600 mm, and a 30-cycle sine burst with frequency 98860 Hz.

3.7 Signal setup and processing

For all measurements performed in this work, the number of pulse cycles is set to 60. This selection is based on the arrival time of the first reflection from the vertical steel bar behind the transducer found in Sect. 3.6. To avoid reflection from other places in the measuring cage and give reflections from the cage time to die out and have no destructive effect on the measuring signal, a burst rate of 25 Hz is selected. This burst rate also gives the piezoelectric disk reverberations time to stop before the next cycle is sent out of the disk. The voltage out of the signal generator V_{0pp} is 1 V peak-to-peak and is selected to avoid non-linearities in the piezoelectric disk that can occur at high input voltages. Because analyzing a vast amount of signals in this work, there is a need to find a standard interval range for the measured acoustic signal $V_{5m}(t)$ to be Fourier-transformed, which gives good and repetitive results. After performing measurements and analyzing the acoustic voltage signal $V_{5m}(t)$ over a more extended period, it is observed that the time for the signal to reach a steady state is approximately 30 pulses. The end time of the signal interval to Fourier transform is set to 5 pulses before the estimated end of the signal to ensure the interval is within the transmitted signal and no transient part is included. All measurements performed in this work are averaged 128 times.

3.7.1 Transmitted signal

The transfer function H_{0m1}^{VV} in Eq. 2.21 is used to calculate the voltage V_1 across the electrodes of the piezoelectric disk by multiplying the transfer function with the Fourier-transformed measured voltage signal $V_{0m}(t)$. This measured voltage $V_{0m}(t)$ example is shown in Fig. 3.24, and to Fourier transform the signal, a steady state range is selected. This steady state range can change depending on the measuring frequency. The Fourier transform of the steady state range gives the voltage $V_{0m}(f)$.

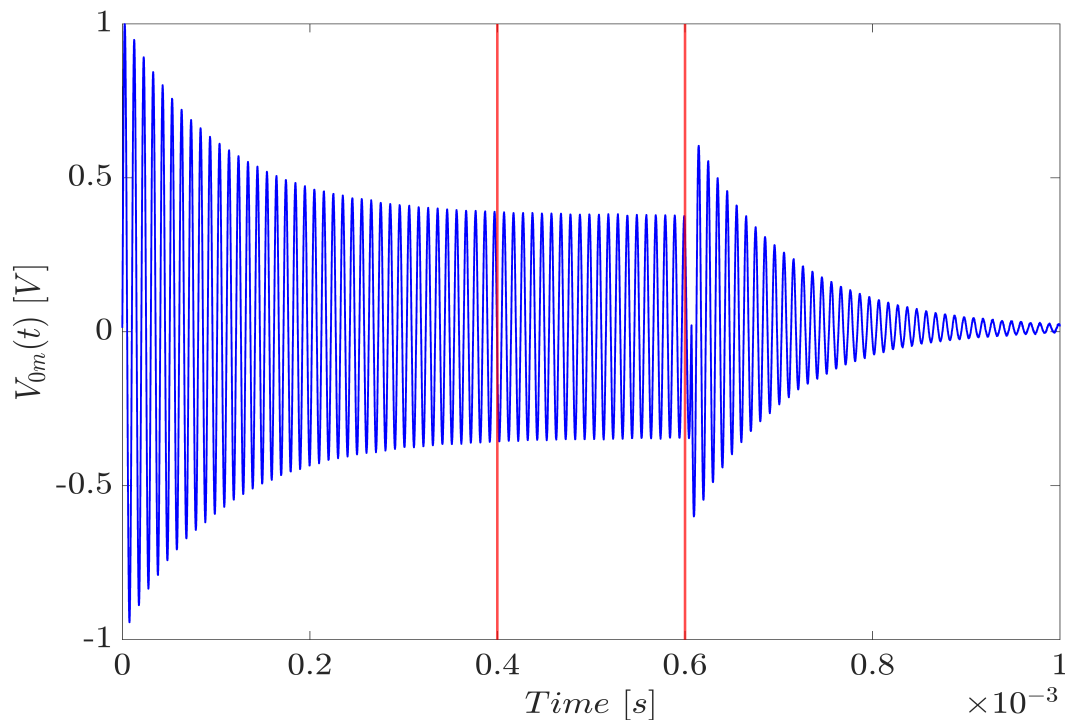


Figure 3.24: The measurement voltage $V_{0m}(t)$ measured at the input channel one on the oscilloscope with signal generator frequency and voltage $V_0(t)$ set to 98860 Hz and 1 Vp-p. The two red vertical lines represent the time interval's start and end, which is the interval that is FFT.

3.7.2 Received signal

The transfer function H_{55m}^{VV} in Eq. 2.29 is used to calculate the output voltage V_5 from the microphone by taking the Fourier transformed measured acoustic voltage signal $V_{5m}(t)$ and dividing it by the transfer function. This measured voltage $V_{5m}(t)$ example is shown in Fig. 3.25, and to Fourier transform the signal, a steady state range is selected based on observation of vast measurements. These observations led to the interval start of 30 pulses from the estimated arrival time and 5 pulses before the estimated end time. This interval is used for all angles and all distances from the microphone. The Fourier transform of the steady state range gives the voltage signal $V_{5m}(f)$

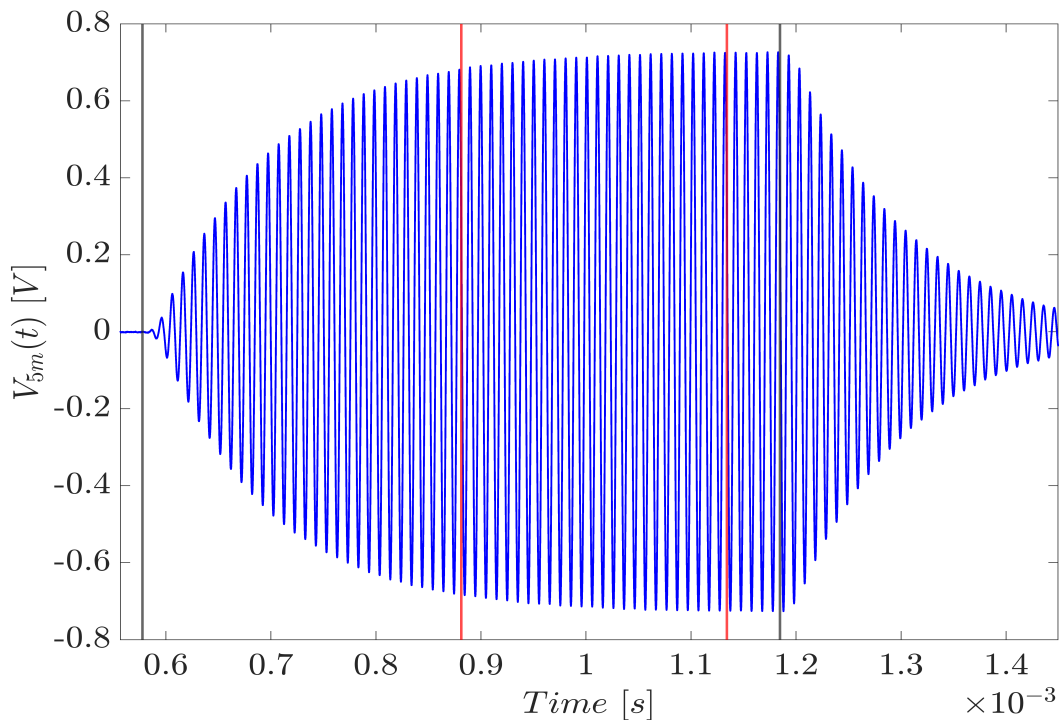


Figure 3.25: The measurement voltage $V_{5m}(t)$ measured at the input channel two on the oscilloscope with signal generator frequency and voltage $V_0(t)$ set to 98860 Hz and 1 Vp-p. The distance between the microphone and the piezoelectric disk Pz27 z_0 is 200 mm, and the rotation angle θ_R is 0 degrees. The first black vertical line represents the estimated arrival time of the signal at the microphone, and the second black vertical line estimates the end of the signal. The two red vertical lines represent the time interval's start and end, which is the interval that is FFT.

3.7.3 Signal filtering

The vertical resolution of the measured $V_{0m}(t)$ and $V_{5m}(t)$ depends on the vertical scaling selected and the oscilloscope's bit resolution. With 16-bit resolution, the signal is relatively good, but the waveform data can be somewhat choppy and uneven. To even out the vertical resolution of the measurement signal, a Savitzky-Golay filter [63] is used, which is a built-in function in MatLab's signal processing toolbox. A Savitzky-Golay filter tries to fit a polynomial of a selected degree to the dataset using a frame length to the date input vector, time, t , of a selected size. In this work, a fifth-degree polynomial is used for the measured signals and a frame length of 21. In Fig. 3.26, it is shown the effect of the Savitzky-Golay filter on a measured signal.

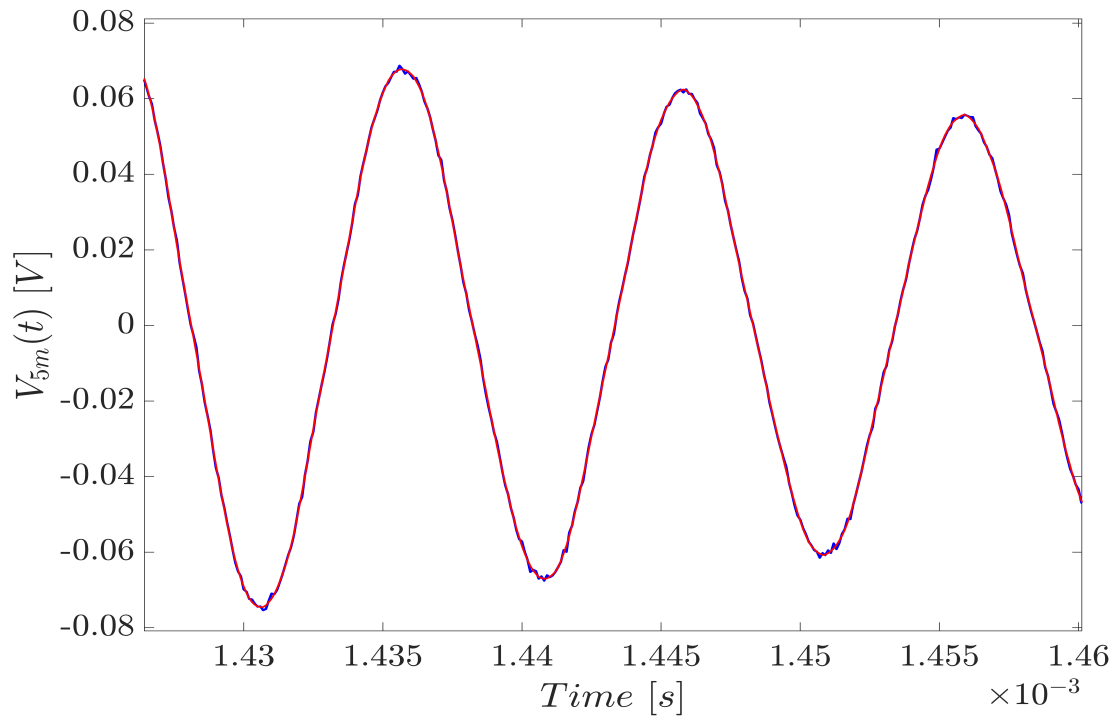


Figure 3.26: An example of measured receiver signal on input channel 2 of the oscilloscope filtered with Savitzky-Golay filter.

3.7.4 Method for calculating peak-to-peak voltage by using the fast Fourier transform

In this work, the Fourier transform method is used to convert a measurement signal that is filtered, DC-compensated, and range limited from being time-dependent to frequency-dependent,

$$V(t) \xrightarrow{FFT} V(f) . \quad (3.23)$$

The DC component is calculated by taking the mean value of the entire measured signal, which is given as

$$DC = \frac{1}{N} \sum_{i=1}^N V_{5m,i_{DC}} , \quad (3.24)$$

where N is the number of samples in $V_{5m_{DC}}(t)$, and $V_{5m,i_{DC}}$ is the discrete measurement sample amplitude. Then the DC component is subtracted from the signal as

$$V_{5m}(t) = V_{5m_{DC}}(t) - DC, \quad (3.25)$$

where $V_{5m_{DC}}(t)$ is the signal containing a DC component. The range limited area is further adjusted, such as the start and end of the interval falling in a zero point, such that it possesses an integer number of periods. The measured and range-limited signal transformed

from time-dependent to frequency-dependent is done with the built-in MatLab function FFT and by using zero padding five times the signal length. Zero padding increases the Fourier-transformed signal $V(f)$ vector's frequency resolution, leading to increased voltage accuracy for the exact applied transmitting frequency, as seen in Fig. 3.27. To find the peak-to-peak voltage of the FFT signal, the FFT signal $V(f)$ vector must be multiplied by four and divided by the number of bins of the FFT signal. It must be multiplied by four because the $V(f)$ vector is split between negative and positive frequencies, which halves the voltage amplitude, and a voltage amplitude is half the peak-to-peak value. This leads to the equation,

$$V_{5m_{pp}}(f) = \frac{V(f) \cdot 2 \cdot 2}{N_{bins}} = 4V_{5m}(f), \quad (3.26)$$

where $V_{5m}(f)$ is the vector output of the FFT, N_{bins} is the number of samples in $V(f)$, and the final result plotted in Fig. 3.27.

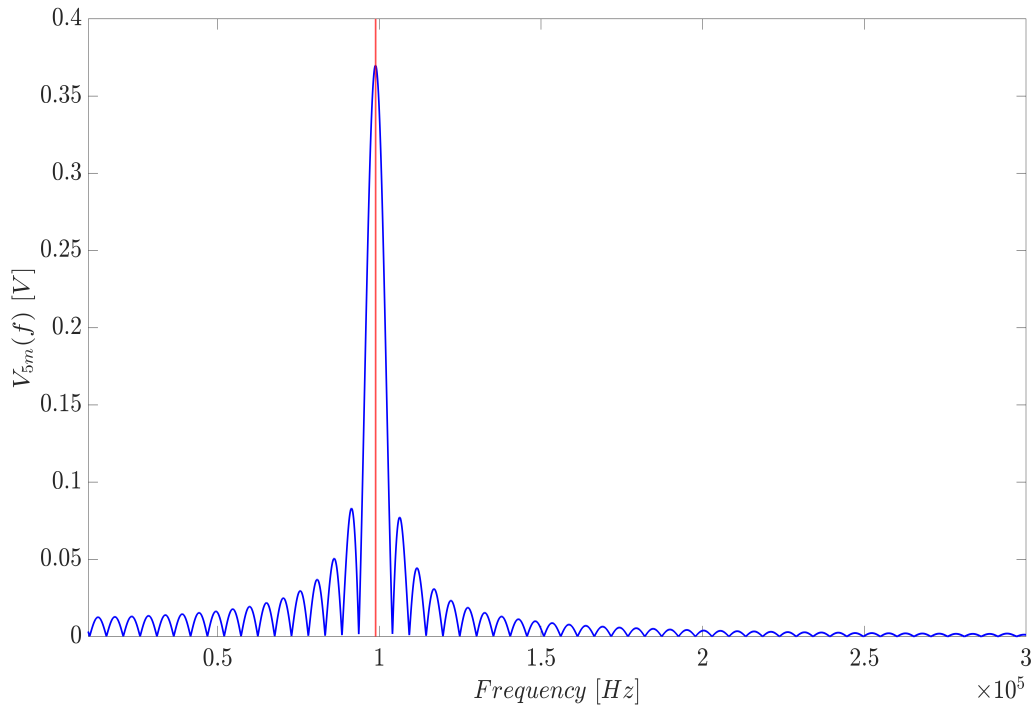


Figure 3.27: FFT of measurement receiver signal in Fig. 3.25 on input channel two of the oscilloscope filtered with Savitzky-Golay filter and with signal generator frequency and voltage $V_0(t)$ set to 98860 Hz and 1 Vp-p. The red vertical line marks the transmitting frequency 98860 Hz. The distance between the microphone and the piezoelectric disk Pz27 z_0 is 200 mm, and the rotation angle θ_R is 0 degrees.

3.7.5 Method of calculating pressure

In order to be able to calculate the peak-to-peak free-field pressure $p_{4pp}(f)$, the voltage $V_5(f)$ and the microphone sensitivity $|M_{cal}(f)|$, see Fig 3.15, for the transmitter frequency f must

be calculated. Then, the free-field pressure is calculated using measurement voltage and calibrated microphone sensitivity, which is

$$p_{4pp}(f) = \frac{V_{5pp}(f)}{M_{cal}(f)}, \quad (3.27)$$

where $p_{4pp}(f)$ is the calculated peak-to-peak free field pressure at the microphone.

3.7.6 Signal to noise ratio

This work uses the same method to calculate background noise as in previous works [29][48][24]. This method takes a time window with enough noise samples, which is about a 1 ms time window containing about 10 000 samples just before the transmission signal's estimated arrival. With the time window selected, the background noise is calculated by the root-mean-square-voltage as

$$V_{rms}^{noise} = \sqrt{\frac{1}{N} \sum_{i=1}^N (V_{5m,i} - \hat{V}_{5m})^2}, \quad (3.28)$$

where N is the number of samples of the measurement voltage signal interval $V_{5m}(t)$, $V_{5m,i}$ is the voltage value of a single sample, and \hat{V}_{5m} is the mean value of the voltage signal. Furthermore, the acoustic measurement signal $V_{5pp}(f)$ is calculated for the frequency of transmitted signal, which is further used to calculate the root mean squared voltage of the measured signal as

$$V_{5rms} = \frac{V_{5pp}(f)}{2\sqrt{2}}, \quad (3.29)$$

where V_{5rms} is the root mean squared voltage of the received acoustic signal. With the root mean squared voltage of the acoustic signal and background noise, the signal to noise [12] can be calculated as

$$SNR = 20 \log_{10} \left(\frac{V_{5rms}}{V_{rms}^{noise}} \right). \quad (3.30)$$

Chapter 4

Positioning setup and measurements with the MatLab app

At the beginning of this work, it was not possible to control the air setup's X, Y, Z, and R-stages through MatLab and has instead been controlled through the motion controller software PIMikroMove. In previous works, this has led to all measurements performed over different positions, such as directivity, on-axis pressure, and 2-D horizontal pressure field, being measured manually, which are highly time-consuming. If the measurement had only been over a few different positions, it would not have been a problem to manually move the position of the stages through PIMikroMove. However, automation is a must due to a single 2-D horizontal pressure field measurement consisting of nearly 10 000 different position measurements, where one measurement manually takes at least 20 seconds. There have previously been able to control some of the stages through MatLab. However, after the years have passed, the company Physik Instrumente no longer supports updates for some of the stages, which has led to communication problems for MatLab with the stages. This issue occurred because MatLab could not read a C++ script, and this issue is resolved in this work.

This chapter goes through the Matlab app designed to easily control the air setup's X, Y, Z, and R-stages in Sects. 4.1 and 4.2, and find the correct position of the piezoelectric disk relative to the microphone with a setup wizard in Sect. 4.3. The Matlab app is also designed to take individual measurements directly through the app or load a set of measurement parameters and start a measurement series, see Sect. 4.4. Starting a measurement series is the automation part, where the app takes in parameters through **MeasurementParameters.m** shown in Appendix A.3 and performs the measurements based on the given parameters. The app then takes the measurement results and saves them into a specified folder in an organized manner. The app also has built-in codes for safety to stop the motions of the machine, preventing undesirable crashes and personal injury or material damage. The app's script is included in Appendix B. Sect. 4.5 describes the importance of positioning the piezoelectric

disk and what uncertainty the positioning entails.

4.1 MatLab app screen

The first showing when the air controller is opened is the app's screen, see Fig. 4.1. This screen contains buttons, labels, LEDs, input fields, and a text window.

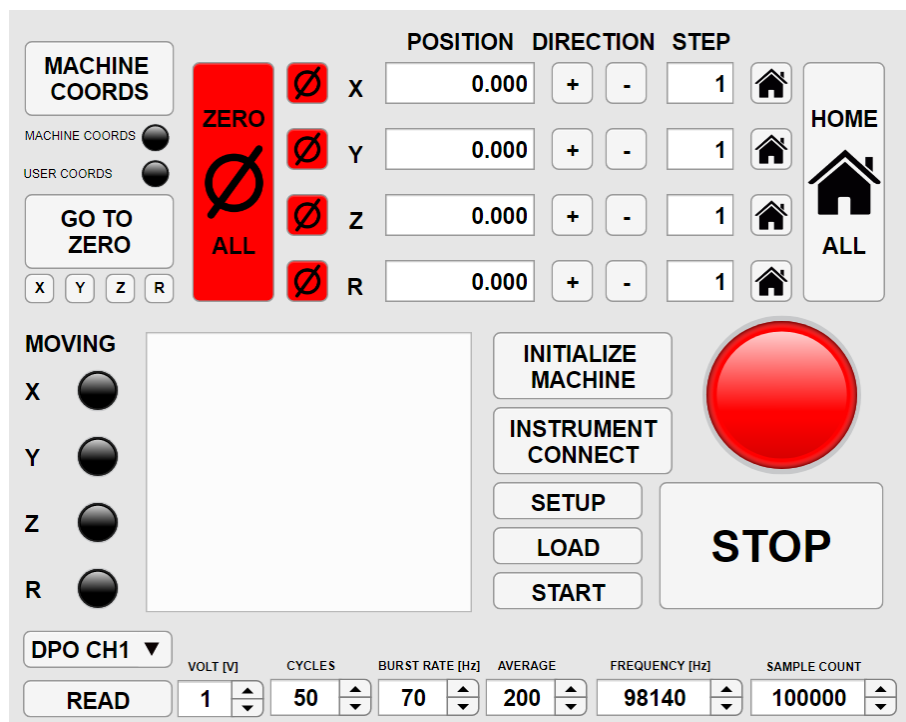


Figure 4.1: The MatLab Air Controller app's screen.

Buttons are an essential element of the app. Pressing one of the buttons executes an action, such as the stop button, see Fig. 4.2a, which stops the motion of the stages and halts all actions until the restart button is pushed, see Fig. 4.2b. All buttons use functions inside the Matlab app.



Figure 4.2: (a) Stop button and (b) Restart button. If the stop button is pushed, all motions of the stages stop and halt all actions, and the stop button turns into a restart button. The control over the app is regained when the restart button is pushed.

Labels serve as informative text. They can be constant, like all labels, not on a button. Labels on buttons can either be constant or change depending on the state of a button. An

example of such a state change is the stop/restart button in Fig. 4.2. LEDs show a current state or action being active or not by either being on (green) or off (red/black), see Fig. 4.3, and the app automatically updates the LED's state.

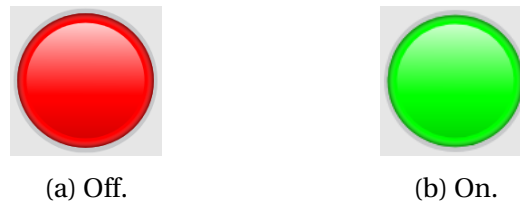


Figure 4.3: Indicates if the stop button is active or not. (a) The stop button is pushed if it is red and prevents stages movements. (b) If the LED is green, the system is up and running.

Input fields are fields with values that can be manually changed, and an example of a changeable input value is a step value, see Fig. 4.4. A step is a value related to travel distance, where one step is the same as one millimeter.



Figure 4.4: One out of the four input fields for step.

The text window is to display actions in the form of text. The text window is the white field in Fig. 4.1 or shown with information as in Fig. 4.5. It helps keep track of all actions, such as informing about the estimated time of completion of a measurement series. A log is kept for all messages displayed in the text window. If anything happens, such as the PC turning off, instruments freezing, or MatLab crashing, the app log can contain the last information displayed in the text window. In case of a failure happens in a middle of a large measurement series, the last known position can be extracted from the log, and the measurement series can quickly be resumed at the last known position.

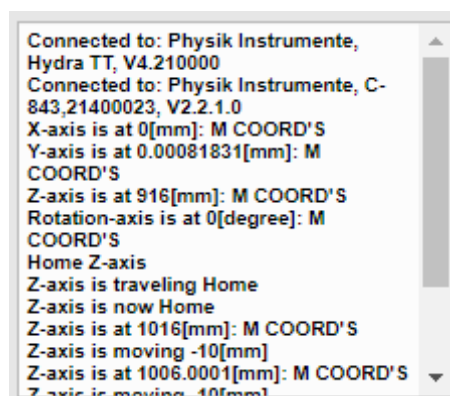


Figure 4.5: Text window with an illustration of live information from the action performed in the app.

4.2 Startup of the MatLab app

When starting the air controller app and the screen in Fig. 4.1 is displayed, certain steps must be taken to ready the measurement setup for measurements. The first action is initializing the machine with the button in Fig. 4.6. The initialize machine button is a function (Appendix B.2) that sets up a connection between the Hydra TT motion controller and PC and between the C-843 motion controller and PC, as illustrated in Fig. 3.16. The initialize machine button also assigns the correct parameter values, such as velocity and acceleration, to the stages. Parameters and other values assigned to the stages are within the script in Appendix B.2.

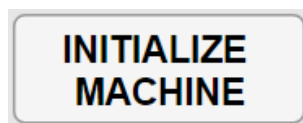


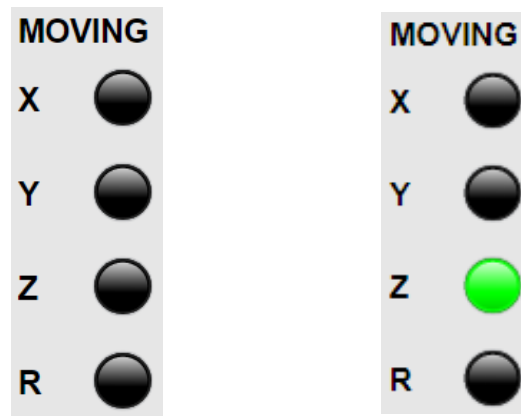
Figure 4.6: The initialize machine button.

After pressing the initialize machine button, all stages need to be "homed" with the home all button, Fig 4.8a, or the individual home button, Fig 4.8b. The home all button is a function (Appendix B.3) that starts a sequence in the following order Z, R, X, and Y-stage to search for their respective reference point. The search for a reference point is when the stage moves as far as possible in a specific direction until induction sensors detect that the stage is at its farthest limit range it can travel. At this limit, the position of the machine coordinates for each stage is defined as the reference point and given in Table 4.1. In the same Table 4.1, the travel limits of the stages are also given.

Table 4.1: Individual stages reference point after a homing function is run, and the individual stages travel range given as lower and upper limit.

	Reference point	Lower limit	Upper limit	Unit
X-stage	0	0	300	[mm]
Y-stage	0	0	300	[mm]
Z-stage	1016	0	1016	[mm]
R-stage	0	-Inf	Inf	[degrees]

Whenever the stages search for a reference point or move in general, the LEDs in Fig. 4.7 indicate which stage is moving.

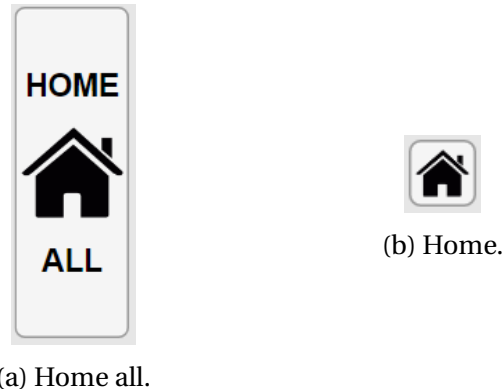


(a) No stages in motion.

(b) Z-stage is moving.

Figure 4.7: Indicates the movement of the stages. If the stage is in motion, the LED is green. No light, no motion.

The individual home button executes the same function as the home all button, but "homes" only the stage associated with the button. The great thing about the reference points is that they are repeatable. This means if the app is closed with Z-stage at the machine coordinates 500 mm, and the app is opened again, the machine coordinates 500 mm of the Z-stage can be found by first using homing function and then traveling from reference points to the machine coordinates 500 mm.



(a) Home all.

(b) Home.

Figure 4.8: The home all button (a) and the individual home button (b).

With all stages "homed", the user coordinates need to be found. User coordinates are an offset value from reference points, where the user coordinates are set to 0 mm at this offset. Setting the coordinate to 0 mm means that if the machine coordinates for Z-stage are at 500 mm, and the zero button for that individual stage is used, Figs. 4.9c/4.9d, the user coordinates will display this coordinate position as 0 mm in the app screen position field (Fig. 4.1). If this stage is moved 10 steps with writing 10 in the input field shown in Fig. 4.4 and moved in the positive direction with the (+) button seen in the app screen in Fig. 4.1, the user coordinates would display 10 mm, and the machine coordinates would display 510 mm for that individual stage.

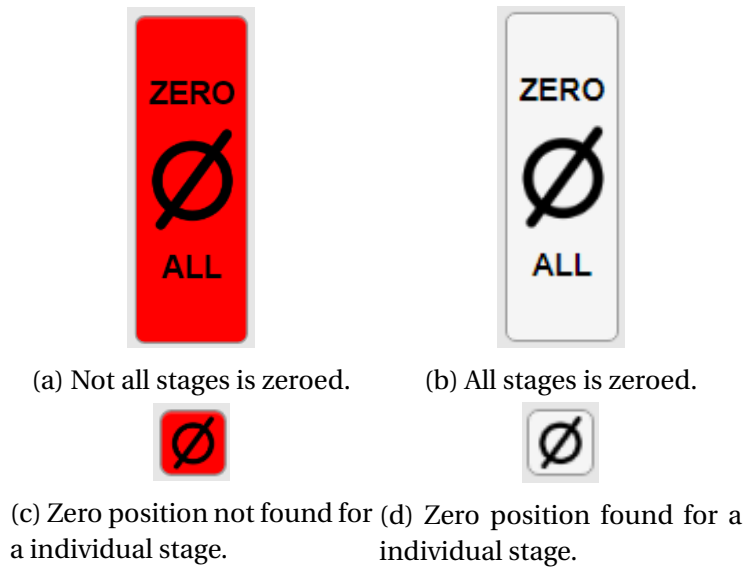


Figure 4.9: The zero all button (a)/(b) sets all current positions of stages to 0 mm in the user coordinates. If it is white (b), it indicates that all stages are zeroed, and (b) indicates that some or all stages are not using offsets from reference points. The zero button (c)/(d) sets the current position of the individual stage to 0 mm in the user coordinate. If it is white (d), it indicates that the stage is zeroed, and (c) indicates that it is not using offsets from reference points.

The button in Figs. 4.10a/4.10b can be used to switch between machine and user coordinates, and the label on the button and the LEDs in Fig. 4.11 will change depending on which coordinate system is active.



Figure 4.10: (a) indicates that the machine coordinates are active. If pushed, it turns into (b) and indicates that the user coordinates are active.

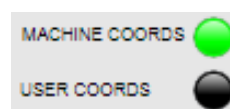


Figure 4.11: Indicates the active coordinate system. In this figure, it is the machine coordinates system that is active.

4.3 Positioning of the piezoelectric disk

User coordinates are used to find zero coordinates for X, Y, and Z-stages that are as close as possible to the origin of the X, Y, and Z axis defined in Fig. 2.4 and to avoid the effects that can

occur, which is described in Sect. 4.5. The user coordinates for the R-stage θ_R is zeroed when the piezoelectric disk's Z-axis is parallel with Z-stage. To find these coordinates, the setup wizard is used by pushing the setup button in Fig. 4.12.

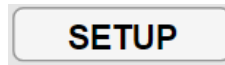


Figure 4.12: The setup button

This setup wizard provides guidance, and a choice of five setups, as seen in Fig. 4.13, where: the setup one is used to find θ_T , see Figs. 4.19 and 4.32; the setup two is used to find σ , see Figs. 4.23 and 4.37; the setup three is used to set θ_R equals 0 degrees; the setup four is used to find the distance z_0 ; the setup five is used to find θ_T and z_0 and calculate constants of a slope such that the position of the microphone is adjusted respect to θ_T and the distance z_0 such that angle θ_T equals θ_M , see Fig. 4.33, for all distances between the microphone and piezoelectric disk. However, this work never used setup five and linear compensation, and compensation was always turned off.

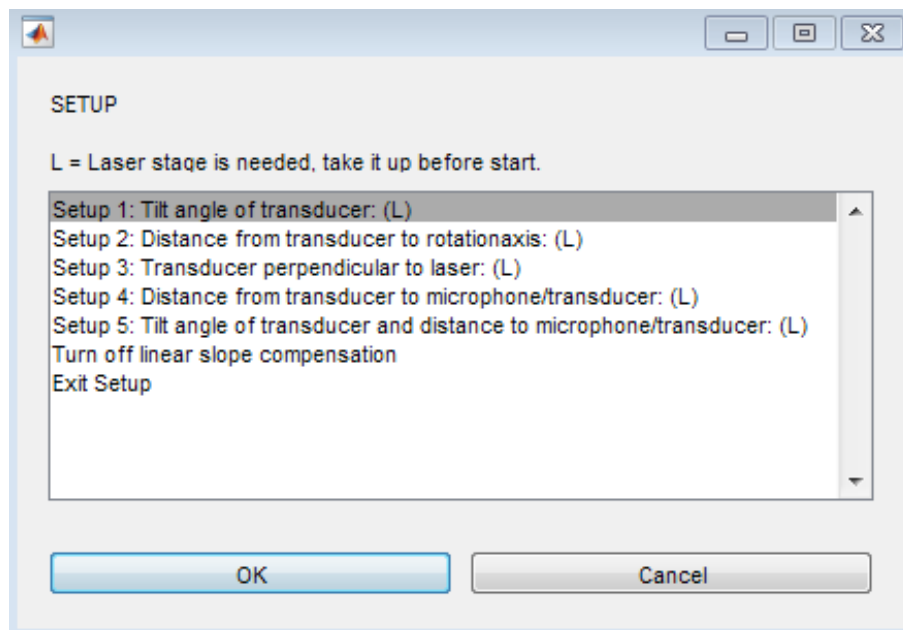


Figure 4.13: Setup wizard that makes the user able to choose different setups.

In Fig. 4.13, it says L equals laser stage (see Fig. 3.6 (D)), which is the laser stage set up by [7], and the laser sensors are of the type LK-G32 from Keyence used with a controller LK-G3001PV and listed in Table 3.2. For all the setup choices, the laser stage needs to be elevated all the way up before starting to measure. The distance d_x denoted in Fig. 4.14 is the distance between the two fronts of the lasers and calibrated by [7] and given in Table 4.2. In Table 4.2, there are also listed key features of the lasers. The distance denoted d_{ref} equals 30 mm and is the reference distance. From d_{ref} , the measuring range of the laser is ± 5 mm.

When measuring with lasers 1 and 2, they measure a distance d_1 and d_2 , which are negative values for distances from the laser front to the object that are greater than d_{ref} or positive if the distance is less than d_{ref} .

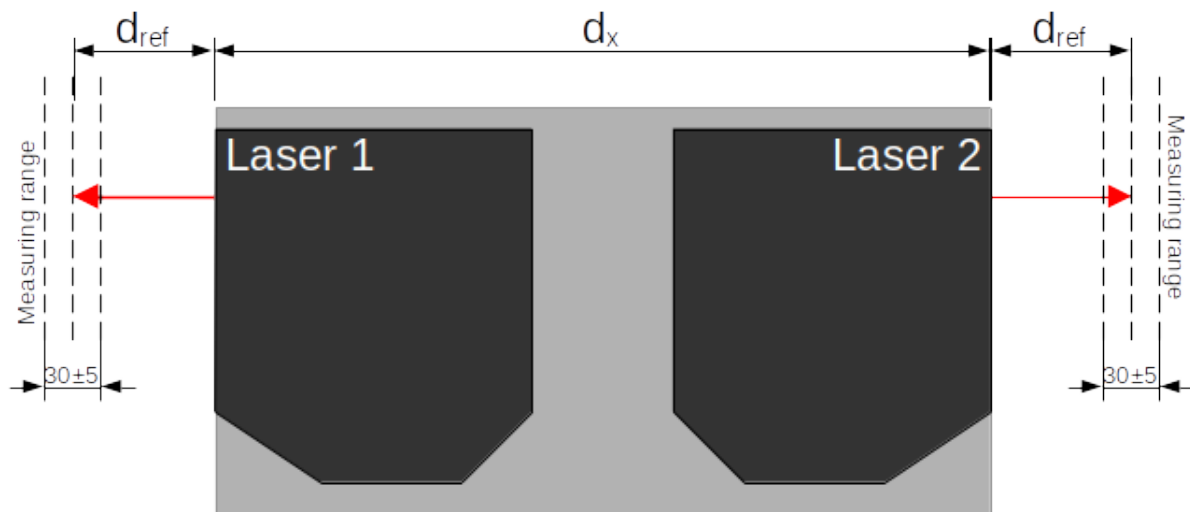


Figure 4.14: Schematic of the two lasers LK-G32 and illustrating the measuring ranges. The distance d_{ref} is the reference distance of 30 mm, and d_x is the distance of 182.5692 mm between the two laser fronts. [35]

Table 4.2: Different key features of the two lasers LK-G32, given in [35], and the distance d_x is the calibrated distance by [7].

LK-G32 laser sensor		Unit
d_x	182.5692	[mm]
d_{ref}	30	[mm]
Range	± 5	[mm]
Spot diameter	Approx. $\varnothing 30$	[μm]
Linearity	$\pm 0.05\%$ (of full scale = ± 5 mm)	[-]
Repeatability	0.05	[μm]
Light source	(viable light) 655	[nm]

4.3.1 Setup 1

For all setup choices in Fig. 4.13, the Z-stage moves in front of the laser after clicking the measure button in Fig 4.15.

MEASURE

Figure 4.15: The measure button.

When the Z-stage has arrived in front of the laser and the piezoelectric disk is within the laser's measuring range, as illustrated in Fig. 4.16, the laser's software opens.

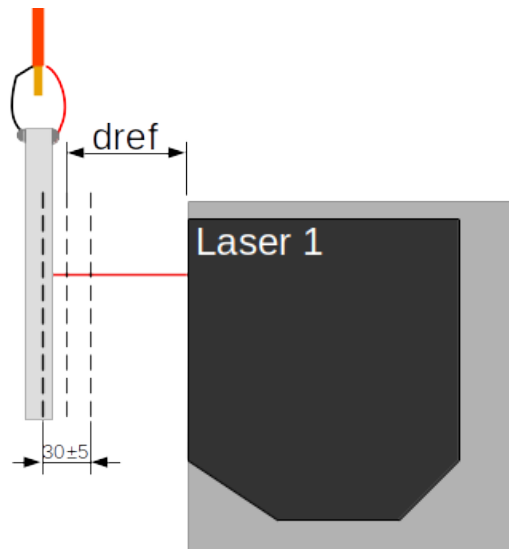


Figure 4.16: Side view of the piezoelectric disk being within the laser 1 measuring range.

The laser software that came with the purchase of the lasers is called LK-navigators. This LK-navigators screen is seen in Fig. 4.17.

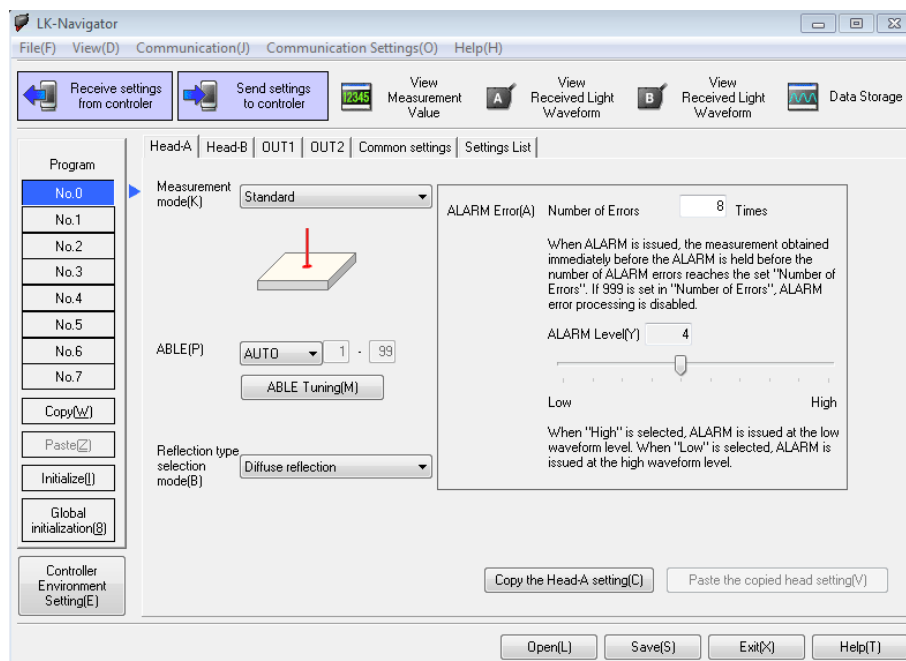


Figure 4.17: LK-navigator screen from Keyence.

Adjustment screws on the laser stage are used to move the laser point to the highest point of the piezoelectric disk front surface. The disk must be slightly rotated, clock, or counterclockwise, so the solder lump is not at the highest point of the disk's front surface. By clicking the

view measurement value from the LK-navigator screen and clicking the measurement value acquisition start, see Fig. 4.18, it starts averaging the distance d_{11} value from the reference distance d_{ref} . The measured value is then written into an open GUI, and measurements are repeated at the bottom of the disk's front surface, measuring d_{12} , see Fig 4.19

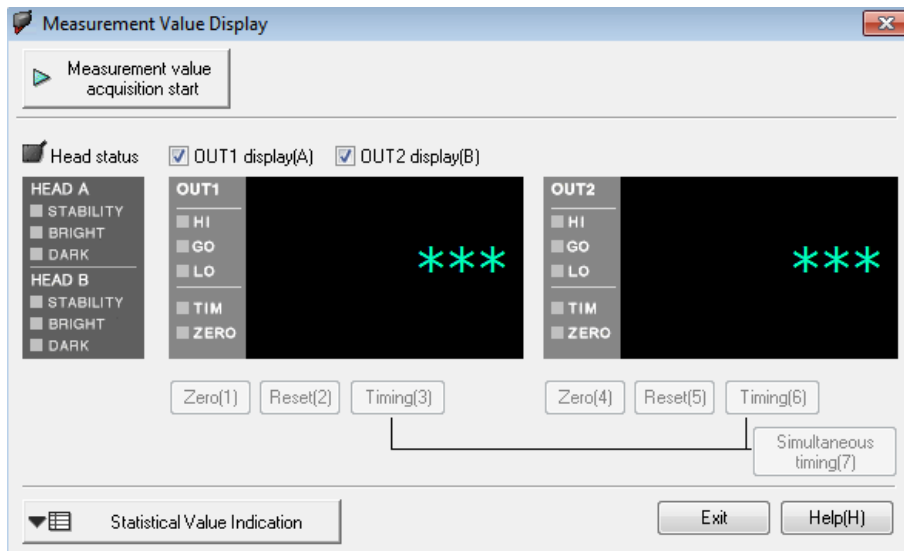


Figure 4.18: LK-navigator measurement value display.

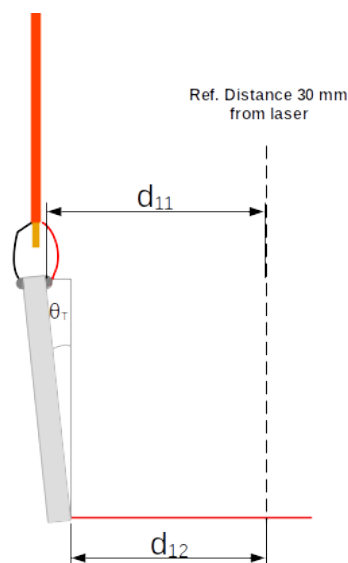


Figure 4.19: Side view of the tilt angle θ_T of the piezoelectric disk relative to the laser one beam direction and distances d_{11} (highest point) and d_{14} (lowest point).

After measuring the top and bottom distances and inserting the diameter of the piezoelectric disk in the open GUI (Graphical User Interface), the app calculates the tilting angle θ_T with the equation

$$\theta_T = \sin^{-1} \left(\frac{d_{12} - d_{11}}{d} \right), \quad (4.1)$$

where d is the diameter of the disk. With known angle θ_T , and if the angle of the piezoelectric disk is more significant than 0.5 degrees, the tilt is adjusted, and the setup one is repeated. This tilt is manually adjusted, and the goal is to get the angle as small as possible. This adjustment reduces the effect of θ_T modeled in Sect. 4.5 is not significant in the measuring frequency range up to 300 kHz.

4.3.2 Setup 2

Before starting this setup, it is essential to get the middle of the vertical rod and horizontal rod, which is attached to the R-stage, and the pointy bolt on the R-stage, which is aligned with the R-stage rotation axis, to construct a vertical plane in between them. The reason for creating this plane is to create a parallel plane with the YZ-stage plane. This opens up to move the front center of the piezoelectric disk with the 3-D-printed part that now moves in the XZ-stage plane, see Fig. 4.20. Then the Y-axis, which passes through the front center of the disk, is defined in Sect. 4.5 can be moved as close as possible to the R-stage axis of rotation after finding σ .

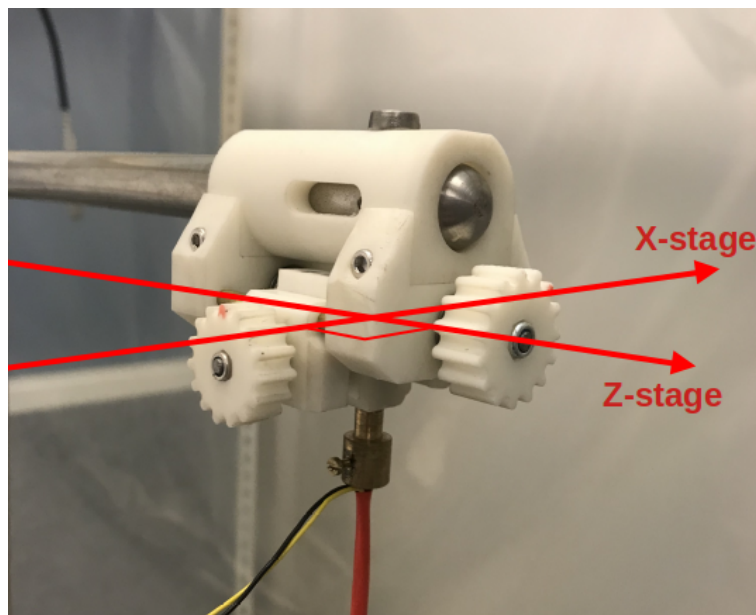


Figure 4.20: Movement of the piezoelectric disk front center in the XZ-stage plane with 3-D printed part adjustment screws.

A vertical laser is used to find this vertical plane passing through the rods and the bolt, see Fig. 4.21. First, in Fig. 4.21a, the vertical laser overlaps the black line on a white tape in the back of the measuring cage that has the same distance to the Z-stage as the pointy bolt. Secondly, in Fig. 4.21b, a piece of paper behind the pointy bolt is used to see the casted shadow of the bolt tip being in the center of the laser line. And lastly, in Figs. 4.21c and 4.21d, The laser line is in the middle of the vertical and horizontal rod.

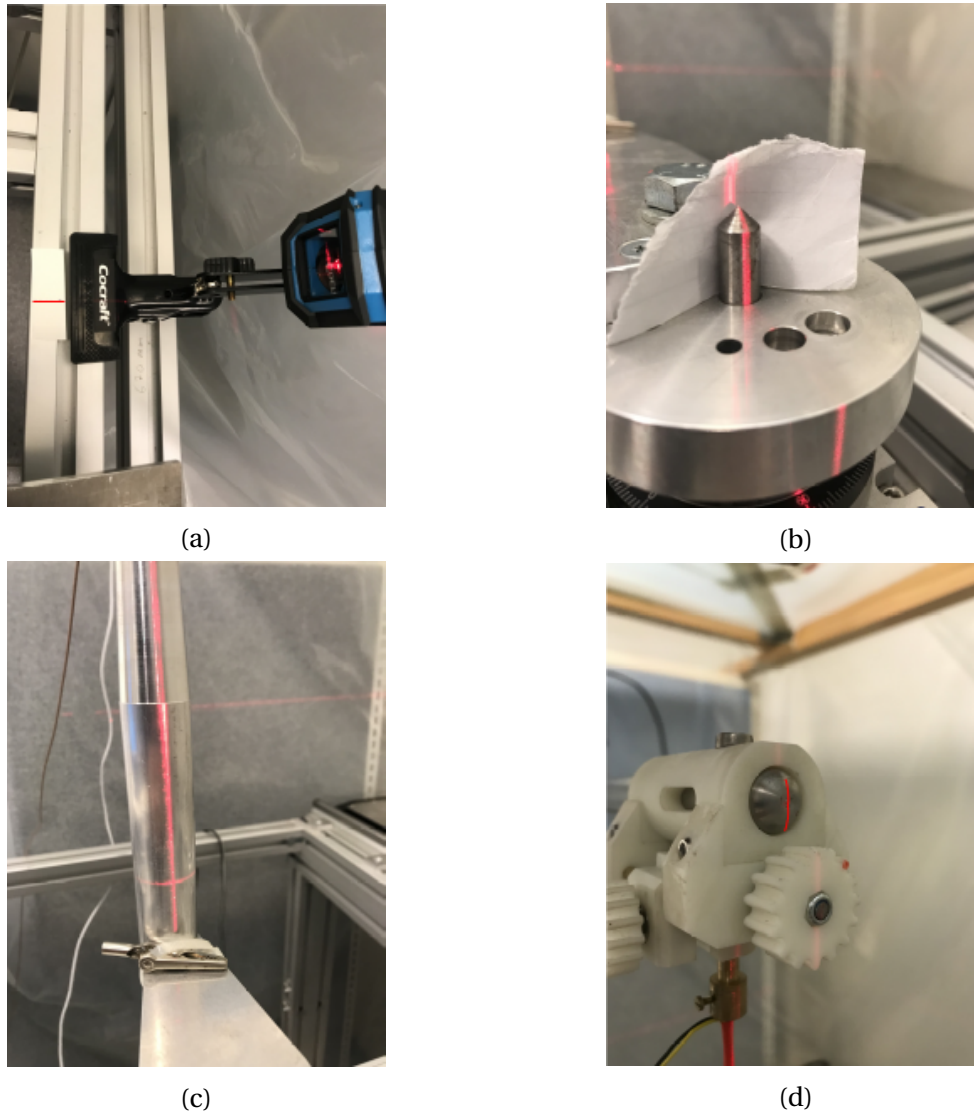


Figure 4.21: Illustrating the vertical laser creating the vertical plane parallel with the YZ-stage plane by laser (a) overlapping the black line on a white tape in the back of the measuring cage, (b) casted shadow of the bolt tip being in the center of the laser line, (c) and (d) the laser line is in the middle of the vertical and horizontal rod.

When selecting setup two, the procedure is the same as the setup one. Instead of measuring the piezoelectric disk front surface's highest point d_{11} and lowest point d_{12} distances, it is measured on the front surface farthest right side of the disk d_{13} and left side d_{14} , see Fig. 4.22. The measured values and diameter d is written into an opened GUI. The app calculates the θ_r as

$$\theta_r = \sin^{-1} \left(\frac{d_{13} - d_{14}}{d} \right). \quad (4.2)$$

Furthermore, θ_r is used in the subsequent calculations to determine the distance σ to the R-stage rotation axis.

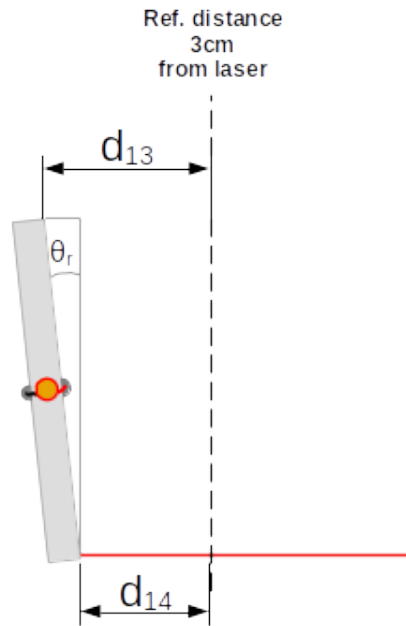


Figure 4.22: Top view of the rotation angle θ_r of the piezoelectric disk relative to the laser one beam direction and distances d_{13} (farthest right point) and d_{14} (farthest left point).

Then following three distances in Fig 4.23 are measured. First distance, d_{15} on the piezoelectric disk front center surface, and the result is written into the open GUI. The R-stage then rotates with an angle θ_R equals γ , then the second distance d_{16} is measured without adjusting the laser's position. It is worth noting that gamma is a negative angle because R-stage rotates in a clockwise direction which is a negative direction. Then the last distance, d_{17} , is measured after adjusting the laser stage position by moving the laser point back to the disk's center, and the results are written into the open GUI. Fig 4.23 illustrates these three measurements.

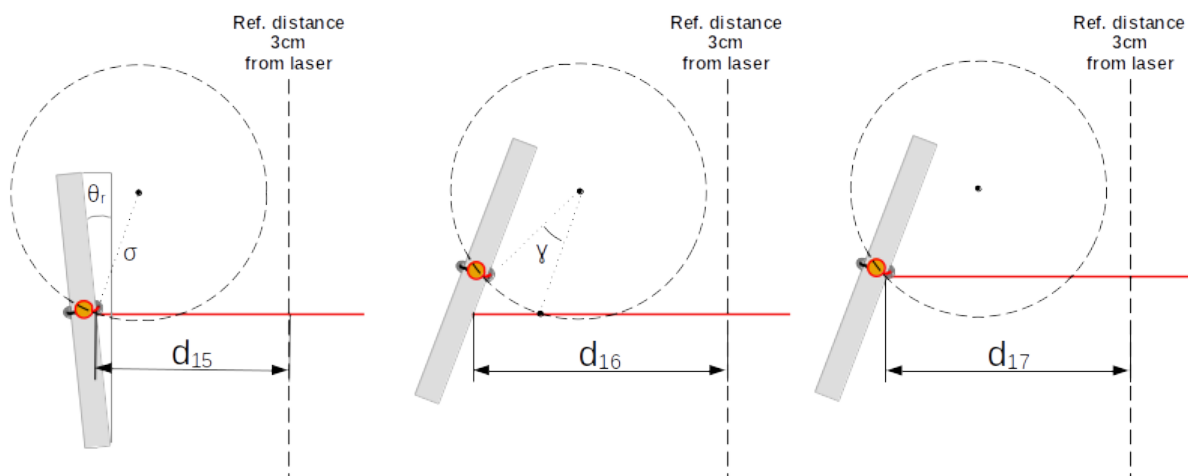


Figure 4.23: Illustration of the three measured distances d_{15} , d_{16} , and d_{17} , where σ is the distance between the center of the piezoelectric disk and the horizontal distance to the R-stage rotation axis and γ is the θ_R rotation angle.

With these three distances measured, d_{15} , d_{16} , and d_{17} the app can calculate the distances X_{mov} and Z_{mov} , which are the distances to move the piezoelectric disk front center with adjustment screws of the 3-D printed part seen in Fig. 4.20. This movement of the front surface will reduce the distance σ and its effect analyzed in Sect. 4.5. By illustrating this trigonometric problem first, as in Fig. 4.24, and calculate the distance a as

$$a = \frac{d_{16} - d_{17}}{\tan(\theta_r + \gamma)} \quad (4.3)$$

where $d_{17} - d_{16}$ equals the opposite distance of the triangle with angle $\theta_r + \gamma$ in Fig 4.24, θ_r is the calculated value from Eq. 4.2 and γ is the rotated angle by R-stage.

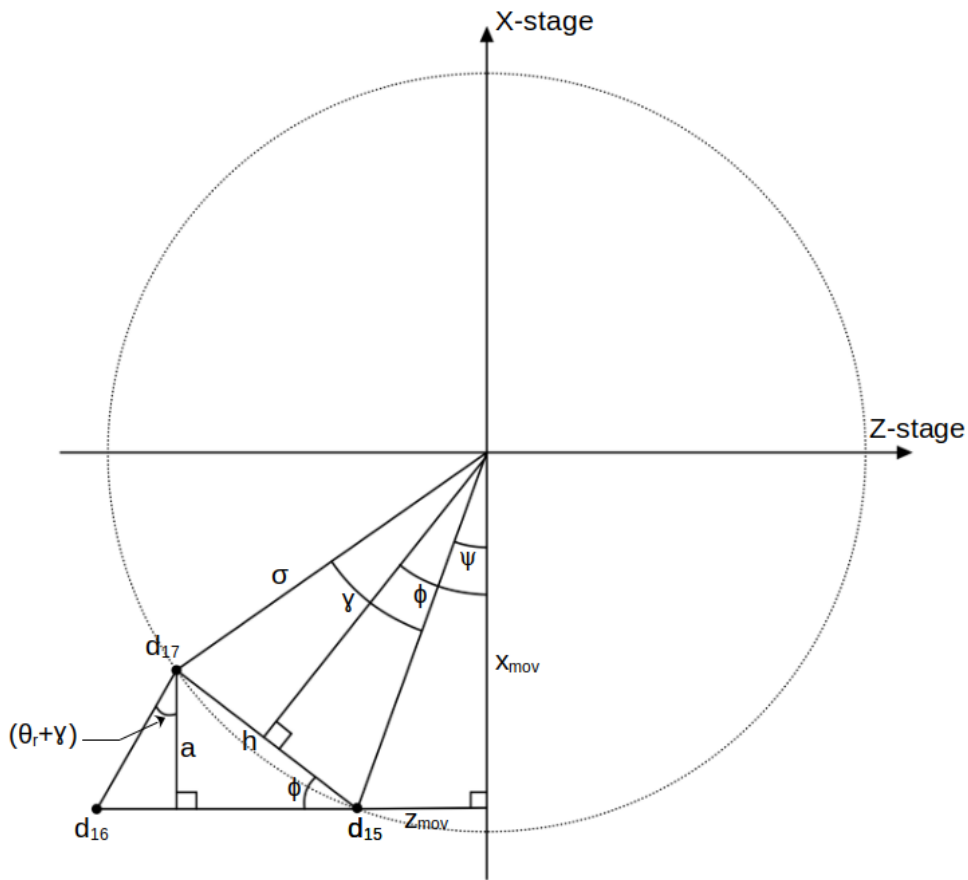


Figure 4.24: Trigonometric problem used in calculating the movement distances X_{mov} and Z_{mov} , which is used to reduce the distance σ . The distances d_{15} , d_{16} , and d_{17} are the measured distances and are marked as three points. The angle θ_r is a calculated angle from measurements, and γ is a (negative) rotation angle of the R-stage. The angle ϕ and ψ are calculated angles.

Then the angle ϕ in Fig. 4.24 is calculated by using the calculated distance a and the distance d_{15} and d_{17} as

$$\phi = \tan^{-1} \left(\frac{a}{d_{15} - d_{17}} \right), \quad (4.4)$$

where $d_{15} - d_{17}$ is the adjacent distance of the smaller triangle with angle ϕ in Fig. 4.24. Furthermore, the hypotenuse distance h for this same triangle is calculated as

$$h = \frac{d_{15} - d_{17}}{\cos(\phi)}. \quad (4.5)$$

Now, the angle ψ and radius σ in Fig. 4.24 can be calculated by using the distances a , and h , and the angle, ϕ , which gives

$$\psi = \phi - \frac{|\gamma|}{2}, \quad (4.6)$$

and

$$\sigma = \frac{h/2}{\sin(\gamma/2)}. \quad (4.7)$$

Then it is easy to calculate the distances X_{mov} and Z_{mov} by using the calculated radius σ and the angle ψ , which gives

$$X_{mov} = \cos(\psi)\sigma, \quad (4.8)$$

and

$$Z_{mov} = \sin(\psi)\sigma. \quad (4.9)$$

After finding the X_{mov} and Z_{mov} distances with Eqs. 4.8 and 4.9, the app calculates the rotation of the 3-D printed part in Fig 4.20 adjustment screws to move the front center of the piezoelectric disk to the R-stage rotation axis and reduce the effects of σ . By using the model in Sect. 4.5, and analyzing the results for different values of σ and the angle α , it is found that for σ equal to 2 mm, the effects are insignificant in the measuring frequency range up to 300 kHz.

4.3.3 Setup 3

In this setup, the same method is used for finding θ_r as in setup two. The difference is that θ_r is now used to straighten up the R-stage of the measured angle, so the piezoelectric disk surface is now perpendicular relative to the laser one's beam. When the piezoelectric disk is perpendicular to the laser beam, the R-stage is zeroed such that θ_R is equal to 0 degrees in the user coordinates. This angle for θ_R is now saved into a zero.mat file such that the angle is stored safely in case of computer failure. In case of failure, these coordinates are loaded into the app with the load button in Fig. 4.25.

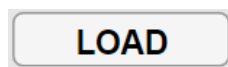


Figure 4.25: The load button.

4.3.4 Setup 4

The last setup used is setup four, which is used to find the distance between the piezoelectric disk front surface and the microphone. This measurement is illustrated in Fig. 4.26. Before selecting this setup, the laser position is adjusted such that the laser point is in the center of the piezoelectric disk. After selecting setup four, the app asks to move the X and Y-stage to position the microphone's center in the laser.

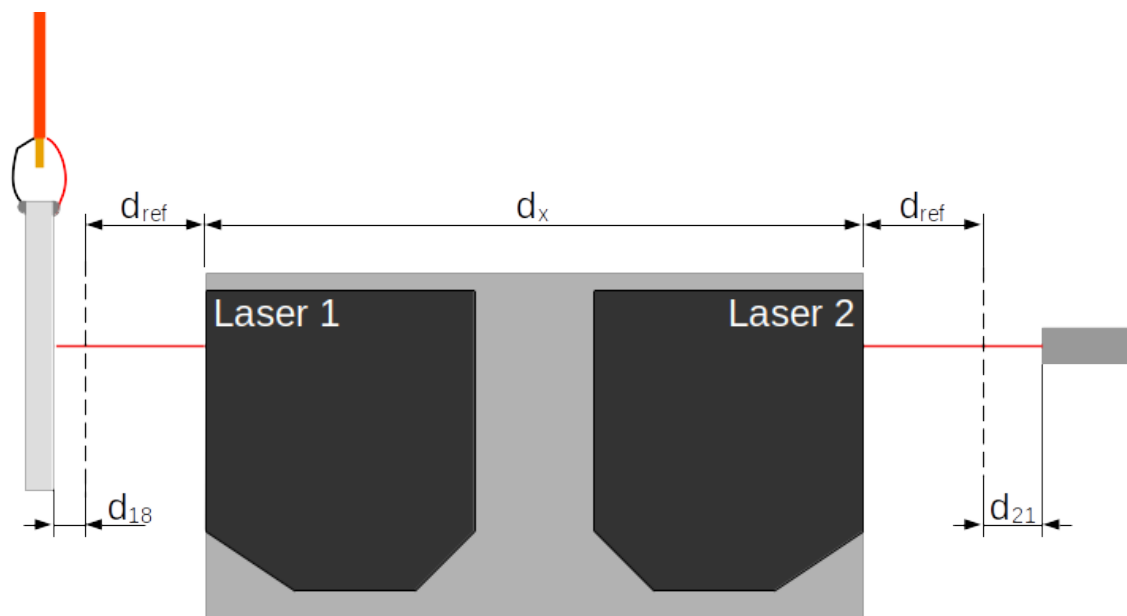


Figure 4.26: Illustration of laser stage measuring the distance between the piezoelectric disk (left side) and the microphone (right side).

With the laser in the center of the disk and microphone, the X and Y-stage are zeroed, setting the user coordinates equal to 0 mm. Then by clicking the measure button in Fig. 4.15, the LK-navigator software opens and is used as described earlier, and then the distances d_{18} and d_{21} in Fig. 4.26 are measured, and the results are written into the open GUI. The app calculates the total distance between the transducer and the microphone as

$$d_{tot} = (d_{ref} - d_{18}) + d_x + (d_{ref} - d_{21}) \quad (4.10)$$

where d_{ref} and d_x distances are given in Table 4.2. The app then uses d_{tot} to take the current machine coordinate of the Z-stage and subtract that position with d_{tot} , and that result is set as Z-stage user coordinates to equal 0 mm. When all the setup wizards are completed, the exit setup in Fig. 4.13 is chosen, the Z-stage backs away from the laser stage, and the laser stage is manually lowered.

4.4 Single or series of measurements of electrical and acoustical signals

When the instrument connect button is pushed, see Fig. 4.27; all instruments in the experimental setup, see Fig. 3.3, are connected to the app.



Figure 4.27: Instrument connect button.

When calibrating the microphone, it is used the DPO CH2 read-only in the drop-down list, accessed by the down arrow in Fig. 4.28, which only reads the oscilloscope screen. When identifying and measuring the reflection, a single measurement is used by using DPO CH2 accessed by the down arrow in Fig. 4.28, and the settings are set in Fig. 4.29. When measuring the reflection, the setting used is 1 V which is the signal generator voltage V_{0pp} , a sinus burst of 30 cycles, and a 25 Hz burst rate. It is also used in the reflection measurement frequency of 98860 Hz and a sample count of 10 000 samples, and the signal is averaged 128 times.

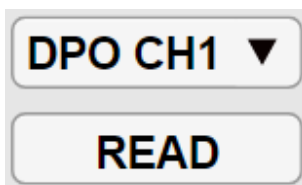


Figure 4.28: Measurement read button.

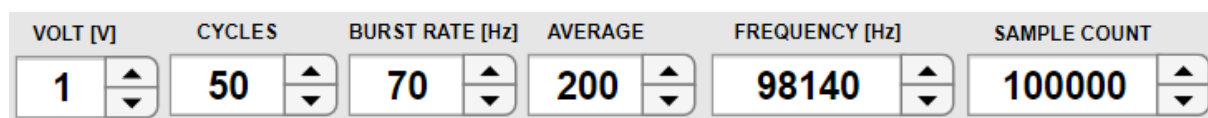


Figure 4.29: Single measurement adjustable parameters.

When it is performed, large measurements, such as directivity, on-axis pressure, and 2-D sound pressure field, the **MeasurementParameters.m** script in Appendix A.3 is used. This script is used to preset the type of measurement being conducted, the measurement frequency, the measuring range in angle and distance direction, the peak-to-peak voltage of the signal generator, the signal averaging, the number of cycles of the measurement signal, the burst rate, the filter setting, the number of sample count, and which channel that measures the electrical or acoustical signal at the oscilloscope. When the correct parameters are set

in the script for the type of measurement being conducted, the parameters are then loaded into the app with the load button in Fig. 4.25, and the start button in Fig. 4.30 is pushed.



Figure 4.30: Start button.

This starts the measurement series by the app automatically driving the stages to the first measuring position. When the stages arrive at the first measuring position, the app sends all settings to the different instruments, and the electrical voltage $V_{0m}(t)$ is first measured. Then the time window of the oscilloscope is adjusted automatically to fit the acoustical signal $V_{5m}(t)$, the acoustical voltage is measured, and environmental parameters are measured. After the first measurement is complete, the results are automatically saved into a specific folder, and the measurement series continues to its next position and repeats the measurements cycle until it is finished with the measurement series.

4.5 Transmitter and receiver mounting and positioning sensitivity analysis

It is vital to go through the MatLab Air Controller app's setup, which is designed to adjust and find the correct position of the piezoelectric disk relative to the microphone. The setup wizard helps to set the user coordinates to be as near as possible to the origin of the X, Y, and Z axis given in Fig. 4.31. Sects. 4.3.1-4.3.4 goes through the actual setup wizard in more detail and explains the user coordinates. The coordinates of the X, Y, and Z axis origin are defined in Figs. 2.4 and 4.31 as the piezoelectric disk front center, where Y-axis is parallel to the Y-stage and overlaps the R-stage rotation axis. The XZ-axis-plane is the horizontal plane. Further, the XY-axis-plane is vertical and matches the piezoelectric disk surface plane under perfect conditions of the orientation of the piezoelectric disk.

However, the world is rarely under perfect conditions, leading to different orientations that can affect the measured pressure. These influences lead to changes in the directivity, on-axis pressure, and 2-D sound pressure measurements from their true values relative to perfect orientations. In this work, three different orientations are analyzed that can affect the measured pressure and modeled how it affects the FE simulation directivity. These modeled deviations can be analyzed and indicate how large a deviation can be allowed from perfect orientation without affecting the measurement results.

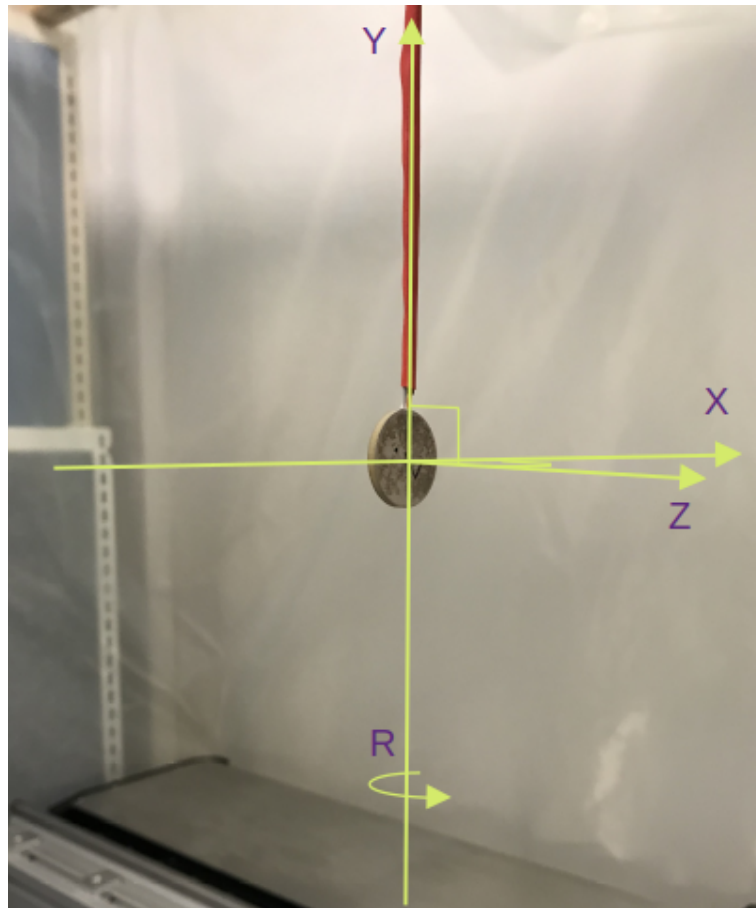


Figure 4.31: X, Y, and Z coordinate with origin in the piezoelectric disk's front center, where the XZ-axis-plane is the horizontal plane, and the XY-axis-plane is the vertical plane overlapping the piezoelectric disk's front surface. Y-axis is parallel with Y-stage and lies on the R-stage rotation axis.

The three analyzed orientations that can affect the measurements come from tilt angles or offset distances. The first orientation is the piezoelectric disk being tilted at an angle θ_T forward or backwards, see Fig. 4.32. The second orientation is an offset value β from the XZ-axis-plane to the microphone's front center resulting in an angle θ_M relative to the Z-axis, see Fig. 4.33. The difference between the first and second orientations is that the tilt angle θ_T of the piezoelectric disk is constant for all distances z_0 between the piezoelectric disk and microphone centers, and the angle θ_M depends on β and the distance z_0 between the piezoelectric disk and microphone centers. Since θ_M depends on β and the distance z_0 between the microphone and the piezoelectric disk centers, θ_M can have a significant impact in the near field for small β . However, into the far field, the impact of θ_M would decrease rapidly. The third and last orientation is a horizontal offset σ from the piezoelectric disk's front center or seen as an offset from the X, Y, and Z-axis origo to the R-stage rotation axis, as illustrated later in Fig. 4.37. This orientation leads to the center of the microphone's front no longer orbits with a constant distance of z_0 around the piezoelectric disk front center. This orbit changes the distance between the microphone and the piezoelectric disk depending on the

R-stage rotation angle θ_R .

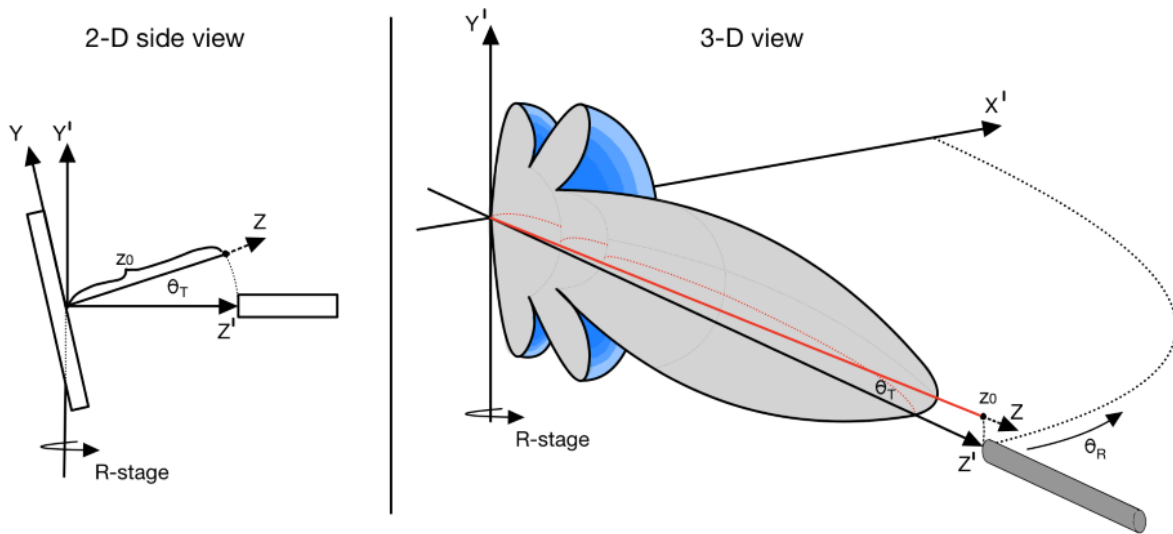


Figure 4.32: Left illustrates the 2-D view of the YZ-plane where the XY-plane crosses the piezoelectric disk's front center. The disk is tilted with an angle θ_T and distanced a distance of z_0 from origo to the microphone's front center. The right illustrates the case in a 3-D view.

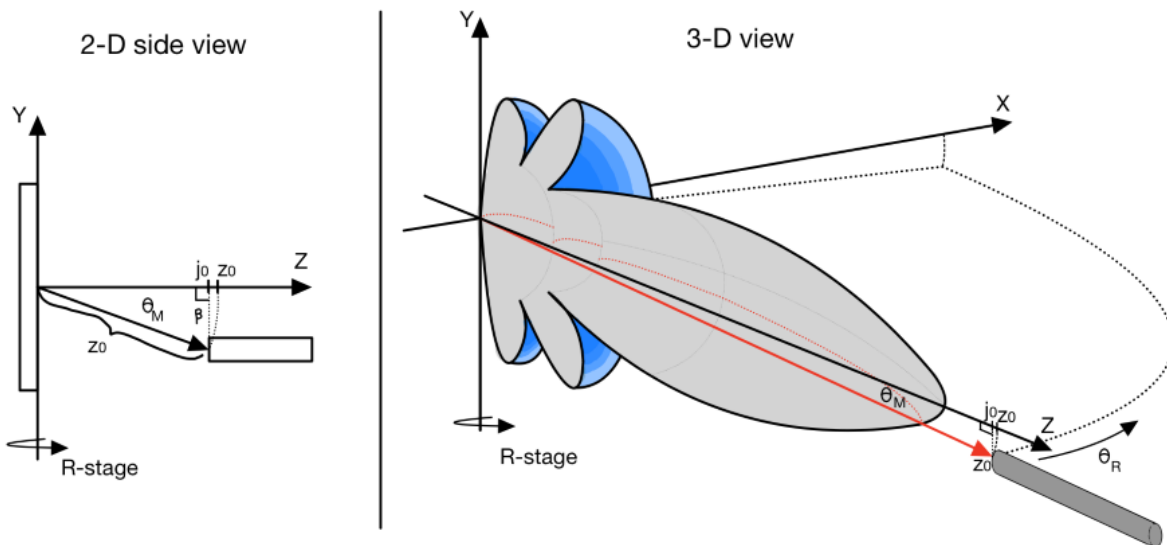


Figure 4.33: Left illustrates the 2-D view of the YZ-plane where the XY-plane lies on the piezoelectric disk's surface. The microphone's front center is offset a distance β from the XZ-plane and distanced at a distance of z_0 from origo. The right illustrates the case in a 3-D view.

The first and second orientations can be described as two points A and B on a sphere with a radius of z_0 and an angular distance θ between the points, see Fig. 4.34. The distance from the X, Y, and Z-axis origin to the directivity $D(\theta = 0, z_0, f)$ is described as the OA vector in Fig. 4.34, where θ equal to zero is the on-axis perpendicular to the piezoelectric disk surface, z_0 as the simulated distance and f as simulated frequency. The distance from the X, Y, and

Z-axis origin to the front center of the microphone is described as OB in Fig. 4.34. The θ_T is the tilt of the piezoelectric disk, θ_M is the angle to the center of the microphone's front dependent on β from $X'Z'$ -axis-plane in Fig. 4.34 and z_0 , θ is the angle between points A and B on the sphere, and θ_R is the R-stage rotation in Fig. 4.34.

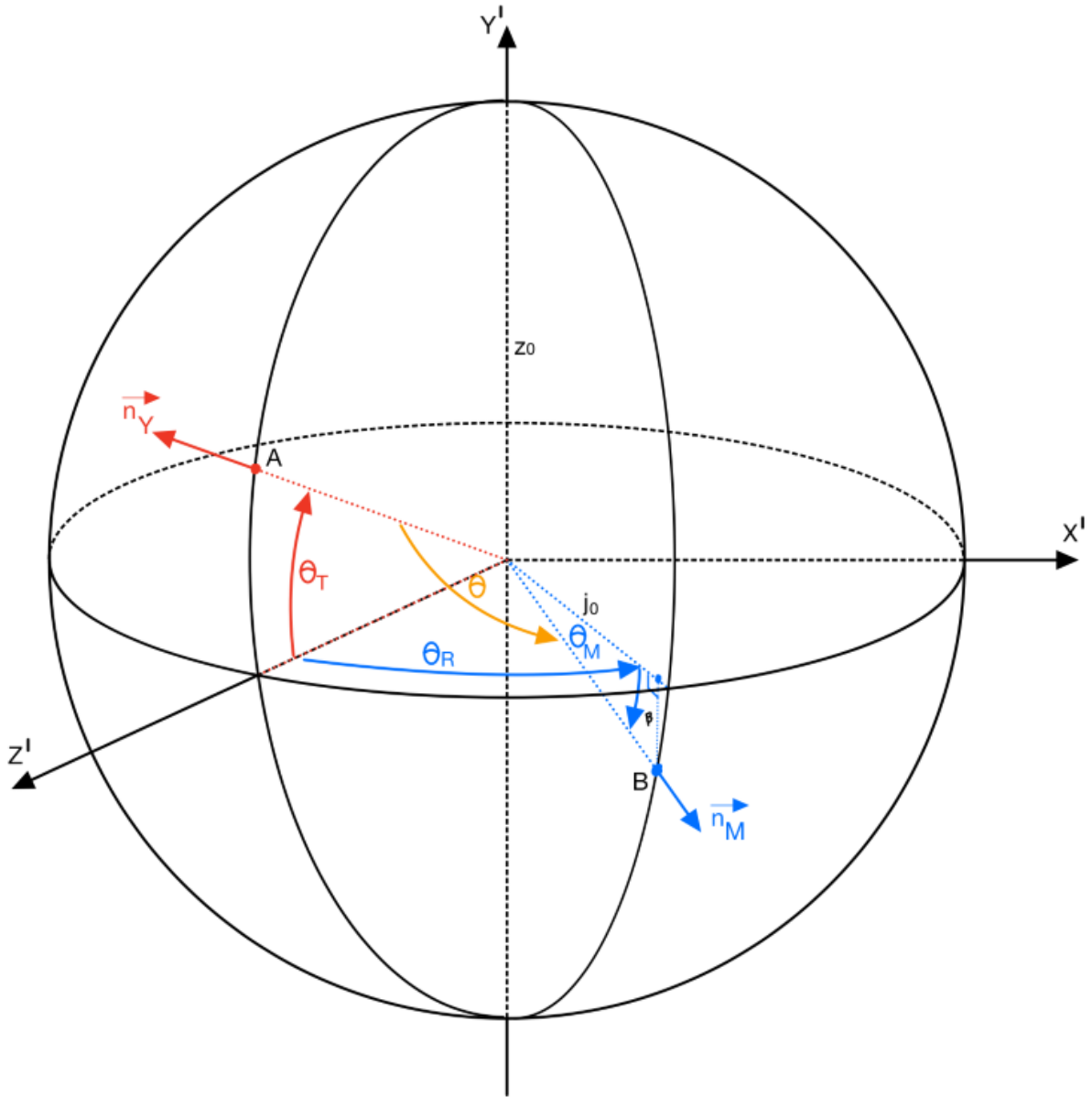


Figure 4.34: Illustration of the first (OA) and second (OB) orientations and the different values of θ_T disk tilt, β microphone offset, z_0 sphere radius, \vec{n}_Y normal unit vector of point A, \vec{n}_M normal unit vector of point B, θ angle distance between A and B, and θ_R R-stage rotation [76].

The angle θ_R ranges from 0 to 2π , and θ_T and θ_M range from $-\pi/2$ to $\pi/2$. To derive the angle distance θ , one first looks at the dot product of the vectors OA and OB as

$$\vec{OA} \cdot \vec{OB} = z_0^2 \cos\theta, \quad (4.11)$$

which is equivalent to the dot product between the normal unit vectors of OA and OB, which equals to

$$\vec{n}_Y \cdot \vec{n}_M = \cos\theta . \quad (4.12)$$

In the X', Y', and Z'-axis frame in Fig. 4.34, the normal unit vectors can be written as

$$\vec{n}_Y = \begin{pmatrix} 0 \\ \sin(\theta_T) \\ \cos(\theta_T) \end{pmatrix} , \quad (4.13)$$

and

$$\vec{n}_M = \begin{pmatrix} \cos(\theta_M)\sin(\theta_R) \\ \sin(\theta_M) \\ \cos(\theta_M)\cos(\theta_R) \end{pmatrix} , \quad (4.14)$$

and solving Eq. 4.12 for θ by inserting the normal unit vectors, the angle is written as

$$\theta = \cos^{-1} (\sin(\theta_M)\sin(\theta_T) + \cos(\theta_M)\cos(\theta_T)\cos(\theta_R)) . \quad (4.15)$$

With an equation for θ , it can now be analyzed the effect of θ_T and θ_M of the R-stage rotation range θ_R from -90 to 90 degrees and plot the logarithmic result of $D(\theta, z_0, f)$ against the measured angle θ_R . Plotting against θ_R is due to it being the perceived angle, while θ describes the actual angle between the microphone's front center and $D(\theta = 0, z_0, f)$, see Figs. 4.35 and 4.36 for the results of the modeling. The script used to model this is included in Appendix A.2.

By analyzing Fig. 4.35, it can be seen that simulated directivity with the frequency 98100 Hz is affected by the tilt of two degrees. The modeled tilts affect the sidelobes by increasing dB strength, where the first side lobes increase by approximately 0.64 dB, and the maximum of the first sidelobes shifts slightly inwards. By analyzing Fig. 4.36, it can be seen that simulated directivity with the frequency 249050 Hz is affected by the tilt of two degrees in a higher degree than for 98100Hz. The modeled tilts affect the sidelobes by increasing dB strength, and the main lobe is highly affected by having a decrease of 3.835 dB. Such an effect in the main lobe should be easily recognized in measurements.

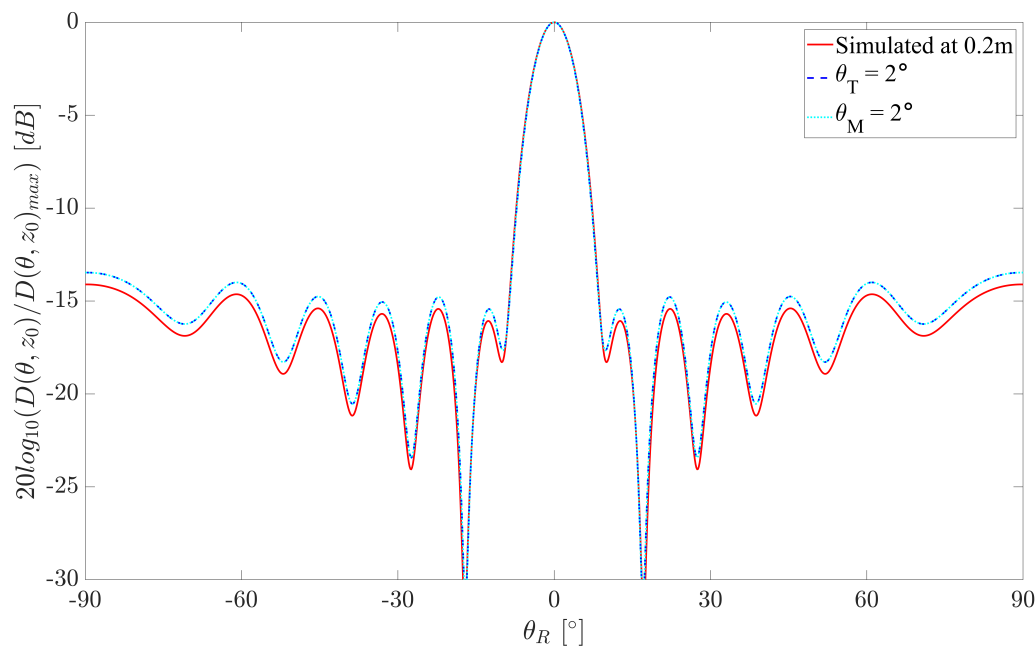


Figure 4.35: Simulated directivity at 0.2 m and frequency of 98100 Hz and analyzing the effect of the θ_T and θ_M equals two.

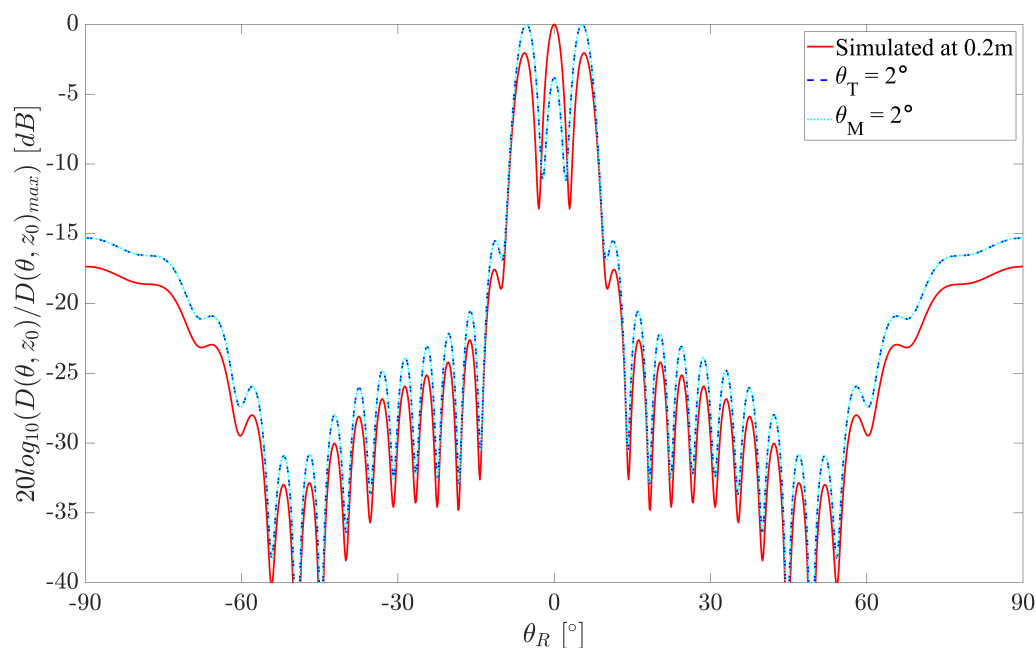


Figure 4.36: Simulated directivity at 0.2 m and frequency of 249050 Hz and analyzing the effect of the θ_T and θ_M equals two.

The third orientation is a horizontal offset σ from the piezoelectric disk's front center to the R-stage rotation axis, as illustrated later in Fig. 4.37. The distance from the R-stage rotation axis to the microphone front center is R and is constant. The center of the microphone's

front no longer orbits with a constant distance of z_0 around the piezoelectric disk front center, instead orbits with an changing distance $z(\theta_R)$ dependent on the rotation angle. The angle α is the angle from the line passing through the R-stage rotation axis and microphone front center when θ_R equals zero and to the piezoelectric disk's front center. The distance z_0 is the horizontal distance from the piezoelectric disk to the microphone when θ_R equals zero.

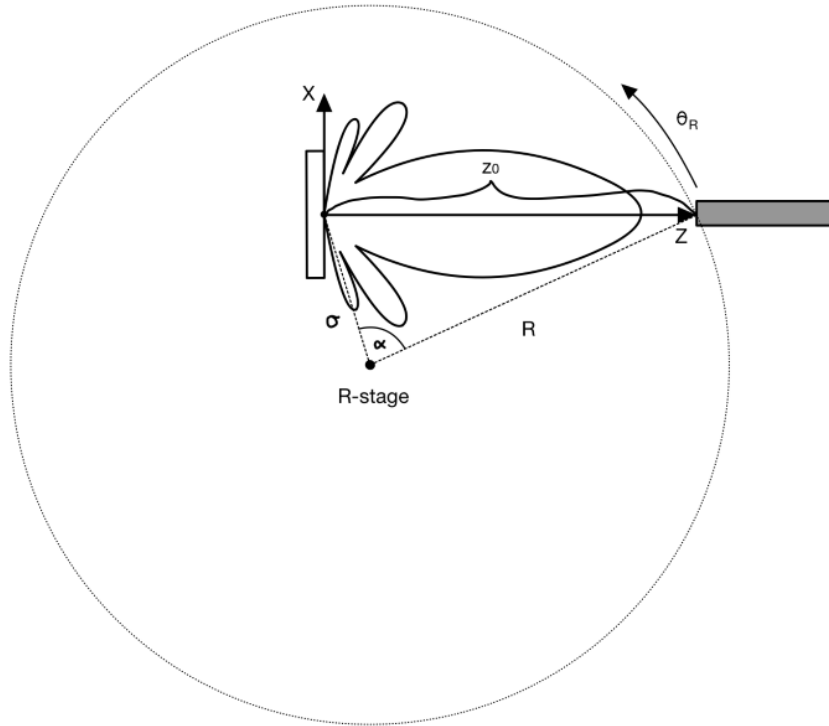


Figure 4.37: Illustration of the top view XZ-plane of the third orientation with a distance sigma from R-stage to disk's front center. The orbital radius of the microphone is the distance R. The angle alpha is the angle from the R line to the disk's front center.

The third, including first and second orientations, can be described as two points on a sphere with a radius of z_0 and an angular distance θ between the points. The distance from the X, Y, and Z-axis origin to the directivity $D(\theta = 0, z_0, f)$ is described as the OA vector in Fig 4.38, where θ equal to zero is the on-axis perpendicular to the piezoelectric disk surface, z_0 as the simulated distance and f as simulated frequency. The distance from the X, Y, and Z-axis origin to a point on the sphere where the line passes through the front center of the microphone is described as OB in Fig 4.38. The θ_T is the tilt of the piezoelectric disk, θ_m is the angle to the center of the microphone's front dependent on β from $X'Z'$ -axis-plane and j , θ is the angle between points A and B on the sphere, and the θ_r is the horizontal rotation in Fig 4.38.

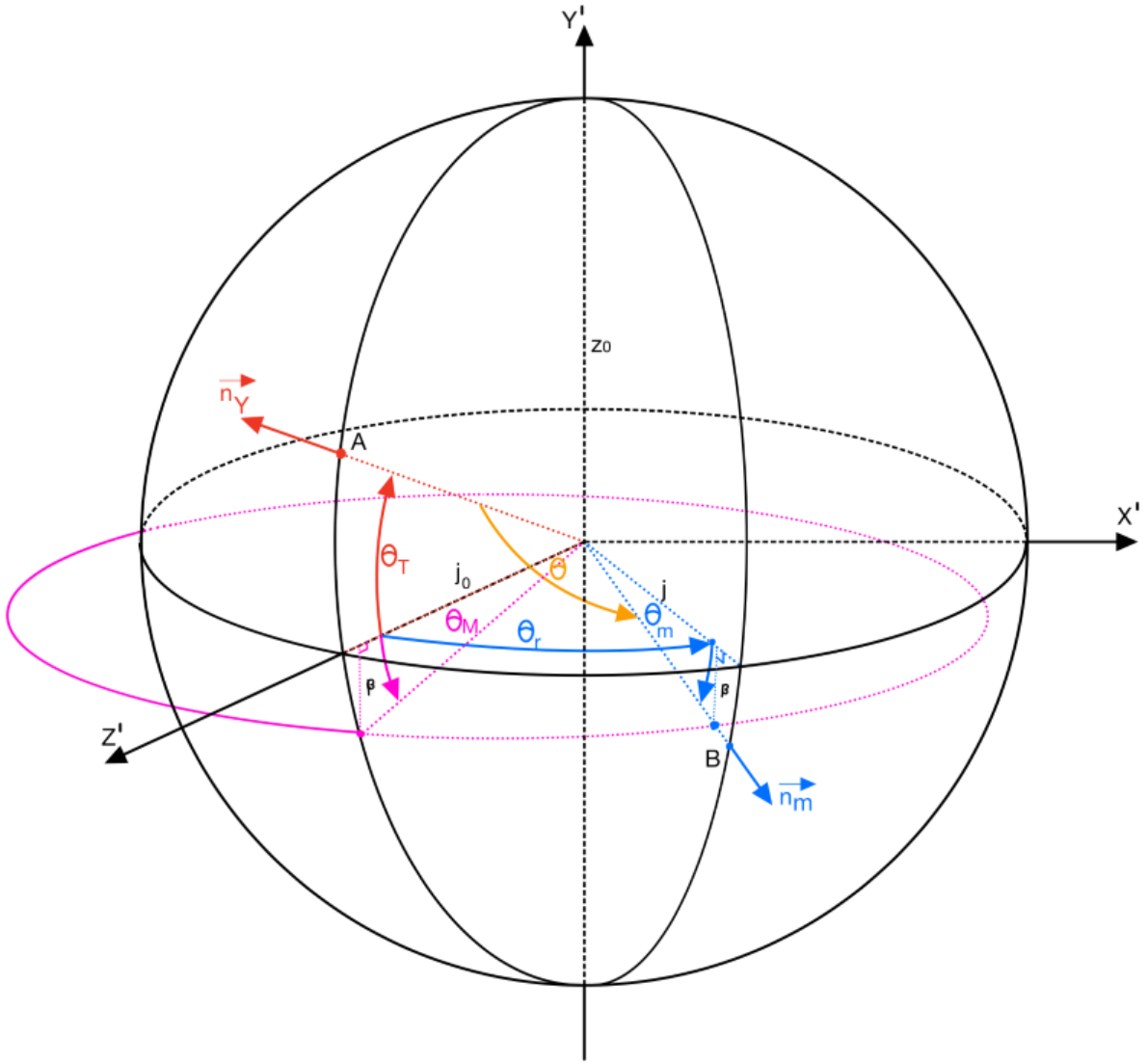


Figure 4.38: Illustration of the third, including first and second orientations, OA and OB, and the different values of θ_T disk tilt, β microphone offset, z_0 sphere radius, \vec{n}_Y normal unit vector of point A, \vec{n}_m normal unit vector of point B, θ angle distance between A and B, and θ_r horizontal rotation.

The dot product between the normal unit vectors of OA and OB equals to

$$\vec{n}_Y \cdot \vec{n}_m = \cos\theta, \tag{4.16}$$

where in the X, Y, and Z-axis frame, the normal unit vector can be written as

$$\vec{n}_m = \begin{pmatrix} \cos(\theta_m)\sin(\theta_r) \\ \sin(\theta_m) \\ \cos(\theta_m)\cos(\theta_r) \end{pmatrix}. \tag{4.17}$$

The offset beta can be set to a constant or calculated with θ_M and the distance z_0 and equals

$$\beta = z_0 \sin(\theta_M) , \quad (4.18)$$

and the distance j_0 , which is the horizontal distance from the piezoelectric disk to the microphone when θ_R equals zero, is

$$j_0 = z_0 \cos(\theta_M) . \quad (4.19)$$

The radius of the microphones orbit R is derived in Appendix D.1 and equals

$$R = \sigma \cos(\alpha) + \sqrt{j_0^2 + \sigma^2 (\cos^2(\alpha) - 1)} , \quad (4.20)$$

and the distance j from the piezoelectric disk front center to any point on the microphones orbit is derived in Appendix D.2 and is

$$j = \sqrt{R^2 - 2R\sigma \cos(\alpha - \theta_R) + \sigma^2} . \quad (4.21)$$

With the equation for the distance j and offset β , the angle θ_m can be calculated as

$$\theta_m = \tan^{-1} \left(\frac{\beta}{j} \right) , \quad (4.22)$$

and with the distances j , j_0 , and R , the $\cos(\theta_r)$ is derived in Appendix D.3 and equals to

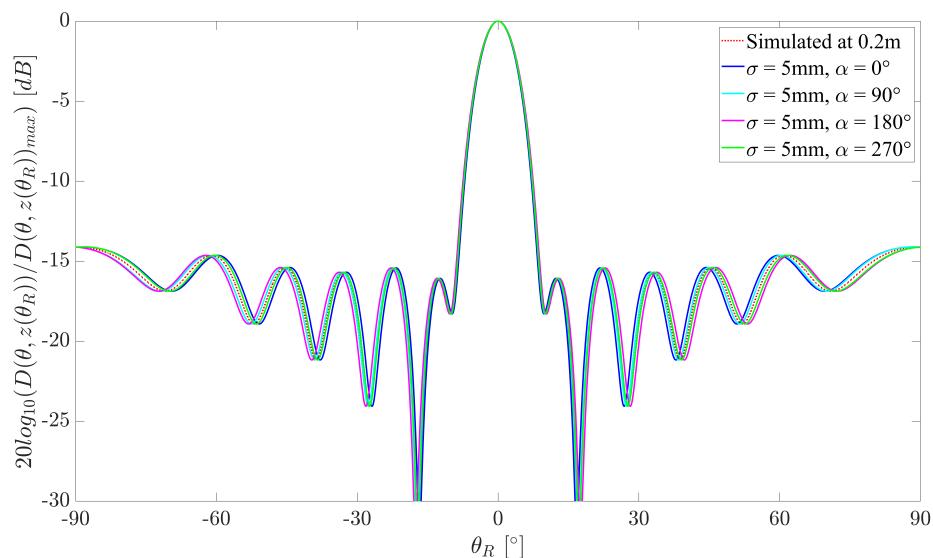
$$\cos(\theta_r) = \frac{j^2 + j_0^2 - 4R^2 \sin^2(\theta_R/2)}{2jj_0} . \quad (4.23)$$

With Eqs 4.22 and 4.23, it is possible to calculate θ with Eq. 4.16 by inserting the normal unit vectors and θ equals to

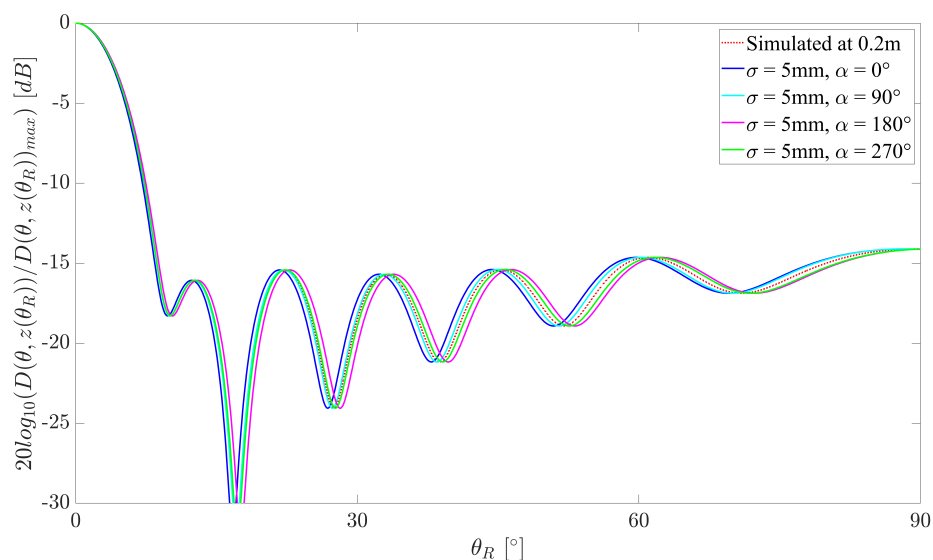
$$\theta = \cos^{-1} (\sin(\theta_m) \sin(\theta_T) + \cos(\theta_m) \cos(\theta_T) \cos(\theta_r)) . \quad (4.24)$$

Now with θ deduced for all three orientations, the effects of the distance σ and starting angle α can be analyzed in the R-stage rotation range θ_R from -90 to 90 degrees. The results are then plotted by taking the logarithmic result of $D(\theta, z(\theta_R), f) / \max(D(\theta, z(\theta_R), f))$ and plotting it against the measured angle θ_R . The distance between the microphone's front center to the piezoelectric disk's front center z is now dependent on the change in θ_m 's angle. This change in the distance z is solved by using interpolation between several distance simulations. In Fig. 4.39, the simulated directivity at 98100 Hz and the effect of distance σ equals 5 mm, and the angle α equals 0, 90, 180, and 270 degrees are analyzed. From Fig. 4.39, it is seen that the modeled effects are largely dependent on the starting angle α . At α equals 0 degrees, the

entire signal is compressed closer to θ_R equals 0 degrees, and for α equals 180 degrees, the entire signal is stretched out relative to θ_R equals 0 degrees. At α equal 90 and 270 degrees, the signal is either stretched out on one side of θ_R equals 0 degrees and compressed closer to θ_R equals 0 degrees on the other side. In Fig. 4.40, the simulated directivity at 249050 Hz and the effect of distance σ equals 5 mm, and the angle α equals 0, 90, 180, and 270 degrees are analyzed. From Fig. 4.40, it is seen that the modeled effects of σ and α behave in the same matter as in Fig 4.39.

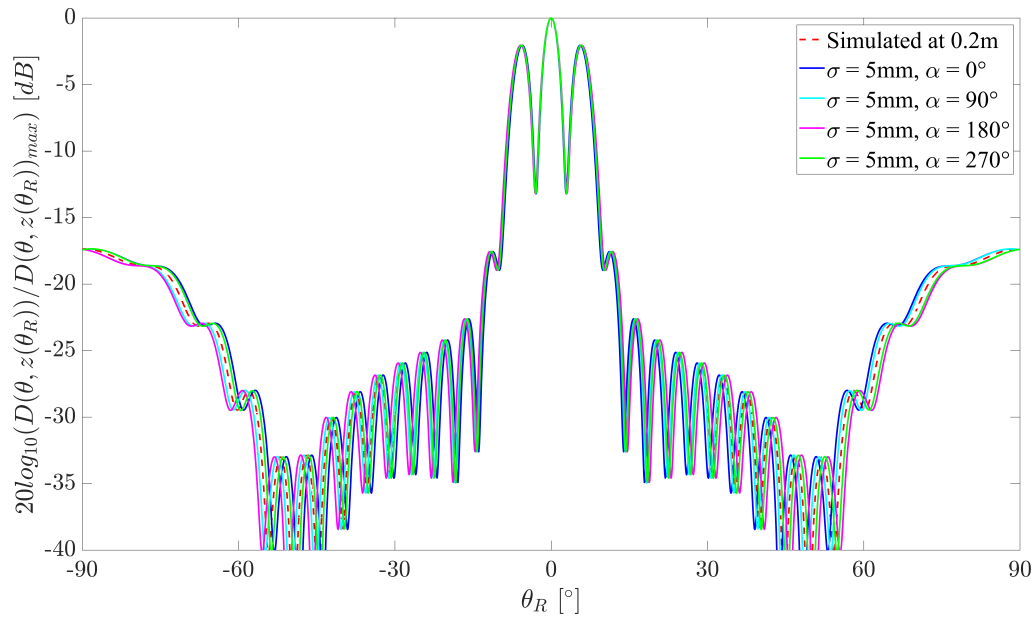


(a)

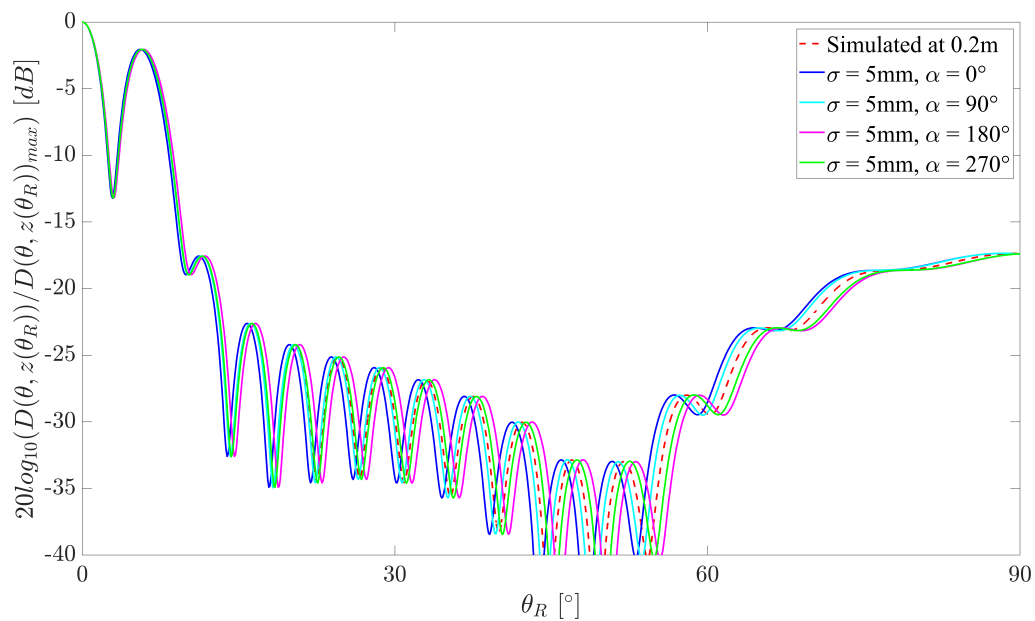


(b)

Figure 4.39: Simulated directivity at 0.2 m and frequency of 98100 Hz and analyzing the effect of the σ equals 5 mm and α equals 0, 90, 180, 270 degrees.



(a)



(b)

Figure 4.40: Simulated directivity at 0.2 m and frequency of 249050 Hz and analyzing the effect of the σ equals 5 mm and α equals 0, 90, 180, 270 degrees. (a) is the simulated and modeled effect from -90 to 90 degrees (b) is the simulated and modeled effect from 0 to 90 degrees.

Chapter 5

Finite element setup

This work uses the finite element method to simulate the piezoelectric disk Pz27 vibrating in a vacuum and fully immersed in a air. Sect. 5.1 gives information on FEMP and the current version used in this work, the different files FEMP uses, and a brief description of FEMP. Sect. 5.2 gives info on the material parameters, the material parameters of the piezoelectric element, and the parameters for the fluid. Sect. 5.3 gives information on the simulation parameters used in this work and their associated values. Sect. 5.4 describes the conversion of simulated pressure to comparable pressure with the measured pressure. Sect. 5.5 gives a visualization of the simulation structures.

5.1 FEMP 6.1

This work performs finite element simulations with the simulation tool FEMP developed by Kocbach [38] in a cooperation between the University of Bergen (UiB) and Christian Michelsen Research AS (CMR). Students and researchers at UiB and CMR/NORCE have continued developing FEMP ever since, and the current version used is FEMP 6.1. The programming language MATLAB [68] allows for fast implementation and visualization [38], making it the choice for the programming language of FEMP.

Different files are needed to alter variables, parameters, areas, points, boundary conditions, and materials to be able to run simulations. The file **material.dat** in Appendix C.5 defines the transducer material and fluid parameters. The file **_inn** in Appendix C.4 defines the set parameters; dimension of the structure, elements in the fluid or structure, material or fluid number, radius from origo to infinite elements region. The rest of the file defines simulation variables and parameters; material file, elements per wavelength frequency, order of the finite elements, order of the infinite elements, the frequency range, and type of simulations like direct harmonic analysis used to calculate, e.g., admittance. The scripts **read_inn_project.m** and **init_const_project.m** in Appendix C.1, C.2, and C.3 defines struc-

ture, areas, points and boundary conditions. It also uses the set parameters from the `_.inn` file.

FE approximates structures with a given number of volumes/elements, where computational time relies on the size and complexity of the structures. To reduce the complexity and, thereby, the computational time, FEMP implements axis symmetry which reduces volumes to rectangles. A problem modeled in FEMP may consist of up to two domains, finite elements and infinite elements domains. The finite elements domain uses 8 node isoparametric elements to solve the parameters inside the element, and the global to local coordinates transition with interpolation functions [21], see Fig. 5.1. In this domain, finite elements consist of the transducer region Ω_p and can consist of the inner fluid region Ω_{f1} [38], depending on the type of simulation. The infinite elements domain is not isoparametric but described by conjugates Astley-Leis infinite elements [9] and is solved using 10th order infinite elements. In this domain, infinite elements consist of the outer fluid region Ω_{f2} [38], see Fig. 5.2.

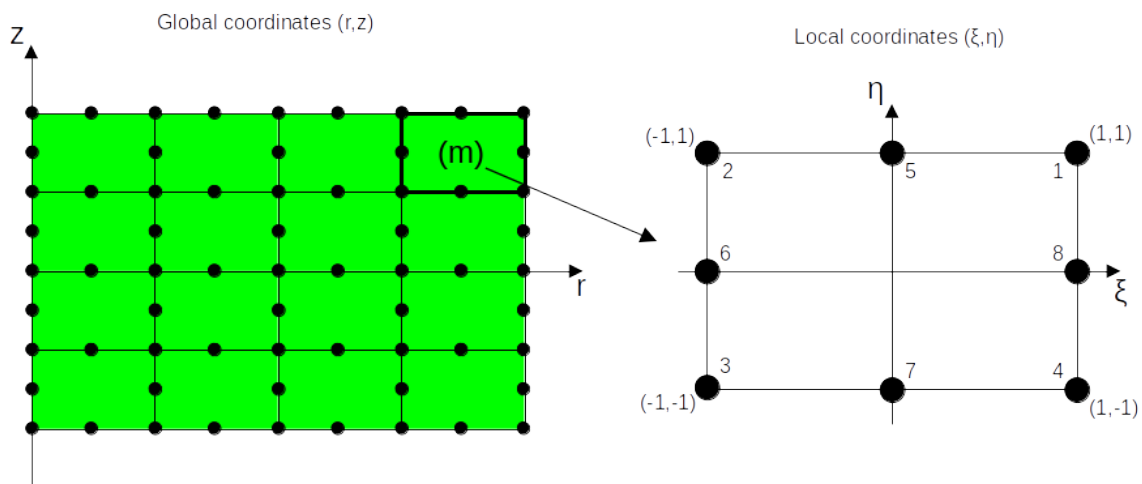


Figure 5.1: The colored area is the piezoelectric discs volume Ω_p split into a number of elements in the global coordinates and shows the connection from one element, m , from the global coordinates to the local coordinates for the 8 node isoparametric element [38].

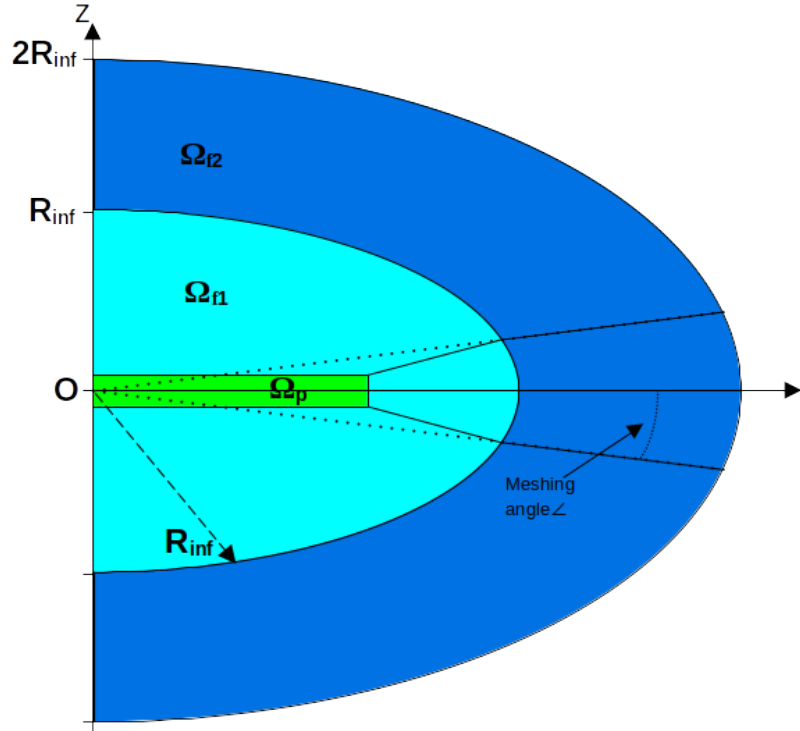


Figure 5.2: Illustration of the piezoelectric disc volume Ω_p , the surrounding finite fluid volume Ω_{f1} and the infinite volume Ω_{f2} , the distance R_{inf} described in Sect. 5.3, and the meshing angle \angle splitting the surrounding fluid volume Ω_{f1} and Ω_{f2} into three regions [38].

5.2 Material parameters

Piezoelectrical material data provided by manufacturers can often be incomplete or inaccurate. This incompleteness and inaccuracy can arise from variations in the composition in different batches, uncertainties, or lack of methods to provide better results of the material parameters. In simulations, it is essential to have as accurate material parameters as possible such that simulations match measurements. This matching is a demanding task to accomplish, and this work uses material parameters found in [37] and presented in Table 5.1. The material parameters of the piezoelectric element that FEMP uses are elastic stiffness matrix with a constant electric field [c^E], piezoelectric stiffness matrix [e], and dielectric stiffness matrix with constant strain [ϵ^S] [38]. The fluid parameters that FEMP uses are bulk modulus K and density ρ . With complex values of the piezoelectric constants, it is possible to describe mechanical and electrical losses in the piezoelectric element, but fluid losses are not considered [38]. The material numbers are set in the `_.inn` file to select the materials or fluid for simulations. These numbers correspond to the material found in the `material_.dat` file.

5.2.1 Piezoelectric element, Pz27

The manufacturer of the piezoelectric element Pz27 used in this work is Meggitt, earlier known as Ferroperm. They state that their element has a variation of $\pm 5\%$ for all parameters and the lowest variation from batch to batch [46]. Previous work has shown that the parameters provided by Meggitt are not in the best agreement when used in simulations and compared with measurements [42][37][1]. This inaccuracy led to an adjusted dataset of Pz27 by Lohne and Knappskog [42][37], which has improved the agreement in the first and second radial mode. This dataset is shown in Tabel 5.1 and used to compare the simulations and measurements in this work.

Table 5.1: Because of inaccuracy in the original dataset from Meggitt and others manufacturers, there is used in present work the adjusted dataset set for piezoelectric element Pz27 made by Lohne and further improved by Knappskog [42][37].

Parameters	Unit	Lohne/Knappskog [42][37]
c_{11}^E	$[10^{10} Pa]$	$11.8750 \left(1 + i \frac{1}{95.7500}\right)$
c_{33}^E	$[10^{10} Pa]$	$11.2050 \left(1 + i \frac{1}{177.990}\right)$
c_{44}^E	$[10^{10} Pa]$	$2.11000 \left(1 + i \frac{1}{75.0000}\right)$
c_{12}^E	$[10^{10} Pa]$	$7.43000 \left(1 + i \frac{1}{71.2400}\right)$
c_{13}^E	$[10^{10} Pa]$	$7.42500 \left(1 + i \frac{1}{120.190}\right)$
e_{15}	$[C/m^2]$	$11.2000 \left(1 - i \frac{1}{200.000}\right)$
e_{31}	$[C/m^2]$	$-5.40000 \left(1 - i \frac{1}{166.000}\right)$
e_{33}	$[C/m^2]$	$16.0389 \left(1 - i \frac{1}{323.770}\right)$
ϵ_{11}^S	$[10^{-9} F/m]$	$8.11043 \left(1 + i \frac{1}{50.0000}\right)$
ϵ_{33}^S	$[10^{-9} F/m]$	$8.14585 \left(1 + i \frac{1}{86.2800}\right)$
ρ	$[kg/m^3]$	7700

5.2.2 Air

When doing finite element simulations in a fluid, the dataset needs the parameters density ρ and bulk modulus K for the given fluid. Since the given fluid in this work is air, and density and bulk modulus are dependent on environmental conditions, setting the temperature and pressure is necessary. At $20^\circ C$ and $1 atm$, Appendix A10 in Kinsler & Frey [36] gives the density and sound speed. Using the definition of the thermodynamic speed of sound given as [36]

$$c = \sqrt{\frac{K}{\rho}}, \quad (5.1)$$

the bulk modulus can be calculated by rewriting this definition as

$$K = c^2 \rho . \quad (5.2)$$

The values found, calculated, and used in the material dataset are given in Table 5.2.

Table 5.2: The material dataset for air used in this work, for 1 *atm* and 20 °C. [36].

Name	Parameter	Unit	Value
Sound speed	c	[<i>m/s</i>]	343
Density	ρ	[<i>kg/m³</i>]	1.21
Bulk modulus	K	[<i>10⁵Pa</i>]	1.42355

5.3 Simulation parameters

Simulation in FEMP requires a set of parameters defined in the **.inn** file, where the number of parameters depends on the type of simulation or structural complexity. The parameters used in this work are only those accounted for here.

Radius and thickness are the dimensions that define the piezoelectric element in this work. They are measured with a Mitutoyo M310-25 micrometer [47] and given in Table 5.3. These dimensions are then used in FEMP when simulating. The element simulation's accuracy and computational time depend on elements per wavelength and frequency [38]. In the case of vacuum, the elements per wavelength used are 98 in radius and thickness direction. For the non-vacuum case, the element per wavelength is 7 in the fluid, 25 in radius, and 98 in thickness. When calculating the wavelength, the frequency is the maximum simulated frequency [38]. Fluids use the wavelength for longitudinal waves, while materials use the wavelength for shear waves [38]. The reason for using shear waves, the shortest wavelength, over longitudinal waves is that the number of elements per wavelength needed to obtain a specific accuracy is almost equal in radial and thickness directions [38]. This investigation of comparing shear waves against longitudinal waves is done by [38].

Table 5.3: Measured dimensions of the piezoelectric element Pz27 with calculated uncertainties. The dimensions measured with Mitutoyo M310-25 micrometer [47] and are mean values of ten measurements.

Element number in batch	Diameter	Thickness	Unit
#7	20.25±0.01	2.048±0.011	[mm]

Studies of [38] make it possible to calculate the optimal distance from origo to the boundary between finite and infinite elements. Using 10th order infinite elements in simulation, [38] suggest the normalized distance

$$R_{inf}/(a^2/\lambda) = S \quad (5.3)$$

should be larger or equal to the critical distance $S = 0.32$. This normalized value corresponds to R_{inf} , approximately 28 mm at the maximum simulated frequency of 300 kHz and sound speed in the air. Therefore R_{inf} is set to 30 mm in this work. When it comes to the order of finite elements, 8 nodes are used, corresponding to 2nd order isoparametric elements [2]. Typically the meshing angle \angle for fluid regions is set to 1.3 rad [2], see Fig. 5.2.

FEMP uses direct harmonic analysis to solve the FE problem over a set range of frequencies [38]. For simulation of the element fully immersed in the fluid, a wide frequency range can take a lot of computing power and computation time. Therefore, all simulations performed in this work only simulate the frequency range of interest from 1-300 kHz with a step of 50 Hz. These simulations also account for complex losses in the element. The main computed quantities in this work are admittance $Y_T(f)$, directivity $D(r, \theta, f)$, 2-D near-field and far-field pressure $p(x, z, f)$, and on-axis pressure $p_{ax}(z, f)$.

5.4 Simulated pressure

The voltage V_1 over the piezoelectric disk, described in Sect. 2.7.2, will change according to the measuring frequency. At around resonance, this voltage decreases rapidly relative to the V_0 voltage generated by the signal generator. The voltage over the piezoelectric disk can be calculated by measuring V_{0m} with the oscilloscope and using the transfer function H_{0m1}^{VV} , see Eq. 2.21. Due to the simulated pressure amplitude being linear dependent on the input voltage amplitude

$$\frac{\{p_{sim}\}}{V_{sim}} = \frac{\{p_{pp}\}}{V_{1pp}}, \quad (5.4)$$

where p_{sim} is the simulation pressure, V_{sim} is the simulation voltage applied to the piezoelectric disk, V_{1pp} is the peak-to-peak voltage calculated over the piezoelectric disk, and p_{pp} is the adjusted peak-to-peak simulation pressure, which is used to compare to peak-to-peak measurement pressure p_{4pp} . The simulated pressure p_{sim} can be scaled by the measured peak-to-peak voltage V_{1pp} as

$$\{p_{pp}\} = \frac{\{p_{sim}\}}{V_{sim}} V_{1pp}, \quad (5.5)$$

where V_{sim} is equal to 1 V in these simulations.

5.5 Structure setup

This work uses two different `read_inn_project.m` scripts given in Appendix C.1 C.2, one for the element fully immersed in the fluid and one for vacuum simulations. Plotting the mesh view, Fig. 5.3 and 5.4, visualize the result of the two scripts and the FE problem to solve.

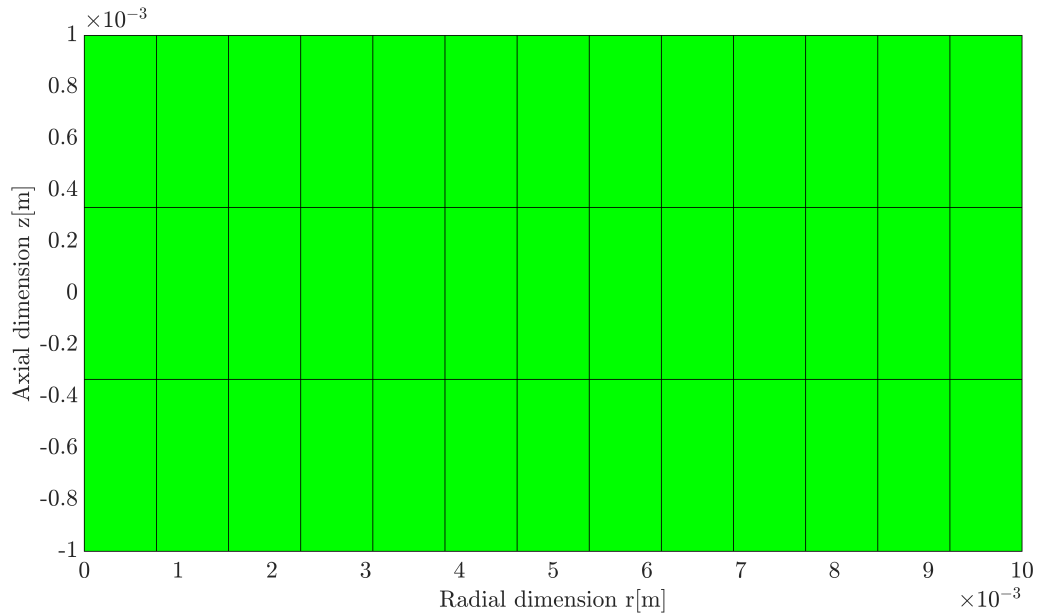


Figure 5.3: For illustration purposes is the mesh view of vacuum simulation, plotted with 7 elements per wavelength in radial and thickness direction at a frequency of 300 kHz.

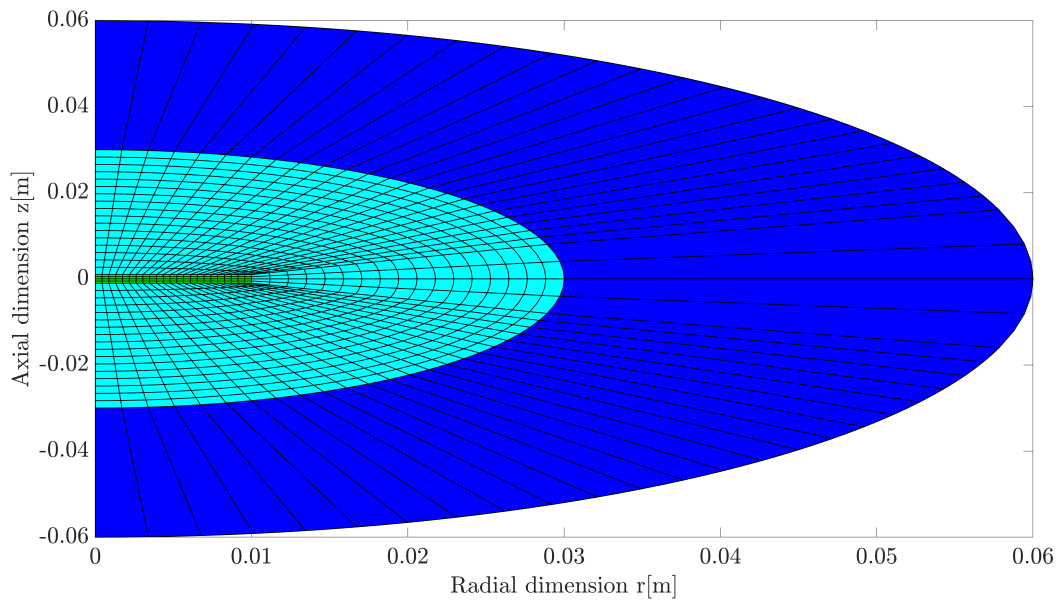


Figure 5.4: For illustration purposes is the mesh view of piezoelectric disc fully immersed in fluid simulation, plotted with 2 element per wavelength in fluid at a frequency of 100 kHz. Elements per wavelength in radial and thickness direction are set to 7 and 28.

Chapter 6

Results and discussion

This chapter presents the results obtained with the FE simulations method described in Chapter 5. The results obtained by performing measurements of the piezoelectric disk's electrical properties with an impedance analyzer (Table 3.2) described in Sect. 3.2 are also presented. And finally, acoustic measurements with the piezoelectric disk transmitting ultrasound and measured with a condenser microphone by Brüel & Kjær are presented. Sect. 6.1 presents all the electrical properties from FE simulations and the measurements results. Sect. 6.2 presents all the acoustically measurements results compared to FE simulations.

6.1 Electrical properties of the piezoelectric disk

This section studies the FE simulated electrical properties of a piezoelectric disk with the same dimensions as piezoelectric disk in Table 5.3. The electrical properties of piezoelectric disk are studied by measuring the properties and compared with the FE simulated electrical properties performed in FEMP.

6.1.1 Comparison of electrical properties between FE simulations in a vacuum and air

The piezoelectric disk's electrical admittance FE simulations are done in a vacuum and air from 1-300 kHz. This frequency range covers the two first radial modes, given the datasets in Tables 5.1 and 5.2, and the dimension of the piezoelectric disk in Table 5.3 is used. The reason for doing the simulations in both vacuum and air is to see how the air impacts the electrical properties of the piezoelectric disk. Based on the plots in Fig. 6.1, there is considerable overlap between simulated admittance for vacuum and air. One has to zoom in significantly to see that they do not overlap perfectly in the plot. The reason for this is that the acoustic impedance in the air is small, which can cause the piezoelectric disk to be considered to

oscillate in a vacuum.

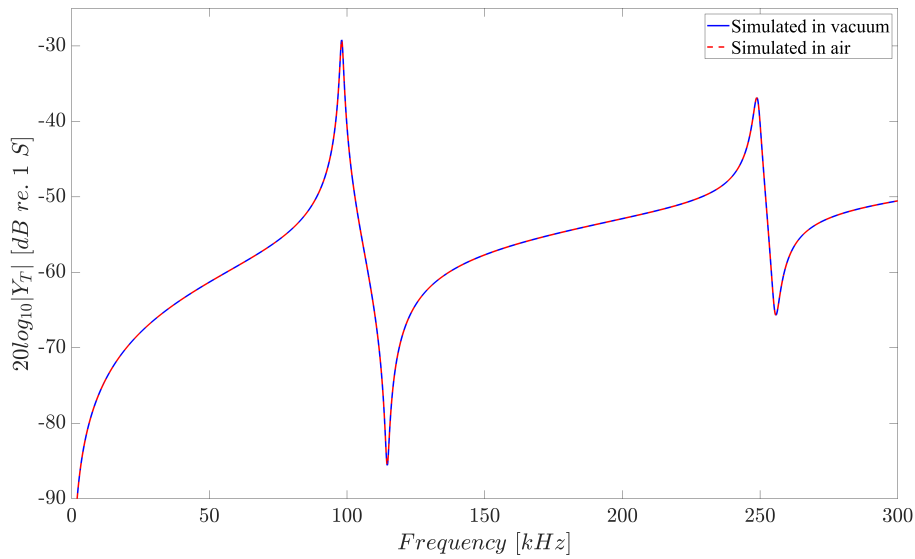


Figure 6.1: FE simulation of the piezoelectric's admittance plotted in dB relative to one siemens over the frequency range of 1-300 kHz. FE simulation of the disk in a vacuum is the blue line, and the FE simulation of the disk in the air is the stippled red line.

The radial modes are found by determining the maximum conductance defined as the serial resonance frequency [32] (Sect. 2.1). By studying Fig. 6.2, the maximum conductance is found at 98.1 kHz for the first radial mode R1 and 249.05 kHz for the second radial mode R2. For completeness of the comparison of the FE simulated piezoelectric disk are, the susceptance shown in Fig. 6.3.

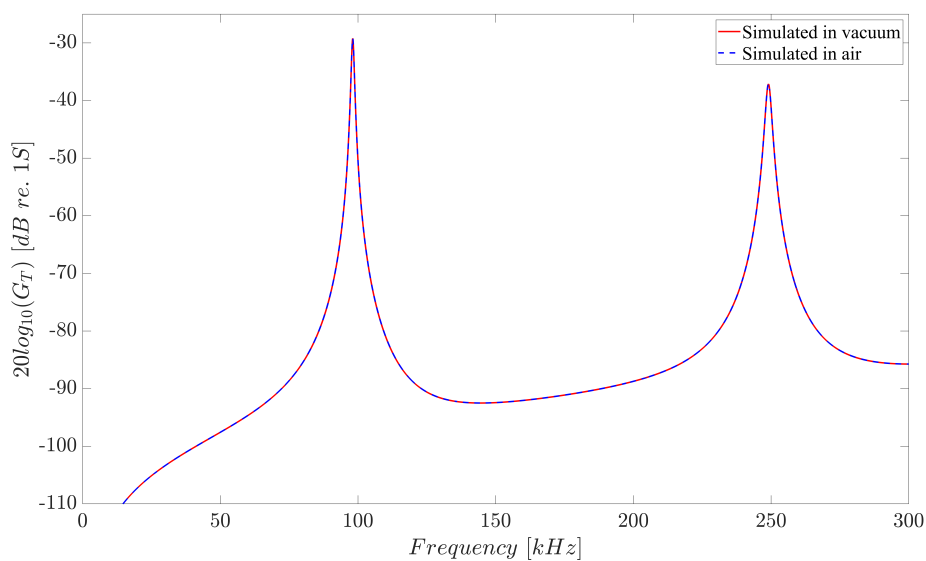


Figure 6.2: FE simulation of the piezoelectric's conductance plotted in dB relative to one siemens over the frequency range of 1-300 kHz. FE simulation of the disk in a vacuum is the blue line, and the FE simulation of the disk in the air is the stippled red line.

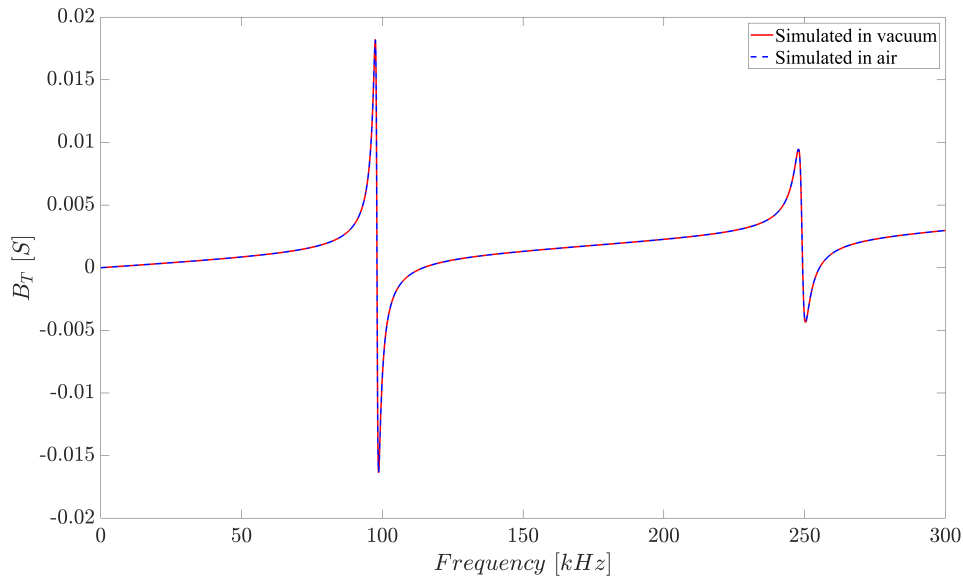


Figure 6.3: FE simulation of the piezoelectric's susceptance over the frequency range of 1-300 kHz. FE simulation of the disk in a vacuum is the blue line, and the FE simulation of the disk in the air is the stippled red line.

6.1.2 Comparison of electrical properties between measurements and FE simulations

The piezoelectric disk's electrical conductance and susceptance are measured with the impedance analyzer as described in Sect. 3.2. It is measured directly on the electrodes and measured on the wires that are soldered onto the electrodes. This is done to see if the short, thin wires soldered to the electrodes affect the measurement results. The results from the impedance analyzer are then compared to the FE simulation in air. The frequency range of the measurements of the electrical properties on the piezoelectric disk matches the FE simulations frequency range, 1-300 kHz. Fig. 6.4 compares the conductance of the measurement results directly on the electrodes, the measurements on the wires, and the FE simulations. In Fig. 6.4, there is a large overlap between the electrode and wire measurements. However, in the frequency range from approx. 50 kHz to 75 kHz in this figure, there are small irregular spikes in the conductance of the electrode measurement. There is a much more consistent measurement result on the wires than the electrodes' measurement. This smoother result may be due to the wires soldered to the electrodes providing better current flow than measuring directly on the electrodes. However, this statement does not explain why irregularities only appear in the specific measuring range from 50 kHz to 75 kHz and are only positive in order of magnitude. Furthermore, it also does not explain why it is only shown in the conductance and not for the susceptance and admittance of the same measurement, see Figs. 6.5 and 6.6. Since the irregularity is frequency-dependent, it is possible that the wires touching the elec-

trodes may have a spring load effect on the electrodes. This "spring" then vibrates close to a resonant frequency and contributes to the irregularities in this frequency range. One thought is that the spikes may occur due to a certain vibration of the disk, but this is weakened because they are not seen in the wire measurement. The last thought is that these irregularities happen due to noise. Regarding the large difference between measured and simulated conductance in the frequency range from approx. 110 kHz to 165 kHz. It is thought that this arises due to the piezoelectric constants used in the FE simulations not perfectly matching the piezoelectric constant of the piezoelectric disk or the fact that these measurements are performed with solder lump, which is not considered in the FE simulations.

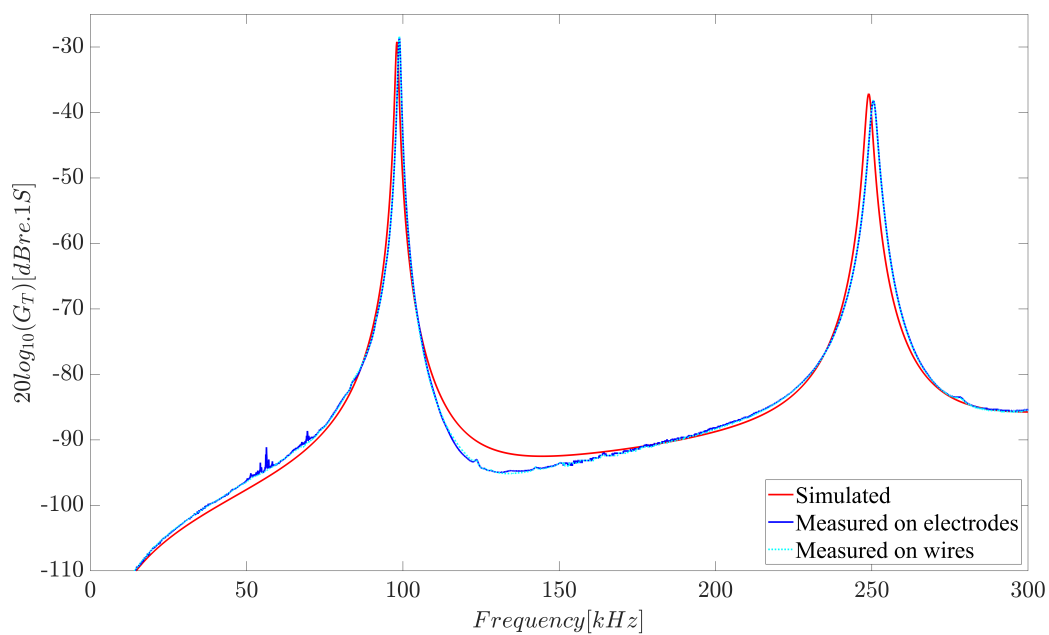


Figure 6.4: FE simulation and measurement of the piezoelectric's conductance plotted in dB relative to one siemens over the frequency range of 1-300 kHz. FE simulation of the disk in a vacuum is the red line, the measured on the disk electrodes is the blue line, and the measured on the wired soldered to the disk electrode is the stippled turquoise line.

By comparing the measurement and FE simulated conductances, it is seen that the simulated conductance's first radial extension mode, R1, frequency is shifted slightly down, and the magnitude is not as large as the measured values. The same shift is seen in comparing simulated and measured radial mode, R2, but to a greater extent. The frequencies of the maximum conductances are given in Table 6.1, and the frequency differences and magnitude differences of the maximum conductances of FE simulated relative to the measured are shown in Table 6.2.

Table 6.1: Comparison of the frequencies of the maximum conductances found in Fig. 6.4 of the FE simulation in air and measurements made with the impedance analyzer. R1 is the first radial extension mode, and R2 is the second radial extension mode.

Mode	Simulated	Measured on wires	Measured on electrodes	Unit
R1	98100	98860	98870	[Hz]
R2	249050	250500	250550	[Hz]

Table 6.2: Comparison of the magnitude difference Δ Magnitude and frequency difference Δf of the maximum conductances found in Fig. 6.4 of the FE simulation in air relative to the measurements made with the impedance analyzer. R1 is the first radial extension mode, and R2 is the second radial extension mode.

Simulated vs Measured on wires		
Mode	Δ Magnitude	Δf
R1	0.86 dB	760 Hz
R2	-1.01 dB	1450 Hz
Simulated vs Measured on electrodes		
Mode	Δ Magnitude	Δf
R1	0.61 dB	770 Hz
R2	-1.1 dB	1500 Hz

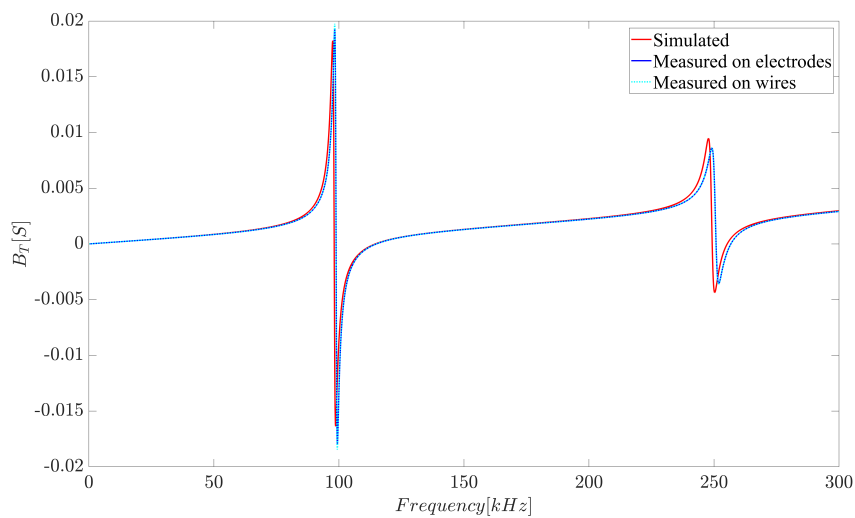


Figure 6.5: FE simulation and measurement of the piezoelectric's susceptance over the frequency range of 1-300 kHz. FE simulation of the disk in a vacuum is the red line, the measured on the disk electrodes is the blue line, and the measured on the wired soldered to the disk electrode is the stippled turquoise.

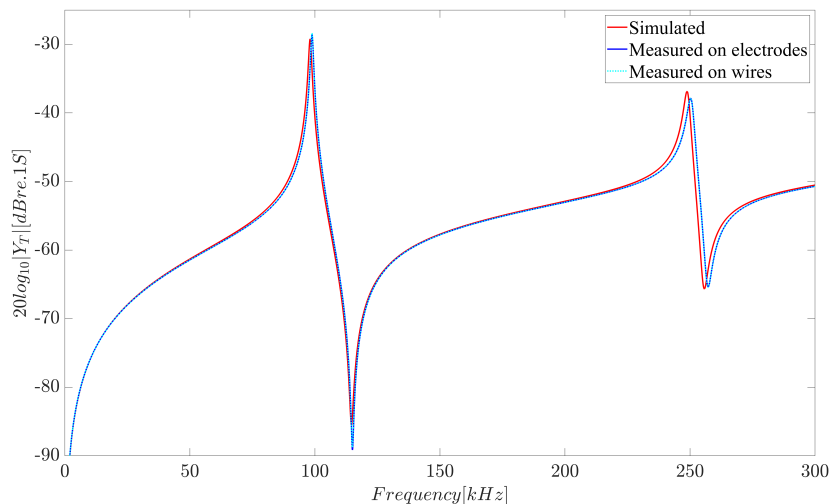


Figure 6.6: FE simulation and measurement of the piezoelectric's conductance plotted in dB relative to one siemens over the frequency range of 1-300 kHz. FE simulation of the disk in a vacuum is the red line, the measured on the disk electrodes is the blue line, and the measured on the wired soldered to the disk electrode is the stippled turquoise line.

6.2 Acoustic characteristics of the piezoelectric disk

In this section, acoustic measurements made with the piezoelectric disk are studied and compared with FE simulations. First, the frequencies used in the acoustic measurements and which simulation frequencies to compare with the measurements are determined. Then directivity measurements are presented, then on-axis pressure measurements, and finally, 2-D sound pressure field of the near and far field.

6.2.1 Frequency selection for measurements and FE simulations

For the on-axis pressure and 2-D pressure field, the frequencies used correspond to 1:2, 2:3, 1:1, 3:2, and 2:1 of the first radial modes given in Table 6.1. For the directivity, the frequencies used correspond to the same frequencies as for the on-axis pressure and 2-D pressure field and, in addition, the second radial mode given in Table 6.1. This method of scaling the frequency relative to the first radial modes is due to the FE simulation, and the measurement results of the radial modes in Table 6.1 are not equal. In order to be able to compare the acoustic characteristics of simulations and measurements with each other, it is then chosen to use the first radial modes of the FE simulation and measurement as the reference frequency when comparing results outside the resonance. The final frequencies used for comparing measurements to FE simulations are shown in Table 6.3.

A reason for only measuring directivity at the second radial mode is due to directivity being a normalized quantity, making it feasible to compare FE simulations with directivity

measurements. Another reason is that the second radial mode only is used to measure directivity is that microphone sensitivity is not valid for such high frequencies, see Fig 3.14. Therefore, only qualitative measurements can be made for such frequencies, and only chosen to do so for directivity due to lack of time.

Table 6.3: The scaling factor of the modes in parentheses and the calculated frequency result, used to compare acoustic characteristics between simulation and measurement. Delta f is the frequency difference between the simulations and the measurements comparisons.

Scaling of mode	Simulation frequency	Measurement frequency	Δf	Unit
1:2 (R1)	49050	49430	380	[Hz]
2:3 (R1)	65400	65907	507	[Hz]
1:1 (R1)	98100	98860	760	[Hz]
3:2 (R1)	147150	148290	1140	[Hz]
2:1 (R1)	196200	197720	1520	[Hz]
1:1 (R2)	249050	250500	1470	[Hz]

6.2.2 Acoustic signals examples over three different angles and for all used frequencies

This section gives examples of the measurement results of the acoustic signal $V_{5m}(t)$, measured at channel two on the oscilloscope at three different angles and for all frequencies in Table 6.3. These examples demonstrate that the acoustic signal quality changes with changing measuring angles. This change can be due to measurements performed in the nodes in the directivity pattern or with too low voltage amplitude V_{0pp} used outside resonance frequencies, which can lead to low signal-to-noise ratio (SNR) and low-pressure amplitudes.

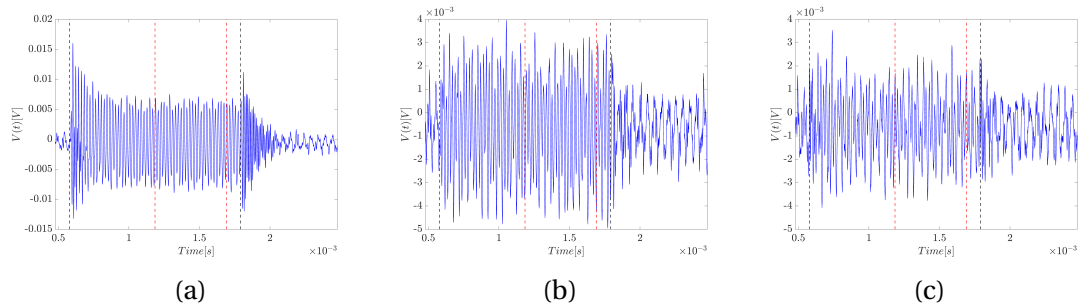


Figure 6.7: Comparison of the acoustic measurement signal for the frequency 49430 Hz, and for the angles (a) 0 degrees, (b) 25 degrees, and (c) 50 degrees. The plot is given in voltage vs. time. The red dotted lines represent the time domain used in FFT, and the black dotted represents the start and end of the signal. The distance between the piezoelectric disk and microphone is 0.2 m. ($T = 25.2$ °C, $RH = 32.6$ %, $P = 990$ hPa).

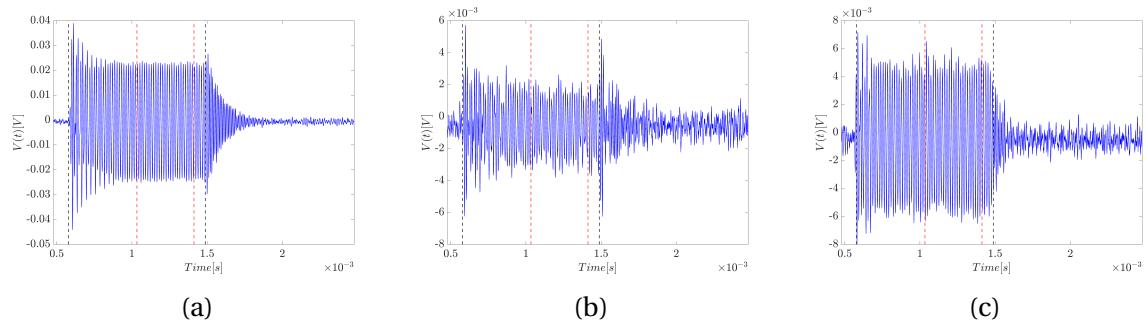


Figure 6.8: Comparison of the acoustic measurement signal for the frequency 65906 Hz, and for the angles (a) 0 degrees, (b) 25 degrees, and (c) 50 degrees. The plot is given in voltage vs. time. The red dotted lines represent the time domain used in FFT, and the black dotted represents the start and end of the signal. The distance between the piezoelectric disk and microphone is 0.2 m. ($T = 25.3$ °C, $RH = 35.3$ %, $P = 990$ hPa).

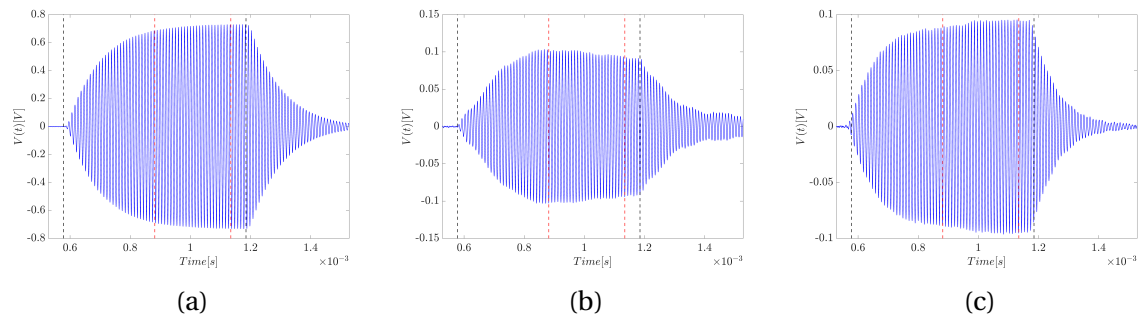


Figure 6.9: Comparison of the acoustic measurement signal for the frequency 98860 Hz, and for the angles (a) 0 degrees, (b) 25 degrees, and (c) 50 degrees. The plot is given in voltage vs. time. The red dotted lines represent the time domain used in FFT, and the black dotted represents the start and end of the signal. The distance between the piezoelectric disk and microphone is 0.2 m. ($T = 25.1$ °C, $RH = 33.4$ %, $P = 991$ hPa).

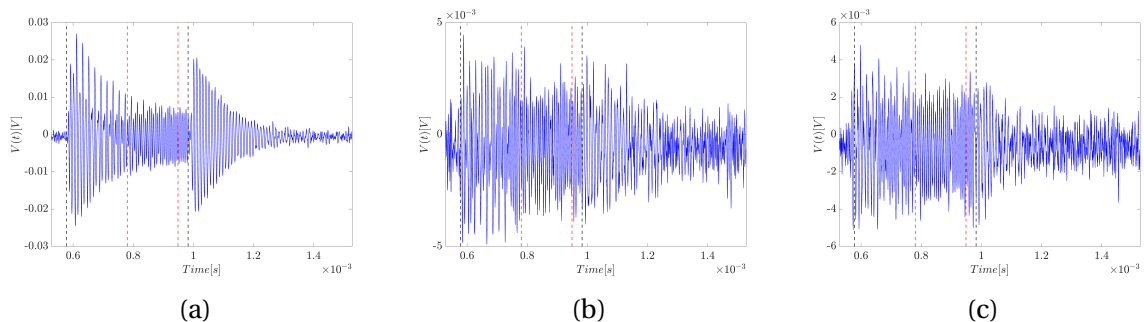


Figure 6.10: Comparison of the acoustic measurement signal for the frequency 148290 Hz, and for the angles (a) 0 degrees, (b) 25 degrees, and (c) 50 degrees. The plot is given in voltage vs. time. The red dotted lines represent the time domain used in FFT, and the black dotted represents the start and end of the signal. The distance between the piezoelectric disk and microphone is 0.2 m. ($T = 25.3$ °C, $RH = 36.3$ %, $P = 990$ hPa).

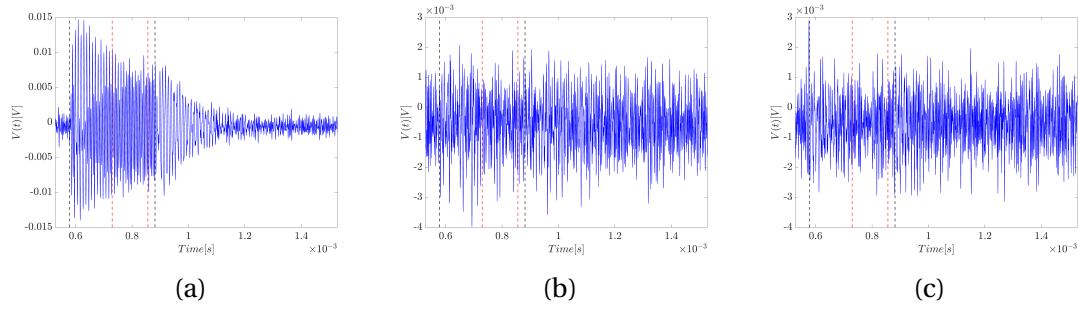


Figure 6.11: Comparison of the acoustic measurement signal for the frequency 197720 Hz, and for the angles (a) 0 degrees, (b) 25 degrees, and (c) 50 degrees. The plot is given in voltage vs. time. The red dotted lines represent the time domain used in FFT, and the black dotted represents the start and end of the signal. The distance between the piezoelectric disk and microphone is 0.2 m. ($T = 25.4$ °C, $RH = 37.8$ %, $P = 991$ hPa).

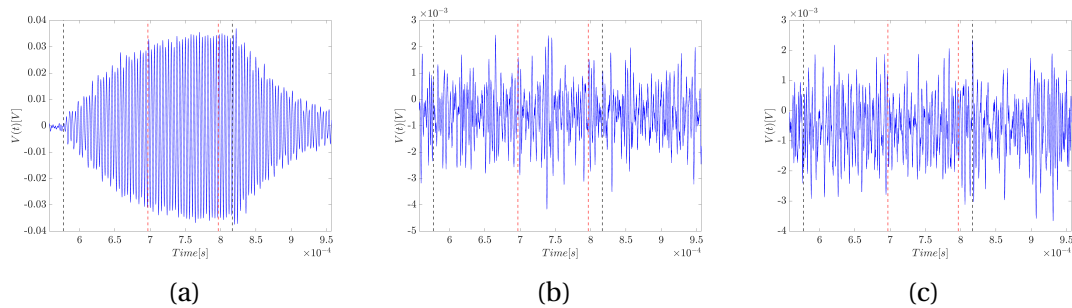


Figure 6.12: Comparison of the acoustic measurement signal for the frequency 250500 Hz, and for the angles (a) 0 degrees, (b) 25 degrees, and (c) 50 degrees. The plot is given in voltage vs. time. The red dotted lines represent the time domain used in FFT, and the black dotted represents the start and end of the signal. The distance between the piezoelectric disk and microphone is 0.2 m. ($T = 26.3$ °C, $RH = 40.2$ %, $P = 1007$ hPa).

6.2.3 Comparison of directivity between FE simulations and measurements

The directivity measurements of the piezoelectric disk are performed at the frequencies given in Table 6.3 and over the angles -90 to 90 degrees with one-degree resolution. These measurement results are compared to the corresponding FE simulations of the directivity with the frequencies in Table 6.3. All directivity measurements and simulations are conducted at a distance of 0.2 m between the disk and microphone. The voltage from the signal generator was $1 V_{0pp}$, and the received signal was amplified by 60 dB. The measurement results are normalized relative to the maximum voltage and plotted linearly and logarithmically. At the measuring distance of 0.2 m, all measurements are performed except for one frequency in the far field, see Table 6.4, where the Rayleigh distance defines the far field as

$$z_R = \frac{\pi a^2}{\lambda}, \quad (6.1)$$

where λ is the wavelength defined by sound speed divided by the frequency. The measurements are desirable to carry out in the far field but not too far out in the far field because it is also desirable to obtain a good SNR.

For Fig. 6.13, the measurement shows good agreement in the main and first side lobe relative to the simulation. However, from the first side lobe and with the angle continuing to increase, there appears to be noise present in the measurement. In the first side lobe, effects due to tilting θ_T or angle θ_M from the model in Sect. 4.5 can be seen as being present in the measurement, and a σ effect at α approx. 0 degrees can also seem to be present. However, these effects are not consistent for all degrees, which leads to the probability that there are other reasons why these effects occur. In the second side lobe, the magnitude of the measurements is lower compared to the simulation and can be due to SNR. At this second side lobe, which is at about 50 degrees, Fig. 6.7c does show a significant amount of noise is present relative to the measurement signal.

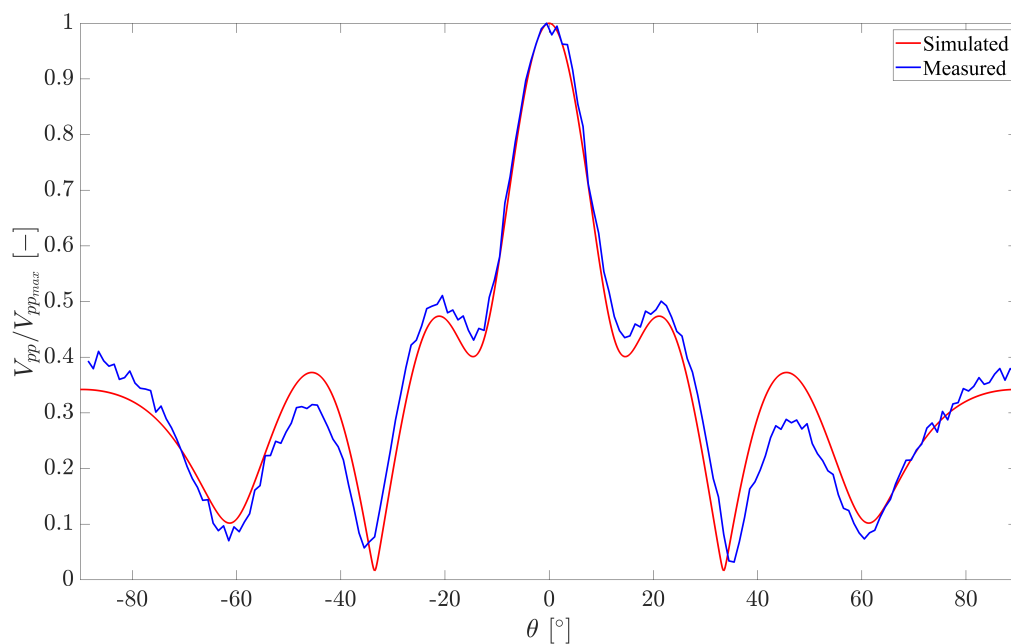
Table 6.4: Rayleigh distance for the different measurement frequencies where sound speed $c = 343$ m/s and radius of the disk $a = 10$ mm are used when calculating the distance.

Rayleigh distance	Frequency
46.3 mm	49430 Hz
60.4 mm	65907 Hz
90.6 mm	98860 Hz
135.8 mm	148290 Hz
181.1 mm	197720 Hz
229.4 mm	250500 Hz

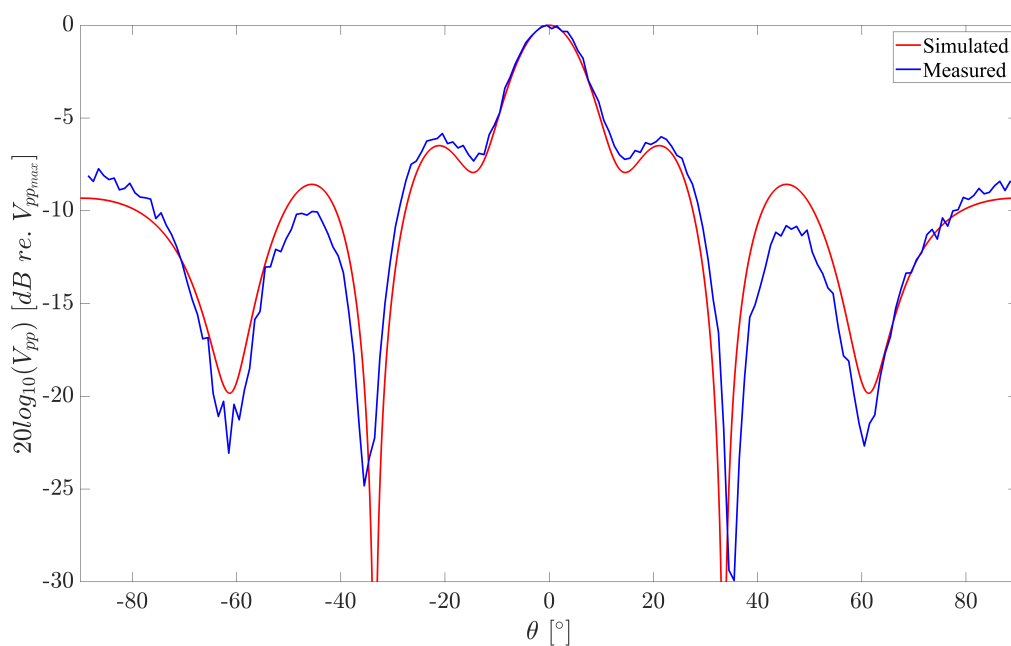
In Fig. 6.14, the measurement shows good agreement in the main lobe relative to the simulations. Regarding the first side lobe, there is a magnitude difference between the negative and positive degrees where the negative is greater than the positive degree. Furthermore, this magnitude difference is shifted for the second side lobe, where the positive is greater than the negative degree. This directivity behavior is one of the reasons for the method in Sect. 4.5, were developed. This was to study if this behavior was due to the disk's positioning relative to the microphone when the R-stage rotates. But this behavior is not absent in the developed method in Sect. 4.5, which leads to the thought that this occurs due to the disk not being perfectly axisymmetric. This discrepancy may be due to the wires soldered to the electrodes and causes anti-axisymmetric effects, damage in the polarization after soldering on the electrodes, or some aging or structural defects.

In Fig 6.15, the measurement shows similar behaviors as Fig. 6.14, but both first side lobes are larger in magnitude relative to the simulation. When it comes to the second and

third side lobes, they seem to melt into each other, especially seen on the negative angle side.



(a)



(b)

Figure 6.13: The directivity is given linearly (a) and logarithmically (b), and at the angles from -90 to 90 degrees with one-degree resolution. Directivity frequency is 49430 Hz for measurement and 49050 Hz for simulation, both conducted at a distance of 0.2 m. ($T = 25.2^\circ\text{C}$, $\text{RH} = 32.6\%$, $P = 990\text{ hPa}$).

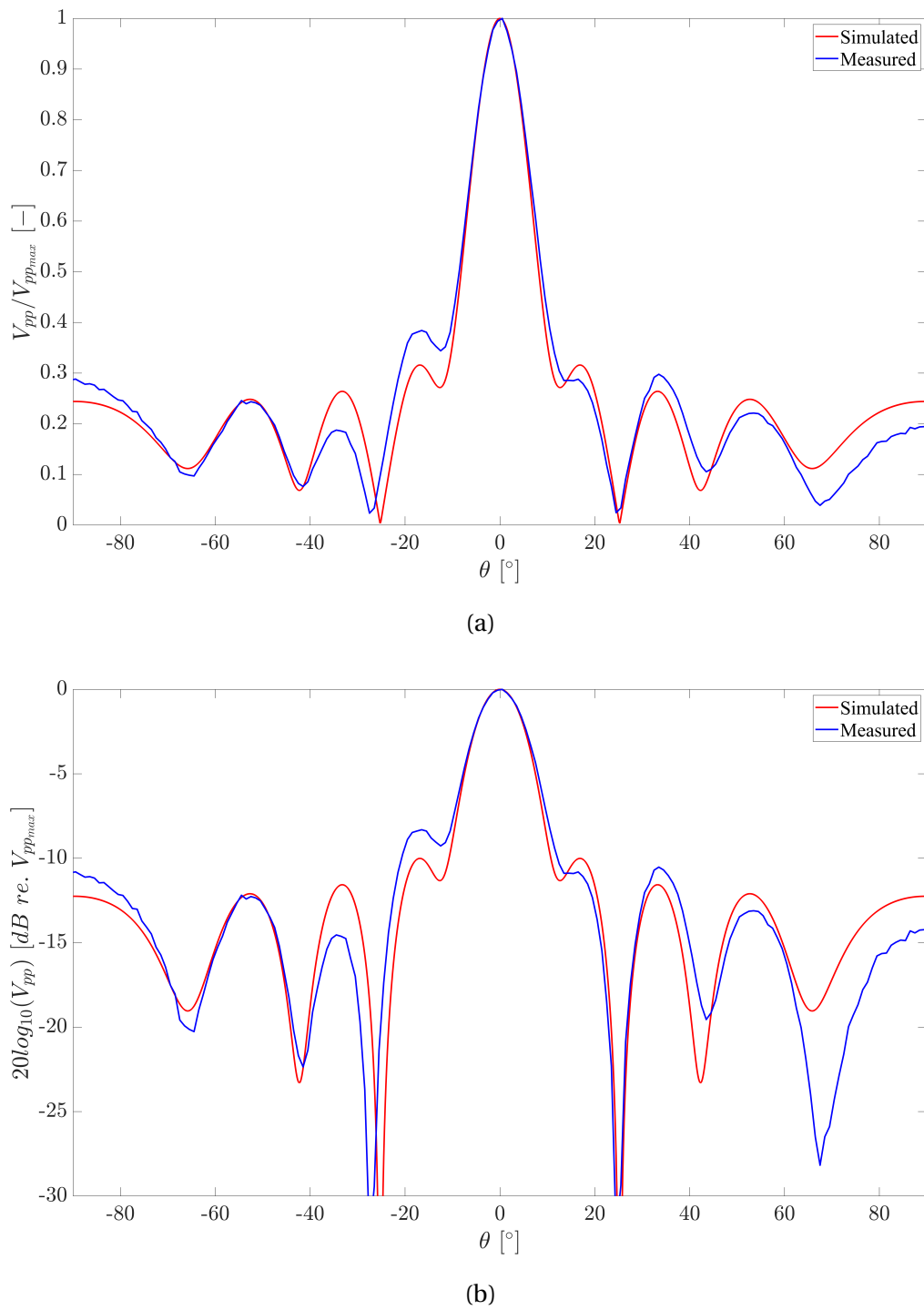


Figure 6.14: The directivity is given linearly (a) and logarithmically (b), and at the angles from -90 to 90 degrees with one-degree resolution. Directivity frequency is 65907 Hz for measurement and 65400 Hz for simulation, both conducted at a distance of 0.2 m. ($T = 25.3^\circ\text{C}$, $\text{RH} = 35.3\%$, $P = 990\text{ hPa}$).

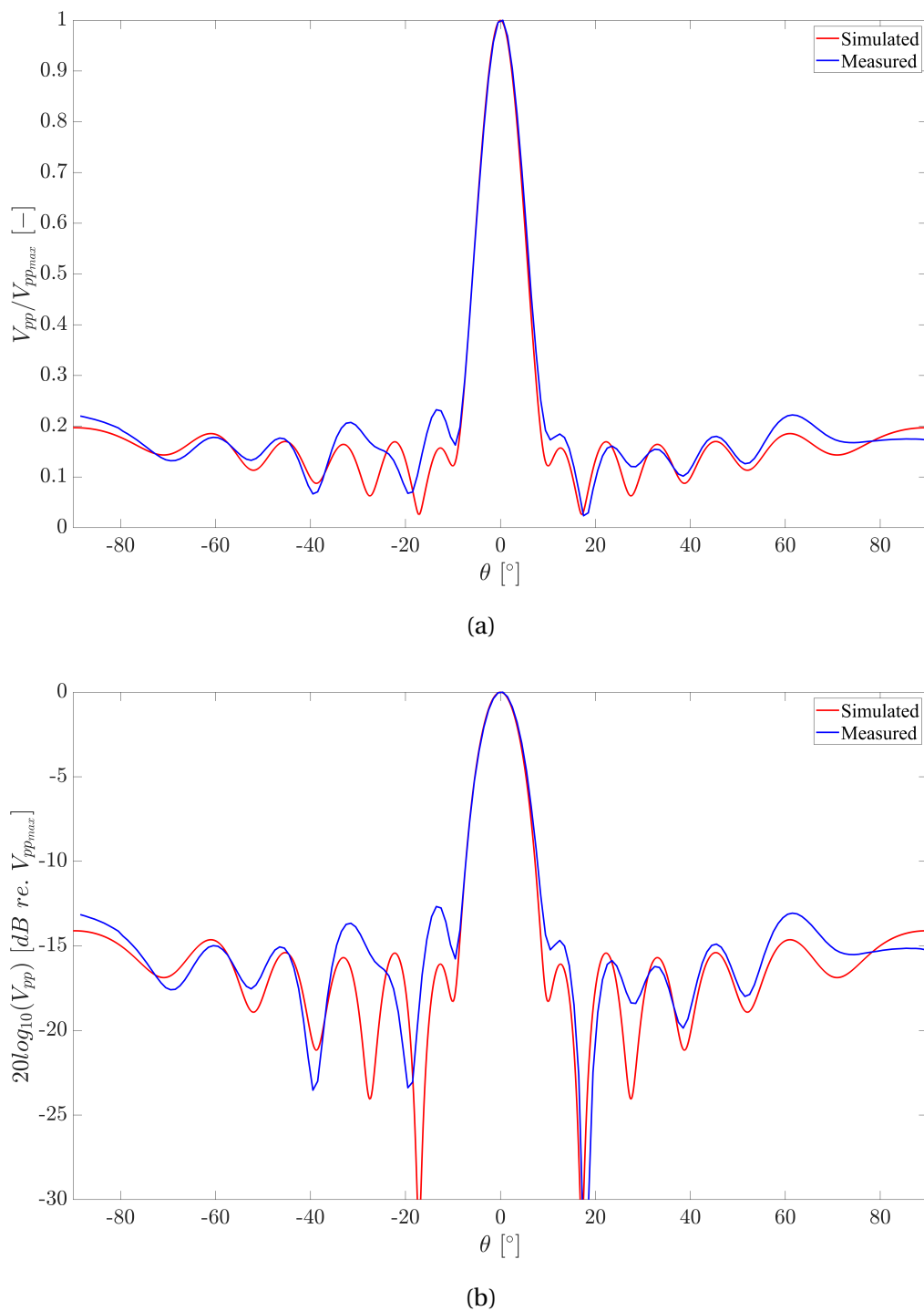


Figure 6.15: The directivity is given linearly (a) and logarithmically (b), and at the angles from -90 to 90 degrees with one-degree resolution. Directivity frequency is 98860 Hz for measurement and 98100 Hz for simulation, both conducted at a distance of 0.2 m. ($T = 25.1^\circ\text{C}$, $\text{RH} = 33.4\%$, $P = 991\text{ hPa}$).

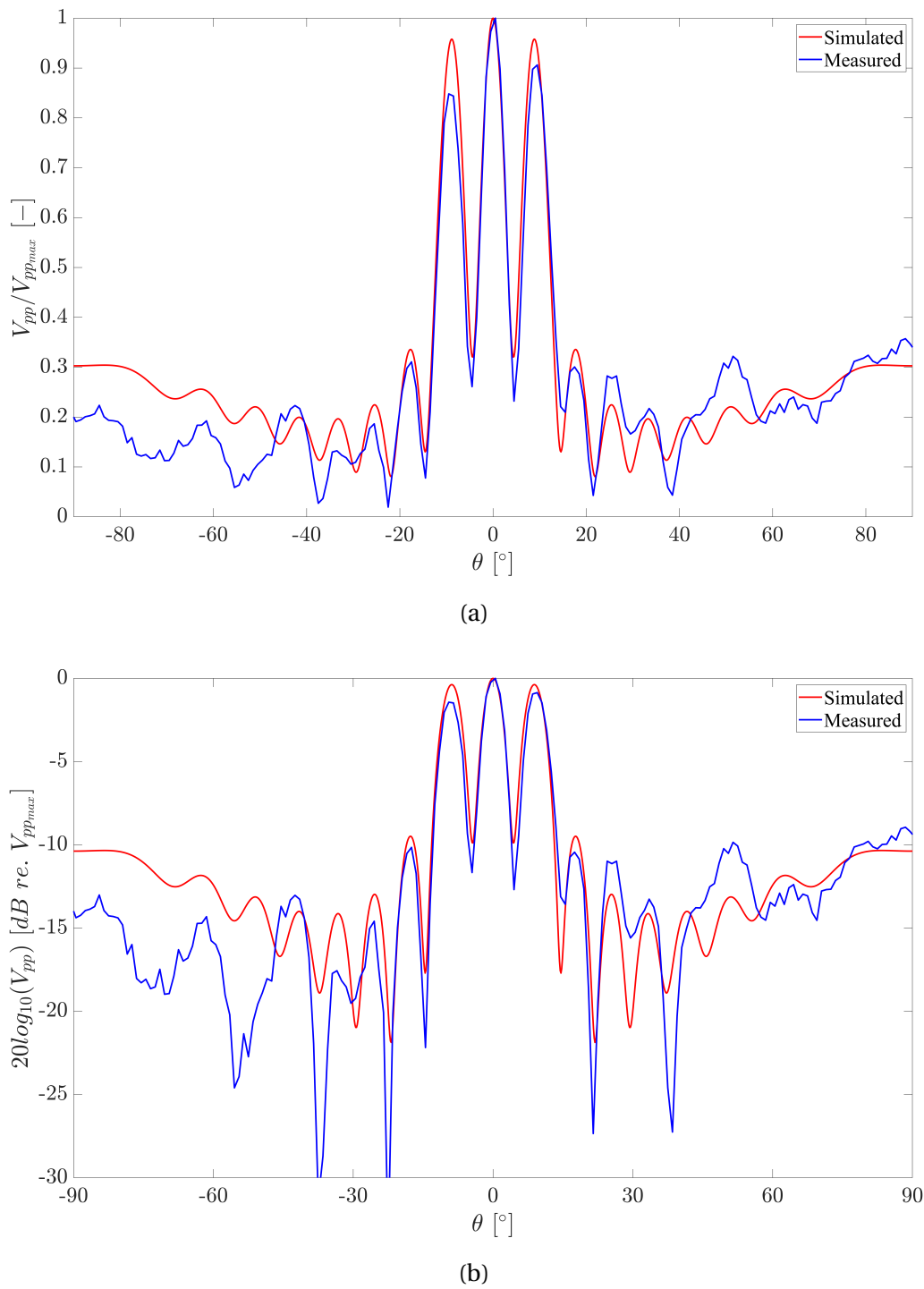


Figure 6.16: The directivity is given linearly (a) and logarithmically (b), and at the angles from -90 to 90 degrees with one-degree resolution. Directivity frequency is 148290 Hz for measurement and 147150 Hz for simulation, both conducted at a distance of 0.2 m. ($T = 25.3^\circ\text{C}$, $\text{RH} = 36.3\%$, $P = 990\text{ hPa}$).

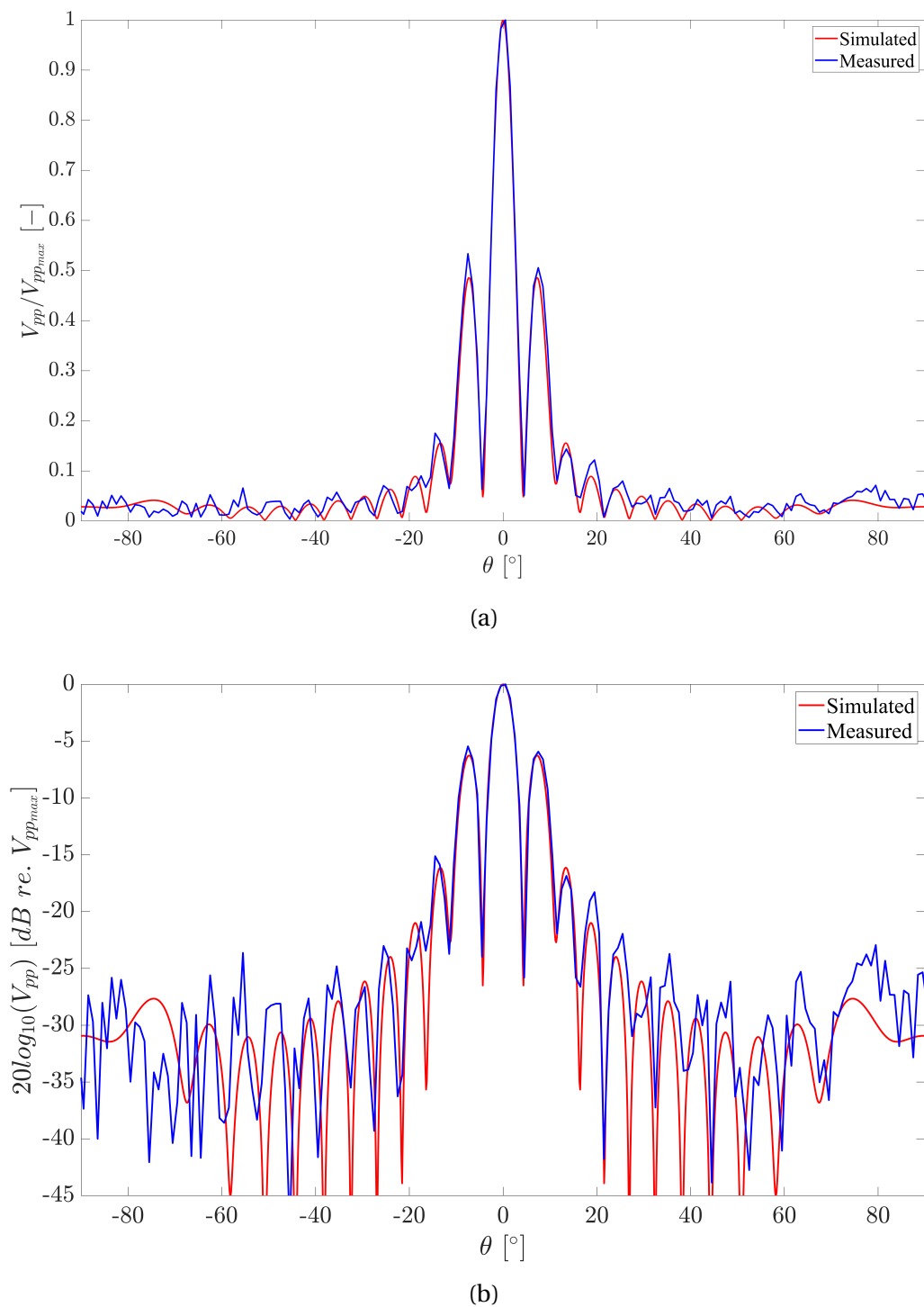


Figure 6.17: The directivity is given linearly (a) and logarithmically (b), and at the angles from -90 to 90 degrees with one-degree resolution. Directivity frequency is 197720 Hz for measurement and 196200 Hz for simulation, both conducted at a distance of 0.2 m. ($T = 25.4^\circ\text{C}$, $\text{RH} = 37.8\%$, $P = 991\text{ hPa}$).

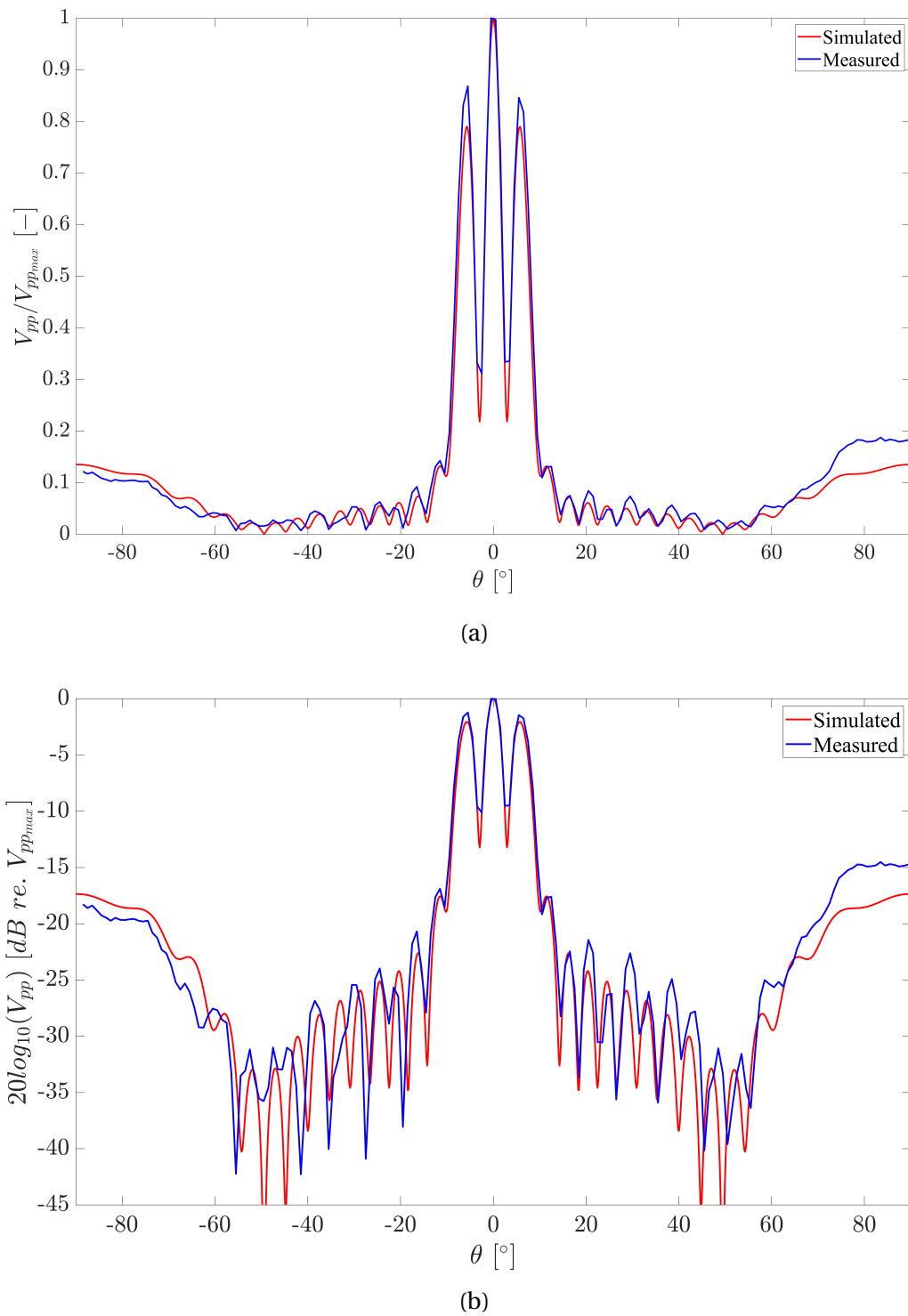


Figure 6.18: The directivity is given linearly (a) and logarithmically (b), and at the angles from -90 to 90 degrees with one-degree resolution. Directivity frequency is 250500 Hz for measurement and 249050 Hz for simulation, both conducted at a distance of 0.2 m. ($T = 26.3^\circ\text{C}$, $\text{RH} = 40.2\%$, $P = 1007\text{ hPa}$).

In Fig 6.16, the measurement shows good agreement in the main lobe relative to the simulations and, to some degree, good agreement in the first and second side lobes. Beyond the second side lobes, there seems to be relatively much noise present in measurement, which seems to be true for the measurement signal as well, see Figs. 6.10b and 6.10c. It is worth noting that it is used a relatively low signal generator output voltage, V_{0pp} , which is 1 V. With this low voltage and compared to Fig. 1.1, measured by [48], it can be seen that the transmitting voltage response S_V of this type of piezoelectric disk for this particular frequency range is relatively low. This low S_V impacts the transmitting efficiency, which most likely is the cause of much noise being present in the measurement due to bad SNR. Since this is not at a resonance frequency, the measuring voltage should and can be much higher and still not cause a non-linear effect in the piezoelectric disk.

In Fig 6.17, the measurement shows good agreement in the main, first and second side lobes. Beyond the second side lobes, there seems to be relatively much noise present in measurement, which is true for the measurement signal as well, see Figs. 6.11b and 6.11c. In the first side lobe, effects due to tilting θ_T or angle θ_M from the model in Sect. 4.5 can be seen as being present in the measurement. These effects can be due to θ_T or θ_M exceeding 0.5 degrees.

For the last directivity measurement seen in Fig. 6.18, the measurement results are similar to the result in Fig. 6.17, but with less noise.

6.2.4 SNR of directivity measurements

In Fig 6.19, the SNR of directivity measurements is presented for all measurement frequencies in Tabel 6.3 and at the measurement distance of 0.2 m between the piezoelectric disk and microphone. Generally, a good SNR magnitude is 20 dB when the measurement voltage $V_{5_{rms}}$ is 10 times greater than the rms noise voltage V_{rms}^{noise} . The highest SNR magnitude is 63 dB and is related to the frequency 98860 Hz (the first radial mode). The lowest SNR magnitude is -25.4 dB and is related to the frequency 197720 Hz. With an SNR less than 0 dB, the rms noise voltage V_{rms}^{noise} is larger than the measurement voltage $V_{5_{rms}}$.

For the directivity measurement with a frequency of 49430 Hz, the SNR magnitude of the main lobe stays above 20 dB. The SNR magnitude starts to drop below 20 dB when the angle passes 30 degrees. When the SNR drops below 20 dB, noise starts appearing in the measurements, as seen in Fig. 6.13.

For the directivity measurement with a frequency of 65907 Hz, the SNR magnitude is generally above 20 dB, except for node points of the directivity beam where the SNR magnitude goes below 20 dB. This measurement is generally stable, as seen in Fig. 6.14.

For the directivity measurement with a frequency of 98860 Hz, the SNR magnitude stays well above 40dB, except for the node points of the directivity beam at approx. 20 de-

degrees where the SNR magnitude goes below 40 dB. This measurement is stable, as seen in Fig. 6.15.

For the directivity measurement with a frequency of 148290 Hz, the SNR magnitude is below 20 dB. At some point, the V_{rms}^{noise} is calculated to be larger than the measurement voltage $V_{5_{rms}}$. This measurement is generally unstable from approx 20 degrees, as seen in Fig. 6.16.

For the directivity measurement with a frequency of 197720 Hz, the SNR magnitude is generally below 20 dB, and for all angles larger than 20 degrees, the V_{rms}^{noise} is calculated to be larger than the measurement voltage $V_{5_{rms}}$. This measurement is generally unstable from approx 15 degrees, but appear to follow the simulation even if there is noise visibly present, as seen in Fig. 6.17.

For the last directivity measurement with a frequency of 250500 Hz, the main, first, and second side lobes stay above the SNR magnitude of 20 dB. The angles between approximately 15 to 60 degrees remain between the SNR magnitude of 0 dB and 20 dB. For the angles increasing past 60 degrees, the SNR magnitude is larger than 20 dB. Between 0 dB and 20 dB, the measurements may appear to follow simulation to some degree in Fig. 6.18, but noise is visibly present.

Measurements of the directivity beam pattern for different frequencies show relatively good agreements with the simulations. However, the SNR is quite low and negative for some of the frequencies used, especially for the measurement frequencies 148290 Hz and 197720 Hz. This can be due to the low signal generator peak-to-peak voltage equal to 1 $V_{0_{pp}}$. If the transmitting voltage response S_V information in Fig. 1.1 had been considered when conducting measurements, the signal generator voltage would have been increased for frequencies outside the first and second radial modes. This is due to work done by Mosland [48], which shows that high signal generator voltages at the first and second radial modes give non-linear effects at these frequencies. Therefore the work conducted by [48] did measure S_V with two different signal generator voltages, which are $V_{0_{pp}} = 20$ V outside resonance and $V_{0_{pp}} = 2$ V at resonance to avoid non-linear effects. If these measurements conducted in this work had used the same voltages as [48], it would most likely increase the SNR ratio giving better measurement results.

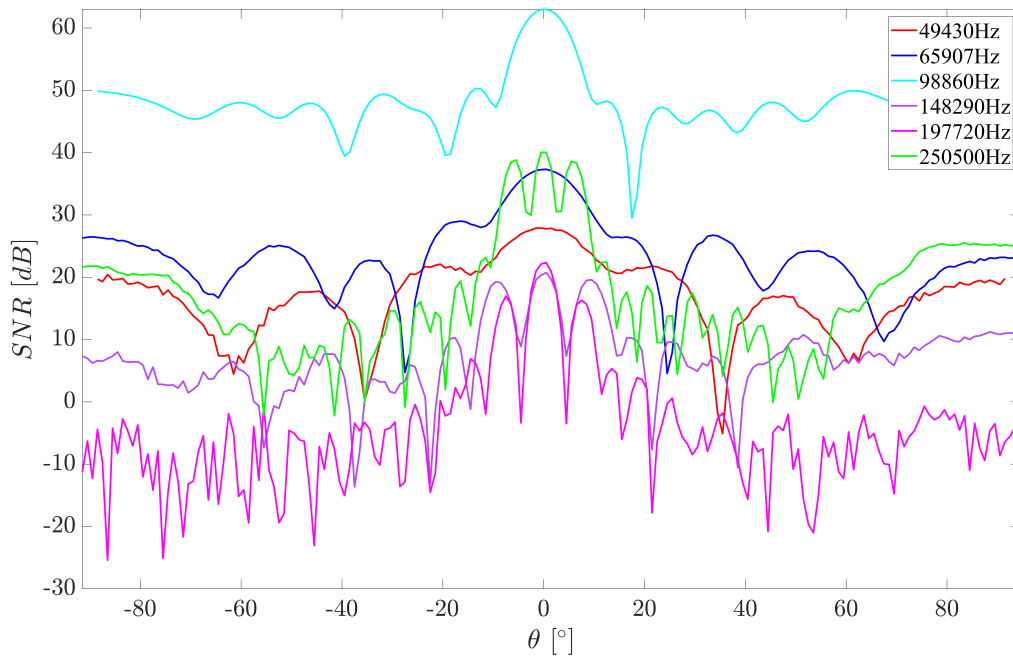
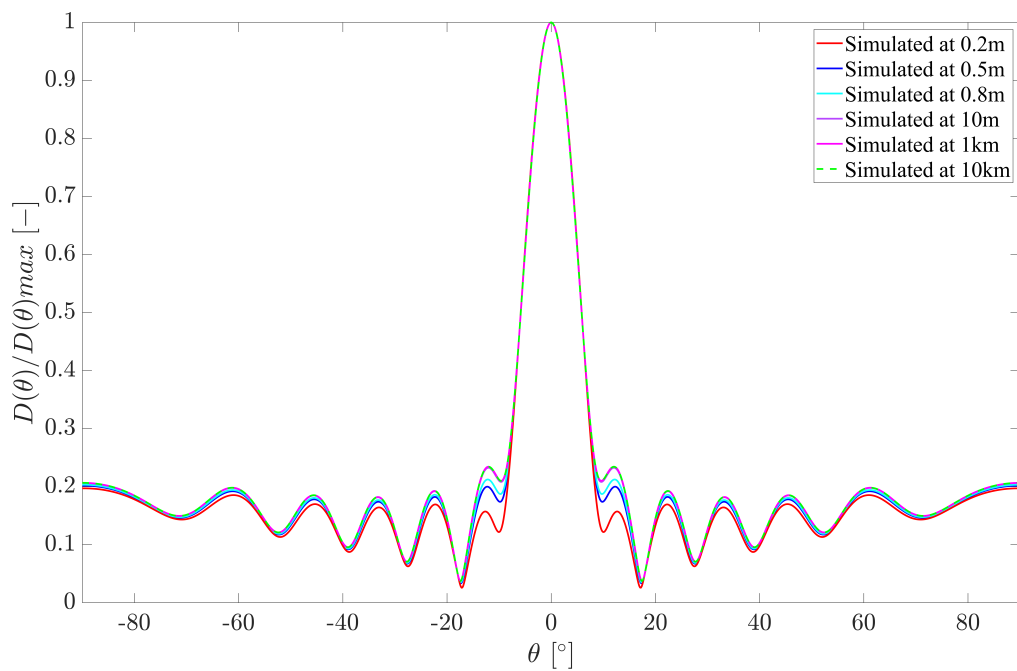


Figure 6.19: Signal-to-noise ratio of all directivity measurements at the distance of 0.2 m.

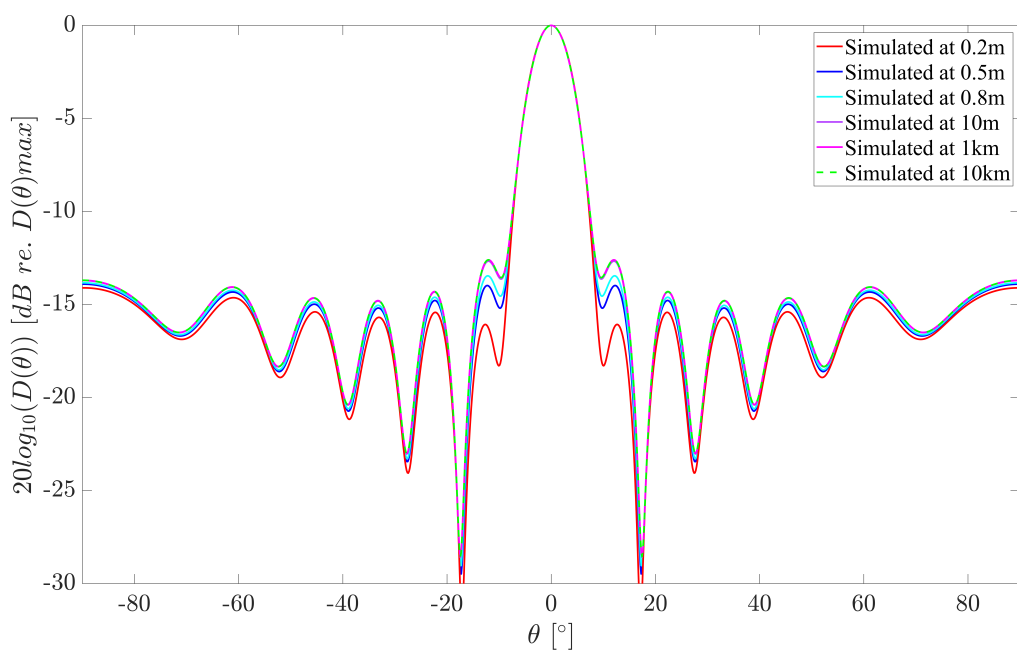
6.2.5 Comparison of directivity at different z distances of FE simulations and measurements

In Fig. 6.20 it is studied the change in the FE directivity simulations as a function of increasing distance z . This is to investigate how increasing the distance affects the directivity and investigate how large the distance must be before the directivity stabilizes. The same study is performed for directivity measurements, but not to the same extent since it is not measured further out than to $z = 0.8$ m, see Fig 6.21.

For the FE directivity simulations, shown in Fig. 6.20, it can be seen that the amplitude of the side lobes of the directivity changes with the distance. The amplitude difference is most noticeable for simulations that have not been performed far enough into the far field, where the far field distance for this frequency is 90.6 mm, see Tabel 6.4. The further into the distant far field that simulations are performed, the more stable the directivity becomes. After 10 m into the far field, there is minimal change up to 10 km and can be seen as they overlap in Fig. 6.20. The directivity measurements at the distances 0.2 m, 0.5 m, and 0.8 m, shown in Fig. 6.21, and the FE directivity simulations at 0.2 m, 0.5 m, and 0.8 m, shown in Fig. 6.20, do not share the same effects. For the directivity measurements in Fig. 6.21, the largest difference in the first side lobe is between 0.2 m and 0.8 m on the positive angle side and is 1.38 dB. Compare this magnitude to the FE directivity simulations first side lobe between 0.2 m and 0.8 m, which is 2.61 dB. The directivity measurement side lobes in Fig. 6.21 vary for which distance is greatest in magnitude.



(a)



(b)

Figure 6.20: The FE directivity simulations is given linearly (a) and logarithmically (b), and at the angles from -90 to 90 degrees with one-degree resolution. Directivity simulation frequency is 98100 Hz and conducted at a distance of 0.2 m, 0.5 m, 0.8 m, 10 m, 1 km, and 10 km.

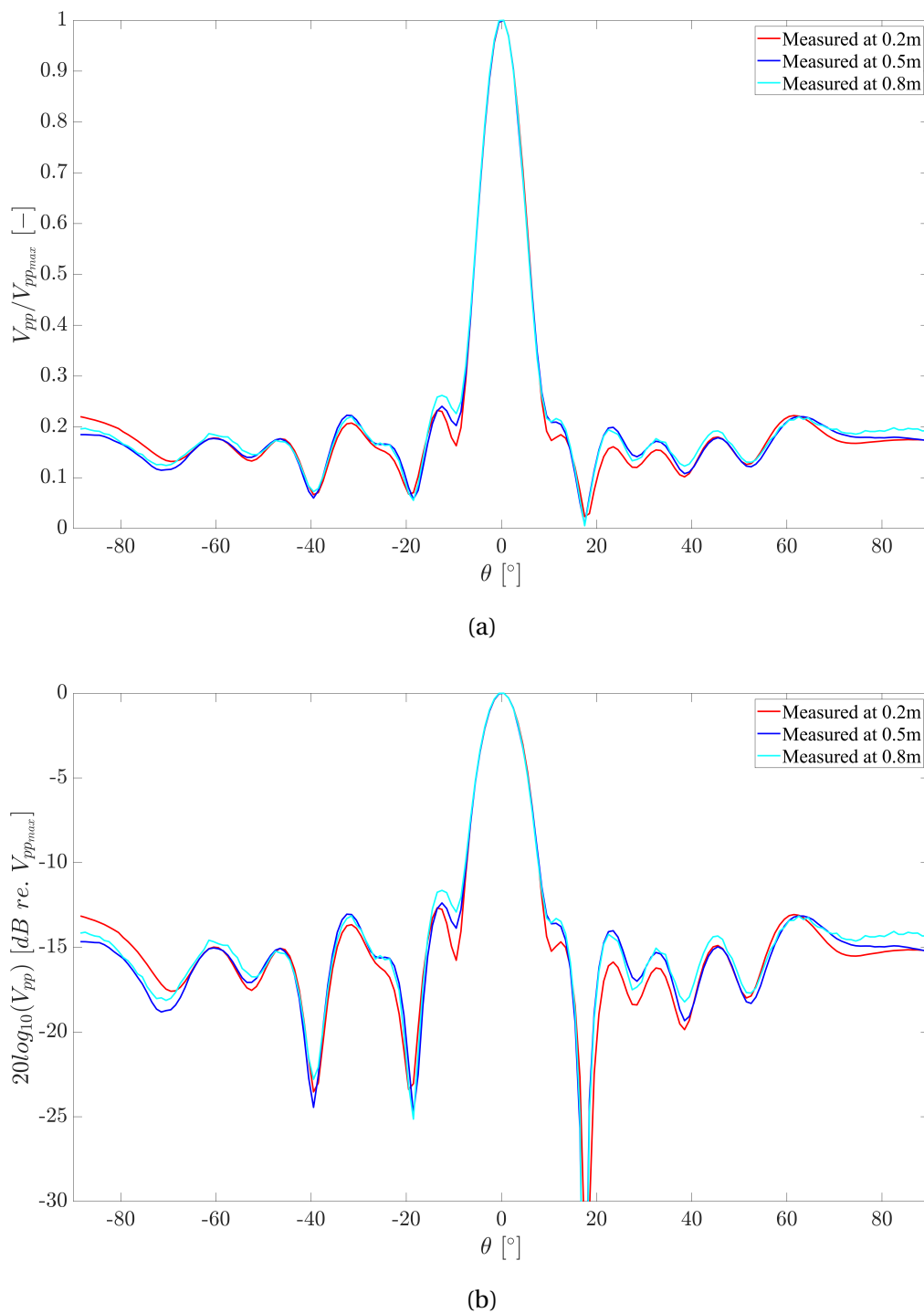


Figure 6.21: The directivity measurements is given linearly (a) and logarithmically (b), and at the angles from -90 to 90 degrees with one-degree resolution. Directivity measurement frequency is 98860 Hz and conducted at a distance of 0.2 m, 0.5 m, and 0.8 m. ($T = 25.2^\circ\text{C}$, $\text{RH} = 32.6\%$, $P = 990\text{ hPa}$).

6.2.6 Comparison of on-axis pressure between FE simulations and measurements

The on-axis pressure of the piezoelectric disk is measured with frequencies given in Table 6.3, excluding 250500 Hz, and at the z distance from 0.1 mm to 0.3 m. The spatial resolutions of the z distance vary with increasing distance and are given in Table 6.5. With increasing z distance, the spatial resolution decreases when it approaches far field, and the on-axis pressure approaches $1/z$ dependency. The resolution is more significant in the near field due to several pressure nodes and maximums that need to be documented. If the spatial resolution is too low in the near field, it is easy to miss relevant pressure changes. All on-axis pressure measurements and simulations are plotted as pressure amplitude vs. distance z and sound pressure level (SPL) vs. distance z .

Table 6.5: Spatial resolution of on-axis pressure measurements from 0.1-300 mm.

Start of Interval	Spatial resolution	Stop of Interval	Unit
0.1	0.1	30	[mm]
31	1	100	[mm]
105	5	300	[mm]

In Fig. 6.22, the on-axis pressure measurement shows good agreement with the FE simulation. It is seen some ripples in the measurements with the increasing z distance. The distance between each maximum of the ripples is approximately 3.2-3.6 mm. The ripples slowly die out and can't be seen anymore from about 0.1 m. For the pressure node, the simulation pressure is higher than for measurement. The $1/z$ dependency shows good agreement with measurement until at around 0.15 m.

In Fig 6.23, the on-axis pressure measurement shows good agreement with the FE simulation. As for earlier on-axis pressure measurement, this also contains ripples with the increasing z distance. The distance between each maximum of the ripples is approximately 2.2-2.7 mm. The ripples slowly die out and can't be seen anymore from about 0.1 m. The simulation pressure is higher for the first pressure maximum and node than for measurement. At the last pressure maximum, the measurement pressure is higher than for simulation. The $1/z$ dependency shows excellent agreement with measurement.

In Fig 6.24, the on-axis pressure measurement shows good agreement with the FE simulation but starts to deviate when z becomes less than 0.0145 m. As for all earlier on-axis pressure measurements, this also contains ripples with the increasing z distance. The distance between each maximum of the ripples is approximately 1.6-1.8 mm. The ripples slowly die out and can't be seen anymore from about 0.075 m. At the last pressure maximum, the

simulation pressure is higher than for the measurement and continues to be higher with increasing distance z . The $1/z$ dependency shows good agreement with measurement and starts to deviate in the near field at approximately 0.075 m.

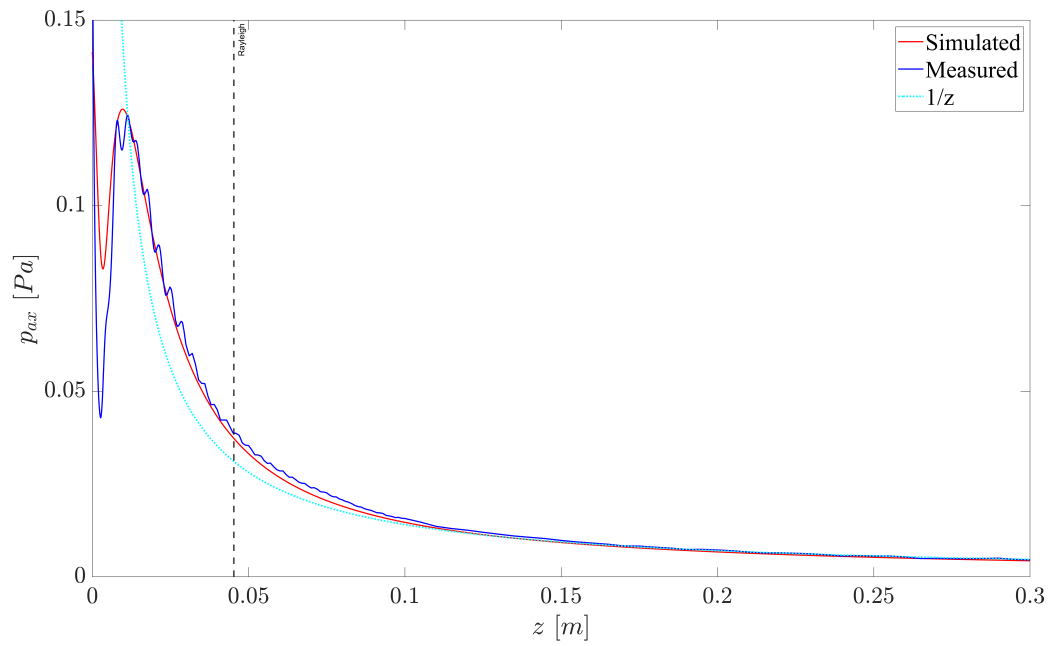
In Fig. 6.25, the on-axis pressure measurement shows some agreement with the FE simulation, but a significant deviation can be seen from the last pressure maximum. As for all earlier on-axis pressure measurements, this also contains ripples, but the ripples are more significant for this frequency than all earlier measurements. The distance between each maximum of the ripples is approximately 1.1-1.2 mm, and the ripples die abruptly out at about 0.03 m. The $1/z$ dependency shows some agreement with measurement in the far field. For the pressure nodes and maximums, it can be seen that they are shifted a little to the left.

In Fig. 6.26, the on-axis pressure measurement shows good agreement with the FE simulation, but a significant deviation can be seen. For the last maximum pressure, the measurements deviate by about 30 % less than for simulated pressure. As for all earlier on-axis pressure measurements, this also contains ripples, and they abruptly die out at about 0.029 m. The distance between each maximum of the ripples is approximately 0.8-0.9 mm. The pressure nodes and maximums show good agreement with the FE simulation but with lesser pressure amplitude.

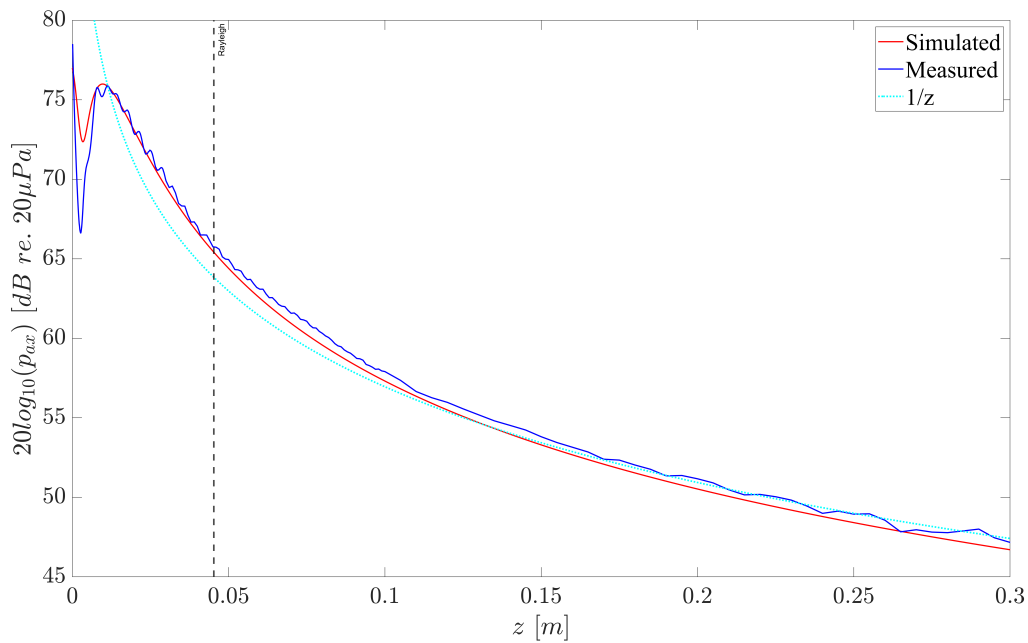
By comparing all distances between the ripple maximums with the wavelength in Table 6.6, it can be seen that all wavelengths divided by two lies within the distance ranges of the ripple maximums with the corresponding frequency. This implies that these ripples are probably caused by standing waves between the microphone and the piezoelectric disk. The pressure shape for all measurements seems to agree well with simulations when one disregards the magnitude. All on-axis pressure plots also have a $1/z$ dependency, which usually happens in the far field at around Rayleigh distance, where pressure amplitude decreases with the inverse of the increasing z distance. For Fig 6.22, 6.25, and 6.26, there also seems to be some noise present at around 0.15 m and continues with increasing distance z .

Table 6.6: Signal length and wavelength λ for the different frequencies used in on-axis measurements. It is used 60-cycle sine burst, and the sound speed $c = 343$ m/s.

Frequency	Signal Length	λ
49430 Hz	416.3 mm	6.939 mm
65907 Hz	312.3 mm	5.204 mm
98860 Hz	208.2 mm	3.470 mm
148290 Hz	138.8 mm	2.313 mm
197720 Hz	104.1 mm	1.735 mm

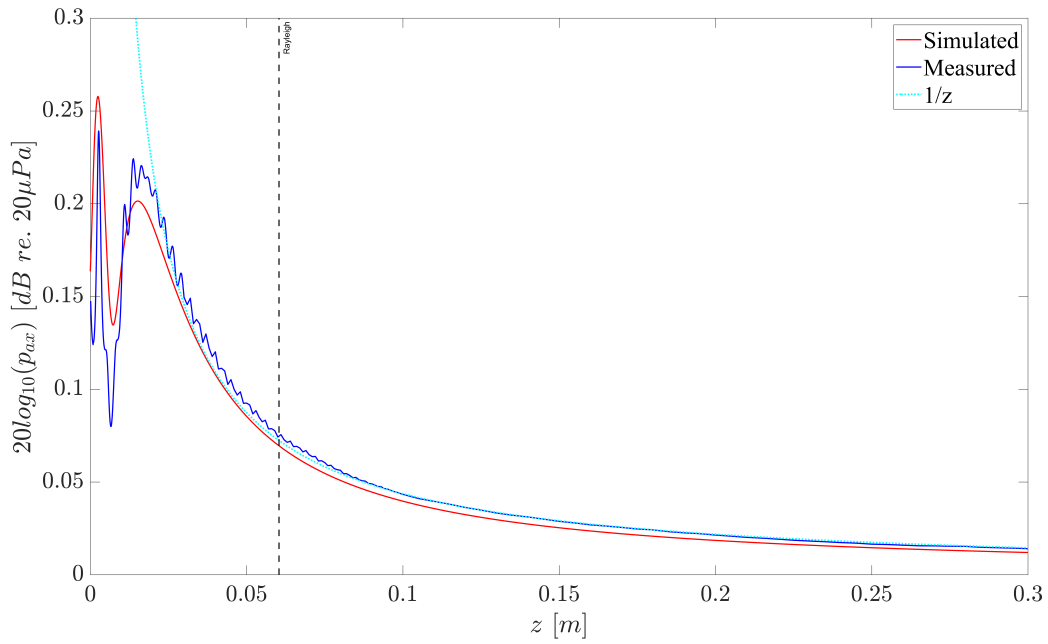


(a)

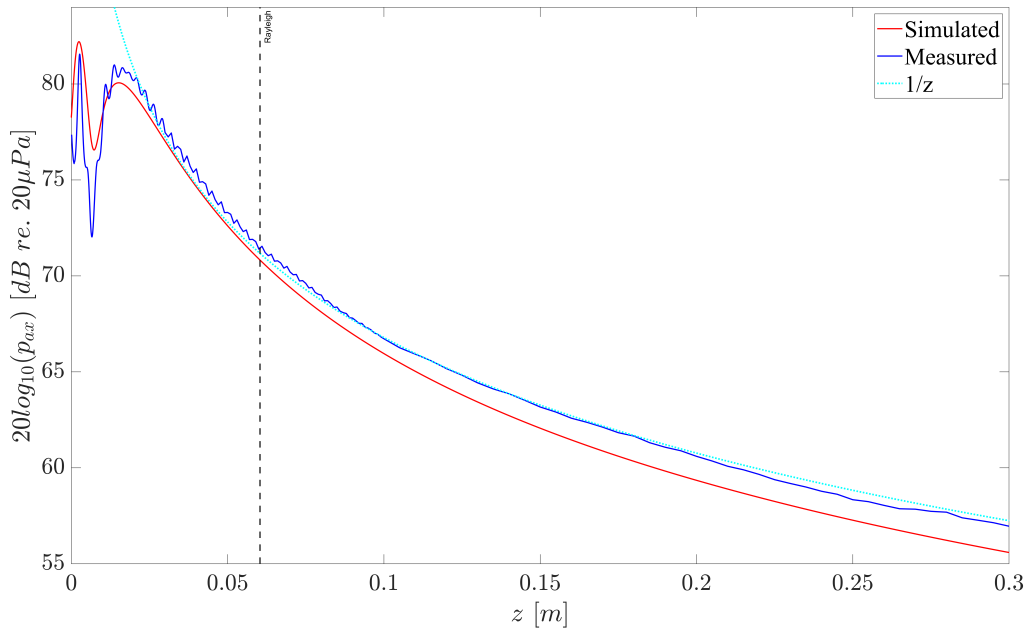


(b)

Figure 6.22: On-axis pressure given in pressure amplitude (a) and SPL (b), from 0.1 mm to 0.3 m with decreasing spatial resolution with increasing distance z . On-axis pressure frequency is 49430 Hz for measurement and 49050 Hz for simulation. The Black stippled line represents Rayleigh distance, and turquoise represents $1/z$ dependency. ($T = 26.2^\circ\text{C}$, $\text{RH} = 31.7\%$, $P = 1010\text{ hPa}$).

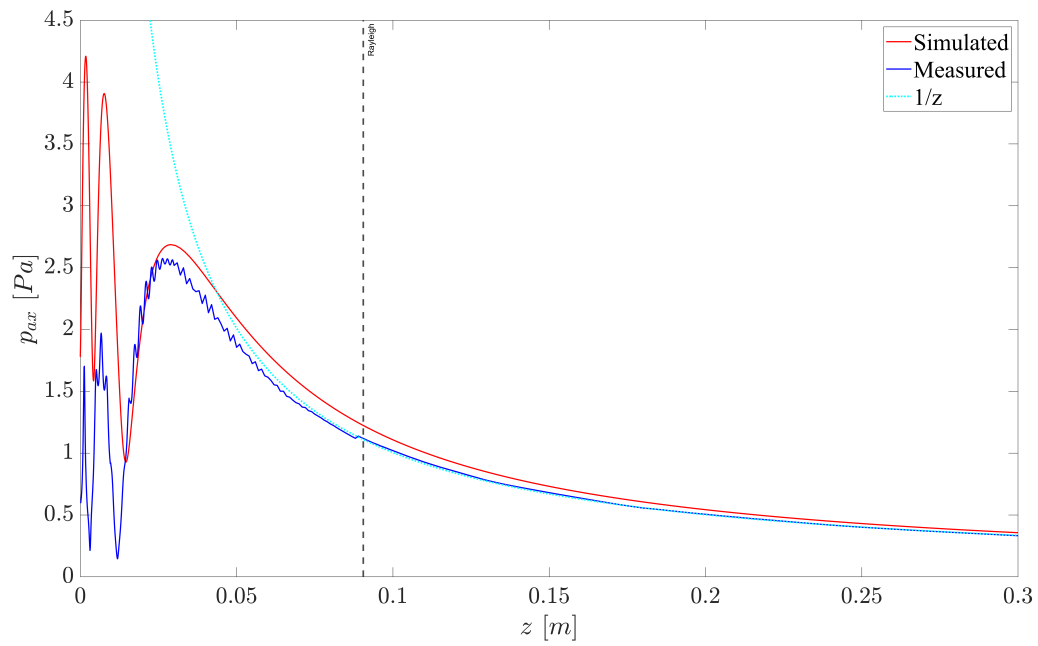


(a)

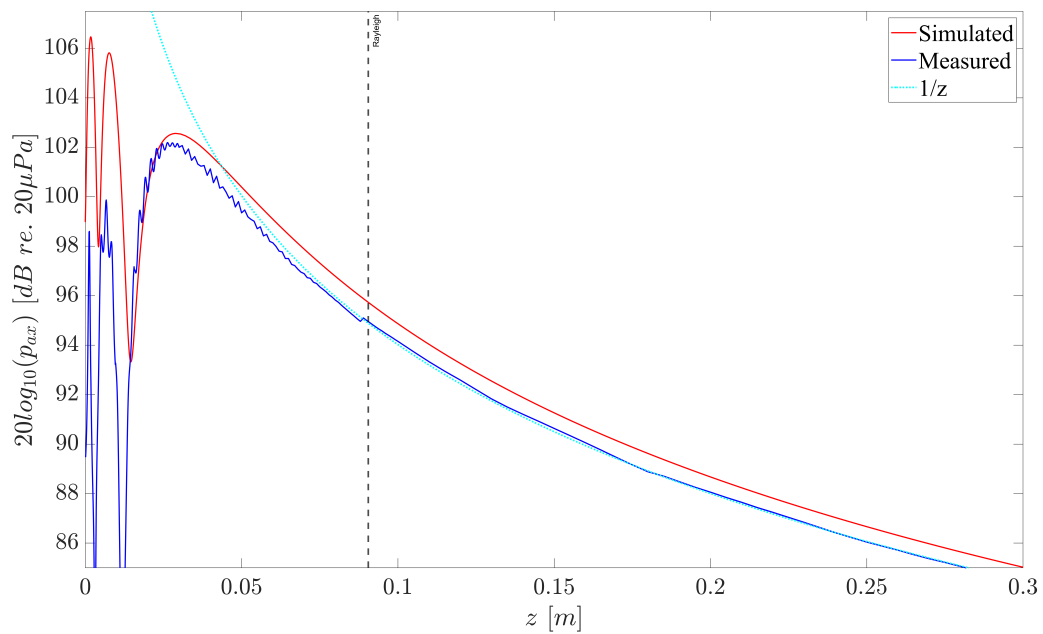


(b)

Figure 6.23: On-axis pressure given in pressure amplitude (a) and SPL (b), from 0.1 mm to 0.3 m with decreasing spatial resolution with increasing distance z . On-axis pressure frequency is 65907 Hz for measurement and 65400 Hz for simulation. The Black stippled line represents Rayleigh distance, and turquoise represents $1/z$ dependency. ($T = 25.1^\circ\text{C}$, $\text{RH} = 42.1\%$, $P = 999\text{ hPa}$).

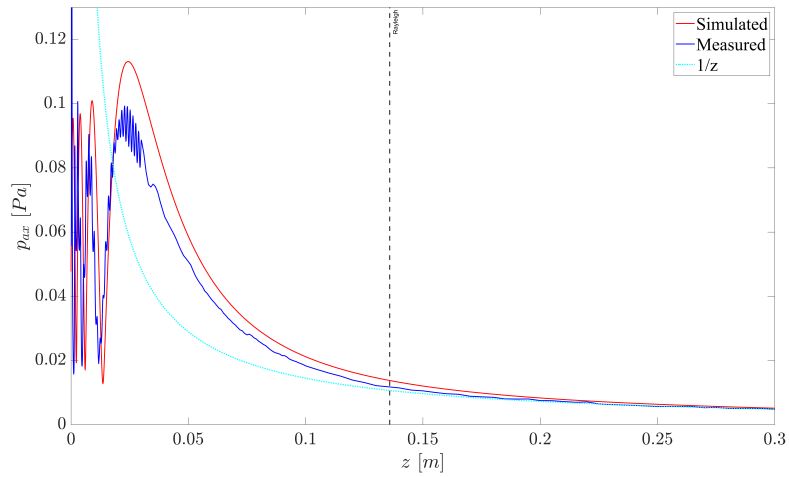


(a)

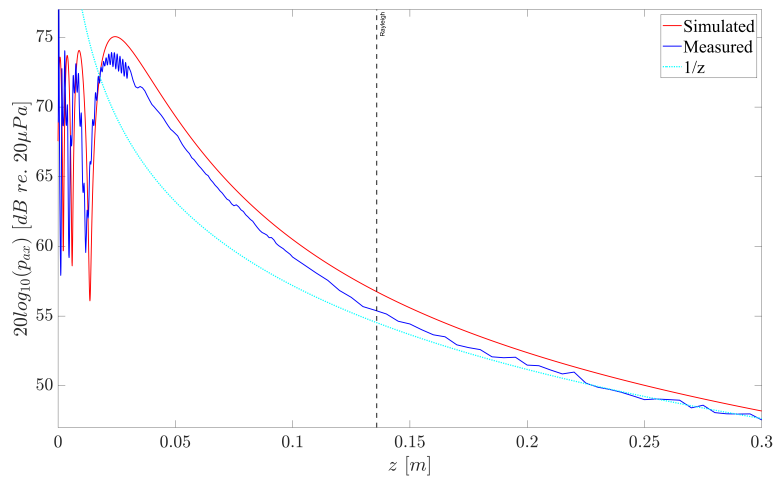


(b)

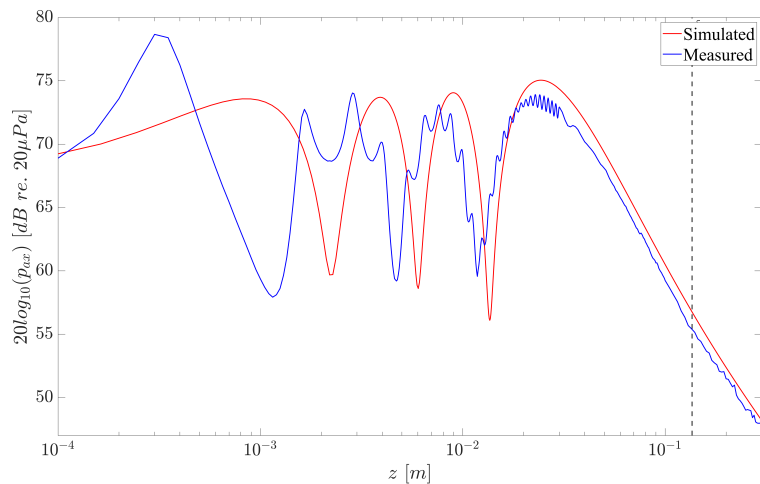
Figure 6.24: On-axis pressure given in pressure amplitude (a) and SPL (b), from 0.1 mm to 0.3 m with decreasing spatial resolution with increasing distance z . On-axis pressure frequency is 98860 Hz for measurement and 98100 Hz for simulation. The Black stippled line represents Rayleigh distance, and turquoise represents $1/z$ dependency. ($T = 26.0\text{ }^{\circ}\text{C}$, $\text{RH} = 35.0\%$, $P = 1012\text{ hPa}$).



(a)

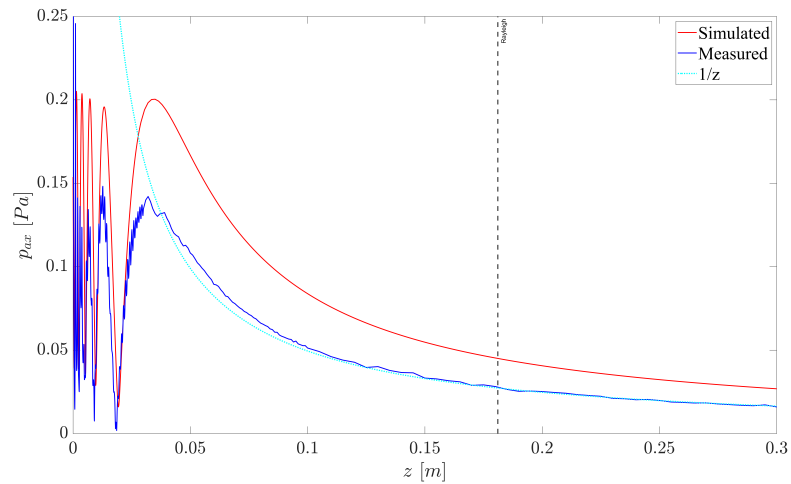


(b)

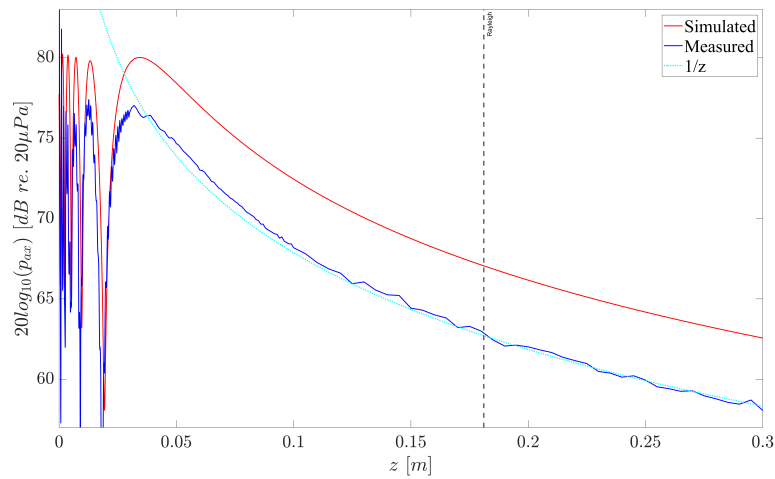


(c)

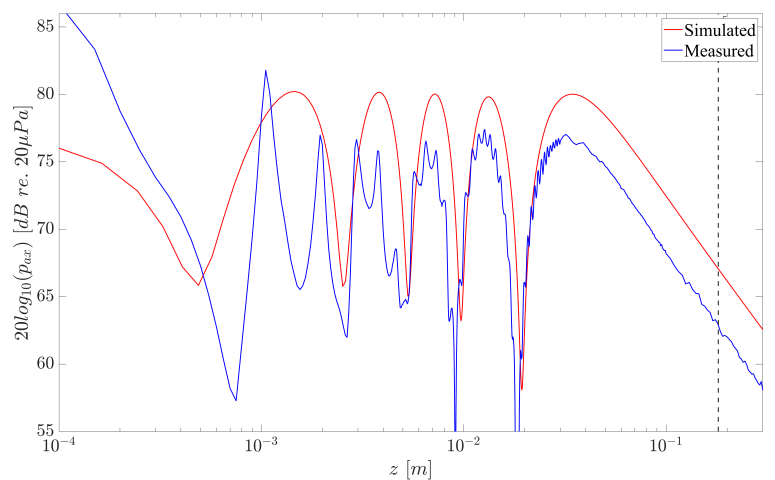
Figure 6.25: On-axis pressure given in pressure amplitude (a), SPL (b), and z distance log scaled (c), from 0.1 mm to 0.3 m with decreasing spatial resolution with increasing distance z . On-axis pressure frequency is 148290 Hz for measurement and 147150 Hz for simulation. The Black stippled line represents Rayleigh distance, and turquoise represents $1/z$ dependency. ($T = 25.2$ °C, $RH = 42.4$ %, $P = 998$ hPa).



(a)



(b)



(c)

Figure 6.26: On-axis pressure given in pressure amplitude (a), SPL (b), and z distance log scaled (c), from 0.1 mm to 0.3 m with decreasing spatial resolution with increasing distance z . On-axis pressure frequency is 197720 Hz for measurement and 196200 Hz for simulation. The Black stippled line represents Rayleigh distance, and turquoise represents $1/z$ dependency. ($T = 24.5^\circ\text{C}$, $\text{RH} = 40.1\%$, $P = 1007\text{ hPa}$).

6.2.7 SNR of on-axis pressure measurements

In Fig 6.27, the SNR of on-axis pressure measurements is presented for all measurement frequencies in Tabel 6.3, excluding 250500 Hz, and at the z distance from 0.1 mm to 0.3 m. The on-axis pressure SNR is generally good for all frequencies and stays well above 20 dB. For the frequency 148290 Hz, the SNR measurement drops below 20 dB at about a z distance equal to 0.2 m. For the frequency 197720 Hz, the SNR measurement drops below 20 dB at about a z distance equal to 0.25 m.

These results in this work have not presented examples of the acoustic signal with increasing distance, such as it was presented for different angles in Sect. 6.2.2, due to lack of time. However, from the on-axis SNR in Fig 6.27, it can be assumed that with increasing z distance, the SNR for different angles will be worsened relative to the SNR given in Fig 6.19.

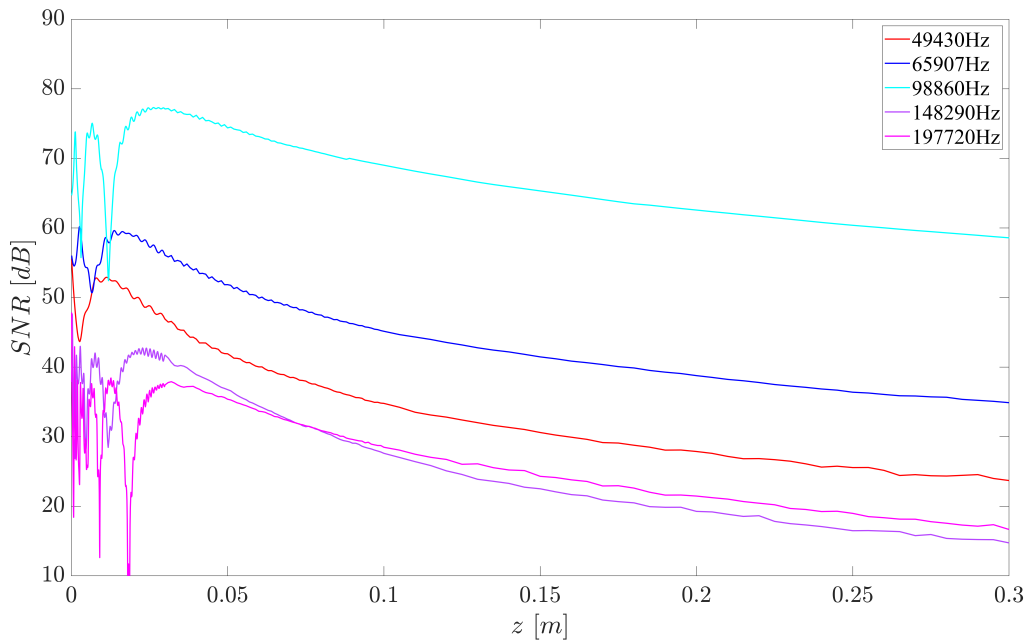


Figure 6.27: Signal to noise ratio of all measured on-axis pressure from 0.1 mm to 0.3 m. (T, RH, and P see individual measurements, Figs 6.22-6.26).

6.2.8 Comparison of 2-D sound pressure field between FE simulations and measurements

In this section, the 2-D sound pressure field for near and far fields is studied, and FE simulations are compared with measurements. Because the diameter of the piezoelectric disk is 10 mm in radius, the sound pressure field of the disk starts at a z distance of 15 mm to avoid crashing with the microphone and extends as far as the z distance of 300 mm. The measurements for each 2-D pressure field are composed of 9350 individual measurements for different positions and angles and performed with the frequencies given in Table 6.3,

excluding 250500 Hz. The resolution of the angle stays constant throughout each measurement series and is set to one degree. The measurement is performed from -93 to 93 degrees for each measured 2-D pressure field with varying spatial resolution z given in Table 6.7. The spatial resolution closest to the receiver provides the best spatial resolution, and with increasing distance z , the spatial resolution decreases.

Table 6.7: The z distance spatial resolution of 2-D sound pressure field measurements from 15-300mm.

Start Interval	Spatial resolution	Stop Interval	Unit
15	1	30	[mm]
35	5	100	[mm]
110	10	300	[mm]

The FE-simulated 2-D pressure field has no distance limitations in the near field, such as measurements performed with the piezoelectric disk. This means that simulations calculate the pressure from the structure's surface and out as far as 300 mm.

In Fig. 6.28, the measurement of the 2-D pressure field compared to the FE simulated pressure field shows good agreement. All lobes present in the measurement are present in the FE simulation.

In Fig. 6.29, the measurement of the 2-D pressure field compared to the FE simulated pressure field shows good agreement. All lobes present in the measurement are present in the FE simulation.

In Fig 6.30, the measurement of the 2-D pressure field compared to the FE simulated pressure field shows relatively good agreement. However, all lobes seen in the FE simulation are not as easy to identify in the measurement. The same effect in the 2-D pressure field measurement can be seen as for the directivity in Fig. 6.15, where some of the lobes discussed seem to melt into each other. This overlap between lobes mainly applies to the second and third side lobes for the negative angle side.

In Fig 6.31, the measurement of the 2-D pressure field compared to the FE simulated pressure field shows good agreement. However, it becomes more difficult to see the side lobes with the increasing angle, and some side lobes overlap. The difficulties occur probably due to low SNR shown in Fig. 6.19 and deviations seen in the directivity beam pattern from approximately 20 degrees in Fig. 6.16.

In Fig. 6.32, the measurement of the 2-D pressure field compared to the FE simulated pressure field shows reasonable agreement. However, it becomes more difficult to see the side lobes with the increasing angle, probably due to the low SNR shown in Fig. 6.19. Even though the SNR is low, it is possible to see that the side lobes are present. It is worth noting

the one pressure node at zero degrees and from about 15-20 mm, see Fig 6.26, is documented in the measurement and agrees well with the FE simulation.

For all 2-D pressure field measurements seen in Fig. 6.28-6.32, the main lobe and first side lobes can be identified and correspond well to the FE simulations.

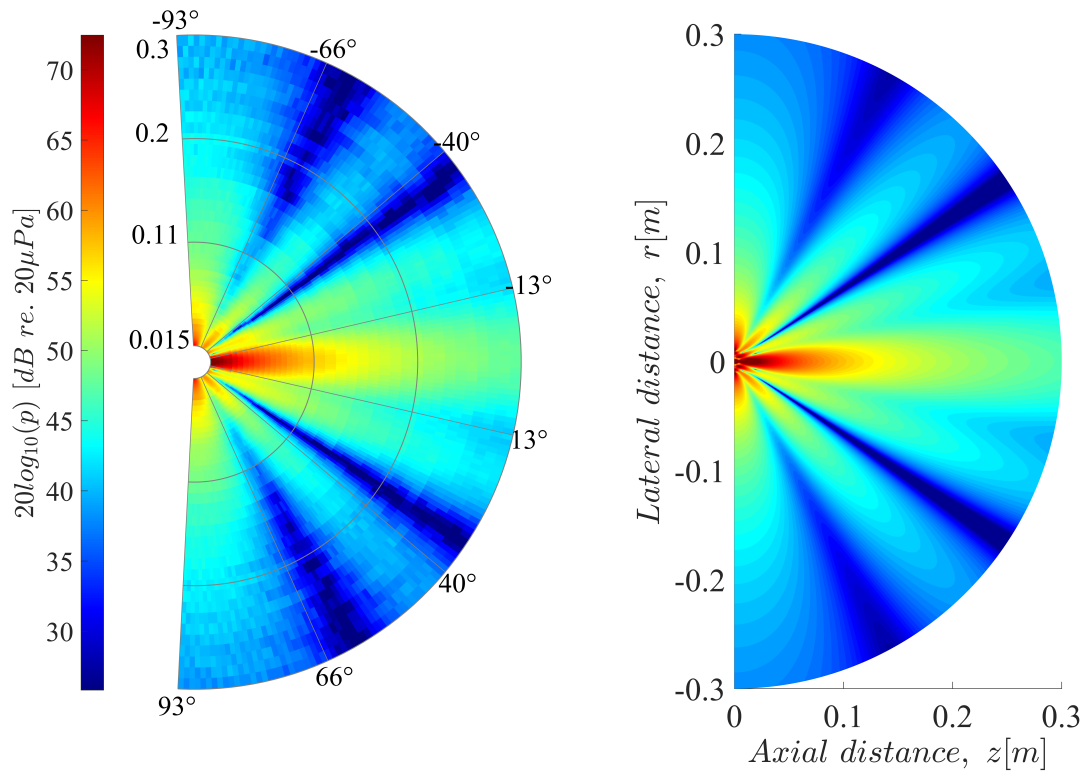


Figure 6.28: Measured (**left**) 2-D pressure field from 0.015-0.3 m with frequency 49430 Hz and simulated (**right**) from 0-0.3 m with frequency 49050 Hz with matching dB scale.

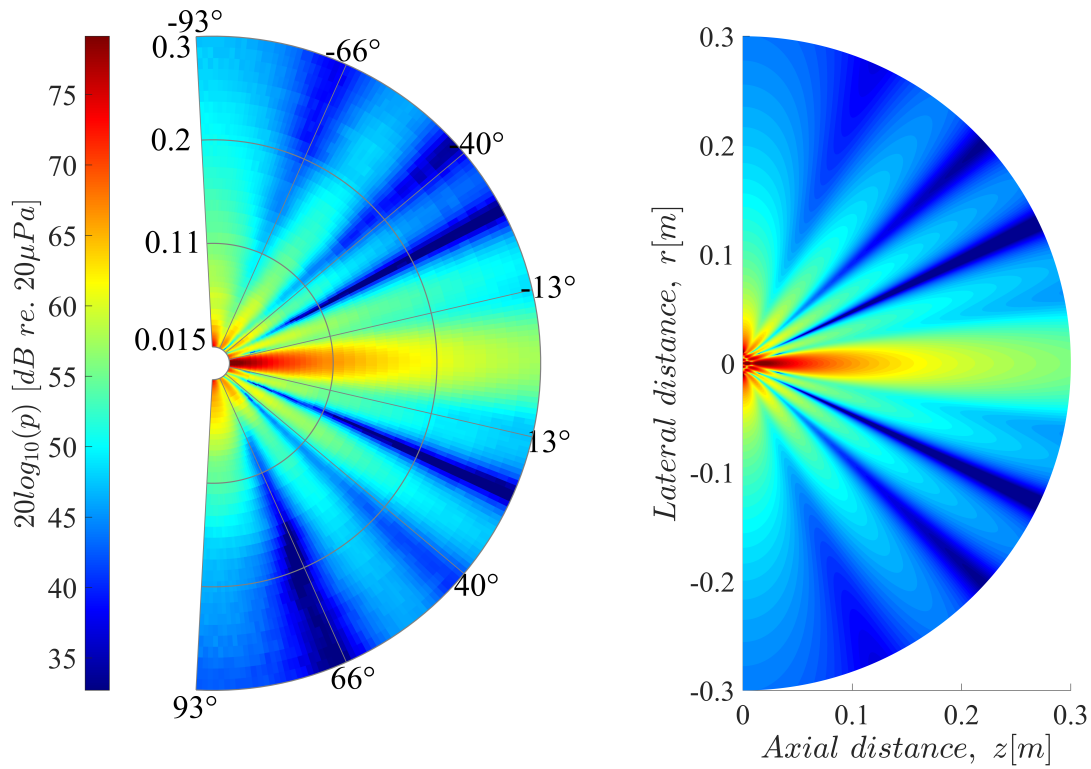


Figure 6.29: Measured (**left**) 2-D pressure field from 0.015-0.3 m with frequency 65907 Hz and simulated (**right**) from 0-0.3 m with frequency 65400 Hz with matching dB scale.

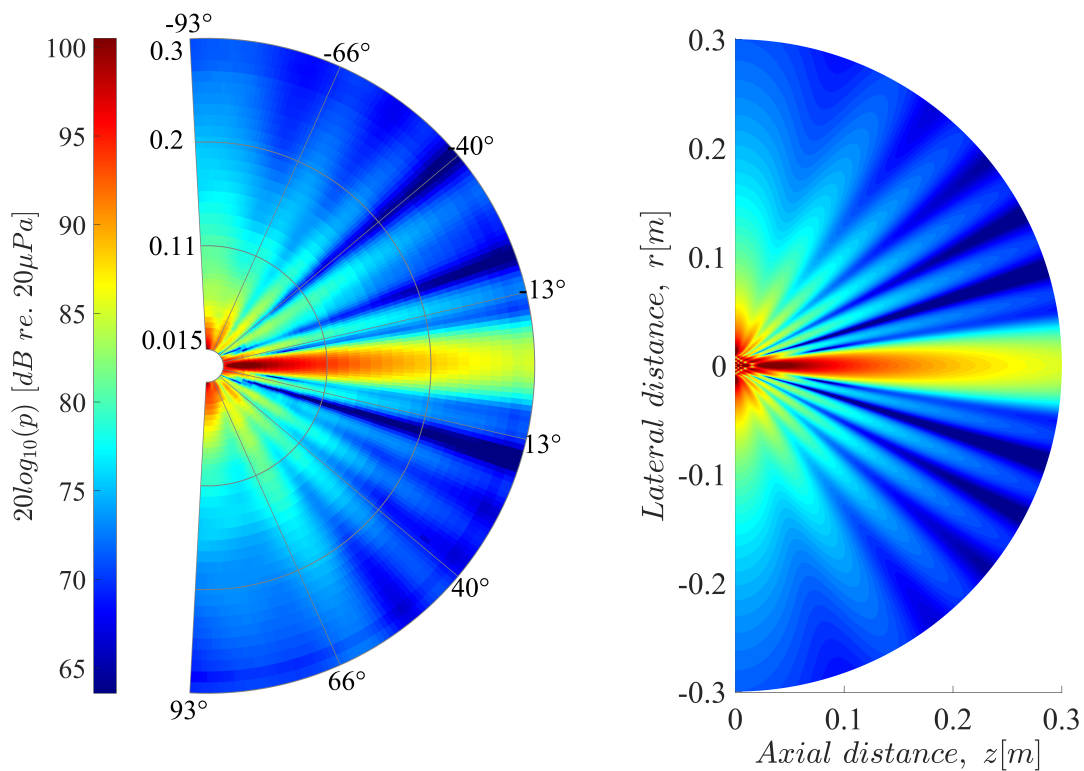


Figure 6.30: Measured (**left**) 2-D pressure field from 0.015-0.3 m with frequency 98860 Hz and simulated (**right**) from 0-0.3 m with frequency 98100 Hz with matching dB scale.

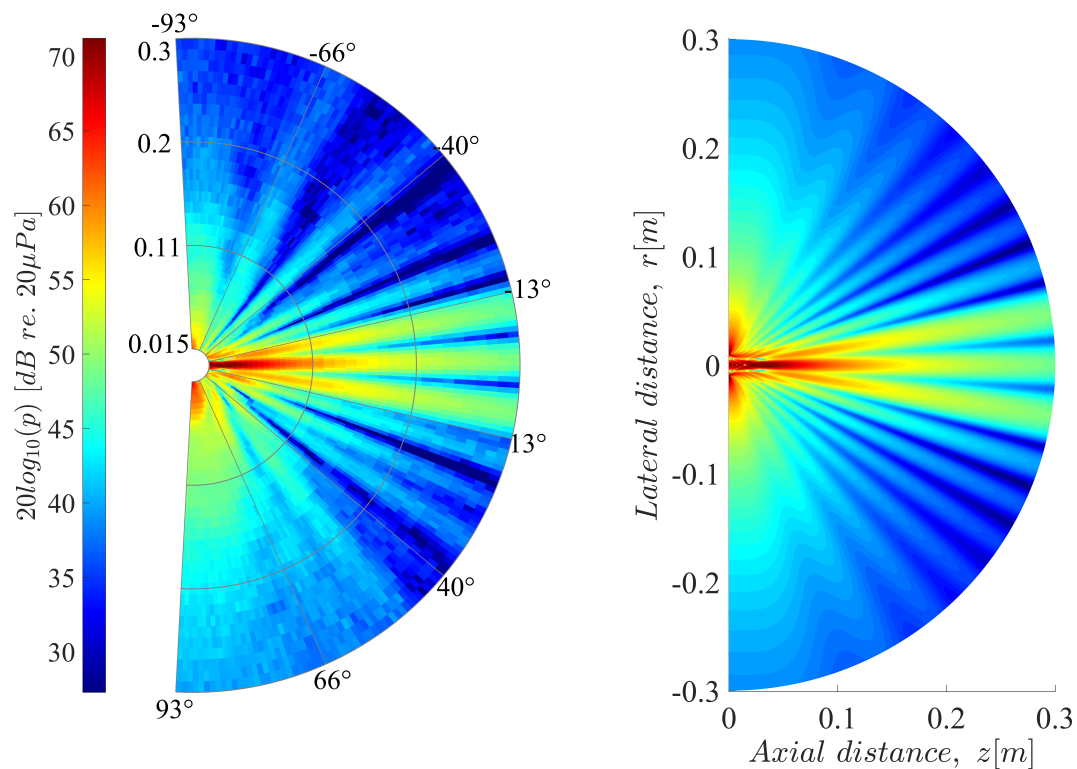


Figure 6.31: Measured (**left**) 2-D pressure field from 0.015-0.3 m with frequency 148290 Hz and simulated (**right**) from 0-0.3 m with frequency 147150 Hz with matching dB scale.

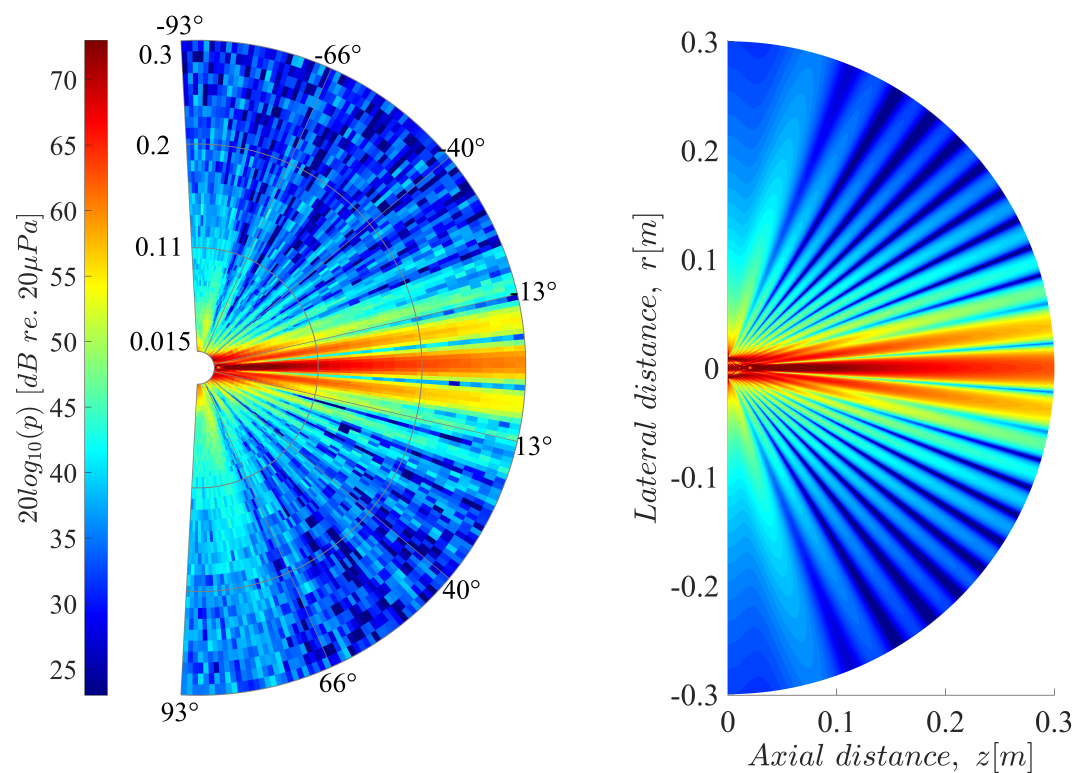


Figure 6.32: Measured (**left**) 2-D pressure field from 0.015-0.3 m with frequency 197720 Hz and simulated (**right**) from 0-0.3 m with frequency 196200 Hz with matching dB scale.

Chapter 7

Conclusions and further work

7.1 Conclusions

The measuring system, which consists of the piezoelectric disk Pz27, the receiver microphone Brüel & Kjær 4138, and the associated electronics for the measuring setup, has been studied when conducting measurements in the air in this work. All measurements performed with the measurement setup are compared with FE simulations. A MatLab app has also been created that has automated the measurement process, which has been very important to be able to carry out this work and will benefit everyone else who will continue to work with this measurement setup. Without automation, the large number of measurements performed in this work would not have been possible to conduct.

The electrical measurements and FE simulations gave good and comparable results. The radial extension modes R1 and R2 measurement performed on the wires soldered to the piezoelectric electrodes corresponded well with the FE simulation and deviated no more than 0.77 % and 0.58 % in frequency, respectively. The magnitude difference of the R1 and R2 modes deviated no more than 0.86 dB and -1.01 dB, respectively. Based on this, it can be said that the measurement and FE simulation of the electrical properties correspond well due to the good matching of the piezoelectric constants. However, there is room for improvements in the 110 kHz to 165 kHz range by adding solder lump in FE simulations to improve the results even more.

This work has studied two types of comparison between measurement and FE simulation of the directivity. The first type is the directivity measurements and FE simulations performed with a constant distance between the piezoelectric disk and microphone using different frequencies (Figs. 6.13 - 6.18). The second type is the directivity measurements and FE simulations performed with a constant frequency over several distances between the piezoelectric disk and microphone (Figs. 6.20 and 6.21). The first type of directivity measurement gave good results in all the main lobes, and, in general, the results are comparable to

the FE simulations. After increasing the angle beyond the first side lobes, the measurements in Fig 6.13, 6.16 - 6.18 suffers from low SNR, which is concluded to be due to the low signal generator peak-to-peak voltage 1 V that was used when conducting the measurement. For all directivity measurements, asymmetry mirrored around the main lobe is present, which is concluded to be due to the solder lump on each side of the electrodes and a combination of not a perfect symmetry within the disk due to aging effects and changes in polarization after soldering. The second type of directivity measurement gave good results but not the same increase in the magnitude of the side lobes as for the FE simulations. The directivity measurements did more or less give similar results for all the different distances with small deviations in between the results. A conclusion about this behavior has not been drawn.

The number of measured pressure nodes agrees with simulations of the on-axis pressure. It is concluded that there are standing waves between the microphone and the piezoelectric disk in the on-axis measurements in Figs. 6.22 - 6.26, and these are difficult to avoid. It has been measured with a given number of pulse cycles that have been constant throughout all measurements performed in this work. This constant number of cycles has proven to be a good choice for achieving good measurement results but did cause problems with standing waves deep into the near field. The pressure amplitude differs in the near field regarding the measurement compared to FE simulation for the first radial mode, Fig. 6.24, and the cause is unknown. The larger deviation in pressure of the measurements compared to FE simulations in Figs 6.25 and 6.26 is concluded to be due to conducting measurements outside the Brüel & Kjær 1/8-inch pressure microphone's stated flat frequency response from 6.5 Hz to 140 kHz ± 2 dB, the measurements results will entail larger uncertainties than expected. It can be concluded that $1/z$ dependency in the pressure is present for all on-axis measurements.

The 2-D pressure field measurements give good results compared to FE simulated 2-D pressure fields. However, it is clear that measurement and simulation results are not perfect matches, but it is still a substantial overlap between them. The most noticeable difference between measurement and simulation results is due to the SNR, as clearly seen in Figs. 6.31, 6.32, and noticeable in 6.28, and concluded to be due to the low signal generator peak-to-peak voltage of 1 V. For the 2-D pressure measurements in Figs. 6.30 and 6.31, it is clearly asymmetry mirrored around the main lobe is present, which is concluded to be due to the solder lump on each side of the electrodes and a combination of not a perfect symmetry within the disk due to aging effects and changes in polarization after soldering.

All measurement results conducted in this work and compared to FE simulation gave good agreements, and it can be concluded that using FE simulations is a good tool for approximating the admittance, directivity, on-axis pressure, and 2D pressure fields in the near and far fields.

7.2 Further work

Further work can be, exploring the effect of a solder lump on the edge of the electrodes of the piezoelectric disk with 3-D simulations in air to try recreating the asymmetric effects that occur in the present work.

Since it used a constant number of cycles throughout this work, further work can increase the number of cycles for frequencies higher than the first radial mode at 98860 Hz, e.g., 150 kHz to 90 cycles, 200 kHz to 120 cycles, and 250 kHz to 150 cycles and still avoid reflections from vertical rod and study if this can improve measurements results by obtaining a longer steady state area.

If possible, a suggestion for further work is to increase the accuracy of the microphone sensitivity beyond 140 kHz with a frequency-dependent factor.

Further work can be, performing measurements with a higher signal generator output voltage, e.g., 2-volt peak-to-peak at resonances and 20-volt peak-to-peak outside resonance, and studying improvements on the SNR ratio, which can further improve measurement results. It can also be suggested to improve the method of calculating the SNR.

More work can be conducting measurements on different-sized piezoelectric disks or other types of disks that can be interesting for gas measurements.

Finally, work regarding on-axis measurements in the near field to try to lower the effects of standing waves between the piezoelectric disk and microphone.

References

- [1] Aanes, M. (2009). Undersøkelser av piezokeramiske skiver. Målinger og endelig element analyser. Master's thesis, University of Bergen, Department of Physics and Technology, Bergen, Norway.
- [2] Aanes, M. (2011). *A Guide to "inn-files" to FEMP 5*. University of Bergen, Department of Physics and Technology, Bergen, Norway.
- [3] AGA-9 (1998). Measurement of Gas by Multipath Ultrasonic Meters. *Transmission Measurement Committee Report No.9, A.G.A, American Gas Association, Wilson Boulevard, Arlington, USA*.
- [4] Agilent Technologies (2007). *Agilent 33220A 20 MHz Waveform Generator User's Guide*. 3501 Stevens Creek Blvd. Santa Clara, CA 95052 USA: Agilent Technologies Inc.
- [5] American National Standard (ANSI S1.26-1995(ASA 113-1995)). *Method for Calculating of the Absorption of Sound by the Atmosphere*. New York, USA: Reaffirmed by ANSI 2004.
- [6] Amundsen, Ø. S. (2011). Material constants determination for piezoelectric disks, and influence on source sensitivity. Measurements and simulations. Master's thesis, University of Bergen, Department of Physics and Technology, Bergen, Norway.
- [7] Andersen, K. K. (2015). Reciprocity calibration of ultrasonic piezoelectric disks in air. Master's thesis, University of Bergen, Department of Physics and Technology, Bergen, Norway.
- [8] ASL (1997). *F250 MKII precision Thermometer. Operator's Handbool*. 40 Tanners Drive, Blakelands. Milton Keynes, MK 14 5BN, England: Automatic Systems Laboratoties LTD.
- [9] Astley, R. J. (2000). Infinite elements for wave problems: a review of current formulations and an assessment of accuracy. *International Journal for Numerical Methods in Engineering* 49(7), 951–976.

- [10] Baby, S., T. Balasubramanian, and R. Pardikar (2003). Ultrasonic study for detection of inner diameter cracking in pipeline girth welds using creeping waves. *International Journal of Pressure Vessels and Piping* 80(2), 139–146.
- [11] Benny, G., G. Hayward, and R. Chapman (2000). Beam profile measurements and simulations for ultrasonic transducers operating in air. *The Journal of the Acoustical Society of America* 107(4), 2089–2100.
- [12] Bentley, J. P. (2005). *Principles of Measurement Systems* (Fourth Edition ed.). Harlow, England: Pearson Prentice Hall.
- [13] Blackburn, John, F and M. G. Cain (2006). Nonlinear piezoelectric resonance: A theoretically rigorous approach to constant IV measurements. *Journal of Applied Physics* 100(11), 114101.
- [14] Brassier, P., B. Hosten, and F. Vulovic (2001). High-frequency transducers and correlation method to enhance ultrasonic gas flow metering. *Flow Measurement and Instrumentation* 12(3), 201–211.
- [15] Brigham, E. O. (1988). *The fast Fourier transform and its applications*. Englewood Cliffs, USA: Prentice-Hall, Inc.
- [16] Brüel & Kjær (1982). *Product Data, Pistonphone — Type 4228*. Nærum, Denmark: Brüel & Kjær, Sound & Vibration Measurement A/S.
- [17] Brüel & Kjær (1982). *Condenser Microphones and Microphone Preamplifiers for acoustic measurements*. Nærum, Denmark: Brüel & Kjær, Sound & Vibration Measurement A/S.
- [18] Brüel & Kjær (1985). *Instruction Manual, Measuring Amplifier Type 2636*. Nærum, Denmark: Brüel & Kjær, Sound & Vibration Measurement A/S.
- [19] Brüel & Kjær (1995). *Calibration data for Type 4138 microphone serial no. 1832479*. Nærum, Denmark: Brüel & Kjær, Sound & Vibration Measurement A/S.
- [20] Brüel & Kjær (1996). *Calibration data for Type 4228 pistonphone serial no. 1918465*. Nærum, Denmark: Brüel & Kjær, Sound & Vibration Measurement A/S.
- [21] Burnett, D. S. (1987). *Finite Element Analysis, From Concepts To Application* (Reprinted with correction May, 1988 ed.). Whippany New Jersey, USA: Addison-Wesley Publishing Company.
- [22] Chillara, V. K., E. S. Davis, C. Pantea, and D. N. Sinha (2019). Ultrasonic bessel beam generation from radial modes of piezoelectric discs. *Ultrasonics* 96, 140–148.

- [23] Cocraft (2022). *Instruction manual Cocraft Cross-Line Laser Level HL 10-S*. Jungfernstieg, Hamburg: Cocraft.
- [24] Finstad, S. K. (2021). Characterization and finite element modelling of piezoelectric ceramic discs vibrating in air, for a frequency range including the first two radial modes. Master's thesis, University of Bergen, Department of Physics and Technology, Bergen, Norway.
- [25] Getman, I. and S. Lopatin (2000). Matching of series and parallel resonance frequencies for ultrasonic piezoelectric transducers. In *ISAF 2000. Proceedings of the 2000 12th IEEE International Symposium on Applications of Ferroelectrics (IEEE Cat. No.00CH37076)*, Volume 2, pp. 713–715 vol. 2.
- [26] Grindheim, R. (2019). Ultrasonic measurement systems for gas. Experimental and theoretical characterization using piezoelectric elements at radial mode vibration in air. Master's thesis, University of Bergen, Department of Physics and Technology, Bergen, Norway.
- [27] Hagen, A. (2017). Ultrasonic measurement systems with diffraction correction for gas. Master's thesis, University of Bergen, Department of Physics and Technology, Bergen, Norway.
- [28] Hatano, H. and J. Oosumi (1983). Effect of bevelling on the thickness vibration of high-frequency Pb(ZrTi)O₃ ceramic transducers. *Ultrasonics* 21(5), 205–210.
- [29] Hauge, R. (2013). Finite element modeling of ultrasound measurement systems for gas. Comparison with experiments in air. Master's thesis, University of Bergen, Department of Physics and Technology, Bergen, Norway.
- [30] Hauptmann, P., N. Hoppe, and A. Püttmer (2002). Application of ultrasonic sensors in the process industry. *Measurement Science and Technology* 13, R73.
- [31] Hewlett-Packard (1982). *Operation and service manual. Model 4192A LF Impedance Analyzer*. Japan, Tokyo: Hewlett-Packard Company.
- [32] IEEE Standard on Piezoelectricity (1987). *The Institute of Electrical and Electronics Engineers*. 345 East 47th Street, New York, NY 10017, USA.
- [33] ISO 17089-1: (2019). Measurement of fluid flow in closed conduits - Ultrasonic meters for gas — Part 1: Meters for custody transfer and allocation measurement.
- [34] Kenny, A., I. Cato, M. Desprez, G. Fader, R. Schüttenhelm, and J. Side (2003, 01). An overview of seabed-mapping technologies in the context of marine habitat classification. *ICES Journal of Marine Science* 60(2), 411–418.

- [35] Keyence (2013). *High-speed, High-accuracy CCD Laser Displacement Sensor LK-G Series User's Manual*. 500 Park Boulevard, USA: Keyence.
- [36] Kinsler, L. E., A. R. Frey, A. B. Coppens, and J. V. Sanders (2000). *Fundamentals of Acoustics* (Fourth Edition ed.). Hoboken, USA: John Wiley & Sons Inc.
- [37] Knappskog, V. (2007). Radiellmode Svingninger i Piezoelektriske Ultralydtransdusere for Luft. Målinger og Endelig Element Analyser. Master's thesis, University of Bergen, Department of Physics and Technology, Bergen, Norway.
- [38] Kocbach, J. (2000). *Finite Element Modeling of Ultrasonic Piezoelectric Transducers*. Ph. D. thesis, University of Bergen, Department of Physics, Bergen, Norway.
- [39] Kocbach, J., P. Lunde, and M. Vestrheim (1999). Femp - finite element modeling of piezoelectric structures. theory and verification for piezoceramic disks. Technical report, No 1999-07 University of Bergen, Department of Physics, Christian Michelsen Research, Bergen, Norway.
- [40] Krohn-Hite (2014). *Operating and Maintenance Manual KH Model 3940/3944*. Brockton, USA: Krohn-Hite Corporation.
- [41] Kunkel, H., S. Locke, and B. Pikeroen (1990). Finite-element analysis of vibrational modes in piezoelectric ceramic disks. *IEEE Transactions on Ultrasonics, Ferroelectrics, and Frequency Control* 37(4), 316–328.
- [42] Lohne, K. D. (2005). Undersøkelse og Utnyttelse av Svingemoder i Ultralyd Transduserkonstruksjoner. Master's thesis, University of Bergen, Department of Physics and Technology, Bergen, Norway.
- [43] Lunde, P., K.-E. Frøysa, V. Martinez, and Torvanger (2008). Pressure and temperature effects for Ormen Lange ultrasonic gas flow meters,-Results from a follow-up study. University of Bergen, Department of Physics and Technology, Christian Michelsen Research, CMR Prototech. Bergen, Norway.
- [44] Lygre, A., M. Vestrheim, P. Lunde, and V. Berge (1987). Numerical simulation of ultrasonic flowmeters. pp. 196–201.
- [45] Lynnworth, L. and Y. Liu (2007). Ultrasonic flowmeters: Half-century progress report 1955-2005. *Ultrasonics* 44 Suppl 1, e1371–8.
- [46] Meggitt (2018). *Data Sheet Type PZ27*. Porthusvej 4, DK3490, Kvistgaard, Denmark: Meggitt A/S.

- [47] Mitutoyo (2018). *Outside Micrometer User's Manual*. Mitutoyo.
- [48] Mosland, E. (2013). Reciprocity calibration method for ultrasonic piezoelectric transducers in air. Master's thesis, University of Bergen, Department of Physics and Technology, Bergen, Norway.
- [49] Øyerhamn, R., E. Mosland, E. Storheim, P. Lunde, M. Vestrheim, and J. Kocbach (2018). Finite element modeling of ultrasound measurement systems for gas. comparison with experiments in air. *The Journal of the Acoustical Society of America, Department of Physics and Technology, University of Bergen, Bergen, Norway*.
- [50] Paroscientific (2002). *Digiquartz Precision Pressure Instruments. Model 770*. Paroscientific, Inc.
- [51] Physik Instrumente (1995). *Operating Manual MS44 E C-852 Signal Processor For Incremental Encoders*. D-763337 Waldbronn, Germany: Physik Instrumente (PI) GmbH & Co. KG.
- [52] Physik Instrumente (1996). *Product Instruction MP 30 E M-500 Linear Positioning Stages*. D-763337 Waldbronn, Germany: Physik Instrumente (PI) GmbH & Co. KG.
- [53] Physik Instrumente (1998). *Operating Manual MP 33E M-501.xx Series Linear Positioning Stages*. D-763337 Waldbronn, Germany: Physik Instrumente (PI) GmbH & Co. KG.
- [54] Physik Instrumente (2007). *MP 34E M-037/M-038 Worm-Gear Rotation Stages*. Auf der Romerstr. 1 76228 Karlsruhe, Germany: Physik Instrumente (PI) GmbH & Co. KG.
- [55] Physik Instrumente (2009). *MS77E User Manual, C-843 Motor Controller Card*. Auf der Romerstr. 1 76228 Karlsruhe, Germany: Physik Instrumente (PI) GmbH & Co. KG.
- [56] Physik Instrumente (2016). *Hydra Handbook*. Auf der Romerstr. 1 76228 Karlsruhe, Germany: Physik Instrumente (PI) GmbH & Co. KG.
- [57] Physik Instrumente (2018). *Linear Stage for Very High Loads, LS-270*. Auf der Romerstr. 1 76228 Karlsruhe, Germany: Physik Instrumente (PI) GmbH & Co. KG.
- [58] Pickrill, R. A. and B. J. Todd (2003). The multiple roles of acoustic mapping in integrated ocean management, canadian atlantic continental margin. *Ocean & Coastal Management* 46(6), 601–614.
- [59] Ricci, R. and A. Sona (2013). Experimental validation of an ultrasound-based measurement system for human motion detection and analysis. In *2013 IEEE International Instrumentation and Measurement Technology Conference (I2MTC)*, pp. 300–305.

- [60] Rohatgi, A. (2021). Webplotdigitizer: Version 4.5.
<https://automeris.io/WebPlotDigitizer> , last accessed:11.04.2022.
- [61] Ronold W. P. King, Harry Rowe Mimno, A. H. W. (1945). *Transmission Lines Antennas and Wave Guides* (First Edition ed.). New York, USA: McGraw-Hill Book Company, INC.
- [62] Sanabria, S. J., T. Marhenke, R. Furrer, and J. Neuenschwander (2018). Calculation of volumetric sound field of pulsed air-coupled ultrasound transducers based on single-plane measurements. *IEEE Transactions on Ultrasonics, Ferroelectrics, and Frequency Control* 65, 72–84.
- [63] Schafer, R. W. (2011). What is a savitzky-golay filter? [lecture notes]. *IEEE Signal Processing Magazine* 28(4), 111–117.
- [64] Søvik, A. A. (2015). Ultrasonic measurement systems for gas. Finite element modelling compared with measurements in air. Master's thesis, University of Bergen, Department of Physics and Technology, Bergen, Norway.
- [65] Storheim, E. (2015). *Diffraction effects in the ultrasonic field of transmitting and receiving circular piezoceramic disks in radial mode vibration FE modelling and comparison with measurements in air*. Ph. D. thesis, University of Bergen, Department of Physics and Technology, Bergen, Norway.
- [66] Tektronix (2012). *Mixed Signal Oscilloscopes MSO3000 Series, DPO3000 Series Data Sheet*. Beaverton, Oregon, USA, Tektronix Inc.
- [67] TESA Technology (2022). *Analogue dial gauges, metric, Standard model, resolution 0.01 mm, measuring range 30 mm*. Brown& Sharpe TESA, USA.
- [68] The Mathworks, Inc. (2022). *MATLAB version (R2021b)*. Natick, Massachusetts: The Mathworks, Inc.
- [69] The Norwegian Petroleum Directorate (2001). Regulations relating to measurement of petroleum for fiscal purposes and for calculation of CO₂-tax (the measurement regulations).
- [70] Vaisala Oyj (2014). *User's Guide. Vaisala HUMICAP Humidity and Temperature Transmitter HMT310*. Vanha Nurmijärventie 21, FI-01670 Vantaa, Finland: Vaisala Oyj.
- [71] Vervik, S. (2000). *Methods for characterization of gas-coupled ultrasonic sender-receiver measurement systems*. Ph. D. thesis, University of Bergen, Department of Physics and Technology, Bergen, Norway.

- [72] Vestrheim, M. (2013). *PHYS 373 Akustiske Målesystemer, Lecture notes*. Bergen, Norway: University of Bergen, Department of Physics and Technology.
- [73] Vestrheim, M. (2013). *PHYS 272 Akustiske Transdusere, Lecture notes*. Bergen, Norway: University of Bergen, Department of Physics and Technology.
- [74] Wang, Z., Q. Cao, N. Luan, and L. Zhang (2008). Development of new pipeline maintenance system for repairing early-built offshore oil pipelines. In *2008 IEEE International Conference on Industrial Technology*, pp. 1–6.
- [75] Whitworth M, Bricker L, M. C. (2015). Ultrasound for fetal assessment in early pregnancy.
- [76] Wikipedia (2022). Angular distance. https://en.wikipedia.org/wiki/Angular_distance, last accessed:15.06.2022.
- [77] Yu, Y., A. Safari, X. Niu, B. Drinkwater, and K. V. Horoshenkov (2021). Acoustic and ultrasonic techniques for defect detection and condition monitoring in water and sewerage pipes: A review. *Applied Acoustics* 183, 108282.

Appendix A

MatLab-scripts

A.1 impanal.m

```

1 clear all
2 clc
3 close all
4 instrreset
5 vinfo = instrhwinfo('visa','agilent');
6 vinfo.ObjectConstructorName
7 obj1 = visa('agilent','GPIB0::17::INSTR');
8
9 % Connect to instrument object, obj1.
10 fopen(obj1);
11 fprintf(obj1, 'V1');
12     %%%%%%%%%%%%%%%%%%%%%%%%%%%%%%%%%%%%%%%%%%%%%%%%%%%%%%%%%%%
13
14     % Osc. level [V]
15     amplitude = 0.3;
16     f = [100:50:97450,97500:10:99500,99550:50:300000]/1000; % Hz
17
18     %%%%%%%%%%%%%%%%%%%%%%%%%%%%%%%%%%%%%%%%%%%%%%%%%%%%%%%%%%%
19     ol = sprintf('%3.3f',amplitude);
20     % Sett analysator i mode for admittans-måling
21     fprintf(obj1, ['A2C3F1OL',ol,'EN']);
22
23     % Tids-streng på format yyyyymmddHHMMSS
24     time = datestr(now, 'yyyyymmddHHMMSS');
25     % Tittelen som målingen blir lagra under
26
27     i = 1;

```

```

28     ii = 1;
29     antal = length(f);
30     g = ones(1,antal);
31     b = ones(1,antal);
32     fr = ones(1,antal);
33     disp([num2str(antal),' frekvenser.'])
34     disp('Starter måling...')
35     for freq = f
36         percent = i/antal*100;
37         if percent >= ii*10
38             disp([num2str(ii*10),' %'])
39             ii = ii + 1;
40         end
41         s = sprintf('%3.3f',freq);
42         fprintf(obj1, ['FR',s,'ENEX']);
43         pause(0.1)
44         data1 = fscanf(obj1);
45         d=sscanf(data1,'%4c%f,%4c%f,%2c%f');
46         g(i)=d(5);b(i)=d(10);fr(i)=d(13);
47         i = i + 1;
48     end
49     disp('Måling ferdig.')
50     disp('Lagrer data...')
51     stoptime = datestr(now, 'yyyymmddHHMMSS');
52     save(stoptime,'g','b','fr')
53     disp('Ferdig!')

```

A.2 positioninganalyze directivity.m

```

1  %%%%%%%%%%%%%%%%%%%%%%%%%%%%%%%%%%%%%%%%%%
2  % The script was created to analyze how much
3  % incorrect positioning affects the simulated
4  % directivity of the piezoelectric disk
5  %
6  % Created by Espen Fosse 2022
7  %%%%%%%%%%%%%%%%%%%%%%%%%%%%%%%%%%%%%%%%%%
8
9  clear all
10
11 % loading the values
12 d1 = load('PZ27_result_0.2m.mat');
13 d2 = load('PZ27_result_0.5m.mat');

```

```

14 d3 = load('PZ27_result_0.8m.mat');
15
16 sim = 1;
17 % frequency indeks
18 % 1963 - 98100Hz
19 % 2944 - 147150Hz
20 % 4982 = 249050Hz
21 mode = 4982;
22 % decimal distance and angle for interpolation functions
23 decdist = 3;
24 decang = 2;
25
26 disp(['simulation frequency ', num2str(d1.result.directivity_f{1}(mode))...
       ])
27
28 ang(1,:) = rad2deg(d1.result.directivity_theta{sim})+90;
29 Y_k(1,:) = abs(d1.result.directivity{sim}(:,mode).');
30 ang(2,:) = rad2deg(d2.result.directivity_theta{sim})+90;
31 Y_k(2,:) = abs(d2.result.directivity{sim}(:,mode).');
32 ang(3,:) = rad2deg(d3.result.directivity_theta{sim})+90;
33 Y_k(3,:) = abs(d3.result.directivity{sim}(:,mode).');
34
35 Y_org = [fliplr(abs(d1.result.directivity{sim}(:,mode).')),abs(...
           d1.result.directivity{sim}(:,mode).')];
36 ang_org = [-fliplr(rad2deg(d1.result.directivity_theta{sim})+90),rad2deg...
            (d1.result.directivity_theta{sim})+90];
37 % interpolated amplitude over new angles
38 angle = (0:10^-(decang):180);
39 p(1,:) = interp1(ang(1,:),Y_k(1,:),angle,'spline');
40 p(2,:) = interp1(ang(2,:),Y_k(2,:),angle,'spline');
41 p(3,:) = interp1(ang(3,:),Y_k(3,:),angle,'spline');
42
43 % original distances in mm
44 dist = [200,500,800];
45
46 % plotting angle in degrees
47 theta_R = (-90:0.1:90);
48 % tilt angle of piezoelectric disk in degrees
49 theta_T = 0;
50 % radius to center of from piezoelectric disk to rotation stage in mm
51 sigma = 5;
52 % line going through rotation stage to center of microphone's
53 % start position and alpha is the angle from line to center of
54 % piezoelectric disk front in degrees
55 alpha = 180;

```

```

56 % start distance to in mm
57 z0 = 200;
58 % initial angle from microphone center to xz-plane
59 theta_M = 0;
60
61 beta = z0*sind(theta_M);
62 r0 = z0*cosd(theta_M);
63 R = sigma*cosd(alpha)+sqrt(r0^2+sigma^2*(cosd(alpha)^2-1));
64 r = sqrt(R^2-2*R*sigma*cosd(alpha-theta_R)+sigma^2);
65 theta_m = atand(beta./r);
66 costheta_r = (r.^2+r0^2-4*R^2*sind(theta_R/2).^2)./(2*r.*r0);
67 theta = acosd(sind(theta_m)*sind(theta_T)+cosd(theta_m)*cosd(theta_T).*...
        costheta_r );
68
69 % sound propagation distance
70 z = r./cosd(theta_m);
71
72 % interpolated amplitudes over distances
73 distance = (round(min(z),decdist):10^-(decdist):round(max(z),decdist));
74
75 for i = 1:length(p)
76     p2(:,i) = interp1(dist,p(:,i),distance,'spline');
77 end
78
79 for i = 1:length(theta)
80     col = find(round(angle,declang)==round(theta(i),declang));
81     row = find(round(distance,decdist)==round(z(i),decdist));
82     D(i) = p2(row,col);
83 end
84
85 Y_orgplot = 20*log10(Y_org./max(Y_org));
86 Y_orgplot2 = Y_org./max(Y_org);
87 D_plot = 20*log10(D./max(D));
88
89 % plot(ang_org,Y_orgplot,'r')
90 % plot(ang_org,Y_orgplot2,'r')
91
92 plot(ang_org,Y_orgplot,'r',theta_R,D_plot,'b')
93 xlim([-90 90])
94 xticks([-90 -60 -30 0 30 60 90])
95 ylim([-30 0])

```

A.3 MeasParameters.m

```

1 %%%%%%%%%%%%%%%%%%%%%%%%%%%%%%%%%%%%%%%%%%%%%%%%%%%%%%%%%%%%%%%%%%%%%%%%%
2 % Information about the calibration of the measurement microphone.
3 % Part of the software for acoustic measurements in air.
4 % Espen Storheim, 2011
5 % Based on work by Vidar Knappskog and Magne Aanes.
6 %
7 % Modified by Rune Hauge and Eivind Mosland, 2012/2013
8 % Modified by Espen Fosse 2021/2022
9 %%%%%%%%%%%%%%%%%%%%%%%%%%%%%%%%%%%%%%%%%%%%%%%%%%%%%%%%%%%%%%%%%%%%%%%%%
10
11 function meas = MeasParameters()
12     %% General measurement info.
13
14     % Version of this software which was used to make the measurements. ...
15     % Should
16     % be taken from elsewhere.
17
18     % Name of the person performing the measurement.
19     meas.name = 'E_F';
20
21     % Information about the transmitting transducer.
22     meas.source = 'Pz27 disk, D = 20.0 mm, T = 2.0 mm, Element No. 7 in ...
23     % batch 9/12.';
24
25     % Information about the receiving transducer.
26     meas.receiver = 'B&K Type 4138 mic';
27
28     % Additional notes regarding the specific simulation.
29     meas.notes = 'Sensitivity';
30     meas.notes = 'Directivity';
31     meas.notes = 'On Axis Pressure';
32
33     meas.info = 'Måler direktiviteten over mangen distanser for å plotte...
34     % 2d feltet';
35     %% Measure distances for primary axis and secondary axis [mm]
36
37     % Primary axis is z-axis, distance between transducer to
38     % microphone/transducer
39     meas.primary_axis = [120:10:300];
40     % Secondary axis can be your x, y or rotation axis, if no secondary...
41     % is
42     % used, set value to 0

```

```
42     meas.secondary_axis = [-93:1:93];
43 %     meas.secondary_axis = [0];
44     %% Measure frequency [Hz]
45     meas.frequency = [98.86e3*3/2];
46 %     meas.frequency = [97e3:0.1e3:97.9e3];
47     %% Define initial bandpass filter low and high cutoff frequency [kHz...
48     ]
49
50     for i = 1:length(meas.frequency)
51         meas.cutoff_1(i) = (meas.frequency(i)/1000)/2;
52         meas.cutoff_2(i) = (meas.frequency(i)/1000)*2;
53     end
54
55     %% Input waveform data.
56
57     %     Vpp voltage out from the signal generator [V]. This is the ...
58     %     actual voltage
59     %     level of the function generator
60     meas.voltage_inn = 1;
61
62     % measured signal averaging(2,4,8,16,...,512)
63     meas.average = 128;
64
65     % scaling averaging (2,4,8,16,...,512), if set to 1, simple sampel ...
66     % is
67     % taken insted of averaging, which is the smartest choice
68     meas.average_scaling = 1;
69
70     % Time in Hz between burst
71     meas.burst_rate = 25;
72
73     % Approximate time before the signal is averaged.
74     meas.average_time = meas.average/meas.burst_rate;
75     meas.average_time_scaling = meas.average_scaling/meas.burst_rate;
76
77     % Estimated travel time from tranducer to microphone/transducer.
78     % Normally faktor is 2, and then signal duration becomes
79     % faktor*estimated_travle time
80     meas.est_travel_time_faktor = 2;
81     % If signal duration becomes less then ~ faktor*10 cm then min ...
82     % signal
83     % duration is used insted of faktor*estimated_travle time
84     meas.min_sig_duration = meas.est_travel_time_faktor*2.9155e-04;
85
86     % Normally, signal cycles changes based on distance from microphone,...
87     % but
```

```

82     % this can be override with setting sig_cycles to not equal to 0
83     meas.sig_cycles = 60;
84
85     % A note on the input voltage: The signal generator claims that the ...
      voltage
86     % specified above is the peak to peak voltage. This is the case when...
      the
87     % generator is connected to a 50 Ohm load. However, the transmitting
88     % transducer typically has an electrical impedance in the kilo Ohm ...
      range and is connected
89     % directly to the generator. This causes a voltage division which ...
      depends
90     % of the impedance of the transducer, and hence an impedance ...
      mismatch.
91     %% Oscilloscope parameters.
92
93     % Allowed values: 1e3, 10e3, 100e3, 1000e3, or 5000e3.
94     meas.sample_count = 10e3;
95
96     % Channel number where the signal generator is connected.
97     meas.channel_electrical = 1;
98
99     % Channel number where the oscilloscope is connected.
100    meas.channel_acoustical = 2;
101    %% Total input gain in the B&K 2636 measurement amplifier [dB].
102
103    % Only recorded for later reference. Must be set manually.
104    meas.gain_in = 40;
105    meas.gain_out = 20;
106    meas.gain = meas.gain_in + meas.gain_out;
107 end

```

A.4 HVV_0m1.m

```

1 function HVV_0m1 = HVV_0m1(Frequency)
2 % HVV_0m1(f) calculates the transfer function HVV_0m1 from oscilloscope ...
      to
3 % transmitter for given frequency
4 % f:    Frequency [Hz]
5 f = Frequency;
6 % Cable length from oscilloscope to transducer in m
7 x = 3;

```

```

8 % Typical inductance per m values for RG58 coaxial cables
9 Lx = 250e-9;
10 % Typical capacitance per m values for RG58 coaxial cables
11 Cx = 100e-12;
12
13 Z0 = sqrt(Lx/Cx);
14 omega = 2*pi.*f;
15 kem = omega*sqrt(Lx*Cx);
16 Za = 1i*Z0*tan((kem*x)/2);
17 Zb = Z0./(1i*sin(kem*x));
18 load #7_admittance.mat fr b g
19 Z = 1./(g+1i*b);
20 ff = fr*1000;
21 ZT = interp1(ff, Z, f, 'spline');
22
23 HVV_0m1 = ZT.*Zb./(ZT.*(Za+Zb)+(Za+Zb).^2-Zb.^2);

```

A.5 HVV_55m.m

```

1 function HVV_55m = HVV_55m(Frequency, Gain)
2 % HVV_55m(f) calculates the transfer function HVV_0m1 from microphone to
3 % oscilloscope for given frequency
4 % f: Frequency [Hz]
5 f = Frequency;
6 % Cable length from amplifier to filter ch1 in m
7 x1 = 0.5;
8 % Cable length from filter ch1 to filter ch2 in m
9 x2 = 0.8;
10 % Cable length from filter ch2 to oscilloscope in m
11 x3 = 1.5;
12 % Typical inductance per m values for RG58 coaxial cables
13 Lx = 250e-9;
14 % Typical capacitance per m values for RG58 coaxial cables
15 Cx = 100e-12;
16
17 omega = 2*pi*f;
18
19 Zamp_out = 100;
20
21 Cfilt = 100e-12;
22 Rfilt = 1e6;
23 Zfilt_out = 50;

```



```

24 Zfilt = 1./(1i*omega*Cfilt+1/Rfilt);
25
26 Cosc = 11.5e-12;
27 Rosc = 1e6;
28 Zosc = 1./(1i*omega*Cosc+1/Rosc);
29
30 Lx = 250e-9;
31 Cx = 100e-12;
32 Z0 = sqrt(Lx/Cx);
33 kem = omega*sqrt(Lx*Cx);
34
35 Za1 = 1i*Z0*tan((kem*x1)/2);
36 Zb1 = Z0./(1i*sin(kem*x1));
37
38 Za2 = 1i*Z0*tan((kem*x2)/2);
39 Zb2 = Z0./(1i*sin(kem*x2));
40
41 Za3 = 1i*Z0*tan((kem*x3)/2);
42 Zb3 = Z0./(1i*sin(kem*x3));
43 HVV_55a = 10^(Gain/20);
44 HVV_5a51 = Zfilt./((Zamp_out+Za1).*(1+(Zfilt+Za1)./Zb1)+Zfilt+Za1);
45 HVV_5152 = Zfilt./((Zfilt_out+Za2).*(1+(Zfilt+Za2)./Zb2)+Zfilt+Za2);
46 HVV_525m = Zosc./((Zfilt_out+Za3).*(1+(Zosc+Za3)./Zb3)+Zosc+Za3);
47
48 HVV_55m = HVV_55a*HVV_5a51.*HVV_5152.*HVV_525m;

```

A.6 Vpp.m

```

1 function Vpp = Vpp(time, amplitude, start, stop, freq, filtorder, filtframelen...
   )
2 % Finding the DC component by taking the mean value of signal
3 DC = mean(amplitude);
4 % Subtract the DC value from signal
5 amp = amplitude-DC;
6 zeropadding = length(amplitude)*5;
7
8 % SampleInfoStruct.Both = 'IntCycles'; % bør brukes ved zeropad
9 SampleInfoStruct.Both = 'IntPeriods'; % bør brukes ved zeropad
10 SampleInfoStruct.StartVal = start;
11 SampleInfoStruct.EndVal = stop;
12 SigStruct.SigFreq = freq;
13 % Dersom 'intPeriods' eller 'IntCycles' eller bruk av peak_peak

```

```

14 SigStruct.periodFracJump = 1/16;
15 % Program starts
16 SigStruct.x = time;
17 SigStruct.y = amp;
18 CutOffIndxs = find_index_in_sig_advanced(SigStruct, SampleInfoStruct);
19 Sig_wa_reg = SigStruct.y(CutOffIndxs(2) : CutOffIndxs(3));
20
21 % framelenght must be odd
22 if rem(filtframelen,2) == 0
23     filtframelen = filtframelen+1;
24 end
25
26 % filtering the measured signal with Savitzky-Golay method
27 filtered = sgolayfilt(Sig_wa_reg, filtorder, filtframelen);
28
29 % Y_k_tmp = fourier_transform(SigStruct.x, Sig_wa_reg, zeropadding);
30 Y_k_tmp = fourier_transform(SigStruct.x, filtered, zeropadding);
31
32 % finding the peak to peak voltage at given frequency
33 Vpp = 2*2*abs(interp1(abs(Y_k_tmp{1}), Y_k_tmp{2}, freq, 'cubic'));

```

A.7 Receiver_Sensitivity.m

```

1 function Mv_f=Receiver_Sensitivity(Frequency)
2 % Linear interpolation of the dB correction from different ambient
3 % pressures
4 load Mv_measurment.mat
5
6 x = [685 800 940 990 1013 1060];
7 y = [-3.4 -2.05 -0.65 -0.2 0 0.39];
8 s = fit(x.',y.', 'linearinterp');
9
10 % Load volume correction, for DP 0774 = 0dB
11 Lv = 0;
12 % Correction for ambient pressure
13 Lp = s(DPO.pressure);
14 % Stated sound pressure level
15 sSPL = 124.11;
16 % Actual sound pressure level of pistophone
17 aSPL = sSPL + Lp + Lv;
18 % Amplifier gain
19 Gain = 20;

```

```
20
21 % Frequency from pistonphone
22 freq = 251.2;
23 V_ppmax = Vpp(DPO.x,DPO.wf,1,length(DPO.x),freq,5,10);
24 HVV = abs(HVV_55m(250,Gain));
25 Veff = V_ppmax/(HVV*2*sqrt(2));
26 peff = 10^(aSPL/20)*20*1e-6;
27
28 % Calculated calibrated reciver sensitivity. 0.4563mV/Pa in my case. The
29 % given sensitivity of the microphone is 0.822 mV/Pa.
30 Mv = Veff/peff;
31
32 % Open circuit pressure response
33 D1 = [20.058132685561468, -0.03159553295001594
34 21.05087511963177, -0.00497567448031333
35 22.09308910488738, -0.0046992481202954295
36 23.075127239496453, -0.0044504643962790524
37 24.100816983586117, -0.0042016806722635636
38 25.050753654543616, -0.003980539584249598
39 26.038132196432052, -0.003759398496234745
40 27.06442838520751, -0.0035382574082207796
41 28.131176164717257, -0.0033171163202068144
42 29.09901530059949, -0.0031236178681943727
43 30.100152460974538, -0.002930119416181931
44 30.9856398639198, -0.002764263600170125
45 32.05168540481925, -0.0025707651481585714
46 33.15440771277152, -0.002377266696147018
47 34.29506863372019, -0.0021837682441345763
48 35.64681298953859, -0.001962627156120611
49 37.05183651569491, -0.0017414860681066457
50 38.141828818330985, -0.0015756302520957277
51 39.64519370079917, -0.001354489164079986
52 41.207813895344884, -0.001133348076066909
53 43.03950182712216, -0.0008845643520523083
54 44.952608314320514, -0.0006357806280359313
55 47.17890095209987, -0.026702786377701848
56 49.514695074759025, -0.026426360017684836
57 51.966132717579626, -0.026149933657667823
58 54.80312407373893, -0.0258458646616484
59 57.795878408724505, -0.05188522777531457
60 60.65638501271208, -0.025265369305611074
61 63.65943986891338, -0.024988942945593173
62 66.48910290436899, -0.024740159221576796
63 69.44454450323498, -0.024491375497561307
64 72.53135552449893, -0.02424259177354493
```

```
65 75.75537534091245, -0.02399380804952944
66 79.5059705627214, -0.02371738168951154
67 83.44352977364937, -0.049784387439179234
68 87.5747601008906, -0.04950796107916222
69 91.91192875425654, -0.07557496682882991
70 97.39920832615756, -0.07524325519680808
71 102.71653131456982, -0.07493918620078865
72 108.84886181419361, -0.0746074745687677
73 116.46748492230017, -0.07422047766474282
74 124.01861390768617, -0.07386112339672035
75 132.69900855770388, -0.07347412649269547
76 141.98696725722905, -0.07308712958867059
77 153.40041900372466, -0.07264484741264177
78 162.55865338014362, -0.07231313578062082
79 172.2610165824735, -0.04563799203891428
80 182.545256834413, -0.04530628040689244
81 195.32208783488707, -0.04491928350286756
82 208.99320342673101, -0.04453228659884356
83 224.70441044155518, -0.04411764705881627
84 238.11959971942048, -0.04378593542679532
85 256.02040349742686, -0.04337129588676891
86 273.93995662570694, -0.04298429898274403
87 293.1137472285418, -0.042597302078719146
88 312.1176753565441, -0.042237947810695786
89 332.35371657275545, -0.041878593542673315
90 353.9017545018618, -0.041519239274649955
91 376.8468519956459, -0.041159885006627484
92 405.18276132827987, -0.06708867757628667
93 435.64930742610267, -0.09301747014594586
94 461.6582224554411, -0.09268575851392491
95 493.9709168008378, -0.09229876160990003
96 528.5452630893234, -0.09191176470587514
97 571.0317389443935, -0.09146948252984721
98 605.1231875570597, -0.09113777089782538
99 653.7652878517716, -0.09069548872179745
100 720.0916947063869, -0.06379920389207516
101 797.0012625520569, -0.06321870853603784
102 877.8727895316784, -0.06266585581600292
103 953.0337476511787, -0.06219593100397258
104 1029.6422202576316, -0.06175364882794465
105 1101.7096344831245, -0.06136665192391977
106 1190.2692395984482, -0.06092436974789095
107 1311.0455738980609, -0.060371517027856036
108 1389.3169549145211, -0.0600398053958342
109 1515.5722906662636, -0.059542237947802334
```

```
110 1629.5064742385878, -0.05912759840777593
111 1752.0325016325971, -0.085056390977436
112 1883.7427432984218, -0.0846417514374096
113 2015.5909386274632, -0.08425475453338471
114 2146.2710779771282, -0.08389540026536224
115 2318.7964995463685, -0.08345311808933431
116 2481.1331726557723, -0.10940955329499413
117 2654.7943226984075, -0.10902255639096925
118 2786.2313178527374, -0.10874613003095224
119 2952.5734934578413, -0.10841441839893129
120 3113.76358094979, -0.10811034940291187
121 3315.694012410975, -0.1340944272445741
122 3513.645902525506, -0.13376271561255315
123 3759.575381442612, -0.13337571870852827
124 4003.3261471992037, -0.1330163644405049
125 4283.529656781166, -0.13262936753648003
126 4561.2508162331815, -0.13227001326845755
127 4833.638147410243, -0.1582817337461231
128 5197.010201254747, -0.15786709420609668
129 5587.698997786313, -0.1574524546660685
130 5949.975524079862, -0.15709310039804603
131 6335.740123291306, -0.15673374613002267
132 6845.030979856471, -0.15629146395399474
133 7359.723291062311, -0.18222025652365392
134 7874.850018159103, -0.18183325961962993
135 8304.76235267869, -0.1815291906236114
136 8886.034892537247, -0.18114219371958562
137 9462.157882459767, -0.18078283945156226
138 9978.726245725167, -0.18047877045554284
139 10371.880529349377, -0.1539141972578424
140 11044.337805733268, -0.15355484298981903
141 11535.082573171361, -0.12696262715611795
142 12106.176378560287, -0.12668620079610005
143 12583.15059193551, -0.10012162759840049
144 13205.931772154905, -0.0735017691286961
145 13859.74814335345, -0.0732253427686782
146 14758.114661653412, -0.04652255639096836
147 15714.951906534357, -0.04616320212294589
148 16977.920077169827, -0.019377487837231477
149 18342.389582936732, 0.007408226448482047
150 19816.51781154511, 0.03419394073419646
151 21305.91262297363, 0.06095201238390935
152 22796.82221585644, 0.08768244139762071
153 24988.582880231424, 0.11455108359134059
154 27523.327493266388, 0.16779080053074757
```

```
155 29448.859105935688, 0.22086466165414365
156 31662.21355962875, 0.24762273330385653
157 33069.59941653967, 0.24787151702787114
158 35382.60763185681, 0.3272888102609546
159 38040.776002059705, 0.40673374613003865
160 40507.13651879439, 0.407093100398062
161 43341.0152322141, 0.4601669615214581
162 45927.13546765157, 0.513185537372852
163 48432.95961514873, 0.5661764705882435
164 50341.950685981115, 0.5663976116762575
165 52582.864033026635, 0.4612726669615306
166 55456.913162824414, 0.35620300751880585
167 58206.10232391049, 0.2511057054400796
168 61091.57820945313, 0.14600840336135246
169 63197.26505637179, 0.040828173374621635
170 65063.36147790973, -0.14340999557716927
171 66984.56021837509, -0.3276481645289602
172 69294.42319019328, -0.4591718266253775
173 71334.01878699053, -0.48534940291905393
174 72721.8084799586, -0.3798651039363037
175 74859.99778107263, -0.3533558160106054
176 76322.21394529774, -0.3795886775762858
177 78192.3034605607, -0.45848076072533317
178 79719.6084756157, -0.48471362229101267
179 82064.80287834875, -0.48454776647500264
180 84481.5693191942, -0.5370687748783638
181 86969.5082947287, -0.5895897832817241
182 89530.71579967023, -0.6421107916850861
183 92608.14619754962, -0.5892304290137016
184 94870.03632559274, -0.536405351614321
185 97657.94290884356, -0.4835526315789389
186 100530.84790012054, -0.483386775762928
187 103488.26811712357, -0.48322091994691707
188 106529.43511934493, -0.43036819991153585
189 109658.29650014469, -0.3511720477664664
190 112879.05523803871, -0.2719758956213978
191 116192.63547874281, -0.1664363113666445
192 119026.92395984495, -0.06092436974789095
193 121928.48669724895, 0.07093100398054819
194 123699.48719847444, 0.2027310924369825
195 126718.82613948248, 0.2818996019460487
196 129815.82914620957, 0.30838124723574367
197 132337.32807373017, 0.4665524104378651
198 134909.86459873084, 0.5983801415303054
199 137532.4092678341, 0.730207872622743
```

```
200 140205.93420114485, 0.8620356037151797
201 142242.41301320156, 0.993835692171614
202 144306.26707734872, 1.1519792127377348
203 145692.10249991124, 1.3364385227775415
204 147088.99976687875, 1.5472412649270328
205 148499.290498152, 1.7580440070765242
206 149923.103110395, 1.9688467492260155
207 151358.2551025438, 2.2059929234851925
208 152804.81096584388, 2.469482529854056
209 153528.57439263677, 2.6539141972578606
210 155000.60782678, 2.8647169394073515
211 156486.75513151608, 3.0755196815568433
212 157987.15163077012, 3.286322423706334
213 159501.93394595556, 3.497125165855826
214 161033.699921934, 3.6815844758956318
215 164161.5642534129, 3.839755639097754
216 166548.54063330134, 3.9452122954445032
217 168165.95944322916, 3.945267580716507
218 169809.46128984625, 3.839949137549767
219 172304.87949111866, 3.681971472799656
220 173994.14714333607, 3.5239661654135435
221 175708.02838608803, 3.2869305616983735
222 177438.79174219005, 3.0498949579832035
223 179186.6035042316, 2.812859354268034
224 180076.5825961926, 2.602139540026546
225 180970.98201181978, 2.3914197257850605
226 182753.5866375774, 2.1543841220698905
227 184556.56956080245, 1.8910050862450332
228 185470.3868064449, 1.7066287041132338
229 187300.17272927362, 1.4432496682883773
230 188230.4500736161, 1.2325298540468905
231 189165.3478938763, 1.0218100398054037
232 190101.98514062806, 0.8374336576736052
233 191971.5996297703, 0.6267414860681209
234 192928.02601257144, 0.38967823971694937
235 193889.21743055253, 0.15261499336577788
236 195817.0164099142, -0.2424812030075083
237 197751.8993713959, -0.5322036709420512
238 199699.79978422992, -0.7692392746572221];
239
240 % Free field correction for mic B&K type 4138
241 D2 = [4007.553556653379, 0.16216216216216317
242 4171.523985222408, 0.16216216216216317
243 4361.593637668383, 0.16216216216215962
244 4560.34969849724, 0.193050193050194
```

```
245 4768.162992759082, 0.22393822393822482
246 5097.729374567116, 0.22393822393822482
247 5425.876500218985, 0.25482625482625565
248 5826.807002226876, 0.25482625482625565
249 6174.314057706561, 0.28571428571429003
250 6601.108787041513, 0.3166023166023155
251 7025.990009476682, 0.3166023166023173
252 7511.656186541617, 0.34749034749034813
253 8175.30676583339, 0.37837837837837895
254 8701.561343001555, 0.4092664092664098
255 9220.516914934291, 0.4401544401544406
256 9946.116316699288, 0.47104247104246966
257 10681.1802408922, 0.5328185328185313
258 11267.881754716329, 0.5637065637065639
259 12100.560859005827, 0.594594594594593
260 12822.304123128384, 0.6563706563706564
261 13466.479211351674, 0.6872586872586872
262 14333.415276075924, 0.7490347490347471
263 15120.815394438714, 0.8108108108108105
264 15951.562477890415, 0.903474903474903
265 16753.043310019864, 0.9652509652509647
266 17438.69982304954, 1.0270270270270263
267 18233.58344722897, 1.1196911196911188
268 19064.699128981494, 1.2123552123552113
269 19933.69838301448, 1.3050193050193037
270 20749.649446205003, 1.3976833976833962
271 21599.000038410624, 1.4903474903474887
272 22583.646254091753, 1.613899613899612
273 23718.761913320126, 1.7683397683397661
274 24800.042950269042, 1.8918918918918912
275 25700.570216429194, 2.0154440154440145
276 26633.796996808847, 2.1389961389961396
277 27478.205414054573, 2.262548262548263
278 28349.547855592133, 2.416988416988419
279 29379.131512011878, 2.5714285714285694
280 30446.107034819277, 2.7258687258687235
281 31411.562559999464, 2.8803088803088794
282 32407.818818171745, 3.0656370656370644
283 33435.48083424683, 3.2200772200772203
284 34342.37281678526, 3.3745173745173727
285 35431.78649771378, 3.590733590733592
286 36555.339469596234, 3.7451737451737444
287 37883.37113186014, 3.96138996138996
288 39084.888741774914, 4.146718146718147
289 40324.745193745155, 4.362934362934363
```



```
290 41603.6939783443, 4.548262548262544
291 42923.20619330782, 4.733590733590733
292 44087.69264795654, 4.9189189189189175
293 45284.03074875428, 5.135135135135135
294 46512.565266454076, 5.32046332046332
295 47774.42934948241, 5.505791505791505
296 49070.527213316214, 5.69111969111969
297 50401.78760437459, 5.876447876447875
298 51539.014520064986, 6.06177606177606
299 52701.598732028, 6.216216216216214
300 53890.407777012966, 6.370656370656368
301 54861.04856995523, 6.525096525096522
302 55849.17194630681, 6.679536679536676
303 57109.30942505863, 6.864864864864862
304 58397.8796703138, 7.050193050193046
305 59715.524217003884, 7.235521235521232
306 60791.43201484806, 7.420849420849418
307 62163.439290876755, 7.637065637065634
308 63850.270386668846, 7.85328185328185
309 65291.31285998187, 8.069498069498065
310 66764.87834999173, 8.285714285714283
311 67967.4061677525, 8.440154440154437
312 69191.98994649285, 8.625482625482622
313 70753.18444092202, 8.810810810810807
314 72350.01940002342, 9.027027027027025
315 73982.89347039249, 9.243243243243239
316 75652.62002196065, 9.459459459459456
317 77705.93130923978, 9.706563706563703
318 79459.22778529546, 9.891891891891888
319 81252.08428567818, 10.077220077220073
320 83456.41522816512, 10.262548262548261
321 86103.33786363956, 10.447876447876443
322 88833.70149212686, 10.602316602316598
323 91242.14849115594, 10.694980694980691
324 94134.38579384239, 10.787644787644783
325 97117.74570825178, 10.849420849420845
326 99749.07255594028, 10.849420849420845
327 102451.10558398512, 10.818532818532812
328 104757.92713762312, 10.75675675675675
329 107116.07557106025, 10.66409266409266
330 109040.3819306176, 10.57142857142857
331 110999.25784423781, 10.478764478764475
332 113497.2506241556, 10.355212355212352
333 115534.86772433866, 10.200772200772198
334 117086.88349409054, 10.077220077220073
```

```
335 119188.94530354132, 9.922779922779918
336 120788.66213038097, 9.737451737451732
337 122409.8498572236, 9.552123552123547
338 124052.79665978807, 9.366795366795362
339 125717.79458159857, 9.181467181467175
340 127405.13958589552, 8.996138996138992
341 129114.39121616929, 8.779922779922774
342 130845.82363460216, 8.532818532818528
343 132600.4746748429, 8.285714285714281
344 134378.65570012658, 8.038610038610035
345 135576.81927932706, 7.85328185328185
346 136784.09732192638, 7.606177606177602
347 139232.5974887442, 7.173745173745171
348 141096.47927815863, 6.803088803088798
349 143622.17312571823, 6.370656370656365
350 144899.43123038978, 6.061776061776056
351 146183.8568004814, 5.598455598455592
352 147482.20497857765, 5.227799227799224
353 149456.52278259964, 4.857142857142852
354 150783.07285878315, 4.45559845559845
355 152120.52484430978, 4.023166023166018
356 154153.39907145244, 3.5289575289575232
357 154834.6752811324, 3.2818532818532784
358 155518.0705690526, 3.0038610038610045
359 156902.92052218987, 2.7567567567567526
360 157596.34815742142, 2.509652509652506
361 158998.79289760426, 2.2316602316602285
362 160415.55770201754, 2.0154440154440127
363 161844.01856674667, 1.7683397683397644
364 162557.41889281085, 1.4594594594594579
365 164004.95250168373, 1.2123552123552095
366 165466.32488206084, 0.9961389961389937
367 167684.2775382433, 0.718146718146718
368 169178.43468459754, 0.5019305019305005
369 172212.73393191773, 0.2548262548262521
370 174521.11716896, -0.023166023166027117
371 177653.27752833022, -0.20849420849421207
372 180037.68437647808, -0.39382239382239526
373 183267.80058292698, -0.6100386100386093
374 188224.65855738753, -0.8571428571428577
375 193318.91070103558, -1.0115830115830153
376 197666.07300972778, -1.2277992277992293
377 200322.53149526555, -1.3204633204633254];
378
379
```

```

380 % cubic interpolation between points of open circuit pressure response
381 cubic1 = interp1(D1(:,1),D1(:,2),Frequency,'spline');
382
383 % cubic interpolation between points of free field correction for mic B&...
      K type 4138
384 cubic2 = interp1(D2(:,1),D2(:,2),Frequency,'spline');
385
386 % Open circuit response including mikrophone free field correction
387 cubic3 = cubic1+cubic2;
388
389 % Open circuit response including mikrophone free field correction with
390 % calibration
391 Y = 20*log10(Mv)+cubic3;
392 % Go from dB to mV/Pa
393 Mv_f = 10.^(Y/20)*1e3;

```

A.8 plothorizontalpressurefield_basic.m

```

1 % plothorizontalpressurefield_basic.m
2 % Fargeplott av trykkfeltet. Fungerar både for PML og uendelege element.
3 % @author Espen Storheim, 2013(?)
4 %
5 % Skriptet er modifisert litt av Eivind Nag Mosland i desember 2020
6
7 % Simuleringsnummer, dersom parametrisk
8 sim = 1;
9
10 % Frekvens
11 f_ind =2;
12 FFr = result.nearfieldpressure_f{sim};
13 disp(['Viser trykkfeltet for f = ' num2str(FFr(f_ind)/1e3) ' kHz'])
14
15 % modene = find(FFr == f);
16
17 % Sett til ein dersom det er ei pml-køyring, eller ein berre vil sjå på ...
      dei
18 % endelege elementa (ikkje det som er rekna ut i dei uendelege).
19 ispml = 0;
20
21 % Hentar ut koordinatane til nodane og det tilh?yrande komplekse ...
      trykkjet.
22 if ispml

```

```
23     P_r = [result.nearfieldpressure_r{sim}.'];
24     P_z = [result.nearfieldpressure_z{sim}.'];
25     P = [result.nearfieldpressure{sim}(:,f_ind)];
26 else
27     P_r = [result.nearfieldpressure_r{sim}.';result.farfieldpressure_r{...
           sim}];
28     P_z = [result.nearfieldpressure_z{sim}.';result.farfieldpressure_z{...
           sim}];
29     P = [result.nearfieldpressure{sim}(:,f_ind);result.farfieldpressure{...
           sim}(:,f_ind)];
30 end
31
32 % Ser på dB-magnituda til trykket. Kan også sjå på fasen.
33 P = 20*log10(abs(P)*mean(pressurefield_result.V1)/(2*20e-6));
34
35 NEWSIM_press = 0;
36
37 % Delaunay delar matrisa opp i nokre trekantar.
38 TRI = delaunay(P_z,P_r);
39
40 X = [];
41 Y = [];
42 C = [];
43
44 % Her er det endring frå FEMP originalt. Har bytta om P_z og P_r ...
    samanlikna
45 % med originalfila. Grunnen til dette er at det er enklare å plotte det
46 % slik enn å rotere labels og ticks, m.m.
47 for ii = 1:3
48     X(1:size(TRI,1),ii) = P_z(TRI(:,ii));
49     Y(1:size(TRI,1),ii) = P_r(TRI(:,ii));
50     C(1:size(TRI,1),ii) = P(TRI(:,ii));
51 end
52
53 %% Plotting av feltet.
54 % Plottar feltet for r => 0.
55 fig = figure;
56 h1 = patch(X.',Y.',C. ');
57 %h1 = contourf(X.',Y.',C. ');
58 set(h1,'edgecolor','none');
59
60 % Plottar feltet for r <= 0. No har ein dobbelt opp i r = 0.
61 hold on
62 h2 = patch(X.',-Y.',C. ');
63 set(h2,'edgecolor','none');
```

```

64 hold off
65
66 %% Colorbar og aksetekstar.
67 defaxis = gca;
68 h = colorbar;
69 ylabel(h, '20log |p| [dB re 1 Pa/V]')
70 axes(defaxis)
71 xlabel('Axial distance, z [m]')
72 ylabel('Lateral distance, r [m]')
73 axis image
74
75 %% Begrensar områda.
76 xlim([0 0.3])
77 ylim([-0.301 0.301])

```

A.9 polarPcolor.m

```

1 function [varargout] = polarPcolor(R,theta,Z,varargin)
2 % [h,c] = polarPcolor1(R,theta,Z,varargin) is a pseudocolor plot of ...
   matrix
3 % Z for a vector radius R and a vector angle theta.
4 % The elements of Z specify the color in each cell of the
5 % plot. The goal is to apply pcolor function with a polar grid, which
6 % provides a better visualization than a cartesian grid.
7 %
8 %% Syntax
9 %
10 % [h,c] = polarPcolor(R,theta,Z)
11 % [h,c] = polarPcolor(R,theta,Z,'Ncircles',10)
12 % [h,c] = polarPcolor(R,theta,Z,'Nspokes',5)
13 % [h,c] = polarPcolor(R,theta,Z,'Nspokes',5,'colBar',0)
14 % [h,c] = polarPcolor(R,theta,Z,'Nspokes',5,'labelR','r (km)')
15 %
16 % INPUT
17 % * R :
18 %     - type: float
19 %     - size: [1 x Nrr ] where Nrr = numel(R).
20 %     - dimension: radial distance.
21 % * theta :
22 %     - type: float
23 %     - size: [1 x Ntheta ] where Ntheta = numel(theta).
24 %     - dimension: azimuth or elevation angle (deg).

```

```
25 %           - N.B.: The zero is defined with respect to the North.
26 % * Z :
27 %           - type: float
28 %           - size: [Ntheta x Nrr]
29 %           - dimension: user's defined .
30 % * varargin:
31 %           - Ncircles: number of circles for the grid definition.
32 %           - autoOrigin: 'on' (the first circle of the plar grid has a ...
radius
33 %           equal to the lowest value of R) or 'off'.
34 %           - Nspokes: number of spokes for the grid definition.
35 %           - colBar: display the colorbar or not.
36 %           - labelR: title for radial axis.
37 %           - RtickLabel: Tick label for the radial axis.
38 %           - colormap: Colormap for the pcolor function
39 %           - ncolor: Number of colors in the colorbar and pcolor
40 %           - circlesPos: position of the circles with respect to the ...
origin
41 %           (it overwrites Ncircles if necessary)
42 %
43 %
44 % OUTPUT
45 % h: returns a handle to a SURFACE object.
46 % c: returns a handle to a COLORBAR object.
47 %
48 %% Examples
49 % R = linspace(3,10,100);
50 % theta = linspace(0,180,360);
51 % Z = linspace(0,10,360) '*linspace(0,10,100);
52 % figure
53 % polarPcolor(R,theta,Z,'Ncircles',3)
54 %
55 %% Author
56 % Etienne Cheynet, University of Stavanger, Norway. 23/10/2019
57 % see also pcolor
58 %
59 %% InputParseer
60 p = inputParser();
61 p.CaseSensitive = false;
62 p.addOptional('Ncircles',5);
63 p.addOptional('autoOrigin','on');
64 p.addOptional('Nspokes',8);
65 p.addOptional('labelR','');
66 p.addOptional('RtickLabel',[ ]);
67 p.addOptional('colBar',1);
```

```

68 p.addOptional('Rscale','linear');
69 p.addOptional('colormap','parula');
70 p.addOptional('ncolor',[]);
71 p.addOptional('typeRose','meteo'); % 'meteo' or 'default'
72 p.addOptional('circlesPos',[]);
73 p.parse(varargin{:});
74 Ncircles = p.Results.Ncircles;
75 Nspokes = p.Results.Nspokes ;
76 labelR = p.Results.labelR ;
77 RtickLabel = p.Results.RtickLabel ;
78 colBar = p.Results.colBar ;
79 Rscale = p.Results.Rscale ;
80 autoOrigin = p.Results.autoOrigin ;
81 myColorMap = p.Results.colormap ;
82 ncolor = p.Results.ncolor ;
83 circPos = p.Results.circlesPos ;
84 typeRose = p.Results.typeRose ;
85 if ~isempty(circPos)
86     Origin = max([min(circPos),min(R)]);
87     circPos(circPos<min(R))=[];
88     circPos(circPos>max(R))=[];
89 elseif strcmpi(autoOrigin,'on')
90     Origin = min(R);
91 elseif strcmpi(autoOrigin,'off')
92     Origin = 0;
93 else
94     error(' 'autoOrigin' must be 'on' or 'of' ');
95 end
96 if Origin==0 && strcmpi(Rscale,'log')
97     warning(' The origin cannot be set to 0 if R is expressed on a ...
98         logarithmic axis. The value 'Rmin' is used instead')
99     Origin = min(R);
100 end
101 if isempty(circPos)
102     if ~isempty(RtickLabel)
103         if numel(RtickLabel)~=Ncircles
104             error(' The radial ticklabel must be equal to Ncircles');
105         end
106         if any(cellfun(@ischar,RtickLabel)==0)
107             error(' The radial ticklabel must be a cell array of ...
108                 characters');
109         end
110     end
111 end
112 if ~isempty(circPos)

```

```

111     circPos = unique([min(R),circPos,max(R)]);
112 end
113 %% Preliminary checks
114 % case where dimension is reversed
115 Nrr = numel(R);
116 Noo = numel(theta);
117 if isequal(size(Z),[Noo,Nrr]) && Noo~=Nrr,
118     Z=Z';
119 end
120 % case where dimension of Z is not compatible with theta and R
121 if ~isequal(size(Z),[Nrr,Noo])
122     fprintf('\n')
123     fprintf(['Size of Z is : ',num2str(size(Z)),'] \n');
124     fprintf(['Size of R is : ',num2str(size(R)),'] \n');
125     fprintf(['Size of theta is : ',num2str(size(theta)),'] \n\n');
126     error(' dimension of Z does not agree with dimension of R and Theta'...
127         )
127 end
128 %% data plot
129 rMin = min(R);
130 rMax = max(R);
131 thetaMin=min(theta);
132 thetaMax =max(theta);
133 if strcmpi(typeRose,'meteo')
134     theta = theta;
135 elseif strcmpi(typeRose,'default')
136     theta = 90-theta;
137 else
138     error('"type" must be "meteo" or "default" ');
139 end
140 % Definition of the mesh
141 cax = newplot;
142 Rrange = rMax - rMin; % get the range for the radius
143 [rNorm] = getRnorm(Rscale,Origin,R,Rrange); % getRnorm is a nested ...
144     function
145     YY = (rNorm) '*cosd(theta);
146     XX = (rNorm) '*sind(theta);
147     h = pcolor(XX,YY,Z,'parent',cax);
148     if ~isempty(ncolor)
149         cmap = feval(myColorMap,ncolor);
150         colormap(gca,cmap);
151     else
152         colormap(gca,myColorMap);
153     end
153 % disp([max(R/Rrange),max(rNorm)])

```



```

154 shading flat
155 set(cax,'dataaspectratio',[1 1 1]);axis off;
156 if ~ishold(cax);
157     % make a radial grid
158     hold(cax,'on')
159     % Draw circles and spokes
160     createSpokes(thetaMin,thetaMax,Ncircles,circPos,Nspokes);
161     createCircles(rMin,rMax,thetaMin,thetaMax,Ncircles,circPos,Nspokes)
162 end
163 %% PLOT colorbar if specified
164 if colBar==1,
165     c = colorbar('location','WestOutside');
166     caxis([quantile(Z(:),0.01),quantile(Z(:),0.99)])
167 else
168     c = [];
169 end
170 %% Outputs
171 nargoutchk(0,2)
172 if nargout==1,
173     varargout{1}=h;
174 elseif nargout==2,
175     varargout{1}=h;
176     varargout{2}=c;
177 end
178 %...
    %%%%%%%%%%%%%%%%%%%%%%%%%%%%%%%%%%%%%%%%%%%%%%%%%%%%%%%%%%%%%%%%%%%%%%%%%%...

179 % Nested functions
180 %...
    %%%%%%%%%%%%%%%%%%%%%%%%%%%%%%%%%%%%%%%%%%%%%%%%%%%%%%%%%%%%%%%%%%%%%%%%%%...

181 function createSpokes(thetaMin,thetaMax,Ncircles,circlesPos,Nspokes)
182
183     spokeMesh = round(linspace(thetaMin,thetaMax,Nspokes));
184     if isempty(circlesPos)
185         circleMesh = linspace(rMin,rMax,Ncircles);
186     else
187         circleMesh = circlesPos;
188     end
189     contourD = abs((circleMesh - circleMesh(1))/Rrange+R(1)/Rrange);
190
191     if strcmpi(typeRose,'meteo')
192         cost = cosd(90-spokeMesh); % the zero angle is aligned with ...
            North
193         sint = sind(90-spokeMesh); % the zero angle is aligned with ...

```

```

        North
194     elseif strcmpi(typeRose, 'default')
195         cost = cosd(spokeMesh); % the zero angle is aligned with ...
            east
196         sint = sind(spokeMesh); % the zero angle is aligned with ...
            east
197     else
198         error('"type" must be "meteo" or "default" ');
199     end
200
201     for kk = 1:Nspokes
202
203         X = cost(kk)*contourD;
204         Y = sint(kk)*contourD;
205
206         if Origin==0
207             X(1)=Origin;
208             Y(1)=Origin;
209         end
210         plot(X,Y, 'color', [0.5,0.5,0.5], 'linewidth', 0.75, ...
211             'handlevisibility', 'off');
212         % plot graduations of angles
213         % avoid superimposition of 0 and 360
214         if and(thetaMin==0, thetaMax == 360),
215             if spokeMesh(kk)<360,
216
217                 text(1.05.*contourD(end).*cost(kk), ...
218                     1.05.*contourD(end).*sint(kk), ...
219                     [num2str(spokeMesh(kk), 3), char(176)], ...
220                     'horiz', 'center', 'vert', 'middle');
221             end
222         else
223             text(1.05.*contourD(end).*cost(kk), ...
224                 1.05.*contourD(end).*sint(kk), ...
225                 [num2str(spokeMesh(kk), 3), char(176)], ...
226                 'horiz', 'center', 'vert', 'middle');
227         end
228
229     end
230 end
231 function createCircles(rMin,rMax,thetaMin,thetaMax,Ncircles,...
    circlePos,Nspokes)
232
233     if isempty(circlePos)
234         if Origin ==0 % if the origin is set at rMin

```

```

235         contourD = linspace(0,1+R(1)/Rrange,Ncircles);
236     else % if the origin is automatically centered at 0
237         contourD = linspace(0,1,Ncircles)+R(1)/Rrange;
238     end
239 else
240
241     contourD = circlePos-circlePos(1);
242     contourD = contourD./max(contourD)*max(R/Rrange);
243     contourD =[contourD(1:end-1)./contourD(end),1]+R(1)/Rrange;
244 end
245
246 if isempty(circlePos)
247     if strcmpi(Rscale,'linear')||strcmpi(Rscale,'lin'),
248         tickMesh = linspace(rMin,rMax,Ncircles);
249     elseif strcmpi(Rscale,'log')||strcmpi(Rscale,'logarithmic'),
250         tickMesh = logspace(log10(rMin),log10(rMax),Ncircles);
251     else
252         error(''Rscale'' must be ''log'' or ''linear'' ');
253     end
254 else
255     tickMesh = circlePos;
256     Ncircles = numel(tickMesh);
257 end
258
259 % define the grid in polar coordinates
260
261
262 if strcmpi(typeRose,'meteo')
263     angleGrid = linspace(90-thetaMin,90-thetaMax,100);
264 elseif strcmpi(typeRose,'default')
265     angleGrid = linspace(thetaMin,thetaMax,100);
266 else
267     error('"type" must be "meteo" or "default" ');
268 end
269
270 xGrid = cosd(angleGrid);
271 yGrid = sind(angleGrid);
272 spokeMesh = linspace(thetaMin,thetaMax,Nspokes);
273
274 % plot circles
275 for kk=1:length(contourD)
276     X = xGrid*contourD(kk);
277     Y = yGrid*contourD(kk);
278     plot(X,Y,'color',[0.5,0.5,0.5],'linewidth',1);
279 end

```

```

280     % radius tick label
281
282     position = 0.51.*(spokeMesh(min(Nspokes,round(Ncircles/2)))+...
283         spokeMesh(min(Nspokes,1+round(Ncircles/2))));
284     if strcmpi(typeRose,'meteo'),position = 90-position; end
285     if strcmpi(typeRose,'default') && min(90-theta)<5,position = 0; ...
286         end
287     if min(round(theta))==90 && strcmpi(typeRose,'meteo'), position...
288         = 0; end
289     if max(round(theta))==90 && strcmpi(typeRose,'meteo'), position...
290         = 0; end
291
292     for kk=1:Ncircles
293         if isempty(RtickLabel),
294             rtick = num2str(tickMesh(kk),2);
295         else
296             rtick = RtickLabel(kk);
297         end
298
299     % radial graduations
300     t = text(contourD(kk).*cosd(position),...
301         (contourD(kk)).*sind(position),...
302         rtick,'verticalalignment','BaseLine',...
303         'horizontalAlignment','right',...
304         'handlevisibility','off','parent',cax);
305     if min(round(abs(90-theta)))<5 && strcmpi(typeRose,'default'...
306         ),
307         t.Position = t.Position - [0,0.1,0];
308         t.Interpreter = 'latex';
309         clear t;
310     end
311     if min(round(theta))==90 && strcmpi(typeRose,'meteo')
312         t.Position = t.Position + [0,0.02,0];
313         t.Interpreter = 'latex';
314         clear t;
315     elseif max(round(theta))==90 && strcmpi(typeRose,'meteo')
316         t.Position = t.Position - [0,0.05,0];
317         t.Interpreter = 'latex';
318         clear t;
319     end
320
321     % annotate spokes
322     if max(theta)-min(theta)>180,
323         t = text(contourD(end).*1.3.*cosd(position),...
324             contourD(end).*1.3.*sind(position),...

```

```

321         [labelR], 'verticalalignment', 'bottom', ...
322         'horizontalAlignment', 'right', ...
323         'handlevisibility', 'off', 'parent', cax);
324     else
325         t = text(contourD(end).*0.6.*cosd(position), ...
326               contourD(end).*0.6.*sind(position), ...
327               [labelR], 'verticalalignment', 'bottom', ...
328               'horizontalAlignment', 'right', ...
329               'handlevisibility', 'off', 'parent', cax);
330     end
331
332     t.Interpreter = 'latex';
333     if min(round(theta))==90 && strcmpi(typeRose, 'meteo'),
334         t.Position = t.Position + [0, 0.05, 0];
335         clear t;
336     elseif max(round(theta))==90 && strcmpi(typeRose, 'meteo'),
337         t.Position = t.Position + [0, 0.05, 0];
338         clear t;
339     end
340     %             if min(round(abs(90-theta)))<5 && strcmpi(...
341     %             typeRose, 'default'),
342     %             t.Position = t.Position - [0, 0.12, 0];
343     %             t.Interpreter = 'latex';
344     %             clear t;
345     %             end
346
347     end
348
349     function [rNorm] = getRnorm(Rscale, Origin, R, Rrange)
350         if strcmpi(Rscale, 'linear') || strcmpi(Rscale, 'lin')
351             rNorm = R-R(1)+Origin;
352             rNorm = (rNorm)/max(rNorm)*max(R/Rrange);
353         elseif strcmpi(Rscale, 'log') || strcmpi(Rscale, 'logarithmic')
354             if rMin<=0
355                 error(' The radial vector cannot be lower or equal to 0 ...
356                       if the logarithmic scale is used');
357             end
358             rNorm = log10(R); %normalized radius [0,1]
359             rNorm = rNorm-rNorm(1);
360             rNorm = (rNorm)/max(rNorm)*max(R/Rrange);
361         else
362             error(' ''Rscale'' must be ''log'' or ''linear'' ');
363         end
364     end
365 end

```

A.10 absorption_in_air.m

```

1 function alpha = absorption_in_air(Frequency,Pressure,RH,Temperature)
2 %Calculating the absorption coefficient alpha dB/m
3
4 % Measure frequency
5 f=Frequency;
6 % Paroscientific reads pressure in hPa, coverting it to kPa
7 p=Pressure/10;
8 % Relative humidity read by Vaisala
9 h_rel=RH;
10
11 % Triple point isothermal temperature(0.01C)
12 T_01=273.16;
13 % Referance pressure in kPa (1atm)
14 p_ref=101.325;
15 %Referance temperature in Kelvin (20 degC)
16 T_ref=293.15;
17 % Temperature read by ASL f250 konverted to Kelvin
18 T=Temperature+273.15;
19
20 % Molar concentration of water in the air
21 V=10.79586*(1-(T_01/T))-5.02808.*log10(T/T_01)+1.50474*(10^-4)*(1-10^(-8...
    .29692*(T/T_01-1)))+0.42873*(10^-3)*(-1+10^(4.76955*(1-T_01/T)))-2...
    .2195983;
22
23 % Molar humidity
24 h=h_rel*(10^V)*(p/p_ref)^-1;
25
26 % Relaxation frequency for Oxygen
27 f_rO=(p/p_ref)*(24 + ((4.04*(10^4)*h)*(0.02+h)/(0.391+h)));
28
29 % Relaxation frequency for Nitrogen
30 f_rN=(p/p_ref)*(T/T_ref)^(-0.5)*(9+280*h*exp(-4.170*((T/T_ref)^(-1/3)-1)...
    ));
31
32 % Absorption coefficient i dB/m
33 alpha=8.686*f^2*( (1.84*(10^-11)*(p/p_ref)^-1*(T/T_ref)^(0.5)) + (T/...
    T_ref)^(-5/2)*(0.01275*(exp(-2239.1/T))*(f_rO/(f_rO^2+f^2)) + 0.1068*...
    exp(-3352/T)*(f_rN/(f_rN^2+f^2))));

```

A.11 Admittance_plotting.m

```
1 % simulated admittance
2 load('PZ27_result.mat')
3 f = result.admittance_f{1}/1000;
4 YT = result.admittance{1};
5 YT_log = 20*log10(abs(YT));
6 % YT_ang = angle(YT);
7
8 GT = real(YT);
9 GT_log = 20*log10(GT);
10
11 BT = imag(YT);
12
13 load('PZ27_result_fluid.mat')
14 f_fluid = result.admittance_f{1}/1000;
15 YT_fluid = result.admittance{1};
16 YT_log_fluid = 20*log10(abs(YT_fluid));
17 % YT_ang_fluid = angle(YT_fluid);
18
19
20
21 GT_fluid = real(YT_fluid);
22 GT_log_fluid = 20*log10(GT_fluid);
23
24 BT_fluid = imag(YT_fluid);
25
26 % measured admittance
27 % load('20220203132417.mat')
28 % load('20220403155415.mat')
29 f_m = fr(2:end);
30 YT_m = g(2:end)+1i*b(2:end);
31 YT_m_log = 20*log10(abs(YT_m));
32 % YT_m_ang = angle(YT_m);
33
34 GT_m = g(2:end);
35 GT_m_log = 20*log10(GT_m);
36
37 BT_m = b(2:end);
38
39 figure
40 box on
41 hold on
```

```
42 plot(f, YT_log, 'LineWidth', 2, 'Color', 'r')
43 plot(f_fluid, YT_log_fluid, '--', 'LineWidth', 2, 'Color', 'g')
44 plot(f_m, YT_m_log, 'LineWidth', 2, 'Color', 'b')
45 xlabel('Frequency [kHz]')
46 ylabel('20log_{10}|Y_T| [dB re. 1 S]')
47 legend('Simuleted', 'Simuleted fluid', 'Measured')
48 set(gca, 'FontSize', 22, 'FontName', 'Times New Roman')
49 ylim([-90 -25])
50 hold off
51
52 figure
53 hold on
54 box on
55 hold on
56 plot(f, GT_log, 'LineWidth', 2, 'Color', 'r')
57 plot(f_fluid, GT_log_fluid, '--', 'LineWidth', 2, 'Color', 'g')
58 plot(f_m, GT_m_log, 'LineWidth', 2, 'Color', 'b')
59 xlabel('Frequency [kHz]')
60 ylabel('20log_{10}(G_T) [dB re. 1 S]')
61 legend('Simuleted', 'Simuleted fluid', 'Measured')
62 set(gca, 'FontSize', 22, 'FontName', 'Times New Roman')
63 ylim([-110 -25])
64 hold off
65
66 figure
67 hold on
68 box on
69 hold on
70 plot(f, BT, 'LineWidth', 2, 'Color', 'r')
71 plot(f_fluid, BT_fluid, '--', 'LineWidth', 2, 'Color', 'g')
72 plot(f_m, BT_m, 'LineWidth', 2, 'Color', 'b')
73 xlabel('Frequency [kHz]')
74 ylabel('B_T [S]')
75 legend('Simuleted', 'Simuleted fluid', 'Measured')
76 set(gca, 'FontSize', 22, 'FontName', 'Times New Roman')
77 % ylim([-110 -25])
78 hold off
```


Appendix B

MatLab-app

B.1 App's startup values

```
1 properties (Access = public)
2     % color for app design
3     red = [1,0,0];
4     green = [0,1,0];
5     black = [0,0,0];
6     grey = [0.96,0.96,0.96];
7
8     % indicates if a certain axis is homed or zeroed where rotation
9     % axis has no induction sensor activated and therefore rotation axis
10    % is always homed
11    homed = [0,0,0,1];
12    zeroed = [0,0,0,0];
13
14    % the travell distance of y axis had to be callibrated because
15    % y step = 10 was not 10mm; y calibration factor
16    factor = 1.69027948373533;
17
18
19    % values indicates if somthing is acitve or not
20    initialized = 0;
21    initializing = 0;
22    connected = 0;
23    connecting = 0;
24
25    % if initialize or connecting fails
26    initfail = 0;
27    connectfail = 0;
```

```
28
29     % other values app use
30     stop = 0;
31     start = 0;
32     stage = 0;
33     setup = 0;
34     zeroz = 0;
35     safety = 0;
36     limits = 0;
37     comp = 0;
38     distance_transducer_microphone = 0;
39     distance_transducer_rotaxis = 0;
40     transducer_perpendicular_laser = 0;
41     transducer_perpendicular_mainlobe = 0;
42     tilt_angle_and_distance = 0;
43     tilt_angle = 0;
44
45     % empty values for app log and the path for the app
46     text = {};
47     path = '';
48
49
50     % Measurements values
51     meas = {};
52     x = 0;
53     wf = 0;
54     timeDiv = '';
55     maxV = 0;
56     result = {};
57     time = 0;
58     selpath = '';
59     measurement = 0;
60     meas_el_sig = 0;
61     filt_setting = 0;
62     gen_setting = 0;
63     environment = 0;
64     angle = [];
65     distance = [];
66
67     % Number of bytes per word (8-bit if 1, 16-bit if 2, ...) when
68     % reading oscilloscope
69     noB = 2;
70
71     % absolute position or absolute value for the zero position
72     zeropos = {};
```

```

73     abspos = {};
74     field = {'xaxis', 'yaxis', 'zaxis', 'rotaxis'};
75     name = {'X-axis', 'Y-axis', 'Z-axis', 'Rotation-axis'};
76     linearslope = {};
77
78
79     % handels that controll devices
80     controller = {};
81     instrument = {};
82 end

```

B.2 Initialize machine function

```

1  methods (Access = public)
2  %%%%%%%%%%%%%%%%%%%%%%%%%%%%%%%%%%%%%%%%%%%%%%%%%%%%%%%%%%%%%%%%%%%%%%%%%
3  % following function handles the motion controllers and to each
4  % axis in the air setup
5  function InitMotor(app)
6      %%%%%%%%%%%%%%%%%%%%%%%%%%%%%%%%%%%%%%%%%%%%%%%%%%%%%%%%%%%%%%%%%%%%%%%%%
7      % Skript InitMotor is used to connect to the controllers of X,
8      % Y, Z and Rotation-axis in the air setup.
9      % X, Y, Z and Rotation-axis can be used to move relatively or
10     % absolute values.
11     %
12     % Espen Fosse, 2021/2022
13     %%%%%%%%%%%%%%%%%%%%%%%%%%%%%%%%%%%%%%%%%%%%%%%%%%%%%%%%%%%%%%%%%%%%%%%%%
14
15     % clear handle for controllers
16     app.controller = {};
17
18     % Initialisation of LS-270 with HydraTT motor controller
19     app.controller.HydraTT = serialport('COM1',115200);
20     writeline(app.controller.HydraTT, 'version')
21     app.controller.HydraTT_idn = readline(app.controller.HydraTT);
22
23     if isstring(app.controller.HydraTT_idn)
24         app.controller.HydraTT_idn = strip(app.controller.HydraTT_idn);
25         WriteTextInWindow(app, ['Connected to: Physik Instrumente, Hydra ...
26             TT, V' num2str(app.controller.HydraTT_idn)])
27     else
28         WriteTextInWindow(app, 'Could not connenct to Hydra TT')
29         app.initfail = 1;

```

```
29     return
30 end
31
32 % z axis
33 app.controller.HydraTT_LS270 = 1;
34 % Initiate Motor restart
35 writeline(app.controller.HydraTT, [num2str(...
    app.controller.HydraTT_LS270) ' init']);
36
37 % Sets PID constants for motor
38 app.controller.HydraTT_LS270_P = 0;
39 app.controller.HydraTT_LS270_I = 0.001;
40 app.controller.HydraTT_LS270_D = 0;
41 writeline(app.controller.HydraTT, [num2str(...
    app.controller.HydraTT_LS270_P) ' 1 ' num2str(...
    app.controller.HydraTT_LS270) ' setsp']);
42 writeline(app.controller.HydraTT, [num2str(...
    app.controller.HydraTT_LS270_I) ' 2 ' num2str(...
    app.controller.HydraTT_LS270) ' setsp']);
43 writeline(app.controller.HydraTT, [num2str(...
    app.controller.HydraTT_LS270_D) ' 3 ' num2str(...
    app.controller.HydraTT_LS270) ' setsp']);
44
45 % Sets motor acceleration and velocity
46 app.controller.HydraTT_LS270_aks = 2;
47 app.controller.HydraTT_LS270_vel = 10;
48 writeline(app.controller.HydraTT, [num2str(...
    app.controller.HydraTT_LS270_aks) ' ' num2str(...
    app.controller.HydraTT_LS270) ' sna']);
49 writeline(app.controller.HydraTT, [num2str(...
    app.controller.HydraTT_LS270_vel) ' ' num2str(...
    app.controller.HydraTT_LS270) ' snv']);
50
51 % Initialisation of M-535.22, M-531.DG and M-037.PD with C843.41 ...
    motor controller
52
53 % Create Instance of controller class
54 app.controller.C843 = C843_GCS_Controller();
55 % rotation axis name
56 app.controller.C843_M037PD_name = ('M-037.PD');
57 % x axis name
58 app.controller.C843_M531DG_name = ('M-531.DG');
59 % y axis name
60 app.controller.C843_M53522_name = ('M-535.22');
61
```

```
62 % Connect using PCI
63 app.controller.C843 = app.controller.C843.Connect(1);
64 app.controller.C843 = app.controller.C843.InitializeController();
65
66 % Query controller identification
67 WriteTextInWindow(app, ['Connected to: ' app.controller.C843.qIDN()])
68 % Query axes
69 app.controller.C843_availableaxes = app.controller.C843.qSAI_ALL();
70 if isempty(app.controller.C843_availableaxes)
71     noax2 = 'No available axes on C.843.41 Motor Controller';
72     WriteTextInWindow(app, noax2)
73     app.initfail = 1;
74     return
75 end
76
77 % x axis
78 app.controller.C843_M531DG = app.controller.C843_availableaxes(4);
79 % y axis
80 app.controller.C843_M53522 = app.controller.C843_availableaxes(2);
81 % rotation axis
82 app.controller.C843_M037PD = app.controller.C843_availableaxes(3);
83
84 % Connect a stage
85 % connecting to x axis
86 app.controller.C843.CST(app.controller.C843_M531DG, ...
87     app.controller.C843_M531DG_name);
88 % connecting to y axis
89 app.controller.C843.CST(app.controller.C843_M53522, ...
90     app.controller.C843_M53522_name);
91 % connecting to rotation axis
92 app.controller.C843.CST(app.controller.C843_M037PD, ...
93     app.controller.C843_M037PD_name);
94
95 % Initialize x and y rotation axis
96
97 app.controller.C843.INI(app.controller.C843_M531DG);
98 app.controller.C843.INI(app.controller.C843_M53522);
99 app.controller.C843.INI(app.controller.C843_M037PD);
100
101 % set to Acceleration, Deceleration and Velocity of rotation axis
102 app.controller.C843.ACC(app.controller.C843_M037PD, 0.5)
103 app.controller.C843.DEC(app.controller.C843_M037PD, 0.5)
104 app.controller.C843.VEL(app.controller.C843_M037PD, 10)
105
106 %% Configuration values for LS-270
```

```
104 % Verdier som ikke skal endres. Konfigurasjonsinstillingene skal væ...
      re
105 % lagret på HYDRA-TT. Skal det være problemer med bevegelse av LS...
      -270
106 % er det en ide og 'uncomment' denne seksjonen og kjøre InitMotor og
107 % 'comment' alt i denne seksjonen igjen etterpå.
108 % (Etter erfaring, så er det greit å alltid ha disse 'uncomment')
109
110
111 % Sets the Vector velocity
112 writeline(app.controller.HydraTT, [num2str(1) ' sv']);
113
114 % Sets the Vector acceleration
115 writeline(app.controller.HydraTT, [num2str(1) ' sa']);
116
117 % Sets the Emergency switch configuration
118 writeline(app.controller.HydraTT, [num2str(1) ' setemsw']);
119
120 % Sets the Hardware limits
121 writeline(app.controller.HydraTT, [num2str(0) ' ' num2str(1016) ' ' ...
      num2str(app.controller.HydraTT_LS270) ' setnlimit']);
122
123 % Sets the Initial limits
124 writeline(app.controller.HydraTT, [num2str(0) ' ' num2str(1016) ' ' ...
      num2str(app.controller.HydraTT_LS270) ' setinilimit']);
125
126 % Sets the Pitch
127 writeline(app.controller.HydraTT, [num2str(5) ' ' num2str(...
      app.controller.HydraTT_LS270) ' setpitch']);
128
129 % Sets the Motor form
130 writeline(app.controller.HydraTT, [num2str(0) ' ' num2str(...
      app.controller.HydraTT_LS270) ' setmotor']);
131
132 % Sets the Motor current shift value
133 writeline(app.controller.HydraTT, [num2str(0.092540) ' ' num2str(...
      app.controller.HydraTT_LS270) ' setMCShift']);
134
135 % Sets the Stop deceleration
136 writeline(app.controller.HydraTT, [num2str(74) ' ' num2str(...
      app.controller.HydraTT_LS270) ' ssd']);
137
138 % Sets the FRT parameters
139 writeline(app.controller.HydraTT, [num2str(0) ' 1 ' num2str(...
      app.controller.HydraTT_LS270) ' setfrtpara']);
```

```
140 writeline(app.controller.HydraTT,[num2str(0) ' 2 ' num2str(...
    app.controller.HydraTT_LS270) ' setfirtpara']);
141
142 % Sets the Calibration velocity
143 writeline(app.controller.HydraTT,[num2str(10) ' 1 ' num2str(...
    app.controller.HydraTT_LS270) ' setncalvel']);
144 writeline(app.controller.HydraTT,[num2str(0.1) ' 2 ' num2str(...
    app.controller.HydraTT_LS270) ' setncalvel']);
145
146 % Sets the Range measure velocity
147 writeline(app.controller.HydraTT,[num2str(10) ' 1 ' num2str(...
    app.controller.HydraTT_LS270) ' setnrmvel']);
148 writeline(app.controller.HydraTT,[num2str(0.1) ' 2 ' num2str(...
    app.controller.HydraTT_LS270) ' setnrmvel']);
149
150 % Sets the Reference velocity
151 writeline(app.controller.HydraTT,[num2str(1) ' 1 ' num2str(...
    app.controller.HydraTT_LS270) ' setnrefvel']);
152 writeline(app.controller.HydraTT,[num2str(0.1) ' 2 ' num2str(...
    app.controller.HydraTT_LS270) ' setnrefvel']);
153
154 % Sets the Motion function
155 writeline(app.controller.HydraTT,[num2str(7) ' ' num2str(...
    app.controller.HydraTT_LS270) ' setmotionfunc']);
156
157 % Sets the Position origin configuration
158 writeline(app.controller.HydraTT,[num2str(1) ' 1 ' num2str(...
    app.controller.HydraTT_LS270) ' setorgconfig']);
159
160 % Sets Reference configuration
161 writeline(app.controller.HydraTT,[num2str(0) ' ' num2str(...
    app.controller.HydraTT_LS270) ' setref']);
162
163 % Sets the Calibration switch distance
164 writeline(app.controller.HydraTT,[num2str(0) ' ' num2str(...
    app.controller.HydraTT_LS270) ' setncalswdist']);
165
166 % Sets the Motor voltage minimum
167 writeline(app.controller.HydraTT,[num2str(3.6) ' ' num2str(...
    app.controller.HydraTT_LS270) ' setumotmin']);
168
169 % Sets the Motor voltage gradient
170 writeline(app.controller.HydraTT,[num2str(7) ' ' num2str(...
    app.controller.HydraTT_LS270) ' setumotgrad']);
171
```

```
172 % Sets the Motor current limit
173 writeline(app.controller.HydraTT, [num2str(5) ' ' num2str(...
    app.controller.HydraTT_LS270) ' setmaxcurrent']);
174
175 % Sets the Motor pole pairs
176 writeline(app.controller.HydraTT, [num2str(100) ' ' num2str(...
    app.controller.HydraTT_LS270) ' setpolepairs']);
177
178 % Sets the Motor phase number
179 writeline(app.controller.HydraTT, [num2str(2) ' ' num2str(...
    app.controller.HydraTT_LS270) ' setphases']);
180
181 % Sets the Positioning control mode
182 writeline(app.controller.HydraTT, [num2str(2) ' ' num2str(...
    app.controller.HydraTT_LS270) ' setcloop']);
183
184 % Sets the Target window
185 writeline(app.controller.HydraTT, [num2str(0.0002) ' ' num2str(0.0002...
    ) ' ' num2str(app.controller.HydraTT_LS270) ' setclwindow']);
186
187 % Sets the Time on target
188 writeline(app.controller.HydraTT, [num2str(0.02) ' ' num2str(...
    app.controller.HydraTT_LS270) ' setclwintime']);
189
190 % Sets the Scale period
191 writeline(app.controller.HydraTT, [num2str(-0.02) ' ' num2str(...
    app.controller.HydraTT_LS270) ' setclperiod']);
192
193 % Sets the Position display selection
194 writeline(app.controller.HydraTT, [num2str(1) ' ' num2str(...
    app.controller.HydraTT_LS270) ' setselpos']);
195
196 % Configures the Motor brake control function
197 writeline(app.controller.HydraTT, [num2str(0) ' 0 ' num2str(...
    app.controller.HydraTT_LS270) ' setbrakefunc']);
198 writeline(app.controller.HydraTT, [num2str(3) ' 1 ' num2str(...
    app.controller.HydraTT_LS270) ' setbrakefunc']);
199
200 % Enables or disables the Clock and direction function
201 writeline(app.controller.HydraTT, [num2str(0) ' ' num2str(...
    app.controller.HydraTT_LS270) ' setcdfunc']);
202
203 % Sets the Clock and direction width
204 writeline(app.controller.HydraTT, [num2str(250) ' ' num2str(...
    app.controller.HydraTT_LS270) ' setcdwidth']);
```



```
205
206 % Configures the Servo control
207 writeline(app.controller.HydraTT, [num2str(100) ' 4 ' num2str(...
    app.controller.HydraTT_LS270) ' setsp']);
208 writeline(app.controller.HydraTT, [num2str(0) ' 5 ' num2str(...
    app.controller.HydraTT_LS270) ' setsp']);
209 writeline(app.controller.HydraTT, [num2str(24) ' 6 ' num2str(...
    app.controller.HydraTT_LS270) ' setsp']);
210 writeline(app.controller.HydraTT, [num2str(1) ' 7 ' num2str(...
    app.controller.HydraTT_LS270) ' setsp']);
211 writeline(app.controller.HydraTT, [num2str(1) ' 8 ' num2str(...
    app.controller.HydraTT_LS270) ' setsp']);
212 writeline(app.controller.HydraTT, [num2str(0.0000) ' 9 ' num2str(...
    app.controller.HydraTT_LS270) ' setsp']);
213
214 % Configures the Adaptive positioning control
215 writeline(app.controller.HydraTT, [num2str(0) ' 1 ' num2str(...
    app.controller.HydraTT_LS270) ' setadaptive']);
216 writeline(app.controller.HydraTT, [num2str(0.025) ' 2 ' num2str(...
    app.controller.HydraTT_LS270) ' setadaptive']);
217 writeline(app.controller.HydraTT, [num2str(0) ' 3 ' num2str(...
    app.controller.HydraTT_LS270) ' setadaptive']);
218 writeline(app.controller.HydraTT, [num2str(0) ' 4 ' num2str(...
    app.controller.HydraTT_LS270) ' setadaptive']);
219 writeline(app.controller.HydraTT, [num2str(0.1) ' 5 ' num2str(...
    app.controller.HydraTT_LS270) ' setadaptive']);
220 writeline(app.controller.HydraTT, [num2str(0) ' 6 ' num2str(...
    app.controller.HydraTT_LS270) ' setadaptive']);
221 writeline(app.controller.HydraTT, [num2str(0) ' 7 ' num2str(...
    app.controller.HydraTT_LS270) ' setadaptive']);
222 writeline(app.controller.HydraTT, [num2str(0.0001) ' 8 ' num2str(...
    app.controller.HydraTT_LS270) ' setadaptive']);
223 writeline(app.controller.HydraTT, [num2str(0) ' 9 ' num2str(...
    app.controller.HydraTT_LS270) ' setadaptive']);
224
225 % Configures the Auto commutation
226 writeline(app.controller.HydraTT, [num2str(0) ' 1 ' num2str(...
    app.controller.HydraTT_LS270) ' setamc']);
227 writeline(app.controller.HydraTT, [num2str(0) ' 2 ' num2str(...
    app.controller.HydraTT_LS270) ' setamc']);
228 writeline(app.controller.HydraTT, [num2str(1) ' 3 ' num2str(...
    app.controller.HydraTT_LS270) ' setamc']);
229
230 % Sets the specified Motor parameters entry
231 writeline(app.controller.HydraTT, [num2str(0) ' 1 ' num2str(...
```

```

    app.controller.HydraTT_LS270) ' setmotorpara']);
232 writeline(app.controller.HydraTT,[num2str(1) ' 2 ' num2str(...
    app.controller.HydraTT_LS270) ' setmotorpara']);
233 writeline(app.controller.HydraTT,[num2str(0.9) ' 3 ' num2str(...
    app.controller.HydraTT_LS270) ' setmotorpara']);
234 writeline(app.controller.HydraTT,[num2str(0.0025) ' 4 ' num2str(...
    app.controller.HydraTT_LS270) ' setmotorpara']);
235 writeline(app.controller.HydraTT,[num2str(10) ' 5 ' num2str(...
    app.controller.HydraTT_LS270) ' setmotorpara']);
236 writeline(app.controller.HydraTT,[num2str(1) ' 6 ' num2str(...
    app.controller.HydraTT_LS270) ' setmotorpara']);
237
238 % Lagrer parameterene for opsettet som er i bruk
239 writeline(app.controller.HydraTT,'csave');
240 writeline(app.controller.HydraTT,'1 nsave');
241 end

```

B.3 Homing function

```

1 %
2 function HomeMotor(app,a)
3     %%%%%%%%%%%%%%%%%%%%%%%%%%%%%%%%%%%%%%%%%%%%%%%%%%%%%%%%%%%%%%%%%%%%%%%%%
4     % Script HomeMotor is made so that each stage can find its
5     % absolute zero position.
6     %
7     % a:    which stage is to be homed
8     %      a = (1, 'x' or 'X') for X-axis           (M-531.DG)
9     %      a = (2, 'y' or 'Y') for Y-axis           (M-535.22)
10    %      a = (3, 'z' or 'Z') for Z-axis            (LS-270)
11    %      a = (4, 'r' or 'R') for Rotation-axis     (M-037.PD)
12    %
13    % Espen Fosse, 2021/2022
14    %%%%%%%%%%%%%%%%%%%%%%%%%%%%%%%%%%%%%%%%%%%%%%%%%%%%%%%%%%%%%%%%%%%%%%%%%
15
16    if a == 1 || strcmp(a,'x') || strcmp(a,'X')
17        ax = app.controller.C843_M531DG;
18        a = 1;
19    elseif a == 2 || strcmp(a,'y') || strcmp(a,'Y')
20        ax = app.controller.C843_M53522;
21        a = 2;
22    elseif a == 3 || strcmp(a,'z') || strcmp(a,'Z')
23        ax = app.controller.HydraTT_LS270;

```

```
24     a = 3;
25     elseif a == 4 || strcmp(a, 'r') || strcmp(a, 'R')
26         ax = app.controller.C843_M037PD;
27         a = 4;
28     else
29         noaxwtn = 'No axis with that name';
30         WriteTextInWindow(app, noaxwtn)
31         return
32     end
33
34     if ax == app.controller.HydraTT_LS270
35         cmd = [num2str(ax) ' nrm'];
36         writeline(app.controller.HydraTT, cmd);
37         WriteTextInWindow(app, [app.name{a} ' is traveling Home'])
38         MovingMotor(app, a)
39         writeline(app.controller.HydraTT, ['1016 ' num2str(ax) ' setnpos'...
40             ])
41         if app.stop == 1
42             WriteTextInWindow(app, [app.name{a} ' stopped Home'])
43         else
44             WriteTextInWindow(app, [app.name{a} ' is now Home'])
45         end
46         PositionMotor(app, a);
47     elseif ax == app.controller.C843_M037PD
48         app.controller.C843.MOV(ax, 0)
49         WriteTextInWindow(app, [app.name{a} ' is traveling Home'])
50         MovingMotor(app, a)
51         if app.stop == 1
52             WriteTextInWindow(app, [app.name{a} ' stopped Home'])
53         else
54             WriteTextInWindow(app, [app.name{a} ' is now Home'])
55         end
56         PositionMotor(app, a);
57     else
58         app.controller.C843.FNL(ax)
59         WriteTextInWindow(app, [app.name{a} ' is traveling Home'])
60         MovingMotor(app, a)
61         if app.stop == 1
62             WriteTextInWindow(app, [app.name{a} ' stopped Home'])
63         else
64             WriteTextInWindow(app, [app.name{a} ' is now Home'])
65         end
66         PositionMotor(app, a);
67     end
end
```

68 %

B.4 Step function

```

1 function StepMotor(app,s,a,m)
2     %%%%%%%%%%%%%%%%%%%%%%%%%%%%%%%%%%%%%%%%%%%%%%%%%%%%%%%%%%%%%%%%%%%%%%%%%
3     % Skript StepMotor that is used to move X, Y, Z og
4     % Rotation-axis in the air setup.
5     %
6     % s:   amount of steps in [mm] or [degrees]; s = 1 is the same
7     %     as 1[degree] or 1[mm].
8     % a:   axis that is going to move is determed by
9     %     a = (1, 'x' or 'X') for X-axis           (M-531.DG)
10    %     a = (2, 'y' or 'Y') for Y-axis           (M-535.22)
11    %     a = (3, 'z' or 'Z') for Z-axis           (LS-270)
12    %     a = (4, 'r' or 'R') for Rotation-axis     (M-037.PD)
13    % m:   movments is relative m = 0; movments is absolute m = 1
14    %
15    % Espen Fosse, 2021/2022
16    %%%%%%%%%%%%%%%%%%%%%%%%%%%%%%%%%%%%%%%%%%%%%%%%%%%%%%%%%%%%%%%%%%%%%%%%%
17    if a == 1 || strcmp(a,'x') || strcmp(a,'X')
18        ax = app.controller.C843_M531DG;
19        a = 1;
20    elseif a == 2 || strcmp(a,'y') || strcmp(a,'Y')
21        ax = app.controller.C843_M53522;
22        a = 2;
23    elseif a == 3 || strcmp(a,'z') || strcmp(a,'Z')
24        ax = app.controller.HydraTT_LS270;
25        a = 3;
26    elseif a == 4 || strcmp(a,'r') || strcmp(a,'R')
27        ax = app.controller.C843_M037PD;
28        a = 4;
29    else
30        noaxwtn = 'No axis with that name';
31        WriteTextInWindow(app,noaxwtn)
32        return
33    end
34
35    if a == 3
36        if (m==0)
37            cmd = [num2str(s) ' ' num2str(ax) ' nr'];
38            writeline(app.controller.HydraTT,cmd);

```

```

39     txt = [app.name{a} ' is moving ' num2str(s) '[mm]'];
40     WriteTextInWindow(app,txt)
41     MovingMotor(app,a)
42     PositionMotor(app,a);
43     elseif (m==1)
44         cmd = [num2str(s) ' ' num2str(ax) ' nm'];
45         writeline(app.controller.HydraTT,cmd);
46         if strcmpi(app.MACHINECOORDS_Button.Text,'MACHINE COORDS')
47             txt = [app.name{a} ' is moving to ' num2str(s) '[mm]: M ...
                    COORD'S'];
48         else
49             s2 = s-app.zeropos.(app.field{a});
50             txt = [app.name{a} ' is moving to ' num2str(s2) '[mm]: U...
                    COORD'S'];
51         end
52         WriteTextInWindow(app,txt)
53         MovingMotor(app,a)
54         PositionMotor(app,a);
55     else
56         WriteTextInWindow(app,'Wrong value for movement type: ...
                    relative movements m=0; absolute movements m=1')
57         return
58     end
59 else
60     if a == 2
61         s = s*app.factor;
62     end
63     if (m==0)
64         app.controller.C843.MVR(ax,s)
65         if a == 2
66             s = s/app.factor;
67         end
68         if a == 4
69             WriteTextInWindow(app,[app.name{a} ' is moving ' num2str...
                    (s) '[degree]'])
70         else
71             WriteTextInWindow(app,[app.name{a} ' is moving ' num2str...
                    (s) '[mm]'])
72         end
73         MovingMotor(app,a)
74         PositionMotor(app,a);
75     elseif (m==1)
76         app.controller.C843.MOV(ax,s)
77         if a == 2
78             s = s/app.factor;

```

```

79     end
80     if a == 4
81         if strcmpi(app.MACHINECOORDS_Button.Text, 'MACHINE COORDS...
            ')
82             txt = [app.name{a} ' is moving to ' num2str(s) '[...
                degree]: M COORD'S'];
83         else
84             s2 = s-app.zeropos.(app.field{a});
85             txt = [app.name{a} ' is moving to ' num2str(s2) '[...
                degree]: U COORD'S'];
86         end
87         WriteTextInWindow(app,txt)
88     else
89         if strcmpi(app.MACHINECOORDS_Button.Text, 'MACHINE COORDS...
            ')
90             txt = [app.name{a} ' is moving to ' num2str(s) '[mm...
                ]: M COORD'S'];
91         else
92             s2 = s-app.zeropos.(app.field{a});
93             txt = [app.name{a} ' is moving to ' num2str(s2) '[mm...
                ]: U COORD'S'];
94         end
95         WriteTextInWindow(app,txt)
96     end
97     MovingMotor(app,a)
98     PositionMotor(app,a);
99     else
100        WriteTextInWindow(app, 'Wrong value for movement type: ...
            relative movements m=0; absolute movements m=1')
101        return
102    end
103 end
104 end
105 %

```

B.5 Position function

```

1 function PositionMotor(app,a)
2     %%%%%%%%%%%%%%%%%%%%%%%%%%%%%%%%%%%%%%%%%%%%%%%%%%%%%%%%%%%%%%%%%%%%%%%%%
3     % Script PositionMotor tells the absolute position of axis
4     %
5     % a:    which axis to read position

```

```

6      %      a = (1, 'x' or 'X') for X-axis          (M-531.DG)
7      %      a = (2, 'y' or 'Y') for Y-axis        (M-535.22)
8      %      a = (3, 'z' or 'Z') for Z-axis        (LS-270)
9      %      a = (4, 'r' or 'R') for Rotation-axis  (M-037.PD)
10     %
11     % Espen Fosse, 2021/2022
12     %%%%%%%%%%%%%%%%%%%%%%%%%%%%%%%%%%%%%%%%%%%%%%%%%%%%%%%%%%%%%%%%%%%%%%%%%
13
14     if a == 1 || strcmp(a, 'x') || strcmp(a, 'X')
15         ax = app.controller.C843_M531DG;
16         a = 1;
17     elseif a == 2 || strcmp(a, 'y') || strcmp(a, 'Y')
18         ax = app.controller.C843_M53522;
19         a = 2;
20     elseif a == 3 || strcmp(a, 'z') || strcmp(a, 'Z')
21         ax = app.controller.HydraTT_LS270;
22         a = 3;
23     elseif a == 4 || strcmp(a, 'r') || strcmp(a, 'R')
24         ax = app.controller.C843_M037PD;
25         a = 4;
26     else
27         noax = 'No axis with that name';
28         WriteTextInWindow(app, noax)
29         return
30     end
31
32     if a == 3
33         pos = writeread(app.controller.HydraTT, [num2str(ax) ' np']);
34         pos = str2double(strip(pos));
35         if strcmpi(app.MACHINECOORDS_Button.Text, 'MACHINE COORDS')
36             txt = [app.name{a} ' is at ' num2str(pos) '[mm]: M COORD''S'...
37                   ];
38         elseif app.zeroed(a) == 0
39             txt = [app.name{a} ' is at ' num2str(pos) '[mm]: U COORD''S'...
40                   ];
41         else
42             pos2 = pos-app.zeroedpos.(app.field{a});
43             txt = [app.name{a} ' is at ' num2str(pos2) '[mm]: U COORD''S'...
44                   ];
45         end
46         WriteTextInWindow(app, txt)
47         app.abspos.(app.field{a}) = pos;
48     elseif a == 4
49         pos = app.controller.C843.qPOS(ax);
50         if strcmpi(app.MACHINECOORDS_Button.Text, 'MACHINE COORDS')

```

```

48         txt = [app.name{a} ' is at ' num2str(pos) '[degree]: M COORD...
              'S'];
49     elseif app.zeroed(a) == 0
50         txt = [app.name{a} ' is at ' num2str(pos) '[degree]: U COORD...
              'S'];
51     else
52         pos2 = pos-app.zeropos.(app.field{a});
53         txt = [app.name{a} ' is at ' num2str(pos2) '[degree]: U ...
              COORD'S'];
54     end
55     WriteTextInWindow(app,txt)
56     app.abspos.(app.field{a}) = pos;
57 else
58     pos = app.controller.C843.qPOS(ax);
59     if a == 2
60         pos = pos/app.factor;
61     end
62     if strcmpi(app.MACHINECOORDS_Button.Text,'MACHINE COORDS')
63         txt = [app.name{a} ' is at ' num2str(pos) '[mm]: M COORD'S'...
              ];
64     elseif app.zeroed(a) == 0
65         txt = [app.name{a} ' is at ' num2str(pos) '[mm]: U COORD'S'...
              ];
66     else
67         pos2 = pos-app.zeropos.(app.field{a});
68         txt = [app.name{a} ' is at ' num2str(pos2) '[mm]: U COORD'S'...
              '];
69     end
70     WriteTextInWindow(app,txt)
71     app.abspos.(app.field{a}) = pos;
72 end
73 end
74 %

```

B.6 Moving function

```

1 function MovingMotor(app,a)
2     %%%%%%%%%%%%%%%%%%%%%%%%%%%%%%%%%%%%%%%%%%%%%%%%%%%%%%%%%%%%%%%%%%%%%%%%%
3     % Script makes MatLab/app wait until axis that moves is reach its
4     % destination.
5     %
6     % a:    which axis that is moving

```



```

7      %      a = (1, 'x' or 'X') for X-axis          (M-531.DG)
8      %      a = (2, 'y' or 'Y') for Y-axis          (M-535.22)
9      %      a = (3, 'z' or 'Z') for Z-axis          (LS-270)
10     %      a = (4, 'r' or 'R') for Rotation-axis    (M-037.PD)
11     %
12     % Espen Fosse, 2021/2022
13     %%%%%%%%%%%%%%%%%%%%%%%%%%%%%%%%%%%%%%%%%%%%%%%%%%%%%%%%%%%%%%%%%%%%%%%%%
14
15     if a == 1 || strcmp(a, 'x') || strcmp(a, 'X')
16         ax = app.controller.C843_M531DG;
17     elseif a == 2 || strcmp(a, 'y') || strcmp(a, 'Y')
18         ax = app.controller.C843_M53522;
19     elseif a == 3 || strcmp(a, 'z') || strcmp(a, 'Z')
20         ax = app.controller.HydraTT_LS270;
21     elseif a == 4 || strcmp(a, 'r') || strcmp(a, 'R')
22         ax = app.controller.C843_M037PD;
23     else
24         noax = 'No axis with that name';
25         WriteTextInWindow(app, noax)
26         return
27     end
28
29     if a == 3
30         while true
31             pause(0.1)
32             writeline(app.controller.HydraTT, [num2str(ax) ' nst']);
33             beveger_seg = readline(app.controller.HydraTT);
34             number = str2double(beveger_seg);
35             if app.stop == 1
36                 return
37             elseif (number ==32 || number ==36)
38                 return
39             else
40                 continue
41             end
42         end
43
44     else
45         while(app.controller.C843.IsMoving(ax))
46             pause(0.1);
47             if app.stop == 1
48                 return
49             end
50         end
51     % pause set because IsMoving(ax) kan make matlab freeze

```

```

52     pause(0.25);
53     end
54
55 end
56 %

```

B.7 Instrument connect

```

1  % following function handels the instruments and measurements
2  function InstrumentConnect(app)
3      %%%%%%%%%%%%%%%%%%%%%%%%%%%%%%%%%%%%%%%%%%%%%%%%%%%%%%%%%%%%%%%%%%%%%%%%%
4      % Script InstrumentConnect creates a handle to the instruments
5      % that is a part of the air setup
6      %
7      % Espen Storheim, 2011
8      % Based on work by Vidar Knappskog and Magne Aanes.
9      % Modified by Espen Fosse to be used in app, 2021/2022.
10     %%%%%%%%%%%%%%%%%%%%%%%%%%%%%%%%%%%%%%%%%%%%%%%%%%%%%%%%%%%%%%%%%%%%%%%%%
11
12     % clear handle of instruments
13     app.instrument = {};
14     ActionButtons(app)
15     set(app.STOP_Button, 'Enable', 'Off')
16     set(app.INSTRUMENTCONNECT_Button, 'Enable', 'On')
17
18     %% Signal Generator Agilent 33220A. S/N:
19
20     % Find a GPIB object.
21     app.instrument.generator = instrfind('Type', 'gpib', 'BoardIndex', ...
22         0, 'PrimaryAddress', 10, 'Tag', '');
23
24     % Create the GPIB object if it does not exist
25     % otherwise use the object that was found.
26     if isempty(app.instrument.generator)
27         app.instrument.generator = gpib('NI', 0, 10);
28     else
29         fclose(app.instrument.generator);
30         app.instrument.generator = app.instrument.generator(1);
31     end
32
33     fopen(app.instrument.generator);
34     app.instrument.generator_name = 'Agilent 33220A. S/N: ';

```

```

34 app.instrument.generator_idn = query(app.instrument.generator, '*IDN?...'
    ');
35
36 % Test the connection. Should be a command where the response can be
37 % verified.
38 if isempty(app.instrument.generator_idn)
39     WriteTextInWindow(app, 'Warning: The signal generator is not ...
        connected or configured properly.')
40     app.connectfail = 1;
41     return
42 else
43     WriteTextInWindow(app, '1: The signal generator is connected and ...
        appears to be working.')
44 end
45
46 %% Digital Oscilloscope Tektronix DPO3012. S/N:
47
48 app.instrument.scope = visadev("USB0::0x0699::0x0410::C024017::0:...
    INSTR");
49 %     app.instrument.scope = visadev("USB0::0x0699::0x0410::...
    C024018::0::INSTR");
50 %     app.instrument.scope = visadev("USB0::0x0699::0x0410::...
    C011044::0::INSTR");
51 %     app.instrument.scope = visadev('USB0::0x0699::0x0410::...
    C010246::0::INSTR'); %problems, it freezes matlab
52 app.instrument.scope_name = 'Tektronix DPO3012. S/N: ';
53 app.instrument.scope_idn = writeread(app.instrument.scope, '*IDN?');
54
55 % Test the connection. Should be a command where the response can be
56 % verified.
57 if isempty(app.instrument.scope_idn)
58     WriteTextInWindow(app, 'Warning: The oscilloscope is not ...
        connected or configured properly.')
59     app.connectfail = 1;
60     return
61 else
62     WriteTextInWindow(app, '2: The oscilloscope is connected and ...
        appears to be working.')
63 end
64
65 %% Pressure sensor: Paroscientific DigiQuartz 740. S/N:
66
67 app.instrument.pressure = visadev('COM13');
68 app.instrument.pressure_name = 'Paroscientific DigiQuartz 740. S/N:'...
    ;

```

```
69     app.instrument.pressure_idn = writeread(app.instrument.pressure, '...
    *0100P3');
70
71     % Test the connection. Should be a command where the response can be
72     % verified.
73     if isempty(app.instrument.pressure_idn)
74         WriteTextInWindow(app, 'Warning: The paroscientific is not ...
            connected or configured properly.')
75         app.connectfail = 1;
76         return
77     else
78         WriteTextInWindow(app, '3: The paroscientific is connected and ...
            appears to be working.')
79     end
80
81     %% Relative humidity and temperature sensor: Vaisala HMT313. S/N:
82
83     app.instrument.humidity = visadev('COM7');
84     configureTerminator(app.instrument.humidity, "CR")
85     app.instrument.humidity_name = 'Vaisala HMT313. S/N: ';
86     app.instrument.humidity_idn = writeread(app.instrument.humidity, '...
        send');
87
88     % Test the connection. Should be a command where the response can be
89     % verified.
90     if isempty(app.instrument.humidity_idn)
91         WriteTextInWindow(app, 'Warning: The vasisala is not connected or...
            configured properly.')
92         app.connectfail = 1;
93         return
94     else
95         WriteTextInWindow(app, '4: The vasisala is connected and appears ...
            to be working.')
96     end
97
98     %% Bandpass filter: Krohn-Hite 3940A. S/N: AM2626.
99
100    % Find a GPIB object.
101    app.instrument.filter = instrfind('Type', 'gpib', 'BoardIndex', 0, '...
        PrimaryAddress', 25, 'Tag', '');
102
103    % Create the GPIB object if it does not exist
104    % otherwise use the object that was found.
105    if isempty(app.instrument.filter)
106        app.instrument.filter = gpib('NI', 0, 25);
```

```

107     else
108         fclose(app.instrument.filter);
109         app.instrument.filter = app.instrument.filter(1);
110     end
111     fopen(app.instrument.filter);
112     app.instrument.filter_name = 'Krohn-Hite 3940A. S/N: AM2626';
113     app.instrument.filter_idn = query(app.instrument.filter, '*IDN?');
114
115     % Test the connection. Should be a command where the response can be
116     % verified.
117     if isempty(app.instrument.filter_idn)
118         WriteTextInWindow(app, 'Warning: The filter is not connected or ...
119             configured properly.')
120         app.connectfail = 1;
121         return
122     else
123         WriteTextInWindow(app, '5: The filter is connected and appears to...
124             be working.')
125     end
126
127     %% Temperature sensor: ASL F250. S/N:
128     % Find a GPIB object.
129     app.instrument.temperature = instrfind('Type', 'gpib', 'BoardIndex', ...
130         0, 'PrimaryAddress', 3, 'Tag', '');
131
132     % Create the GPIB object if it does not exist
133     % otherwise use the object that was found.
134     if isempty(app.instrument.temperature)
135         app.instrument.temperature = gpib('NI', 0, 3);
136     else
137         fclose(app.instrument.temperature);
138         app.instrument.temperature = app.instrument.temperature(1);
139     end
140
141     fopen(app.instrument.temperature);
142     set(app.instrument.temperature, 'EOSmode', 'read&write');
143     set(app.instrument.temperature, 'EOSCharCode', 10); % Set terminator ...
144     to LF.
145     app.instrument.temperature_name = 'ASL F250 mk II. S/N: ';
146     fprintf(app.instrument.temperature, 'A0');
147     app.instrument.temperature_idn = fscanff(app.instrument.temperature);
148
149     % Test the connection. Should be a command where the response can be
150     % verified.
151     if isempty(app.instrument.temperature_idn)

```

```
148     WriteTextInWindow(app, 'Warning: The thermometer is not connected...
        or configured properly.')
149     app.connectfail = 1;
150     return
151 else
152     WriteTextInWindow(app, '6: The thermometer is connected and ...
        appears to be working.')
153 end
154 end
155 %
```

B.8 Initialize instruments

```
1 function InitInstruments(app)
2     % Initialize the bandpass filter.
3     % There seems to be an overflow when the commands are combined, so ...
        they
4     % have been separated and a pause of 100 ms is set between each
5     % command.
6     %
7     % Set the input and output gain on both channels to 0 dB.
8     txt = 'Initialize Bandpass Filter';
9     WriteTextInWindow(app,txt)
10    fprintf(app.instrument.filter, 'AL;0IG;0OG;B');
11    pause(0.1)
12    % Set channel 1 to high pass mode.
13    fprintf(app.instrument.filter, 'CH1.1;M2');
14    pause(0.1)
15    % Set the cutoff frequency for channel 1.
16    fprintf(app.instrument.filter, ['F' num2str(app.result.cutoff_f1) 'K'...
        ]);
17    pause(0.1)
18    % Set channel 2 to low pass mode.
19    fprintf(app.instrument.filter, 'CH1.2;M1');
20    pause(0.1)
21    % Set the cutoff frequency for channel 2.
22    fprintf(app.instrument.filter, ['F' num2str(app.result.cutoff_f2) 'K'...
        ]);
23
24    % Initialize the oscilloscope.
25    txt = 'Initialize Oscilloscope';
26    WriteTextInWindow(app,txt)
```

```

27 % Code for the Tektronix DPO3012.
28 % Set the acquisition mode to averaging.
29 writeline(app.instrument.scope, 'ACQ:MOD AVE');
30 % Set the number of cycles to average.
31 writeline(app.instrument.scope, ['ACQ:NUMAV ' num2str(...
    app.meas.average)]);
32 % Number of points which shall be read from the scope.
33 writeline(app.instrument.scope, ['HOR:RECO ' num2str(...
    app.meas.sample_count)]);
34 % Start point for the recorded signal
35 writeline(app.instrument.scope, 'DAT:START 1');
36 % Stop point for the recorded signal
37 writeline(app.instrument.scope, ['DAT:STOP ' num2str(...
    app.meas.sample_count)]);
38 % Trigger specifications. Set to edge detection from external ...
    source.
39 writeline(app.instrument.scope, 'TRIG:A:EDGE:SOU EXT');
40 % Set the trigger type to positive edge.
41 writeline(app.instrument.scope, 'TRIG:A:TYP EDG');
42 % 2012.11.19 EM: Added additional initialization.
43 % CH1
44 % Set Offset to zero.
45 writeline(app.instrument.scope, 'CH1:OFFS 0');
46 % Set position to zero.
47 writeline(app.instrument.scope, 'CH1:POS 0');
48 % Set coupling to AC.
49 writeline(app.instrument.scope, 'CH1:COUP AC');
50 % CH2
51 % Set Offset to zero.
52 writeline(app.instrument.scope, 'CH2:OFFS 0');
53 % Set position to zero.
54 writeline(app.instrument.scope, 'CH2:POS 0');
55 % Set coupling to AC.
56 writeline(app.instrument.scope, 'CH2:COUP AC');
57 % Number of bytes per word (8-bit if 1, 16-bit if 2, ...)
58 writeline(app.instrument.scope, ['DATA:ENCDG SRIBINARY;WIDTH ' ...
    num2str(app.noB)]);
59
60
61 % Initialize Signal Generator
62 txt = 'Initialize Signal Generator';
63 WriteTextInWindow(app,txt)
64 fprintf(app.instrument.generator, 'BM:STATe on'); % burst mode
65 fprintf(app.instrument.generator, ['BM:INT:RATE ' num2str(...
    app.meas.burst_rate)]);

```

```

66     fprintf(app.instrument.generator,['BM:NCYC ', num2str(...
        app.result.sig_cycles)]);
67     fprintf(app.instrument.generator,['FREQ ', num2str(...
        app.result.frequency)]);
68     fprintf(app.instrument.generator,['VOLT ' num2str(...
        app.meas.voltage_inn)]);
69 end
70 %

```

B.9 Measure function

```

1 function Measure(app)
2     % Voltage scalings in oscilloscope, unit: V/div
3     voltageScalings = [1e-3, 2e-3, 5e-3, 10e-3, 20e-3, 50e-3, 100e-3, ...
        200e-3, 500e-3 1 2 5 10];
4     % The are 8 visible divisons on the screen and two above/below ...
        outside,
5     % i.e., 10 in total. Maximum amplitude thus corresponds to
6     % 5*verticalScalings, but is set to 4.5 to be on the save side
7     NumVerDivs_max = 4.5;
8     NumVerDivs_min = 1.7;
9
10    % Time scalings in oscilloscope, unit: mus/div
11    timeScalings = [40 100 200 400 1000]*1e-6;
12    maxNumHorDivs = 10;
13
14    % Set scope acquisition mode to SEQUENCE instead of RUNSTOP, so that...
        a
15    % measurement is aquired when prompted, instead of continuously. See...
        page
16    % 2-97 in programming manual for details.
17    writeline(app.instrument.scope,'ACQ:STOPA SEQ');
18
19    txt = ['Measure frequency ' num2str(app.result.frequency/1000) 'kHz'...
        ];
20    WriteTextInWindow(app,txt)
21
22
23    if app.gen_setting == 1
24        txt = 'Adjusting signal generator settings';
25        WriteTextInWindow(app,txt)
26        % Common settings for electrical and acoustical signal

```



```

27     % Update signal generator settings
28     fprintf(app.instrument.generator,['BM:NCYC ', num2str(...
        app.result.sig_cycles)]);
29     fprintf(app.instrument.generator,['FREQ ', num2str(...
        app.result.frequency)]);
30     % Give little time to signal generator to set the setting
31     pause(0.1)
32 end
33
34 % Find appropriate horizontal scaling & update time/Div
35 tScaling = timeScalings(find(timeScalings*maxNumHorDivs >= ...
        app.result.sig_duration*1.5,1));
36 writeline(app.instrument.scope,['HOR:SCA ', num2str(tScaling)]);
37
38 if app.meas_el_sig == 1
39
40     txt = 'Starting measurements of the electrical pulses';
41     WriteTextInWindow(app,txt)
42
43     %% Electrical signal (transmitter excitation)
44
45     % Set the delay of acquisition data so that the resulting ...
        waveform is
46     % centered tScaling*5 after the trigger occurs. (See 2-234 in ...
        manual)
47     writeline(app.instrument.scope,['HOR:DEL:TIM ', num2str(tScaling...
        *5)]);
48
49     % Find appropriate vertical scaling for transmitter excitation ...
        signal
50     vScaling = voltageScalings(find(NumVerDivs_max*voltageScalings ...
        >= app.meas.voltage_inn,1));
51     % Set voltage/div
52     writeline(app.instrument.scope,['CH', num2str(...
        app.meas.channel_electrical), ':SCA ' num2str(vScaling)]);
53
54     % Set the number of cycles to average.
55     writeline(app.instrument.scope,['ACQ:NUMAV ' num2str(...
        app.meas.average)]);
56     % Number of points which shall be read from the scope.
57     writeline(app.instrument.scope,['HOR:RECO ' num2str(...
        app.meas.sample_count)]);
58
59     % Start aquisition.
60     writeline(app.instrument.scope,'ACQ:STATE RUN');

```

```

61     txt = 'Starting aquisition';
62     WriteTextInWindow(app,txt)
63     pause(app.meas.average_time)
64     DPO_read(app,app.meas.channel_electrical);
65     app.result.electric_t = app.x;
66     app.result.electric = app.wf;
67     app.result.electric_timescale = app.timeDiv;
68     app.result.electric_maxV = app.maxV;
69     app.result.electric_Vscale = str2double(writeread(...
        app.instrument.scope,['CH',num2str(...
        app.meas.channel_electrical),':SCA?']));
70     app.result.electric_Termination = str2double(writeread(...
        app.instrument.scope,['CH',num2str(...
        app.meas.channel_electrical),':TER?']));
71     txt = 'Finished reading the electrical pulses';
72     WriteTextInWindow(app,txt)
73 end
74 %% Acoustical signal (receiving transducer)
75
76 txt = 'Starting measurements of the acoustical pulses';
77 WriteTextInWindow(app,txt)
78
79 if app.filt_setting == 1
80     txt = 'Adjusting filter settings';
81     WriteTextInWindow(app,txt)
82     % Adjust the bandwidth of the KH-filter
83     % Set the cutoff frequency for filter channel 1. (Not working ...
        properly)
84     fprintf(app.instrument.filter,['CH1.1;F' num2str(...
        app.result.cutoff_f1) 'K']);
85     pause(0.2)
86     % Set the cutoff frequency for channel 2.
87     fprintf(app.instrument.filter,['CH1.2;F' num2str(...
        app.result.cutoff_f2) 'K']);
88     % Give little time to filter to set the setting
89     pause(0.1)
90 end
91
92 % Set the delay of acquisition data so that the resulting waveform ...
    is
93 % centered [tScaling*5 + (under)estimated plane wave travel time] ...
    after
94 % the trigger occurs. (See 2-234 in manual)
95 writeline(app.instrument.scope,['HOR:DEL:TIM ',num2str(tScaling*5-0...
    .5*tScaling+app.result.est_travel_time)]);

```

```

96
97  if app.meas.average_scaling == 1
98      % Set aquisition mode to single sample instead of averaging
99      % This speeds things up, and ensures that the noise-prior-to-...
      averaging
100     % is not clipped, which could distort the averaged signals. See ...
      meas.
101     % setup chapter in Hauge (2013) or Mosland (2013) for details
102     writeline(app.instrument.scope, 'ACQ:MOD SAM');
103  else
104     % Set the number of cycles to average.
105     writeline(app.instrument.scope, ['ACQ:NUMAV ' num2str(...
      app.meas.average_scaling)]);
106  end
107  % Number of points which shall be read from the scope.
108  writeline(app.instrument.scope, ['HOR:RECO ' num2str(...
      app.meas.sample_count)]);
109
110  % Find appropriate vertical scaling for receiver signal
111  writeline(app.instrument.scope, 'ACQ:STATE RUN');
112  pause(app.meas.average_time_scaling)
113  DPO_read(app, app.meas.channel_acoustical);
114  Scaling = str2double(writeread(app.instrument.scope, ['CH', num2str(...
      app.meas.channel_acoustical), ':SCA?']));
115
116  ind = find(Scaling==voltageScalings);
117  if isempty(ind)
118      txt = 'ind is empty!';
119      WriteTextInWindow(app, txt)
120      ind = 1;
121      writeline(app.instrument.scope, ['CH', num2str(...
      app.meas.channel_acoustical), ':SCA ', num2str(voltageScalings(...
      ind))]);
122      % Start aquisition.
123      writeline(app.instrument.scope, 'ACQ:STATE RUN');
124      txt = 'Checking scaling';
125      WriteTextInWindow(app, txt)
126      pause(app.meas.average_time_scaling)
127      DPO_read(app, app.meas.channel_acoustical);
128  end
129
130  scaling_down = 0;
131  finished = 0;
132  while ~finished
133      % Debugging, app.Vmax or ind is empty inside the while loop

```

```

134     if isempty(app.maxV)
135         % Start aquisition.
136         txt = 'Max voltage not found. Trying to find max voltage...'...
            ;
137         WriteTextInWindow(app,txt)
138         writeline(app.instrument.scope,'ACQ:STATE RUN');
139         pause(app.meas.average_time_scaling)
140         DPO_read(app,app.meas.channel_acoustical);
141         if ~isempty(app.maxV)
142             txt = 'Max voltage found';
143             WriteTextInWindow(app,txt)
144         end
145         continue
146     elseif isempty(ind)
147         txt = 'ind is empty!';
148         WriteTextInWindow(app,txt)
149         ind = 1;
150         writeline(app.instrument.scope,['CH',num2str(...
            app.meas.channel_acoustical),':SCA ',num2str(...
            voltageScalings(ind))]);
151         % Start aquisition.
152         writeline(app.instrument.scope,'ACQ:STATE RUN');
153         pause(app.meas.average_time_scaling)
154         DPO_read(app,app.meas.channel_acoustical);
155
156     end
157     % Continue on finding the correct amplitude scaling
158     if app.maxV >= voltageScalings(ind)*NumVerDivs_max
159         txt = 'Increasing scaling';
160         WriteTextInWindow(app,txt)
161         Scaling = voltageScalings(ind+1);
162         writeline(app.instrument.scope,['CH',num2str(...
            app.meas.channel_acoustical),':SCA ',num2str(Scaling)]);
163         ind = ind +1;
164         % Start aquisition.
165         writeline(app.instrument.scope,'ACQ:STATE RUN');
166         pause(app.meas.average_time_scaling)
167         DPO_read(app,app.meas.channel_acoustical);
168
169     elseif ind ~= 1 && app.maxV <= voltageScalings(ind)*...
        NumVerDivs_min
170         txt = 'Decreasing scaling';
171         WriteTextInWindow(app,txt)
172         Scaling = voltageScalings(ind-1);
173         writeline(app.instrument.scope,['CH',num2str(...

```

```

        app.meas.channel_acoustical), ':SCA ', num2str(Scaling)]];
174     ind = ind -1;
175     % Start aquisition.
176     writeline(app.instrument.scope, 'ACQ:STATE RUN');
177     pause(app.meas.average_time_scaling)
178     DPO_read(app, app.meas.channel_acoustical);
179     scaling_down = scaling_down + 1;
180     % Prevent while loop to scale up and down over, and
181     % over again.
182     if scaling_down == 20
183         if isempty(app.Vmax)
184             txt = 'Max Voltage is empty';
185             WriteTextInWindow(app,txt)
186             scaling_down = scaling_down-1;
187             continue
188         end
189         txt = 'Scaling caught in a loop. The lowest scaling ...
                value is selected';
190         WriteTextInWindow(app,txt)
191         break
192     end
193     else
194         txt = 'Correct scaling';
195         WriteTextInWindow(app,txt)
196         finished = 1;
197     end
198 end
199
200 if app.meas.average_scaling == 1
201     % Reset aquisition mode to averaging
202     writeline(app.instrument.scope, 'ACQ:MOD AVE');
203 end
204
205 % Set the number of cycles to average.
206 writeline(app.instrument.scope, ['ACQ:NUMAV ' num2str(...
        app.meas.average)]);
207 % Number of points which shall be read from the scope.
208 writeline(app.instrument.scope, ['HOR:RECO ' num2str(...
        app.meas.sample_count)]);
209
210 % Start aquisition.
211 writeline(app.instrument.scope, 'ACQ:STATE RUN');
212 txt = 'Starting aquisition';
213 WriteTextInWindow(app,txt)
214 pause(app.meas.average_time)

```

```

215     DPO_read(app, app.meas.channel_acoustical);
216
217     app.result.acoustic_t = app.x;
218     app.result.acoustic = app.wf;
219     app.result.acoustic_timescale = app.timeDiv;
220     app.result.acoustic_maxV = app.maxV;
221     app.result.acoustic_Vscale = str2double(writeread(...
        app.instrument.scope, ['CH', num2str(app.meas.channel_acoustical), '...
            :SCA?']));
222     app.result.acoustic_Termination = str2double(writeread(...
        app.instrument.scope, ['CH', num2str(app.meas.channel_acoustical), '...
            :TER?']));
223     txt = 'Finished reading the acoustical pulses';
224     WriteTextInWindow(app, txt)
225 end
226 %

```

B.10 DPO read function

```

1 function DPO_read(app, ch)
2     % Set data source
3     writeline(app.instrument.scope, ['DAT:SOUR CH' num2str(ch)]);
4
5     % Set what samples to retrieve
6     writeline(app.instrument.scope, 'DAT:START 1');
7     writeline(app.instrument.scope, ['DAT:STOP ' num2str(...
        app.meas.sample_count)]);
8
9     % Read the data
10    writeline(app.instrument.scope, 'CURV?');
11
12    if app.noB == 2
13        ydata = readbinblock(app.instrument.scope, 'int16');
14        txt = 'Reading ydata 16-bit';
15        WriteTextInWindow(app, txt)
16    elseif app.noB == 1
17        ydata = readbinblock(app.instrument.scope, 'int8');
18        txt = 'Reading ydata 8-bit';
19        WriteTextInWindow(app, txt)
20    else
21        WriteTextInWindow(app, 'Unsupported word length');
22    end

```

```

23
24     % Flush the termination character from the scope
25     flush(app.instrument.scope);
26     txt = 'Reading additional data';
27     WriteTextInWindow(app,txt)
28
29     % Horizontal scaling
30     app.timeDiv = str2double(writeread(app.instrument.scope,'HOR:SCA?'))...
31     ;
32     % Horizontal offset
33     xze = str2double(writeread(app.instrument.scope,'WFMO:XZE?'));
34     % Horizontal increment
35     xin = str2double(writeread(app.instrument.scope,'WFMO:XIN?'));
36     % Digital vertical offset
37     YOF = str2double(writeread(app.instrument.scope,'WFMO:YOF?'));
38     % Vertical multiplying factor
39     YMU = str2double(writeread(app.instrument.scope,'WFMO:YMU?'));
40     % Vertical offset
41     YZE = str2double(writeread(app.instrument.scope,'WFMO:YZE?'));
42     % Voltage/current vector
43     app.wf = (ydata-YOF)*YMU + YZE;
44     % Time vector
45     app.x = (0:(length(ydata)-1))*xin + xze;
46     % max voltage
47     app.maxV = max(abs(app.wf));
48 end
49 %

```

B.11 Environmental measurements

```

1 function VaisalaHMT313_read(app)
2     txt = 'Reading Vaisala temperature and humidity';
3     WriteTextInWindow(app,txt)
4     app.result.vaisala = writeread(app.instrument.humidity,'send');
5     app.result.vaisala = regexp(app.result.vaisala,'\d+\.\d*', 'Match');
6     app.result.vaisala_RH = str2double(app.result.vaisala(1));
7     app.result.vaisala_T = str2double(app.result.vaisala(2));
8 end
9 %

```

```

1 function Paroscientific(app)

```

```

2     txt = 'Reading Paroscientific pressure';
3     WriteTextInWindow(app,txt)
4     app.result.pressure = writeread(app.instrument.pressure, '*0100P3');
5     app.result.pressure = str2double(app.result.pressure{1}(6:end-1));
6 end
7 %

1 function ASLF250(app)
2     txt = 'Reading ASL F250 temperature';
3     WriteTextInWindow(app,txt)
4     fprintf(app.instrument.temperature, 'A0');
5     pause(0.1)
6     app.result.temperature = fscanf(app.instrument.temperature);
7     app.result.temperature = regexp(app.result.temperature, '\d+\.\d*', '...
           Match');
8     app.result.temperature = str2double(app.result.temperature(1));
9 end
10 %
11 %%%%%%%%%%%%%%%%%%%%%%%%%%%%%%%%%%%%%%%%%%%%%%%%%%%%%%%%%%%%%%%%%%%%%%%%%

```

B.12 Setup functions

```

1 %%%%%%%%%%%%%%%%%%%%%%%%%%%%%%%%%%%%%%%%%%%%%%%%%%%%%%%%%%%%%%%%%%%%%%%%%
2 % following function handles transducer and microphone position so
3 % you can find user/zero coordinates
4 function ATL(app,y)
5     %%%%%%%%%%%%%%%%%%%%%%%%%%%%%%%%%%%%%%%%%%%%%%%%%%%%%%%%%%%%%%%%%%%%%%%%%
6     % Angle of transducer relativt to laser
7     %
8     % y = 0:   manually measure left and right side of transducer
9     %         and make it perpendicular to laser.
10    %
11    % y = 1:   manually measure top and bottom of transducer to
12    %         find angle of transducer tilted upp or downward.
13    %%%%%%%%%%%%%%%%%%%%%%%%%%%%%%%%%%%%%%%%%%%%%%%%%%%%%%%%%%%%%%%%%%%%%%%%%
14    system('C:\Program Files (x86)\KEYENCE\LK-Navigator\LK-Navigator.exe...
           &');
15    system('Taskkill /IM cmd.exe');
16    if y == 0
17        inputvalues = inputdlg({'Front left side of transducer','Front ...
           right side of transducer','Radius of transducer'}, 'Measured ...

```



```

        average value [mm]', [1, 50], {num2str(0); num2str(0); num2str(10) ...
    });
18  if isempty(inputvalues)
19      return
20  elseif cellfun('isempty', inputvalues(1)) || cellfun('isempty', ...
    inputvalues(2)) || cellfun('isempty', inputvalues(3))
21      return
22  else
23      inputvalues = cellfun(@str2num, inputvalues);
24      theta = asind((inputvalues(2)-inputvalues(1))/(2*inputvalues...
    (3)));
25      StepMotorFunc(app, theta, 4, 0)
26      if app.stop == 1
27          app.stop = 0;
28          return
29      end
30      ZERO_R_ButtonPushed(app, matlab.ui.control.Button)
31  end
32  elseif y == 1
33      inputvalues = inputdlg({'Top of transducer', 'Bottom of ...
    transducer', 'Radius of transducer'}, 'Measured average value [...
    mm]', [1, 50], {num2str(0); num2str(0); num2str(10)});
34      if isempty(inputvalues)
35          return
36      elseif cellfun('isempty', inputvalues(1)) || cellfun('isempty', ...
    inputvalues(2)) || cellfun('isempty', inputvalues(3))
37          return
38      else
39          inputvalues = cellfun(@str2num, inputvalues);
40          app.angle = asind((inputvalues(2)-inputvalues(1))/(2*...
    inputvalues(3)));
41      end
42      if app.angle == 0
43          txt = 'Transducer is perpendicular laser';
44          WriteTextInWindow(app, txt)
45      elseif app.angle < 0
46          txt = ['Transducer is tilted ' num2str(abs(app.angle)) ' ...
    degrees downward'];
47          WriteTextInWindow(app, txt)
48      elseif app.angle > 0
49          txt = ['Transducer is tilted ' num2str(abs(app.angle)) ' ...
    degrees upward'];
50          WriteTextInWindow(app, txt)
51      end
52  end

```

```

53 end
54 %
55 function DTRax(app)
56     %%%%%%%%%%%%%%%%%%%%%%%%%%%%%%%%%%%%%%%%%%%%%%%%%%%%%%%%%%%%%%%%%%%%%%%%%
57     % Distance from transducer midpoint to rotation axis
58     %%%%%%%%%%%%%%%%%%%%%%%%%%%%%%%%%%%%%%%%%%%%%%%%%%%%%%%%%%%%%%%%%%%%%%%%%
59     system('C:\Program Files (x86)\KEYENCE\LK-Navigator\LK-Navigator.exe...
        &');
60     system('Taskkill /IM cmd.exe');
61     inputvalues = inputdlg({'Front left side of transducer','Front right...
        side of transducer','Radius of transducer'},'Measured average ...
        value [mm]', [1,50], {num2str(0);num2str(0);num2str(10)});
62     if isempty(inputvalues)
63         return
64     elseif cellfun('isempty',inputvalues(1)) || cellfun('isempty',...
        inputvalues(2)) || cellfun('isempty',inputvalues(3))
65         return
66     else
67         inputvalues = cellfun(@str2num,inputvalues);
68         theta = asind((inputvalues(1)-inputvalues(2))/(2*inputvalues(3))...
            );
69     end
70
71     inputvalues = inputdlg('Measure with laser in middle of transducer',...
        'Measured average value [mm]', [1,50]);
72     if cellfun('isempty',inputvalues)
73         return
74     else
75         inputvalues = cellfun(@str2num,inputvalues);
76         d1 = inputvalues;
77     end
78
79     alpha = -10;
80     StepMotorFunc(app,alpha,4,0)
81     if app.stop == 1
82         app.stop = 0;
83         return
84     end
85
86     inputvalues = inputdlg({'Measure at point after move transducer','...
        Move and measure with laser in middle of transducer'},'Measured ...
        average value [mm]', [1,50]);
87     if isempty(inputvalues)
88         return
89     elseif cellfun('isempty',inputvalues(1)) || cellfun('isempty',...

```

```

        inputvalues(2))
90     return
91 else
92     inputvalues = cellfun(@str2num,inputvalues);
93     d2 = inputvalues(1);
94     d3 = inputvalues(2);
95 end
96
97 StepMotorFunc(app,-alpha,4,0)
98 if app.stop == 1
99     app.stop = 0;
100    return
101 end
102
103 zpitch = 0.7;
104 xpitch = 0.5;
105
106 a = (d2-d3)/tand(theta+alpha);
107 phi = atand(a/(d1-d3));
108 h = (d1-d3)/cosd(phi);
109 gamma = phi + alpha/2;
110 r = (h/2)/sind(alpha/2);
111 z_mov = sind(gamma)*r;
112 x_mov = cosd(gamma)*r;
113 txt = ['Transducer are at X =' num2str(x_mov) '[mm] and Z =' num2str...
        (z_mov) '[mm] from rotation axis'];
114 WriteTextInWindow(app,txt)
115
116 rotate_x = x_mov/xpitch;
117 rotate_z = z_mov/zpitch;
118 wholerot_x = fix(rotate_x);
119 wholerot_z = fix(rotate_z);
120
121 restrot_x = round(360*abs(rotate_x-wholerot_x));
122 restrot_z = round(360*abs(rotate_z-wholerot_z));
123
124 if rotate_x > 0
125     if wholerot_x == 0
126         txt_1 = ['Rotate X knob ' num2str(restrot_x) ' degrees CW.'...
                ];
127         WriteTextInWindow(app,txt_1)
128     elseif abs(wholerot_x) == 1
129         txt_1 = ['Rotate X knob ' num2str(abs(wholerot_x)) ' time CW...
                , and aditional ' num2str(restrot_x) ' degrees.'];
130         WriteTextInWindow(app,txt_1)

```

```
131     else
132         txt_1 = ['Rotate X knob ' num2str(abs(wholerot_x)) ' times ...
                ' CW, and additional ' num2str(restrot_x) ' degrees.'];
133         WriteTextInWindow(app,txt_1)
134     end
135     else
136         if wholerot_x == 0
137             txt_1 = ['Rotate X knob ' num2str(restrot_x) ' degrees CCW.'...
                    ];
138             WriteTextInWindow(app,txt_1)
139         elseif abs(wholerot_x) == 1
140             txt_1 = ['Rotate X knob ' num2str(abs(wholerot_x)) ' time ...
                    ' CCW, and additional ' num2str(restrot_x) ' degrees.'];
141             WriteTextInWindow(app,txt_1)
142         else
143             txt_1 = ['Rotate X knob ' num2str(abs(wholerot_x)) ' times ...
                    ' CCW, and additional ' num2str(restrot_x) ' degrees.'];
144             WriteTextInWindow(app,txt_1)
145         end
146     end
147
148     if rotate_z > 0
149         if wholerot_z == 0
150             txt_2 = ['Rotate Z knob ' num2str(restrot_z) ' degrees CCW.'...
                    ];
151             WriteTextInWindow(app,txt_2)
152         elseif abs(wholerot_z) == 1
153             txt_2 = ['Rotate Z knob ' num2str(abs(wholerot_z)) ' time ...
                    ' CCW, and additional ' num2str(restrot_z) ' degrees.'];
154             WriteTextInWindow(app,txt_2)
155         else
156             txt_2 = ['Rotate Z knob ' num2str(abs(wholerot_z)) ' times ...
                    ' CCW, and additional ' num2str(restrot_z) ' degrees.'];
157             WriteTextInWindow(app,txt_2)
158         end
159     else
160         if wholerot_z == 0
161             txt_2 = ['Rotate Z knob ' num2str(restrot_z) ' degrees CW.'...
                    ];
162             WriteTextInWindow(app,txt_2)
163         elseif abs(wholerot_z) == 1
164             txt_2 = ['Rotate Z knob ' num2str(abs(wholerot_z)) ' time ...
                    ' CW, and additional ' num2str(restrot_z) ' degrees.'];
165             WriteTextInWindow(app,txt_2)
166         else
```

```

167         txt_2 = ['Rotate Z knob ' num2str(abs(wholerot_z)) ' times ...
168                 CW, and additional ' num2str(restrot_z) ' degrees.'];
169         WriteTextInWindow(app,txt_2)
170     end
171     questdlg({txt_1,txt_2},'Manually move the transducer','Ok','Ok')
172 end
173 %
174 function DTM(app)
175     %%%%%%%%%%%%%%%%%%%%%%%%%%%%%%%%%%%%%%%%%%%%%%%%%%%%%%%%%%%%%%%%%%%%%%%%%
176     % Distance from transducer to microphone/transducer
177     %%%%%%%%%%%%%%%%%%%%%%%%%%%%%%%%%%%%%%%%%%%%%%%%%%%%%%%%%%%%%%%%%%%%%%%%%
178     system('C:\Program Files (x86)\KEYENCE\LK-Navigator\LK-Navigator.exe...
179           &');
180
181     system('Taskkill /IM cmd.exe');
182
183     inputvalues = inputdlg({'Value one at transducer','Value two at ...
184                           microphone/transducer'},'Measured average value [mm]', [1,50]);
185     if isempty(inputvalues)
186         return
187     elseif cellfun('isempty',inputvalues(1)) || cellfun('isempty',...
188                 inputvalues(2))
189         return
190     else
191         inputvalues = cellfun(@str2num,inputvalues);
192         app.distance = 30 + 30 + 182.5692 - inputvalues(1) - inputvalues...
193                 (2);
194         value = app.abspos.(app.field{3})-app.distance;
195         txt = ['Dictance from transducer to microphone/transducer is ...
196               measured to be ' num2str(app.distance) '[mm]'];
197         WriteTextInWindow(app,txt)
198
199         choice = questdlg(['Do you want current position to ' app.name...
200                           {1} ' to be zero?'],'Zero Position','Yes','No','No');
201         switch choice
202             case 'Yes'
203                 SaveZero(app,1, '')
204         end
205         choice = questdlg(['Do you want current position to ' app.name...
206                           {2} ' to be zero?'],'Zero Position','Yes','No','No');
207         switch choice
208             case 'Yes'
209                 SaveZero(app,2, '')
210         end
211         SaveZero(app,3,value)

```

```

204     end
205 end
206 %
207 function MLY(app)
208     %%%%%%%%%%%%%%%%%%%%%%%%%%%%%%%%%%%%%%%%%%%%%%%%%%%%%%%%%%%%%%%%%%%%%%%%%
209     % Main Lobe on y axis, linear slope
210     % constants
211     %%%%%%%%%%%%%%%%%%%%%%%%%%%%%%%%%%%%%%%%%%%%%%%%%%%%%%%%%%%%%%%%%%%%%%%%%
212     if app.zeroed(3) == 0
213         txt = 'Find zero z position with Setup 3, 4 or load zero.mat';
214         WriteTextInWindow(app,txt)
215     elseif app.zeroed(2) == 0
216         txt = 'Find zero y position with Setup 3, 4 or load zero.mat';
217         WriteTextInWindow(app,txt)
218     else
219         if isempty(app.angle)
220             txt = 'No angle is found';
221             WriteTextInWindow(app,txt)
222             return
223         elseif isempty(app.distance)
224             txt = 'No distance from transducer to microphone/transducer ...
                is found';
225             WriteTextInWindow(app,txt)
226             return
227         else
228             delta_y = tand(app.angle)*app.distance;
229             app.linearslope.a = delta_y/app.distance;
230             app.linearslope.b = app.zeropos.(app.field{2});
231             SaveLinearSlope(app)
232         end
233     end
234 end
235 %
236 %%%%%%%%%%%%%%%%%%%%%%%%%%%%%%%%%%%%%%%%%%%%%%%%%%%%%%%%%%%%%%%%%%%%%%%%%

```

B.13 Overall functions

```

1 %%%%%%%%%%%%%%%%%%%%%%%%%%%%%%%%%%%%%%%%%%%%%%%%%%%%%%%%%%%%%%%%%%%%%%%%%
2 % following functions handles different needs in the app
3 function ResetButtons(app)
4     buttons = [app.MACHINECOORDS_Button, app.GO_TO_ZERO_Button, ...
               app.GO_TO_ZERO_X_Button, app.GO_TO_ZERO_Y_Button, ...

```

```

app.GO_TO_ZERO_Z_Button, app.GO_TO_ZERO_R_Button, ...
app.ZERO_ALL_Button, app.ZERO_X_Button, app.ZERO_Y_Button, ...
app.ZERO_Z_Button, app.ZERO_R_Button, app.POSITIVESTEP_X_Button, ...
app.POSITIVESTEP_Y_Button, app.POSITIVESTEP_Z_Button, ...
app.POSITIVESTEP_R_Button, app.NEGATIVESTEP_X_Button, ...
app.NEGATIVESTEP_Y_Button, app.NEGATIVESTEP_Z_Button, ...
app.NEGATIVESTEP_R_Button, app.HOME_ALL_Button, app.HOME_X_Button, ...
app.HOME_Y_Button, app.HOME_Z_Button, app.HOME_R_Button, ...
app.INITISLIZEMACHINE_Button, app.INSTRUMENTCONNECT_Button, ...
app.SETUP_Button, app.LOAD_Button, app.START_Button, app.STOP_Button...
, app.READ_DropDown, app.READ_Button];
5 set(buttons, 'Enable', 'Off')
6 if app.initialized == 0
7     set(buttons(25), 'Enable', 'On')
8 elseif ~all(app.homed)
9     set(buttons, 'Enable', 'On')
10    movebuttons = [app.POSITIVESTEP_X_Button, ...
        app.NEGATIVESTEP_X_Button; app.POSITIVESTEP_Y_Button, ...
        app.NEGATIVESTEP_Y_Button; app.POSITIVESTEP_Z_Button, ...
        app.NEGATIVESTEP_Z_Button; app.POSITIVESTEP_R_Button, ...
        app.NEGATIVESTEP_R_Button];
11    for i = 1:length(app.homed)
12        if app.homed(i) == 0
13            set(movebuttons(i, :), 'Enable', 'Off')
14        else
15            set(movebuttons(i, :), 'Enable', 'On')
16        end
17    end
18 else
19    set(buttons, 'Enable', 'On')
20 end
21 if app.connected == 0
22    set(buttons(31), 'Enable', 'Off')
23    set(buttons(32), 'Enable', 'Off')
24 end
25 end
26 %
27 function ResetColor(app)
28    color = [app.ZERO_ALL_Button, app.ZERO_X_Button, app.ZERO_Y_Button, ...
        app.ZERO_Z_Button, app.ZERO_R_Button];
29    for i = 1:length(app.zeroed)
30        if app.zeroed(i) == 0
31            set(color(1, (i+1)), 'BackgroundColor', app.red)
32        else
33            set(color(1, (i+1)), 'BackgroundColor', app.grey)

```

```

34     end
35 end
36 if all(app.zeroed == 1)
37     set(color(1,1), 'BackgroundColor', app.grey)
38 else
39     set(color(1,1), 'BackgroundColor', app.red)
40 end
41 end
42 %
43 function ActionButtons(app)
44     buttons = [app.MACHINECOORDS_Button, app.GO_TO_ZERO_Button, ...
45               app.GO_TO_ZERO_X_Button, app.GO_TO_ZERO_Y_Button, ...
46               app.GO_TO_ZERO_Z_Button, app.GO_TO_ZERO_R_Button, ...
47               app.ZERO_ALL_Button, app.ZERO_X_Button, app.ZERO_Y_Button, ...
48               app.ZERO_Z_Button, app.ZERO_R_Button, app.POSITIVESTEP_X_Button, ...
49               app.POSITIVESTEP_Y_Button, app.POSITIVESTEP_Z_Button, ...
50               app.POSITIVESTEP_R_Button, app.NEGATIVESTEP_X_Button, ...
51               app.NEGATIVESTEP_Y_Button, app.NEGATIVESTEP_Z_Button, ...
52               app.NEGATIVESTEP_R_Button, app.HOME_ALL_Button, app.HOME_X_Button, ...
53               app.HOME_Y_Button, app.HOME_Z_Button, app.HOME_R_Button, ...
54               app.INITISLIZEMACHINE_Button, app.INSTRUMENTCONNECT_Button, ...
55               app.SETUP_Button, app.LOAD_Button, app.START_Button, app.STOP_Button...
56               , app.READ_DropDown, app.READ_Button];
57     set(buttons, 'Enable', 'Off')
58     set(app.STOP_Button, 'Enable', 'On')
59 end
60 %
61 function ActionLamp(app, onoff, a)
62     lamp = [app.X_Lamp, app.Y_Lamp, app.Z_Lamp, app.R_Lamp];
63     if onoff
64         set(lamp(a), 'Color', app.green);
65     else
66         set(lamp(a), 'Color', app.black);
67     end
68 end
69 %
70 function WritePosition(app)
71     value = [app.X_EditField, app.Y_EditField, app.Z_EditField, ...
72             app.R_EditField];
73     if app.MACHINECOORDS_Lamp.Color == app.green
74         for i = 1:4
75             value(i).Value = app.abspos.(app.field{i});
76         end
77     else
78         for i = 1:4

```



```

67         if app.zeroed(i) == 1
68             value(i).Value = app.abspos.(app.field{i})-app.zeropos.(...
                app.field{i});
69         else
70             value(i).Value = app.abspos.(app.field{i});
71         end
72     end
73 end
74 end
75 %
76 function WriteTextInWindow(app,txt)
77     app.text = app.TextArea.Value;
78     if cellfun(@isempty,app.text)
79         app.text{1} = txt;
80         app.TextArea.Value = app.text;
81     else
82         if length(app.text) >= 100
83             app.text = app.text(2:end);
84         end
85         app.text{length(app.text)+1} = txt;
86         app.TextArea.Value = app.text;
87     end
88     scroll(app.TextArea, 'bottom')
89
90
91     if not(isfolder([app.path '\App_LOG']))
92         mkdir([app.path '\App_LOG'])
93     end
94     celltext{1} = txt;
95     if ~isfile([app.path '\App_LOG\TextWindow' app.time '.txt'])
96         writecell(celltext, [app.path '\App_LOG\TextWindow' app.time '...
                .txt'], 'QuoteStrings',false);
97     else
98         writecell(celltext, [app.path '\App_LOG\TextWindow' app.time '...
                .txt'], 'QuoteStrings',false,'WriteMode','append')
99     end
100 end
101 %
102 function HomeMotorFunc(app,a)
103     if app.stop == 1
104         WritePosition(app)
105         return
106     end
107     ActionButtons(app)
108     ActionLamp(app,true,a)

```

```
109     app.safety = 1;
110     while app.safety == 1
111         HomeMotor(app,a)
112         app.safety = 0;
113     end
114     if app.stop == 1
115         WritePosition(app)
116         return
117     end
118     ActionLamp(app,false,a)
119     app.homed(a) = 1;
120     WritePosition(app)
121     ResetButtons(app)
122 end
123 %
124 function StepMotorFunc(app,s,a,m)
125     if app.homed(a) == 0
126         txt = [app.name{a} ' is not homed'];
127         WriteTextInWindow(app,txt)
128         return
129     end
130
131     if app.stop == 1
132         WritePosition(app)
133         return
134     end
135
136     softlim.xaxis = [0,300];
137     softlim.yaxis = [0,300];
138     softlim.zaxis = [0,1016];
139
140     if a ~=4
141         pos = app.abspos.(app.field{a});
142         lowerlim = softlim.(app.field{a})(1);
143         upperlim = softlim.(app.field{a})(2);
144     end
145
146     if a == 4
147         ActionButtons(app)
148         ActionLamp(app,true,a)
149         app.safety = 1;
150         while app.safety == 1
151             StepMotor(app,s,a,m)
152             app.safety = 0;
153         end
```

```
154     if app.stop == 1
155         WritePosition(app)
156         return
157     end
158     ActionLamp(app, false, a)
159     WritePosition(app)
160     ResetButtons(app)
161 elseif m == 0
162     if s < 0 && pos+s < lowerlim
163         ActionButtons(app)
164         ActionLamp(app, true, a)
165         app.safety = 1;
166         while app.safety == 1
167             StepMotor(app, lowerlim, a, 1)
168             app.safety = 0;
169         end
170         if app.stop == 1
171             WritePosition(app)
172             return
173         end
174         ActionLamp(app, false, a)
175         WritePosition(app)
176         ResetButtons(app)
177         txt = 'Reached lower limit';
178         WriteTextInWindow(app, txt)
179     elseif s > 0 && pos+s > upperlim
180         ActionButtons(app)
181         ActionLamp(app, true, a)
182         app.safety = 1;
183         while app.safety == 1
184             StepMotor(app, upperlim, a, 1)
185             app.safety = 0;
186         end
187         if app.stop == 1
188             WritePosition(app)
189             return
190         end
191         ActionLamp(app, false, a)
192         WritePosition(app)
193         ResetButtons(app)
194         txt = 'Reached upper limit';
195         WriteTextInWindow(app, txt)
196     else
197         ActionButtons(app)
198         ActionLamp(app, true, a)
```

```
199         app.safety = 1;
200         while app.safety == 1
201             StepMotor(app,s,a,m)
202             app.safety = 0;
203         end
204         if app.stop == 1
205             WritePosition(app)
206             return
207         end
208         ActionLamp(app,false,a)
209         WritePosition(app)
210         ResetButtons(app)
211     end
212 else
213     if s <= lowerlim
214         ActionButtons(app)
215         ActionLamp(app,true,a)
216         app.safety = 1;
217         while app.safety == 1
218             StepMotor(app,lowerlim,a,1)
219             app.safety = 0;
220         end
221         if app.stop == 1
222             WritePosition(app)
223             return
224         end
225         ActionLamp(app,false,a)
226         WritePosition(app)
227         ResetButtons(app)
228         txt = 'Reached lower limit';
229         WriteTextInWindow(app,txt)
230     elseif s >= upperlim
231         ActionButtons(app)
232         ActionLamp(app,true,a)
233         app.safety = 1;
234         while app.safety == 1
235             StepMotor(app,upperlim,a,1)
236             app.safety = 0;
237         end
238         if app.stop == 1
239             WritePosition(app)
240             return
241         end
242         ActionLamp(app,false,a)
243         WritePosition(app)
```

```

244         ResetButtons (app)
245         txt = 'Reached upper limit';
246         WriteTextInWindow (app,txt)
247     else
248         ActionButtons (app)
249         ActionLamp (app,true,a)
250         app.safety = 1;
251         while app.safety == 1
252             StepMotor (app,s,a,m)
253             app.safety = 0;
254         end
255         if app.stop == 1
256             WritePosition (app)
257             return
258         end
259         ActionLamp (app, false, a)
260         WritePosition (app)
261         ResetButtons (app)
262     end
263 end
264 end
265 %
266 function SaveZero (app,a,value)
267     if isempty(value)
268         if a == 2
269             app.linearslope.b = app.abspos.(app.field{a});
270             SaveLinearSlope (app)
271         end
272         app.zeropos.(app.field{a}) = app.abspos.(app.field{a});
273         zero = app.zeropos;
274         if isfile([app.path '\zero.mat'])
275             save([app.path '\zero.mat'],'-struct','zero','-append')
276         else
277             save([app.path '\zero.mat'],'-struct','zero')
278         end
279         app.zeroed(a) = 1;
280         WritePosition (app)
281         ResetColor (app)
282     else
283         if a == 2
284             app.linearslope.b = value;
285             SaveLinearSlope (app)
286         end
287         app.zeropos.(app.field{a}) = value;
288         zero = app.zeropos;

```

```
289     if isfile([app.path '\zero.mat'])
290         save([app.path '\zero.mat'],'-struct','zero','-append')
291     else
292         save([app.path '\zero.mat'],'-struct','zero')
293     end
294     app.zeroed(a) = 1;
295     WritePosition(app)
296     ResetColor(app)
297 end
298 end
299 %
300 function SaveLinearSlope(app)
301     slope = app.linearslope;
302     if isfile([app.path '\slope.mat'])
303         save([app.path '\slope.mat'],'-struct','slope','-append')
304     else
305         save([app.path '\slope.mat'],'-struct','slope')
306     end
307 end
308 %
309 function SaveMeasurements(app)
310     if strcmpi(app.meas.notes,'Main Lobe on y-axis')
311         filename_1 = [app.meas.date '_Main_Lobe_Y'];
312     elseif strcmpi(app.meas.notes,'Main Lobe on x-axis')
313         filename_1 = [app.meas.date '_Main_Lobe_X'];
314     else
315         filename_1 = [app.meas.date '_' app.meas.name];
316     end
317     newfolder_1 = [app.selpath '\\' filename_1];
318     if ~isfolder(newfolder_1)
319         mkdir(newfolder_1)
320     end
321     if app.measurement == 1
322         txt = 'Saving Measurement Parameters';
323         WriteTextInWindow(app,txt)
324         savepath_1 = [newfolder_1 '\measurement_parameters.mat'];
325         m = matfile(savepath_1,'Writable',true);
326         m.parameters = app.meas;
327     end
328     if strcmpi(app.meas.notes,'Directivity')
329         filename_2 = ['Primary_axis_' num2str(...
330             app.result.primary_axis_pos) '[mm]'];
331         newfolder_2 = [newfolder_1 '\\' filename_2];
332         if ~isfolder(newfolder_2)
333             mkdir(newfolder_2)
```

```

333     end
334     filename_3 = ['Frequency_' num2str(app.result.frequency) '[Hz]'...
335                 ];
336     newfolder_3 = [newfolder_2 '\\' filename_3];
337     if ~isfolder(newfolder_3)
338         mkdir(newfolder_3)
339     end
340     txt = 'Saving Results';
341     WriteTextInWindow(app,txt)
342     if strcmpi(app.result.secondary_axis,'rotaxis')
343         savepath_2 = [newfolder_3 '\\' num2str(...
344                     app.result.secondary_axis_pos) '[degree].mat'];
345     else
346         savepath_2 = [newfolder_3 '\\' num2str(...
347                     app.result.secondary_axis_pos) '[mm].mat'];
348     end
349     n = matfile(savepath_2,'Writable',true);
350     n.results = app.result;
351 elseif strcmpi(app.meas.notes,'On Axis Pressure')
352     filename_2 = ['Frequency_' num2str(app.result.frequency) '[Hz]'...
353                 ];
354     newfolder_2 = [newfolder_1 '\\' filename_2];
355     if ~isfolder(newfolder_2)
356         mkdir(newfolder_2)
357     end
358     if strcmpi(app.result.secondary_axis,'rotaxis')
359         filename_3 = ['Secondary_axis_' num2str(...
360                     app.result.secondary_axis_pos) '[degree]'];
361     else
362         filename_3 = ['Secondary_axis_' num2str(...
363                     app.result.secondary_axis_pos) '[mm]'];
364     end
365     newfolder_3 = [newfolder_2 '\\' filename_3];
366     if ~isfolder(newfolder_3)
367         mkdir(newfolder_3)
368     end
369     txt = 'Saving Results';
370     WriteTextInWindow(app,txt)
371     savepath_2 = [newfolder_3 '\\' num2str(...
372                 app.result.primary_axis_pos) '[mm].mat'];
373     n = matfile(savepath_2,'Writable',true);
374     n.results = app.result;
375 elseif strcmpi(app.meas.notes,'Sensitivity')
376     filename_2 = ['Primary_axis_' num2str(...
377                 app.result.primary_axis_pos) '[mm]'];

```

```
370     newfolder_2 = [newfolder_1 '\\' filename_2];
371     if ~isfolder(newfolder_2)
372         mkdir(newfolder_2)
373     end
374     if strcmpi(app.result.secondary_axis,'rotaxis')
375         filename_3 = ['Secondary_axis' num2str(...
376             app.result.secondary_axis_pos) '[degree]'];
377     else
378         filename_3 = ['Secondary_axis' num2str(...
379             app.result.secondary_axis_pos) '[mm]'];
380     end
381     newfolder_3 = [newfolder_2 '\\' filename_3];
382     if ~isfolder(newfolder_3)
383         mkdir(newfolder_3)
384     end
385     txt = 'Saving Results';
386     WriteTextInWindow(app,txt)
387     savepath_2 = [newfolder_3 '\\' num2str(app.result.frequency) '[Hz...
388         ].mat'];
389     n = matfile(savepath_2,'Writable',true);
390     n.results = app.result;
391 elseif strcmpi(app.meas.notes,'Main Lobe on y-axis')
392     filename_2 = ['Primary_axis_' num2str(...
393         app.result.primary_axis_pos) '[mm]'];
394     newfolder_2 = [newfolder_1 '\\' filename_2];
395     if ~isfolder(newfolder_2)
396         mkdir(newfolder_2)
397     end
398     filename_3 = ['Frequency_' num2str(app.result.frequency) '[Hz]'...
399         ];
400     newfolder_3 = [newfolder_2 '\\' filename_3];
401     if ~isfolder(newfolder_3)
402         mkdir(newfolder_3)
403     end
404     txt = 'Saving Results';
405     WriteTextInWindow(app,txt)
406     if strcmpi(app.result.secondary_axis,'rotaxis')
407         savepath_2 = [newfolder_3 '\\' num2str(...
408             app.result.secondary_axis_pos) '[degree].mat'];
409     else
410         savepath_2 = [newfolder_3 '\\' num2str(...
411             app.result.secondary_axis_pos) '[mm].mat'];
412     end
413     n = matfile(savepath_2,'Writable',true);
414     n.results = app.result;
```



```

408     elseif strcmpi(app.meas.notes,'Main Lobe on x-axis')
409         filename_2 = ['Primary_axis_' num2str(...
410             app.result.primary_axis_pos) '[mm]'];
411         newfolder_2 = [newfolder_1 '\\' filename_2];
412         if ~isfolder(newfolder_2)
413             mkdir(newfolder_2)
414         end
415         filename_3 = ['Frequency_' num2str(app.result.frequency) '[Hz]'...
416             ];
417         newfolder_3 = [newfolder_2 '\\' filename_3];
418         if ~isfolder(newfolder_3)
419             mkdir(newfolder_3)
420         end
421         txt = 'Saving Results';
422         WriteTextInWindow(app,txt)
423         if strcmpi(app.result.secondary_axis,'rotaxis')
424             savepath_2 = [newfolder_3 '\\' num2str(...
425                 app.result.secondary_axis_pos) '[degree].mat'];
426         else
427             savepath_2 = [newfolder_3 '\\' num2str(...
428                 app.result.secondary_axis_pos) '[mm].mat'];
429         end
430         n = matfile(savepath_2,'Writable',true);
431         n.results = app.result;
432     end
433 end
434 %
435 %%%%%%%%%%%%%%%%%%%%%%%%%%%%%%%%%%%%%%%%%%%%%%%%%%%%%%%%%%%%%%%%%%%%%%%%%

```

B.14 Button functions

```

1 % Callbacks that handle component events
2 methods (Access = private)
3
4 % Code that executes after component creation
5 function startupFcn(app)
6     % At start up, resets all buttons
7     app.path = fileparts(mfilename('fullpath'));
8     addpath(app.path)
9     app.time = strcat(datestr(now,'yyyy_mm_dd_HH_MM'));
10    ResetButtons(app)
11    ResetColor(app)

```

```
12 end
13
14 % Button pushed function: INITISLIZEMACHINE_Button
15 function INITISLIZEMACHINE_ButtonPushed(app, event)
16     % If you accidentaly hit INIT button, you have the ability to
17     % stop
18     if app.initializing == 1
19         return
20     elseif app.initialized == 1
21         choice = questdlg('WARNING: Do you want to initialize again?','...
22             WARNING','Yes','No','No');
23         switch choice
24             case 'No'
25                 return
26         end
27     end
28     app.TextArea.Value = '';
29
30     % Set up connection to the motor controllers with InitMotor and
31     % finds initial position of with PositionMotor.
32     % app.initializing sets everything on pause to initializing and
33     % finding position is done.
34     app.initializing = 1;
35     while app.initializing == 1
36         InitMotor(app)
37         if app.initfail == 1
38             txt = 'Initialize Machine failed';
39             WriteTextInWindow(app,txt)
40             app.initfail = 0;
41             app.initializing = 0;
42             return
43         end
44         for i = 1:4
45             PositionMotor(app,i);
46             app.zeroed(i) = 0;
47             if i == 4
48                 app.homed(i) = 1;
49             else
50                 app.homed(i) = 0;
51             end
52         end
53         app.initialized = 1;
54         app.initializing = 0;
55     end
```

```

56
57 % Set stop lamp to green to tell user that app is ready to and
58 % set machine coordinates/absolute positions to correct state
59 app.STOP_Lamp.Color = app.green;
60 app.MACHINECOORDS_Lamp.Color = app.green;
61 app.MACHINECOORDS_Button.Text = 'MACHINE COORDS';
62 app.SETUP_Button.Text = 'SETUP';
63 app.USERCOORDS_Lamp.Color = app.black;
64 % Write position to position fields and reset buttons and
65 % colors to corret states.
66 WritePosition(app)
67 ResetButtons(app)
68 ResetColor(app)
69 end
70
71 % Button pushed function: INSTRUMENTCONNECT_Button
72 function INSTRUMENTCONNECT_ButtonPushed(app, event)
73 % If you accedentaly hit instr button, you have the ability to
74 % stop
75 if app.connected == 1
76     choice = questdlg('WARNING: Do you want to connect to ...
77         instruments again?', 'WARNING', 'Yes', 'No', 'No');
78     switch choice
79         case 'No'
80             return
81     end
82 InstrumentConnect(app)
83 if app.connectfail == 1
84     txt = 'Instrument Connect failed';
85     WriteTextInWindow(app,txt)
86     app.connectfail = 0;
87     return
88 end
89 app.connected = 1;
90 set(app.STOP_Button, 'Enable', 'On')
91 ResetButtons(app)
92 end
93
94 % Button pushed function: HOME_ALL_Button
95 function HOME_ALL_ButtonPushed(app, event)
96     txt = 'Home All';
97     WriteTextInWindow(app,txt)
98     home_order = [4,3,1,2];
99     for i = 1:length(home_order)

```

```
100     HomeMotorFunc (app,home_order(i))
101     if app.stop == 1
102         app.stop = 0;
103         return
104     end
105 end
106 end
107
108 % Button pushed function: HOME_X_Button
109 function HOME_X_ButtonPushed(app, event)
110     txt = ['Home ' app.name{1}];
111     WriteTextInWindow(app,txt)
112     HomeMotorFunc (app,1)
113     if app.stop == 1
114         app.stop = 0;
115         return
116     end
117 end
118
119 % Button pushed function: HOME_Y_Button
120 function HOME_Y_ButtonPushed(app, event)
121     txt = ['Home ' app.name{2}];
122     WriteTextInWindow(app,txt)
123     HomeMotorFunc (app,2)
124     if app.stop == 1
125         app.stop = 0;
126         return
127     end
128 end
129
130 % Button pushed function: HOME_Z_Button
131 function HOME_Z_ButtonPushed(app, event)
132     txt = ['Home ' app.name{3}];
133     WriteTextInWindow(app,txt)
134     HomeMotorFunc (app,3)
135     if app.stop == 1
136         app.stop = 0;
137         return
138     end
139 end
140
141 % Button pushed function: HOME_R_Button
142 function HOME_R_ButtonPushed(app, event)
143     txt = ['Home ' app.name{4}];
144     WriteTextInWindow(app,txt)
```

```
145     HomeMotorFunc(app,4)
146     if app.stop == 1
147         app.stop = 0;
148         return
149     end
150 end
151
152 % Button pushed function: POSITEIVESTEP_X_Button
153 function POSITEIVESTEP_X_ButtonPushed(app, event)
154     if app.STEP_X_DIR_EditField.Value < 0
155         return
156     end
157     step = app.STEP_X_DIR_EditField.Value;
158     StepMotorFunc(app,step,1,0)
159     if app.stop == 1
160         app.stop = 0;
161         return
162     end
163 end
164
165 % Button pushed function: POSITEIVESTEP_Y_Button
166 function POSITEIVESTEP_Y_ButtonPushed(app, event)
167     if app.STEP_Y_DIR_EditField.Value < 0
168         return
169     end
170     step = app.STEP_Y_DIR_EditField.Value;
171     StepMotorFunc(app,step,2,0)
172     if app.stop == 1
173         app.stop = 0;
174         return
175     end
176 end
177
178 % Button pushed function: POSITEIVESTEP_Z_Button
179 function POSITEIVESTEP_Z_ButtonPushed(app, event)
180     if app.STEP_Z_DIR_EditField.Value < 0
181         return
182     elseif app.setup == 1
183         questdlg('WARNING: Exit setup!', 'WARNING', 'Ok', 'Ok')
184         return
185     end
186     step = app.STEP_Z_DIR_EditField.Value;
187     StepMotorFunc(app,step,3,0)
188     if app.stop == 1
189         app.stop = 0;
```

```
190     return
191 end
192 end
193
194 % Button pushed function: POSITIVESTEP_R_Button
195 function POSITIVESTEP_R_ButtonPushed(app, event)
196     if app.STEP_R_DIR_EditField.Value < 0
197         return
198     end
199     step = app.STEP_R_DIR_EditField.Value;
200     StepMotorFunc(app, step, 4, 0)
201     if app.stop == 1
202         app.stop = 0;
203         return
204     end
205 end
206
207 % Button pushed function: NEGATIVESTEP_X_Button
208 function NEGATIVESTEP_X_ButtonPushed(app, event)
209     if app.STEP_X_DIR_EditField.Value < 0
210         return
211     end
212     step = -app.STEP_X_DIR_EditField.Value;
213     StepMotorFunc(app, step, 1, 0)
214     if app.stop == 1
215         app.stop = 0;
216         return
217     end
218 end
219
220 % Button pushed function: NEGATIVESTEP_Y_Button
221 function NEGATIVESTEP_Y_ButtonPushed(app, event)
222     if app.STEP_Y_DIR_EditField.Value < 0
223         return
224     end
225     step = -app.STEP_Y_DIR_EditField.Value;
226     StepMotorFunc(app, step, 2, 0)
227     if app.stop == 1
228         app.stop = 0;
229         return
230     end
231 end
232
233 % Button pushed function: NEGATIVESTEP_Z_Button
234 function NEGATIVESTEP_Z_ButtonPushed(app, event)
```

```

235     if app.STEP_Z_DIR_EditField.Value < 0
236         return
237     elseif app.setup == 1
238         questdlg('WARNING: Exit setup!', 'WARNING', 'Ok', 'Ok')
239         return
240     elseif app.zeroed(3) == 1 && app.zeroz == 1
241         newpos = app.abspos.zaxis-app.STEP_Z_DIR_EditField.Value;
242         if newpos < app.zeropos.zaxis
243             choice = questdlg('WARNING: You are crossing your zero point...
                , this may cause you to crash with the microphone/...
                transducer.', 'WARNING', 'Don''t cross', 'Ignore', 'Don''t ...
                cross');
244             switch choice
245                 case 'Don''t cross'
246                     return
247                 case ''
248                     return
249                 case 'Ignore'
250                     app.zeroz = 0;
251             end
252         end
253     end
254     step = -app.STEP_Z_DIR_EditField.Value;
255     StepMotorFunc(app, step, 3, 0)
256     if app.stop == 1
257         app.stop = 0;
258         return
259     end
260 end
261
262 % Button pushed function: NEGATIVESTEP_R_Button
263 function NEGATIVESTEP_R_ButtonPushed(app, event)
264     if app.STEP_R_DIR_EditField.Value < 0
265         return
266     end
267     step = -app.STEP_R_DIR_EditField.Value;
268     StepMotorFunc(app, step, 4, 0)
269     if app.stop == 1
270         app.stop = 0;
271         return
272     end
273 end
274
275 % Button pushed function: STOP_Button
276 function STOP_ButtonPushed(app, event)

```

```
277     if strcmpi(app.STOP_Button.Text, 'STOP')
278         txt = 'Stop';
279         WriteTextInWindow(app,txt)
280         app.stop = 1;
281         ActionButtons(app)
282         app.STOP_Lamp.Color = app.red;
283         app.controller.C843.STP();
284         writeline(app.controller.HydraTT, '1 nabort')
285         for i = 1:4
286             ActionLamp(app, false, i)
287         end
288         app.STOP_Button.Text='RESTART';
289     elseif strcmpi(app.STOP_Button.Text, 'RESTART') && app.safety == 0
290         txt = 'Restart';
291         WriteTextInWindow(app,txt)
292         app.STOP_Lamp.Color = app.green;
293         app.STOP_Button.Text='STOP';
294         ResetButtons(app)
295     end
296 end
297
298 % Button pushed function: ZERO_ALL_Button
299 function ZERO_ALL_ButtonPushed(app, event)
300     txt = 'Zero All';
301     WriteTextInWindow(app,txt)
302     for i = 1:4
303         SaveZero(app,i, '')
304     end
305 end
306
307 % Button pushed function: ZERO_X_Button
308 function ZERO_X_ButtonPushed(app, event)
309     txt = ['Zero ' app.name{1}];
310     WriteTextInWindow(app,txt)
311     SaveZero(app,1, '')
312 end
313
314 % Button pushed function: ZERO_Y_Button
315 function ZERO_Y_ButtonPushed(app, event)
316     txt = ['Zero ' app.name{2}];
317     WriteTextInWindow(app,txt)
318     SaveZero(app,2, '')
319 end
320
321 % Button pushed function: ZERO_Z_Button
```



```

322 function ZERO_Z_ButtonPushed(app, event)
323     txt = ['Zero ' app.name{3}];
324     WriteTextInWindow(app,txt)
325     SaveZero(app,3, '')
326 end
327
328 % Button pushed function: ZERO_R_Button
329 function ZERO_R_ButtonPushed(app, event)
330     txt = ['Zero ' app.name{4}];
331     WriteTextInWindow(app,txt)
332     SaveZero(app,4, '')
333 end
334
335 % Button pushed function: GO_TO_ZERO_Button
336 function GO_TO_ZERO_ButtonPushed(app, event)
337     txt = 'All Go To Zero';
338     WriteTextInWindow(app,txt)
339
340     gotozero_order = [4,1,2,3];
341     for i = 1:length(gotozero_order)
342         if app.homed(gotozero_order(i)) == 0
343             txt = [app.name{gotozero_order(i)} ' is not homed.'];
344             WriteTextInWindow(app,txt)
345             continue
346         elseif app.zeroed(gotozero_order(i)) == 0
347             txt = [app.name{gotozero_order(i)} ' have no zero ...
348                 coordinates'];
349             WriteTextInWindow(app,txt)
350             continue
351         elseif app.setup == 1 && gotozero_order(i) == 3
352             txt = ['Exit Setup to move ' app.name{gotozero_order(i)} ' ...
353                 to zero'];
354             WriteTextInWindow(app,txt)
355             continue
356         elseif app.zeroed(gotozero_order(i)) == 1
357             pos = app.zeropos.(app.field{gotozero_order(i)});
358             if gotozero_order(i) == 3
359                 distmic = 10;
360                 choice = questdlg('WARNING: Possible collision can occur...
361                 with the microphone/transducer.','WARNING',['Stop at...
362                 ' num2str(distmic) '[mm]'], 'Ignore',['Stop at ' ...
363                 num2str(distmic) '[mm]']);
364                 switch choice
365                     case ['Stop at ' num2str(distmic) '[mm]']
366                         StepMotorFunc(app, (pos + distmic), gotozero_order...

```

```

        (i),1)
362         if app.stop == 1
363             app.stop = 0;
364             return
365         end
366         case ''
367             return
368         case 'Ignore'
369             StepMotorFunc(app,pos,gotozero_order(i),1)
370             if app.stop == 1
371                 app.stop = 0;
372                 return
373             end
374         end
375     else
376         StepMotorFunc(app,pos,gotozero_order(i),1)
377         if app.stop == 1
378             app.stop = 0;
379             return
380         end
381     end
382 end
383 end
384 end
385
386 % Button pushed function: GO_TO_ZERO_X_Button
387 function GO_TO_ZERO_X_ButtonPushed(app, event)
388     if app.homed(1) == 0
389         txt = [app.name{1} ' is not homed.'];
390         WriteTextInWindow(app,txt)
391         return
392     elseif app.zeroed(1) == 0
393         txt = [app.name{1} ' have no zero coordinates'];
394         WriteTextInWindow(app,txt)
395         return
396     end
397
398     txt = [app.name{1} ' Go To Zero'];
399     WriteTextInWindow(app,txt)
400
401     pos = app.zeropos.(app.field{1});
402     StepMotorFunc(app,pos,1,1)
403     if app.stop == 1
404         app.stop = 0;
405         return

```

```
406     end
407 end
408
409 % Button pushed function: GO_TO_ZERO_Y_Button
410 function GO_TO_ZERO_Y_ButtonPushed(app, event)
411     if app.homed(2) == 0
412         txt = [app.name{2} ' is not homed.'];
413         WriteTextInWindow(app,txt)
414         return
415     elseif app.zeroed(2) == 0
416         txt = [app.name{2} ' have no zero coordinates'];
417         WriteTextInWindow(app,txt)
418         return
419     end
420
421     txt = [app.name{2} ' Go To Zero'];
422     WriteTextInWindow(app,txt)
423
424     pos = app.zeropos.(app.field{2});
425     StepMotorFunc(app,pos,2,1)
426     if app.stop == 1
427         app.stop = 0;
428         return
429     end
430 end
431
432 % Button pushed function: GO_TO_ZERO_Z_Button
433 function GO_TO_ZERO_Z_ButtonPushed(app, event)
434     if app.setup == 1
435         txt = 'Exit Setup';
436         WriteTextInWindow(app,txt)
437         return
438     elseif app.homed(3) == 0
439         txt = [app.name{3} ' is not homed.'];
440         WriteTextInWindow(app,txt)
441         return
442     elseif app.zeroed(3) == 0
443         txt = [app.name{3} ' have no zero coordinates'];
444         WriteTextInWindow(app,txt)
445         return
446     end
447
448     txt = [app.name{3} ' Go To Zero'];
449     WriteTextInWindow(app,txt)
450
```

```
451 pos = app.zeropos.(app.field{3});
452 distmic = 10;
453 choice = questdlg('WARNING: Possible collision can occur with the ...
    microphone/transducer.', 'WARNING', ['Stop at ' num2str(distmic) '[...
    mm]'], 'Ignore', ['Stop at ' num2str(distmic) '[mm]']);
454 switch choice
455     case ['Stop at ' num2str(distmic) '[mm]']
456         StepMotorFunc(app, (pos + distmic), 3, 1)
457         if app.stop == 1
458             app.stop = 0;
459             return
460         end
461     case ''
462         return
463     case 'Ignore'
464         StepMotorFunc(app, pos, 3, 1)
465         if app.stop == 1
466             app.stop = 0;
467             return
468         end
469     end
470 end
471
472 % Button pushed function: GO_TO_ZERO_R_Button
473 function GO_TO_ZERO_R_ButtonPushed(app, event)
474     if app.homed(4) == 0
475         txt = [app.name{4} ' is not homed.'];
476         WriteTextInWindow(app, txt)
477         return
478     elseif app.zeroed(4) == 0
479         txt = [app.name{4} ' have no zero coordinates'];
480         WriteTextInWindow(app, txt)
481         return
482     end
483
484     txt = [app.name{4} ' Go To Zero'];
485     WriteTextInWindow(app, txt)
486
487     pos = app.zeropos.(app.field{4});
488     StepMotorFunc(app, pos, 4, 1)
489     if app.stop == 1
490         app.stop = 0;
491         return
492     end
493 end
```

```
494
495 % Button pushed function: MACHINECOORDS_Button
496 function MACHINECOORDS_ButtonPushed(app, event)
497     if strcmpi(app.MACHINECOORDS_Button.Text, 'MACHINE COORDS')
498         txt = 'User Coordinates';
499         WriteTextInWindow(app,txt)
500         app.MACHINECOORDS_Button.Text = 'USER COORDS';
501         app.MACHINECOORDS_Lamp.Color = app.black;
502         app.USERCOORDS_Lamp.Color = app.green;
503         for i = 1:4
504             WritePosition(app)
505         end
506     elseif strcmpi(app.MACHINECOORDS_Button.Text, 'USER COORDS')
507         txt = 'Machine Coordinates';
508         WriteTextInWindow(app,txt)
509         app.MACHINECOORDS_Button.Text = 'MACHINE COORDS';
510         app.MACHINECOORDS_Lamp.Color = app.green;
511         app.USERCOORDS_Lamp.Color = app.black;
512         for i = 1:4
513             WritePosition(app)
514         end
515     end
516 end
517
518 % Button pushed function: LOAD_Button
519 function LOAD_ButtonPushed(app, event)
520     txt = 'Load';
521     WriteTextInWindow(app,txt)
522     [file,selpathh] = uigetfile({'*m'; '*mat'});
523     selectedfile = fullfile(selpathh,file);
524     if isequal(file,0)
525         txt = 'Canceled Loading';
526         WriteTextInWindow(app,txt)
527         return
528     else
529         txt = ['Loaded File: ', selectedfile];
530         WriteTextInWindow(app,txt)
531     end
532     if strcmpi(file,'zero.mat')
533         app.zeropos = load(selectedfile);
534         app.zeroed(1) = 1;
535         app.zeroed(2) = 1;
536         app.zeroed(3) = 1;
537         app.zeroed(4) = 1;
538         app.zerоз = 1;
```

```

539     elseif strcmpi(file, 'MeasParameters.m')
540         app.meas = MeasParameters;
541         app.start = 1;
542     elseif strcmpi(file, 'MainLobeX.m')
543         app.meas = MainLobeX;
544         app.start = 1;
545     elseif strcmpi(file, 'MainLobeY.m')
546         app.meas = MainLobeY;
547         app.start = 1;
548     elseif strcmpi(file, 'slope.mat')
549         app.linearslope = load(selectedfile);
550         app.comp = 1;
551     else
552         txt = 'File not supported by app';
553         WriteTextInWindow(app,txt)
554     end
555     WritePosition(app)
556     ResetColor(app)
557 end
558
559 % Button pushed function: SETUP_Button
560 function SETUP_ButtonPushed(app, event)
561     if ~all(app.homed)
562         txt = 'Not all axis is homed';
563         WriteTextInWindow(app,txt)
564         return
565     elseif strcmpi(app.SETUP_Button.Text, 'SETUP')
566         txt = 'Setup';
567         WriteTextInWindow(app,txt)
568         set = {'SETUP';'';'L = Laser stage is needed, take it up before ...
569             start.'};
570         list = {'Setup 1: Tilt angle of transducer: (L)';
571             'Setup 2: Distance from transducer to rotationaxis: (L)';
572             'Setup 3: Transducer perpendicular to laser: (L)';
573             'Setup 4: Distance from transducer to microphone/transducer:...
574             (L)';
575             'Setup 5: Tilt angle of transducer and distance to ...
576             microphone/transducer: (L)';
577             'Turn off linear slope compensation';
578             'Exit Setup'};
579         choice = listdlg('PromptString',set,'ListSize',[400,150],'...
580             ListString',list,'SelectionMode','single');
581         if isempty(choice)
582             choice = 0;
583         end

```

```
580     switch choice
581         case 0
582             txt = 'Canceled Setup';
583             WriteTextInWindow(app,txt)
584             return
585         case 1
586             app.setup = 1;
587             txt = 'Setup 1';
588             WriteTextInWindow(app,txt)
589             StepMotorFunc(app,360,3,1)
590             if app.stop == 1
591                 app.stop = 0;
592                 return
593             end
594             txt = 'Ready to measure? Click measure';
595             WriteTextInWindow(app,txt)
596             questdlg(txt, 'Choose', 'Ok', 'Ok');
597             app.SETUP_Button.Text = 'MEASURE';
598             app.tilt_angle = 1;
599         case 2
600             app.setup = 1;
601             txt = 'Setup 2';
602             WriteTextInWindow(app,txt)
603             StepMotorFunc(app,360,3,1)
604             if app.stop == 1
605                 app.stop = 0;
606                 return
607             end
608             txt = 'Ready to measure? Click measure';
609             WriteTextInWindow(app,txt)
610             questdlg(txt, 'Choose', 'Ok', 'Ok');
611             app.SETUP_Button.Text = 'MEASURE';
612             app.distance_transducer_rotaxis = 1;
613         case 3
614             app.setup = 1;
615             txt = 'Setup 3';
616             WriteTextInWindow(app,txt)
617             StepMotorFunc(app,360,3,1)
618             if app.stop == 1
619                 app.stop = 0;
620                 return
621             end
622             txt = 'Ready to measure? Click measure';
623             WriteTextInWindow(app,txt)
624             questdlg(txt, 'Choose', 'Ok', 'Ok');
```

```
625         app.SETUP_Button.Text = 'MEASURE';
626         app.transducer_perpendicular_laser = 1;
627     case 4
628         app.setup = 1;
629         txt = 'Setup 4';
630         WriteTextInWindow(app,txt)
631         StepMotorFunc(app,360,3,1)
632         if app.stop == 1
633             app.stop = 0;
634             return
635         end
636         txt = 'Adjust laser such laser point is in the center of...
        transducer and then adjust the X and Y-axis such ...
        laser point is in center microphone/transducer';
637         WriteTextInWindow(app,txt)
638         questdlg(txt, 'Choose', 'Ok', 'Ok');
639         app.SETUP_Button.Text = 'MEASURE';
640         app.distance_transducer_microphone = 1;
641     case 5
642         app.setup = 1;
643         txt = 'Setup 5';
644         WriteTextInWindow(app,txt)
645         StepMotorFunc(app,360,3,1)
646         if app.stop == 1
647             app.stop = 0;
648             return
649         end
650         txt = 'Adjust laser such laser point is in the center of...
        transducer and then adjust the X and Y-axis such ...
        laser point is in center microphone/transducer';
651         WriteTextInWindow(app,txt)
652         questdlg(txt, 'Choose', 'Ok', 'Ok');
653         app.SETUP_Button.Text = 'MEASURE';
654         app.tilt_angle_and_distance = 1;
655     case 6
656         app.comp = 0;
657     case 7
658         app.setup = 0;
659         txt = 'Exit Setup';
660         WriteTextInWindow(app,txt)
661         app.distance_transducer_microphone = 0;
662         app.distance_transducer_rotaxis = 0;
663         app.transducer_perpendicular_laser = 0;
664         app.tilt_angle_and_distance = 0;
665         app.tilt_angle = 0;
```



```

666         app.SETUP_Button.Text = 'SETUP';
667         if app.abspos.(app.field{3}) < 500
668             StepMotorFunc(app,500,3,1)
669             if app.stop == 1
670                 app.stop = 0;
671                 return
672             end
673         end
674     end
675 else
676     txt = 'Measure';
677     WriteTextInWindow(app,txt)
678     if app.distance_transducer_microphone == 1
679         DTM(app)
680         app.distance_transducer_microphone = 0;
681     elseif app.distance_transducer_rotaxis == 1
682         DTRax(app)
683         app.distance_transducer_rotaxis = 0;
684     elseif app.transducer_perpendicular_laser == 1
685         ATL(app,0)
686         app.transducer_perpendicular_laser = 0;
687     elseif app.tilt_angle_and_distance == 1
688         DTM(app)
689         ATL(app,1)
690         MLY(app)
691         app.tilt_angle_and_distance = 0;
692     elseif app.tilt_angle == 1
693         ATL(app,1)
694         app.tilt_angle = 0;
695     end
696     app.SETUP_Button.Text = 'SETUP';
697 end
698 end
699
700 % Button pushed function: START_Button
701 function START_ButtonPushed(app, event)
702     notes = {'Directivity','Sensitivity','On Axis Pressure','Main Lobe ...
703             on y-axis','Main Lobe on x-axis'};
704
705     if app.start == 0
706         txt = 'No measurement parameters loaded';
707         WriteTextInWindow(app,txt)
708         return
709     elseif ~all(app.homed)
710         txt = 'Not all axis is homed';

```

```
710     WriteTextInWindow(app,txt)
711     return
712 elseif ~all(app.zeroed)
713     txt = 'Not all axis have zero coordinates';
714     WriteTextInWindow(app,txt)
715     return
716 elseif app.connected == 0
717     txt = 'Not connected to instruments';
718     WriteTextInWindow(app,txt)
719     return
720 elseif ~any(strcmp(notes,app.meas.notes))
721     txt = 'No meas.notes of that type, you have to modify ...
722           SaveMeasurements(app) or choose meas.notes!';
723     WriteTextInWindow(app,txt)
724     for i = 1:length(notes)
725         txt = notes{i};
726         WriteTextInWindow(app,txt)
727     end
728     return
729
730 if strcmpi(app.MACHINECOORDS_Button.Text,'MACHINE COORDS')
731     MACHINECOORDS_ButtonPushed(app, ...
732         matlab.ui.eventdata.ButtonPushedData)
733
734 end
735
736 primary_axis = 3;
737 txt = [app.name{primary_axis} ' are the primary axis'];
738 WriteTextInWindow(app,txt)
739
740 mainlobex = 0;
741 if strcmpi(app.meas.notes,'Main Lobe on y-axis')
742     secondary_axis = 2;
743 elseif strcmpi(app.meas.notes,'Main Lobe on x-axis')
744     secondary_axis = 4;
745 mainlobex = 1;
746 else
747     set = {'Secondary axis';'';'Choose your secondary axis'};
748     list = {'X-axis';'Y-axis';'Rotation-axis'};
749     choice = listdlg('PromptString',set,'ListSize',[150,80], '...
750         ListString',list,'SelectionMode','single');
751     if isempty(choice)
752         choice = 0;
753     end
754     switch choice
```

```

752         case 0
753             return
754         case 1
755             secondary_axis = 1;
756         case 2
757             secondary_axis = 2;
758         case 3
759             secondary_axis = 4;
760     end
761 end
762 txt = [app.name{secondary_axis} ' selected as secondary axis'];
763 WriteTextInWindow(app,txt)
764
765 app.selpath = uigetdir(app.path);
766 if isempty(app.selpath)
767     app.selpath = app.path;
768 end
769
770 axis = [1,2,3,4];
771 axis = axis(axis~=primary_axis);
772 axis = axis(axis~=secondary_axis);
773
774 app.meas.zeropos = app.zeropos;
775 app.meas.date = strcat(datestr(now, 'yyyy-mm-dd_HH_MM'));
776
777 app.measurement = 0;
778 started = 0;
779 init = 0;
780
781 freq_change = zeros(length(app.meas.primary_axis),width(...
782     app.meas.secondary_axis)*length(app.meas.frequency));
783 for ii = 1:length(app.meas.primary_axis)
784     ll = 0;
785     for jj = 1:width(app.meas.secondary_axis)
786         for kk = 1:length(app.meas.frequency)
787
788             % Calculate current measurement and total
789             % measurements
790             app.measurement = app.measurement + 1;
791             totmeas = length(app.meas.primary_axis)*width(...
792                 app.meas.secondary_axis)*length(app.meas.frequency);
793             measurementleft = totmeas-app.measurement;
794             app.result.measurement = ['Measurement ' num2str(...
795                 app.measurement) ' of ' num2str(totmeas)];

```

```

794     % Needed to reduce measurement time, and following
795     % script measure only the output signal when
796     % distance in z direction changes, the last signal
797     % before moving in z direction and measure with a
798     % frequency of 10 when no changes in z direction.
799     ll = ll+1;
800     if ~ismember(kk,freq_change(ii,:))
801         if strcmpi(app.meas.notes,'On Axis Pressure')
802             % measure el signal for first or every 10n
803             % distance
804             if ii == 1
805                 app.meas_el_sig = 1;
806             elseif mod(ii,10) == 0
807                 app.meas_el_sig = 1;
808             else
809                 app.meas_el_sig = 0;
810             end
811             freq_change(ii,ll) = kk;
812             z_dist = 1;
813         else
814             % measure el signal because of new z distance
815             freq_change(ii,ll) = kk;
816             app.meas_el_sig = 1;
817             z_dist = 1;
818         end
819     elseif mod(sum(freq_change(ii,')==kk),10) == 0
820         % measure el signal because of 10n frequency
821         freq_change(ii,ll) = kk;
822         app.meas_el_sig = 1;
823         z_dist = 0;
824     elseif width(freq_change) < ll+length(app.meas.frequency...
825         )
826         % measure el signal because of last secondary ...
827         % movment
828         freq_change(ii,ll) = kk;
829         app.meas_el_sig = 1;
830         z_dist = 0;
831     else
832         % measure only acoutical
833         freq_change(ii,ll) = kk;
834         app.meas_el_sig = 0;
835         z_dist = 0;
836     end
837
838     % Prevent to change filter settings if frequency is

```

```

837     % not changed
838     if app.measurement == 1
839         % Set filter settings for first time
840         app.filt_setting = 1;
841     elseif ll == 1 && ii-1 ~= 0 && freq_change(ii-1,width(...
842         freq_change)) ~= freq_change(ii,ll)
843         % Changes filter settings because frequency
844         % changed whith z movment
845         app.filt_setting = 1;
846     elseif ll-1 ~= 0 && freq_change(ii,ll) ~= freq_change(ii...
847         ,(ll-1))
848         % Changes filter settings because of frequency
849         % changed
850         app.filt_setting = 1;
851     else
852         % Frequency is the same and filter stays
853         % unchanged
854         app.filt_setting = 0;
855     end
856
857     % Prevent generator settings to change if frequency
858     % or z distance is unchanged
859     if app.filt_setting == 1
860         app.gen_setting = 1;
861     elseif z_dist == 1
862         app.gen_setting = 1;
863     else
864         app.gen_setting = 0;
865     end
866
867     % Measure enviroment signal with a frequency of 30
868     if app.measurement == 1
869         app.environment = 1;
870     elseif mod(app.measurement,30) == 0
871         app.environment = 1;
872     else
873         app.environment = 0;
874     end
875
876     step_primary = app.zeropos.(app.field{primary_axis})+...
877         app.meas.primary_axis(ii);
878     if mod(ii,2) == 0
879         stepdirrev = fliplr(app.meas.secondary_axis);
880         if height(app.meas.secondary_axis) > 1
881             step_secondary = app.zeropos.(app.field{...

```

```

secondary_axis))+stepdirrev(ii,jj);
879     else
880         step_secondary = app.zeropos.(app.field{...
secondary_axis))+stepdirrev(jj);
881     end
882     else
883         if height(app.meas.secondary_axis) > 1
884             step_secondary = app.zeropos.(app.field{...
secondary_axis))+app.meas.secondary_axis(ii,...
jj);
885         else
886             step_secondary = app.zeropos.(app.field{...
secondary_axis))+app.meas.secondary_axis(jj);
887         end
888     end
889
890     for tt = 1:length(axis)
891         if axis(tt) == 2 && app.comp == 1
892             app.result.lin_slope_const_a = app.linearslope.a...
;
893             app.result.lin_slope_const_b = app.linearslope.b...
;
894             compensation = app.linearslope.a*...
app.meas.primary_axis(ii)+app.linearslope.b;
895             if round((app.abspos.(app.field{axis(tt)})- ...
compensation),4) ~= 0
896                 StepMotorFunc(app,compensation,axis(tt),1)
897                 if app.stop == 1
898                     app.stop = 0;
899                     return
900                 end
901             end
902             elseif axis(tt) == 1 && mainlobex == 1
903                 position = app.zeropos.(app.field{axis(tt)})+...
app.meas.xaxis_offset;
904                 if round((app.abspos.(app.field{axis(tt)})- ...
position),4) ~= 0
905                     StepMotorFunc(app,position,axis(tt),1)
906                     if app.stop == 1
907                         app.stop = 0;
908                         return
909                     end
910                 end
911             elseif started == 0 || round((app.abspos.(app.field{...
axis(tt)})-app.zeropos.(app.field{axis(tt)})),4) ...

```

```

~ = 0
912     step = app.zeropos.(app.field{axis(tt)});
913     StepMotorFunc(app, step, axis(tt), 1)
914     if app.stop == 1
915         app.stop = 0;
916         return
917     end
918 end
919 end
920
921 if length(app.meas.primary_axis) == 1
922     if started == 0 || round((app.abspos.(app.field{...
primary_axis})-app.zeropos.(app.field{...
primary_axis})),4) ~= app.meas.primary_axis(ii)
923     StepMotorFunc(app, step_primary, primary_axis, 1)
924     if app.stop == 1
925         app.stop = 0;
926         return
927     end
928 end
929 elseif round((app.abspos.(app.field{primary_axis})-...
app.zeropos.(app.field{primary_axis})),4) ~= ...
app.meas.primary_axis(ii)
930     StepMotorFunc(app, step_primary, primary_axis, 1)
931     if app.stop == 1
932         app.stop = 0;
933         return
934     end
935 end
936
937 if mod(ii,2) == 0
938     if height(app.meas.secondary_axis) > 1
939         if round((app.abspos.(app.field{secondary_axis})...
-app.zeropos.(app.field{secondary_axis})),4) ...
~ = stepdirrev(ii, jj)
940         StepMotorFunc(app, step_secondary, ...
secondary_axis, 1)
941         if app.stop == 1
942             app.stop = 0;
943             return
944         end
945     end
946 elseif round((app.abspos.(app.field{secondary_axis})...
-app.zeropos.(app.field{secondary_axis})),4) ~= ...
stepdirrev(jj)

```

```
947         StepMotorFunc (app, step_secondary, secondary_axis...
948             ,1)
949     if app.stop == 1
950         app.stop = 0;
951         return
952     end
953 else
954     if height (app.meas.secondary_axis) > 1
955         if round((app.abspos.(app.field{secondary_axis})...
956             -app.zeropos.(app.field{secondary_axis})),4) ...
957             ~= app.meas.secondary_axis(ii,jj)
958             StepMotorFunc (app, step_secondary, ...
959                 secondary_axis,1)
960             if app.stop == 1
961                 app.stop = 0;
962                 return
963             end
964         elseif round((app.abspos.(app.field{secondary_axis})...
965             -app.zeropos.(app.field{secondary_axis})),4) ~= ...
966             app.meas.secondary_axis(jj)
967             StepMotorFunc (app, step_secondary, secondary_axis...
968                 ,1)
969             if app.stop == 1
970                 app.stop = 0;
971                 return
972             end
973         end
974     end
975 end
976
977 app.result.primary_axis = app.field{primary_axis};
978 app.result.secondary_axis = app.field{secondary_axis};
979 app.result.primary_axis_pos = app.meas.primary_axis(ii);
980 if mod(ii,2) == 0
981     if height (app.meas.secondary_axis) > 1
982         app.result.secondary_axis_pos = stepdirrev(ii,jj...
983             );
984     else
985         app.result.secondary_axis_pos = stepdirrev(jj);
986     end
987 else
988     if height (app.meas.secondary_axis) > 1
989         app.result.secondary_axis_pos = ...
990             app.meas.secondary_axis(ii,jj);
```



```

983         else
984             app.result.secondary_axis_pos = ...
985                 app.meas.secondary_axis(jj);
986         end
987     end
988     app.result.pos.(app.field{1}) = app.abspos.(app.field...
989         {1})-app.zeropos.(app.field{1});
990     app.result.pos.(app.field{2}) = app.abspos.(app.field...
991         {2})-app.zeropos.(app.field{2});
992     app.result.pos.(app.field{3}) = app.abspos.(app.field...
993         {3})-app.zeropos.(app.field{3});
994     app.result.pos.(app.field{4}) = app.abspos.(app.field...
995         {4})-app.zeropos.(app.field{4});
996     app.result.abs_pos.(app.field{1}) = app.abspos.(...
997         app.field{1});
998     app.result.abs_pos.(app.field{2}) = app.abspos.(...
999         app.field{2});
1000    app.result.abs_pos.(app.field{3}) = app.abspos.(...
1001        app.field{3});
1002    app.result.abs_pos.(app.field{4}) = app.abspos.(...
1003        app.field{4});
1004
1005    distance_to_microphone = app.result.pos.(app.field{3})*1...
1006        e-3;
1007    if app.environment == 1
1008        VaisalaHMT313_read(app)
1009        Paroscientific(app)
1010        ASLF250(app)
1011    end
1012
1013    app.result.sound_speed = 331*sqrt((...
1014        app.result.temperature+273.15)/273.15);
1015    app.result.est_travel_time = (distance_to_microphone/...
1016        app.result.sound_speed);
1017    % override with own signal cycles if not set to 0
1018    if app.meas.sig_cycles == 0
1019        sig_duration_nominal = max((...
1020            app.meas.est_travel_time_faktor*...
1021            app.result.est_travel_time),...
1022            app.meas.min_sig_duration);
1023        app.result.sig_cycles = floor(app.meas.frequency(kk)...
1024            *sig_duration_nominal);
1025    else
1026        app.result.sig_cycles = app.meas.sig_cycles;
1027    end

```

```
1012     app.result.sig_duration = app.result.sig_cycles/...
        app.meas.frequency(kk);
1013     app.result.frequency = app.meas.frequency(kk);
1014     app.result.cutoff_f1 = app.meas.cutoff_1(kk);
1015     app.result.cutoff_f2 = app.meas.cutoff_2(kk);
1016
1017     % Start time
1018     if started == 0
1019         start_time = datetime('now');
1020         started = 1;
1021     end
1022
1023     % Initialize first time
1024     if init == 0
1025         InitInstruments(app)
1026         init = 1;
1027     end
1028     Measure(app)
1029
1030     app.result.time = datetime('now');
1031     time_used = app.result.time-start_time;
1032     average_time = (time_used)/app.measurement;
1033     time_finished = average_time*measurementleft;
1034
1035     SaveMeasurements(app)
1036
1037     if measurementleft >= 1
1038         txt = ['Measurement ' num2str(app.measurement) ' is ...
                complete'];
1039         WriteTextInWindow(app,txt)
1040         txt = ['There are ' num2str(measurementleft) ' ...
                measurements left'];
1041         WriteTextInWindow(app,txt)
1042         txt = ['The current average time for each ...
                measurement is ' datestr(average_time,'MM:SS')];
1043         WriteTextInWindow(app,txt)
1044         txt = ['Expected to be complete at ' datestr(...
                app.result.time+time_finished)];
1045         WriteTextInWindow(app,txt)
1046     else
1047         txt = ['The measurements are complete and took ' ...
                datestr(time_used,'dd:HH:MM:SS')];
1048         WriteTextInWindow(app,txt)
1049     end
1050
```

```

1051         % Reset scope acquisition mode to RUNSTOP, so that ...
           realtime changes is
1052         % visible on the oscilloscope.
1053         writeline(app.instrument.scope, 'ACQ:STOPA RUNST');
1054     end
1055 end
1056 end
1057 end
1058
1059 % Button pushed function: READ_Button
1060 function READ_ButtonPushed(app, event)
1061     read = app.READ_DropDown.Value;
1062     switch read
1063     case 'DPO CH1'
1064         app.meas = {};
1065         app.meas.sample_count = app.SAMPLE_COUNT_Spinner.Value;
1066         app.meas.average = app.AVERAGE_Spinner.Value;
1067         app.meas.voltage_inn = app.VOLT_Spinner.Value;
1068         app.meas.burst_rate = app.BURST_RATE_Spinner.Value;
1069         app.meas.average_time = app.meas.average/app.meas.burst_rate...
           +1;
1070         app.result.frequency = app.FREQUENCY_Spinner.Value;
1071         app.result.cutoff_f1 = (app.result.frequency/1000)/2;
1072         app.result.cutoff_f2 = (app.result.frequency/1000)*2;
1073         app.result.sig_cycles = app.CYCLES_Spinner.Value;
1074
1075         InitInstruments(app)
1076
1077         % Set scope acquisition mode to SEQUENCE instead of RUNSTOP,...
           so that a
1078         % measurement is aquired when prompted, instead of ...
           continuously. See page
1079         % 2-97 in programming manual for details.
1080         writeline(app.instrument.scope, 'ACQ:STOPA SEQ');
1081
1082         % Reset aquisition mode to averaging
1083         writeline(app.instrument.scope, 'ACQ:MOD AVE');
1084         % Set the number of cycles to average.
1085         writeline(app.instrument.scope, ['ACQ:NUMAV ' num2str(...
           app.meas.average)]);
1086         % Number of points which shall be read from the scope.
1087         writeline(app.instrument.scope, ['HOR:RECO ' num2str(...
           app.meas.sample_count)]);
1088
1089         % Start aquisition.

```

```
1090     writeline(app.instrument.scope, 'ACQ:STATE RUN');
1091     txt = 'Starting aquisition';
1092     WriteTextInWindow(app,txt)
1093     pause(app.meas.average_time)
1094
1095     DPO_read(app,1)
1096     dporeult.x = app.x;
1097     dporeult.wf = app.wf;
1098
1099     Paroscientific(app)
1100     dporeult.pressure = app.result.pressure;
1101     VaisalaHMT313_read(app)
1102
1103     dporeult.vaisala_RH = app.result.vaisala_RH;
1104     dporeult.vaisala_T = app.result.vaisala_T;
1105
1106     ASLF250(app)
1107     dporeult.temperature = app.result.temperature;
1108
1109     for fn = fieldnames(app.result)'
1110         app.meas.(fn{1}) = app.result.(fn{1});
1111     end
1112     dporeult.settings = app.meas;
1113     txt = 'Saving Measurement Parameters';
1114     WriteTextInWindow(app,txt)
1115     savepath = [app.path '\DPO_read_CH1.mat'];
1116     m = matfile(savepath, 'Writable', true);
1117     m.DPO = dporeult;
1118     txt = 'Finished';
1119     WriteTextInWindow(app,txt)
1120     % Reset scope acquisition mode to RUNSTOP, so that realtime ...
1121     % changes is
1122     % visible on the oscilloscope.
1123     writeline(app.instrument.scope, 'ACQ:STOPA RUNSTOp');
1124 case 'DPO CH2'
1125     app.meas = {};
1126     app.meas.sample_count = app.SAMPLE_COUNT_Spinner.Value;
1127     app.meas.average = app.AVERAGE_Spinner.Value;
1128     app.meas.voltage_inn = app.VOLT_Spinner.Value;
1129     app.meas.burst_rate = app.BURST_RATE_Spinner.Value;
1130     app.meas.average_time = app.meas.average/app.meas.burst_rate...
1131         +1;
1132     app.result.frequency = app.FREQUENCY_Spinner.Value;
1133     app.result.cutoff_f1 = (app.result.frequency/1000)/2;
1134     app.result.cutoff_f2 = (app.result.frequency/1000)*2;
```

```
1133     app.result.sig_cycles = app.CYCLES_Spinner.Value;
1134
1135     InitInstruments(app)
1136
1137     % Set scope acquisition mode to SEQUENCE instead of RUNSTOP,...
1138     % so that a
1139     % measurement is aquired when prompted, instead of ...
1140     % continuously. See page
1141     % 2-97 in programming manual for details.
1142     writeline(app.instrument.scope, 'ACQ:STOPA SEQ');
1143
1144     % Reset aquisition mode to averaging
1145     writeline(app.instrument.scope, 'ACQ:MOD AVE');
1146     % Set the number of cycles to average.
1147     writeline(app.instrument.scope, ['ACQ:NUMAV ' num2str(...
1148     app.meas.average)]);
1149     % Number of points which shall be read from the scope.
1150     writeline(app.instrument.scope, ['HOR:RECO ' num2str(...
1151     app.meas.sample_count)]);
1152
1153     % Start aquisition.
1154     writeline(app.instrument.scope, 'ACQ:STATE RUN');
1155     txt = 'Starting aquisition';
1156     WriteTextInWindow(app,txt)
1157     pause(app.meas.average_time)
1158
1159     DPO_read(app,2)
1160     dporeult.x = app.x;
1161     dporeult.wf = app.wf;
1162
1163     Paroscientific(app)
1164     dporeult.pressure = app.result.pressure;
1165     VaisalaHMT313_read(app)
1166
1167     dporeult.vaisala_RH = app.result.vaisala_RH;
1168     dporeult.vaisala_T = app.result.vaisala_T;
1169
1170     ASLF250(app)
1171     dporeult.temperature = app.result.temperature;
1172
1173     for fn = fieldnames(app.result)'
1174         app.meas.(fn{1}) = app.result.(fn{1});
1175     end
1176     dporeult.settings = app.meas;
1177     txt = 'Saving Measurement Parameters';
```

```
1174 WriteTextInWindow(app,txt)
1175 savepath = [app.path '\DPO_read_CH2.mat'];
1176 m = matfile(savepath,'Writable',true);
1177 m.DPO = dporesult;
1178 txt = 'Finished';
1179 WriteTextInWindow(app,txt)
1180 % Reset scope acquisition mode to RUNSTOP, so that realtime ...
      changes is
1181 % visible on the oscilloscope.
1182 writeline(app.instrument.scope,'ACQ:STOPA RUNST');
1183 case 'DPO CH2 Read Only'
1184 % Reading only from screen, only changeable value is
1185 % samplecount. Useful when calibrating microphone.
1186 app.meas = {};
1187 app.meas.sample_count = app.SAMPLE_COUNT_Spinner.Value;
1188
1189 DPO_read(app,2)
1190 dporesult.x = app.x;
1191 dporesult.wf = app.wf;
1192
1193 Paroscientific(app)
1194 dporesult.pressure = app.result.pressure;
1195 VaisalaHMT313_read(app)
1196
1197 dporesult.vaisala_RH = app.result.vaisala_RH;
1198 dporesult.vaisala_T = app.result.vaisala_T;
1199
1200 ASLF250(app)
1201 dporesult.temperature = app.result.temperature;
1202
1203 dporesult.sample_count = app.meas.sample_count;
1204
1205 txt = 'Saving Measurement Parameters';
1206 WriteTextInWindow(app,txt)
1207 savepath = [app.path '\DPO_read_CH2_Read.mat'];
1208 m = matfile(savepath,'Writable',true);
1209 m.DPO = dporesult;
1210 txt = 'Finished';
1211 WriteTextInWindow(app,txt)
1212 case 'PAROSCIENTIFIC'
1213 Paroscientific(app)
1214 txt = num2str(app.result.pressure);
1215 WriteTextInWindow(app,txt)
1216 case 'VAISALA'
1217 VaisalaHMT313_read(app)
```

```
1218         txt = ['Relative Humidity = ' num2str(app.result.vaisala_RH)...
1219             ];
1219         WriteTextInWindow(app,txt)
1220         txt = ['Temperature = ' num2str(app.result.vaisala_T)];
1221         WriteTextInWindow(app,txt)
1222     case 'ASLF250'
1223         ASLF250(app)
1224         txt = ['Temperature = ' num2str(app.result.temperature)];
1225         WriteTextInWindow(app,txt)
1226     end
1227 end
```

Appendix C

FEMP-scripts

C.1 read_inn_project.m (vacuum)

```

1 function [read]=read_inn_project(read,commands);
2 %%%%%%%%%%%%%%%%%%%%%%%%%%%%%%%%%%%%%%%%%%%%%%%%%%%%%%%%%%%%%%%%%%%%%%%%%
3 % Read .inn-file. Note that this function calls a project specific
4 % read_inn_project.m which should be in the working directory
5 %
6 % Part of FEMP (Finite Element Modeling of Piezoelectric structures)
7 % Programmed by Jan Kocbach (jan@kocbach.net)
8 % (C) 2000 Jan Kocbach. This file is free software; you can ...
   redistribute
9 % it and/or modify it only under the the terms of the GNU GENERAL PUBLIC
10 % LICENSE which should be included along with this file.
11 % (C) 2000-2010 Christian Michelsen Research AS
12 %%%%%%%%%%%%%%%%%%%%%%%%%%%%%%%%%%%%%%%%%%%%%%%%%%%%%%%%%%%%%%%%%%%%%%%%%
13
14 % Put a file read_inn_project.m in your project directory to define ...
   local
15 % FEMP input commands. Also include init_const_project.m in this ...
   directory
16 % and define the commands there.
17 global glob;
18 read=read;
19
20
21 %% piezodiskfluid_egen
22     if ~isempty(read.piezodiskfluidtest)
23
24         read.points=[]; read.areas=[]; read.materials=[]; read.dof=[]; ...

```



```

        read.restraints=[];
25
26     r=read.piezodiskfluidtest(1,1,:);
27     t=read.piezodiskfluidtest(1,2,:);
28     rfluid=read.piezodiskfluidtest(1,3,:);
29     elfluid=read.piezodiskfluidtest(1,4,:);
30     matnum=read.piezodiskfluidtest(1,5,:);
31     elr=read.piezodiskfluidtest(1,6,:);
32     elt=read.piezodiskfluidtest(1,7,:);
33     matnumfluid=read.piezodiskfluidtest(1,8,:);
34     theta=read.piezodiskfluidtest(1,9,:);
35
36     for s=1:size(r,3)
37         rfluidtemp=0+rfluid(s);
38         rinffluid=rfluidtemp*2;
39         read.points(:, :, s)=[
40             1 0 -t(s)/2;
41             2 r(s) -t(s)/2;
42             3 0 t(s)/2;
43             4 r(s) t(s)/2];
44
45         read.areas(:, :, s)=[1 1 2 4 3 elr(s) elt(s) 0 0];
46
47         read.materials(:, :, s)=[1 glob.globvariables.piezo matnum(s)];
48
49         read.dof(:, :, s)=[-1 1 t(s)/2-1e-9 t(s)/2+1e-9 glob.free.ep];
50         read.restraints(:, :, s)=[-1 1 -t(s)/2-1e-9 -t(s)/2+1e-9 ...
51             glob.free.ep 1];
52         glob.tfront(s)=t(s)/2;
53     end
end

```

C.2 read_inn_project.m (fluid)

```

1 function [read]=read_inn_project(read,commands);
2 %%%%%%%%%%%%%%%%%%%%%%%%%%%%%%%%%%%%%%%%%%%%%%%%%%%%%%%%%%%%%%%%%%%%%%%%%
3 % Read .inn-file. Note that this function calls a project specific
4 % read_inn_project.m which should be in the working directory
5 %
6 % Part of FEMP (Finite Element Modeling of Piezoelectric structures)
7 % Programmed by Jan Kocbach (jan@kocbach.net)
8 % (C) 2000 Jan Kocbach. This file is free software; you can ...

```

```

    redistribute
9 % it and/or modify it only under the the terms of the GNU GENERAL PUBLIC
10 % LICENSE which should be included along with this file.
11 % (C) 2000-2010 Christian Michelsen Research AS
12 %%%%%%%%%%%%%%%%%%%%%%%%%%%%%%%%%%%%%%%%%%%%%%%%%%%%%%%%%%%%%%%%%%%%%%%%%%
13
14 % Put a file read_inn_project.m in your project directory to define ...
    local
15 % FEMP input commands. Also include init_const_project.m in this ...
    directory
16 % and define the commands there.
17 global glob;
18 read=read;
19
20
21 %% piezodiskfluid_egen
22     if ~isempty(read.piezodiskfluidtest)
23
24         read.points=[]; read.areas=[]; read.materials=[]; read.dof=[]; ...
            read.restraints=[];
25
26         r=read.piezodiskfluidtest(1,1,:);
27         t=read.piezodiskfluidtest(1,2,:);
28         rfluid=read.piezodiskfluidtest(1,3,:);
29         elfluid=read.piezodiskfluidtest(1,4,:);
30         matnum=read.piezodiskfluidtest(1,5,:);
31         elr=read.piezodiskfluidtest(1,6,:);
32         elt=read.piezodiskfluidtest(1,7,:);
33         matnumfluid=read.piezodiskfluidtest(1,8,:);
34         theta=read.piezodiskfluidtest(1,9,:);
35
36         for s=1:size(r,3)
37             rfluidtemp=0+rfluid(s);
38             rinffluid=rfluidtemp*2;
39             read.points(:, :, s)=[
40                 1 0 -t(s)/2;
41                 2 r(s) -t(s)/2;
42                 3 0 t(s)/2;
43                 4 r(s) t(s)/2;
44                 5 0 rfluid(s);
45                 6 rfluid(s)*sin(theta(s)) rfluid(s)*cos(theta(s));
46                 7 rfluid(s)*sin(theta(s)) -rfluid(s)*cos(theta(s));
47                 8 0 -rfluid(s);
48                 9 0 rinffluid;
49                 10 rinffluid*sin(theta(s)) rinffluid*cos(theta(s));

```

```

50     11 rinffluid*sin(theta(s)) -rinffluid*cos(theta(s));
51     12 0 -rinffluid;
52     13 0 0];
53
54     read.areas(:, :, s)=[1 1 2 4 3 elr(s) elt(s) 0 0;
55     2 3 4 6 5 elfluid(s) elfluid(s) 0 13;
56     2 4 2 7 6 elfluid(s) elfluid(s) 0 13;
57     2 2 1 8 7 elfluid(s) elfluid(s) 0 13;
58     3 5 6 10 9 1 1 13 13;
59     3 6 7 11 10 1 1 13 13;
60     3 7 8 12 11 1 1 13 13];
61
62     read.materials(:, :, s)=[1 glob.globvariables.piezo matnum(s);
63     2 glob.globvariables.fluid matnumfluid(s);
64     3 glob.globvariables.infinitefluid matnumfluid(s)];
65
66     read.dof(:, :, s)=[-1 1 t(s)/2-1e-9 t(s)/2+1e-9 glob.free.ep];
67     read.restraints(:, :, s)=[-1 1 -t(s)/2-1e-9 -t(s)/2+1e-9 ...
68         glob.free.ep 1];
69     glob.tfront(s)=t(s)/2;
70     end
end

```

C.3 init_const_project.m

```

1  %%%%%%%%%%%%%%%%%%%%%%%%%%%%%%%%%%%%%%%%%%%%%%%%%%%%%%%%%%%%%%%%%%%%%%%%%
2  % Initialization of constants for FEMP
3  % Part of FEMP (Finite Element Modeling of Piezoelectric structures)
4  % Programmed by Jan Kocbach (jan@kocbach.net)
5  % (C) 2000 Jan Kocbach. This file is free software; you can ...
6  %   redistribute
7  % it and/or modify it only under the the terms of the GNU GENERAL PUBLIC
8  % LICENSE which should be included along with this file.
9  % (C) 2000-2010 Christian Michelsen Research AS
10 %%%%%%%%%%%%%%%%%%%%%%%%%%%%%%%%%%%%%%%%%%%%%%%%%%%%%%%%%%%%%%%%%%%%%%%%%
11
12 %%%%%%%%%%%%%%%%%%%%%%%%%%%%%%%%%%%%%%%%%%%%%%%%%%%%%%%%%%%%%%%%%%%%%%%%%
13 % INIT_CONST_PROJECT: Initialize constants - project specifix
14 %%%%%%%%%%%%%%%%%%%%%%%%%%%%%%%%%%%%%%%%%%%%%%%%%%%%%%%%%%%%%%%%%%%%%%%%%
15
16 % Make a copy of this file in your project folder to

```

```
17 % make project specific definitions
18
19 %'piezodiskfront1',
20
21 commands = [commands, 'piezodiskfluidtest'];
```

C.4 Pz27.inn

```
1 set
2 Radius_P,          10e-3
3 Thickness_P,       2e-3
4 Radius_Infel,      30e-3
5 Elements_FL,       7
6 Materialnumber_P,  77
7 Elements_R_P,      7
8 Elements_T_P,      7
9 Materialnumber_FL, 10101
10 Theta,            1.3
11 end
12
13 materialfile
14 5
15 end
16
17 meshingtype
18 elementsperwavelength, 300e3
19 end
20
21 viewmesh
22 0
23 end
24
25 # The order of the finite elements is 2 - i.e. 8 node isoparametric ...
    elements are applied
26 order
27 2
28 end
29
30 # The order of the infinite elements is set to 10.
31 infiniteorder
32 10
33 end
```

```
34
35 piezodiskfluidtest
36 Radius_P,Thickness_P,Radius_Infel,Elements_FL,Materialnumber_P,...
    Elements_R_P,Elements_T_P,Materialnumber_FL,Theta,q_DampDist_r,...
    q_DampDist_z
37 end
38
39 #directharmonicanalysis
40 #0,50,300e3,complex_loss
41 #end
42
43 #admittance
44 #0,0,0
45 #end
46
47 #save
48 #admittance,admittance_f
49 #end
50
51 #nearfieldpressure
52 #0,0,0,-1,1,-1,1
53 #end
54
55 # Calculate far-field pressure for the frequencies used in the time-...
    harmonic
56 # analysis. Calculate out to 3 times the distance at which the infinite
57 # elements are applied (10*7.0 mm= 70.0 mm), with 20 divisions per 7.0 ...
    mm.
58
59 #farfieldpressure
60 #0,0,0,10,20
61 #end
62
63 #save
64 #farfieldpressure,farfieldpressure_f,farfieldpressure_r,...
    farfieldpressure_z,nearfieldpressure,nearfieldpressure_z,...
    nearfieldpressure_r,nearfieldpressure_f
65 #end
66
67 #onaxispressure
68 #0,0,0,10,20
69 #end
70
71 #directivity
72 #0,0,0,1
```

```

73 #end
74
75 #sensitivity
76 #0,0,0,1
77 #end
78
79 #save
80 #sensitivity,sensitivity_f,directivity,directivity_theta,directivity_f
81 #end
82
83 #save
84 #sensitivity,sensitivity_f,onaxispressure,onaxispressure_r,...
    onaxispressure_f
85 #end
86
87 #save
88 #sensitivity,sensitivity_f,directivity,directivity_theta,directivity_f,...
    onaxispressure,onaxispressure_r,onaxispressure_f
89 #end
90
91 #save('test_res.mat','result','-v7.3');

```

C.5 material5.dat

```

1      77      piezo      pz27 (Lohne/Knappskog)
2 # mechanical terms
3      1.1875E+11 7.43000E+10 7.42500E+10 0.00000E+00 0.00000E+00 0.00000E+00
4      7.43000E+10 1.1875E+11 7.42500E+10 0.00000E+00 0.00000E+00 0.00000E+00
5      7.42500E+10 7.42500E+10 1.12050E+11 0.00000E+00 0.00000E+00 0.00000E...
        +00
6      0.00000E+00 0.00000E+00 0.00000E+00 2.11000E+10 0.00000E+00 0.00000E...
        +00
7      0.00000E+00 0.00000E+00 0.00000E+00 0.00000E+00 2.11000E+10 0.00000E...
        +00
8      0.00000E+00 0.00000E+00 0.00000E+00 0.00000E+00 0.00000E+00 2.22250E...
        +10
9 # coupling terms
10     0.00000E+00 0.00000E+00 0.00000E+00 0.00000E+00 1.12000E+01 0.00000E...
        +00
11     0.00000E+00 0.00000E+00 0.00000E+00 1.12000E+01 0.00000E+00 0.00000E...
        +00
12    -5.40000E+00 -5.40000E+00 1.60389E+01 0.00000E+00 0.00000E+00 0.00000E...

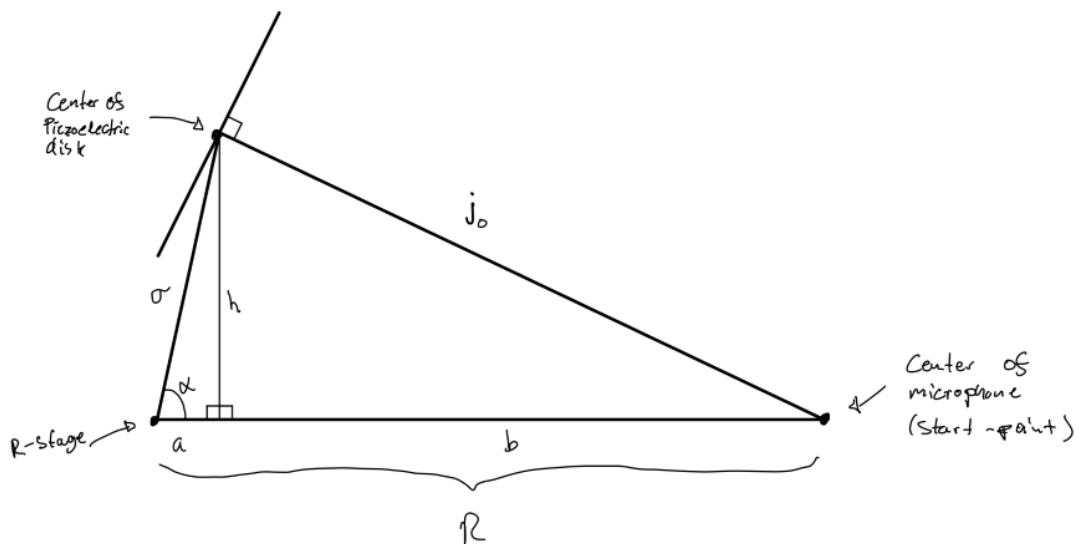
```

```
+00
13 # dielectric terms
14 8.11043e-09 0.00000E+00 0.00000E+00
15 0.00000E+00 8.11043e-09 0.00000E+00
16 0.00000E+00 0.00000E+00 8.14585e-09
17 # density and damping coefficients
18 7.70000E+03 9.99000e+02 9.99000e+02
19 # mechanical Q-factors
20 9.57500e+01 7.12400e+01 1.20190e+02 0.00000e+00 0.00000e+00 0.00000e...
    +00
21 7.12400e+01 9.57500e+01 1.20190e+02 0.00000e+00 0.00000e+00 0.00000e...
    +00
22 1.20190e+02 1.20190e+02 1.77990e+02 0.00000e+00 0.00000e+00 0.00000e...
    +00
23 0.00000e+00 0.00000e+00 0.00000e+00 7.50000e+01 0.00000e+00 0.00000e...
    +00
24 0.00000e+00 0.00000e+00 0.00000e+00 0.00000e+00 7.50000e+01 0.00000e...
    +00
25 0.00000e+00 0.00000e+00 0.00000e+00 0.00000e+00 0.00000e+00 2.25342e...
    +02
26 # piezoelectric Q-factors
27 0.00000e+00 0.00000e+00 0.00000e+00 0.00000e+00 -2.00000e+02 0.00000e...
    +00
28 0.00000e+00 0.00000e+00 0.00000e+00 -2.00000e+02 0.00000e+00 0.00000e...
    +00
29 -1.66000e+02 -1.66000e+02 -3.23770e+02 0.00000e+00 0.00000e+00 0...
    .00000e+00
30 # dielectric Q-factors
31 5.00000e+01 0.00000e+00 0.00000e+00
32 0.00000e+00 5.00000e+01 0.00000e+00
33 0.00000e+00 0.00000e+00 8.62800e+01
34 # end of material data
35
36 10100 fluid air
37 1.20500E+00 1.41767E+05 0.00000E+00 0.00000E+00
38 10101 fluid air20grader
39 1.21000E+00 1.42355e+05 0.00000E+00 0.00000E+00
```

Appendix D

Additional information

D.1 Derivation of R



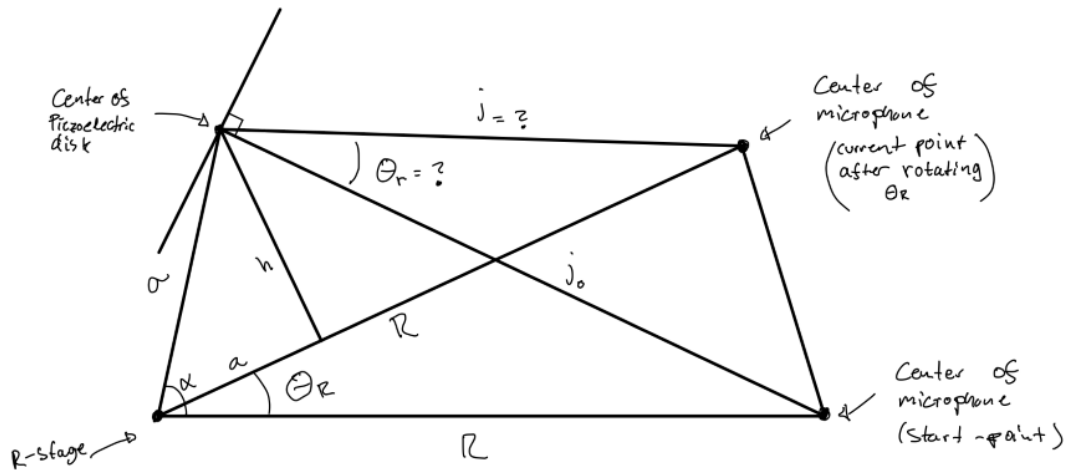
$$R = a + b$$

$$a = \sigma \cos(\alpha)$$

$$\left. \begin{aligned} \sigma^2 &= a^2 + h^2 \\ j_0^2 &= b^2 + h^2 \end{aligned} \right\} \Rightarrow b = \sqrt{j_0^2 + a^2 - \sigma^2}$$

$$\underline{\underline{R = \sigma \cos(\alpha) + \sqrt{j_0^2 + \sigma^2(\cos^2(\alpha) - 1)}}}$$

D.2 Derivation of j



$$a = \sigma \cos(\alpha - \theta_R)$$

$$h = \sigma \sin(\alpha - \theta_R)$$

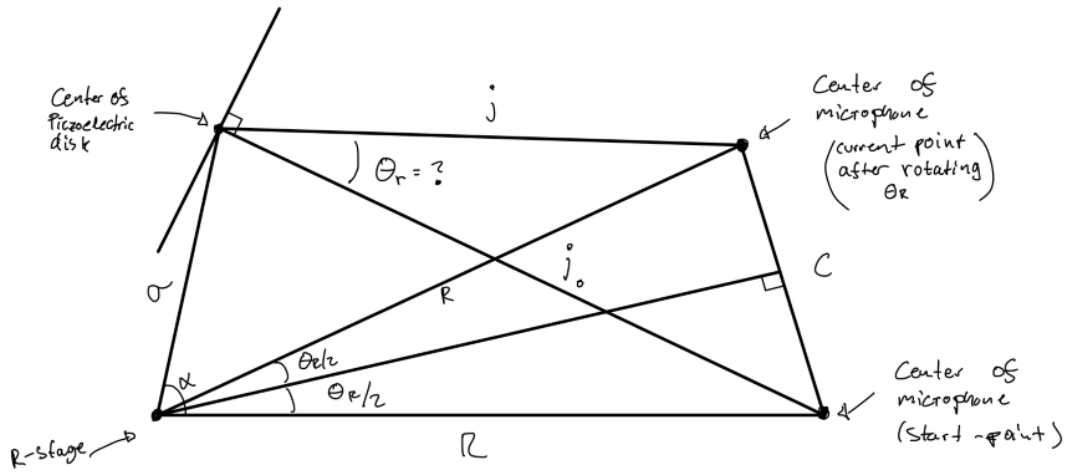
$$j = \sqrt{(R-a)^2 + h^2}$$

$$= \sqrt{(R - \sigma \cos(\alpha - \theta_R))^2 + \sigma^2 \sin^2(\alpha - \theta_R)}$$

$$= \sqrt{R^2 - 2R\sigma \cos(\alpha - \theta_R) + \sigma^2 (\cos^2(\alpha - \theta_R) + \sin^2(\alpha - \theta_R))}$$

$$\underline{\underline{j = \sqrt{R^2 - 2R\sigma \cos(\alpha - \theta_R) + \sigma^2}}}$$

D.3 Derivation of θ_r



$$\frac{C}{2} = R \sin\left(\frac{\theta_r}{2}\right) \quad \Rightarrow \quad C = 2R \sin\left(\frac{\theta_r}{2}\right)$$

$$C^2 = j^2 + j_0^2 - 2jj_0 \cos(\theta_r)$$

$$C^2 = 4R^2 \sin^2\left(\frac{\theta_r}{2}\right)$$

$$\theta_r = \cos^{-1}\left(\frac{j^2 + j_0^2 - 4R^2 \sin^2\left(\frac{\theta_r}{2}\right)}{2jj_0}\right)$$
